Donders Institute
for Brain, Cognition and Behaviour

Radboud University Nijmegen

UNIVERSITEIT TWENTE.

MIRA
INSTITUTE FOR BIOMEDICAL TECHNOLOGY AND TECHNICAL MEDICINE

FMRIB
Oxford Centre for Functional MRI of the Brain

Independent Component Analysis for Discovery and Inference Testing

Christian F. Beckmann

beckmann@fmrib.ox.ac.uk

c.beckmann@donder.ru.nl

NITP Summer Course
UCLA - 21/07/2011

Model-free Functional Data Analysis

MELODIC

Multivariate Exploratory Linear Optimised Decomposition into Independent Components

- decomposes data into a set of statistically independent spatial component maps and associated time courses
- can perform multi-subject/ multi-session analysis
- fully automated (incl. estimation of the number of components)
- inference on IC maps using alternative hypothesis testing

Model-free Functional Data Analysis

MELODIC

Multivariate Exploratory Linear Optimised Decomposition into Independent Components

- decomposes data into a set of statistically independent spatial component maps and associated time courses
- can perform multi-subject/ multi-session analysis
- fully automated (incl. estimation of the number of components)
- inference on IC maps using alternative hypothesis testing

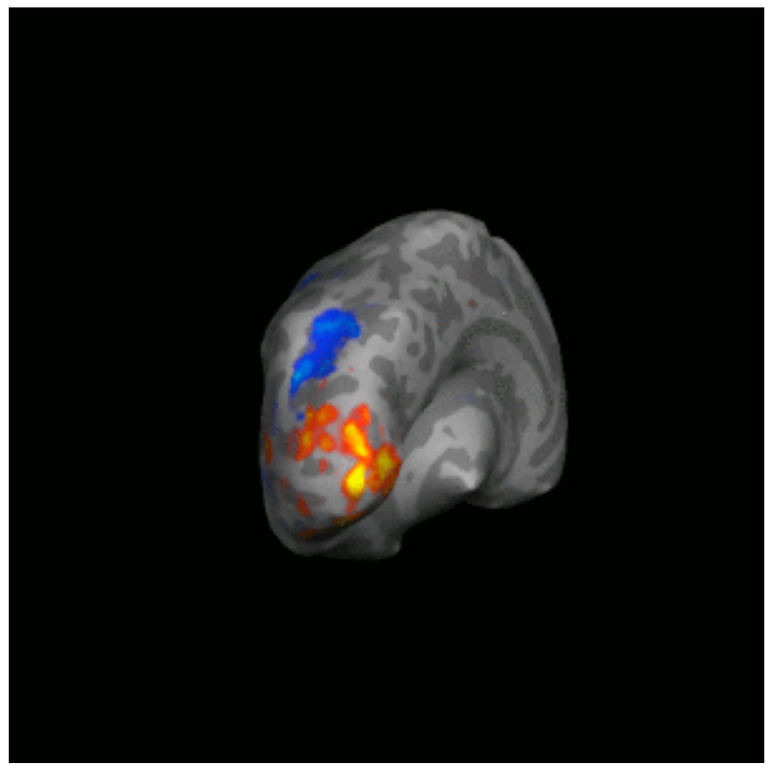

The FMRI inferential path

Experiment

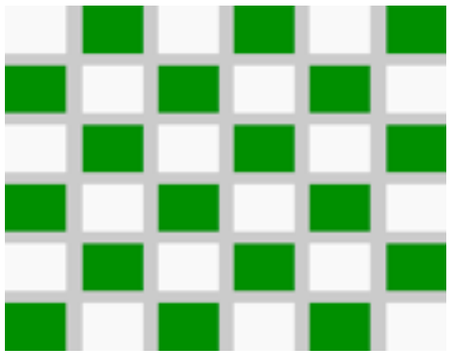

The FMRI inferential path

Experiment

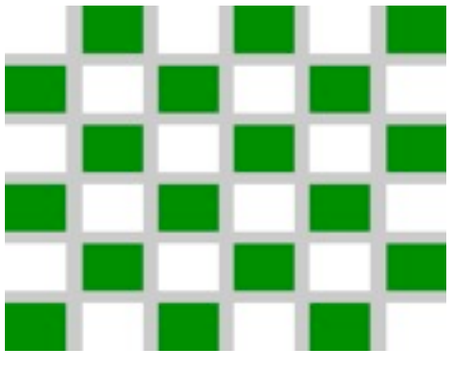

Physiology

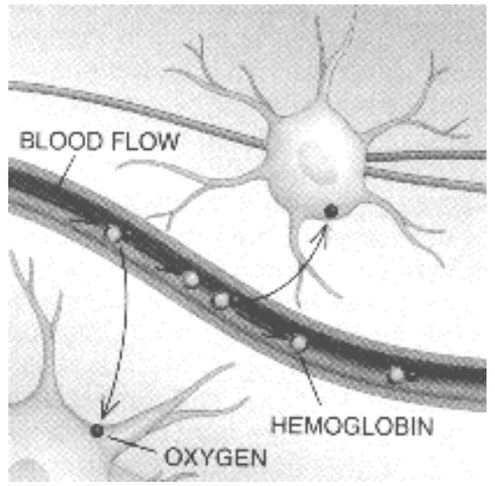

The FMRI inferential path

Experiment

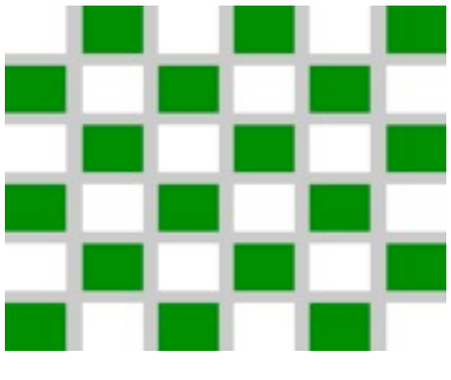

Physiology

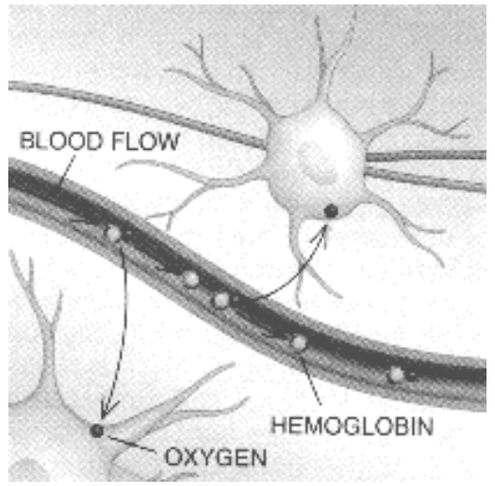

MR Physics

The FMRI inferential path

Experiment

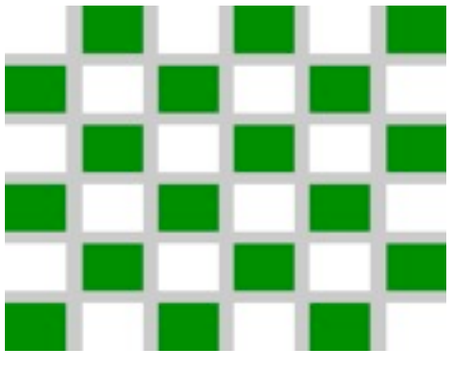

Physiology

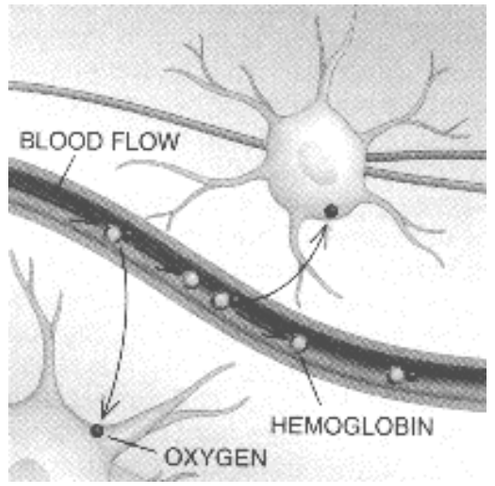

MR Physics

Analysis

The FMRI inferential path

Experiment

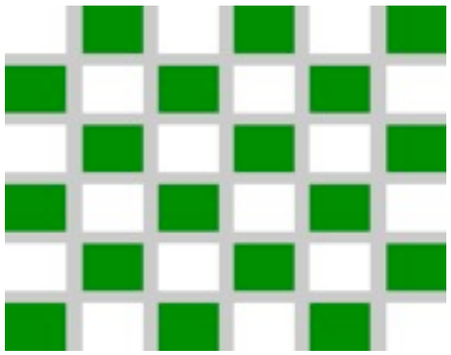

Physiology

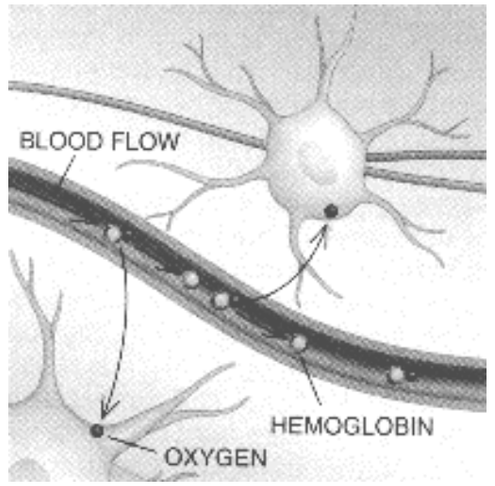

MR Physics

Analysis

Interpretation of final results

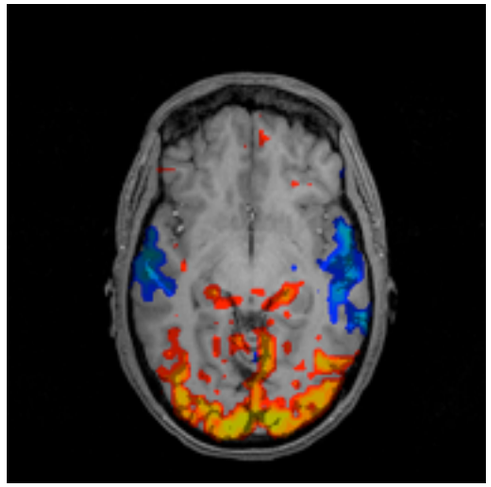

Variability in FMRI

Experiment

suboptimal event timing, inefficient design, etc.

Interpretation of final results

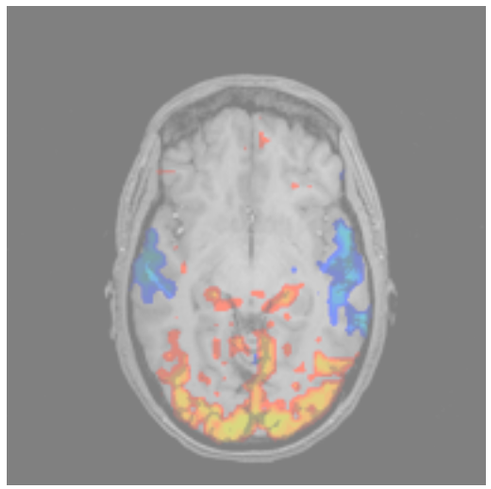

Physiology

Analysis

MR Physics

Variability in FMRI

Experiment

suboptimal event timing, inefficient design, etc.

Physiology

secondary activation, ill-defined baseline, resting-fluctuations etc.

MR Physics

Analysis

Interpretation of final results

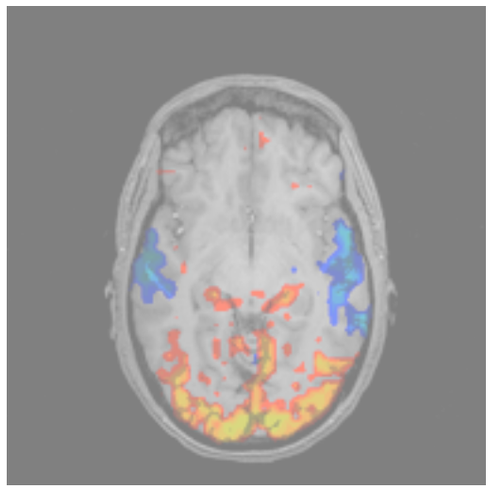

Variability in FMRI

Experiment

suboptimal event timing, inefficient design, etc.

Physiology

secondary activation, ill-defined baseline, resting-fluctuations etc.

MR Physics

MR noise, field inhomogeneity, MR artefacts etc.

Analysis

Interpretation of final results

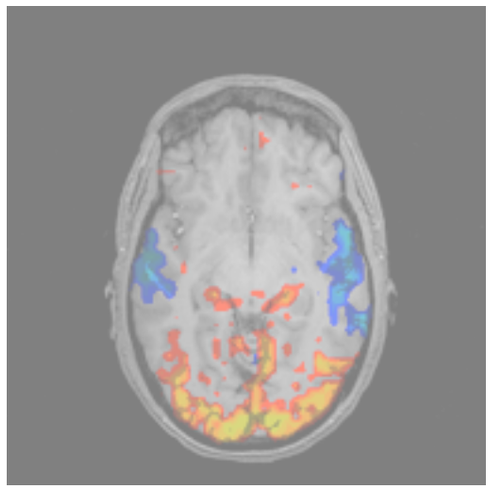

Variability in FMRI

Experiment

suboptimal event timing, inefficient design, etc.

Interpretation of final results

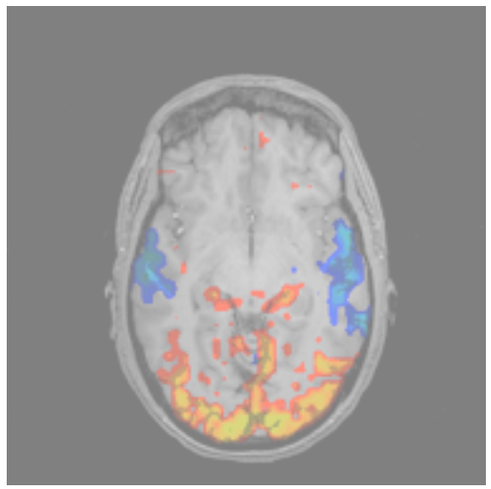

Physiology

secondary activation, ill-defined baseline, resting-fluctuations etc.

Analysis

filtering & sampling artefacts, design misspecification, stats & thresholding issues etc.

MR Physics

MR noise, field inhomogeneity, MR artefacts etc.

Data Analysis

Confirmatory

- *"How well does my model fit to the data?"*

Problem ⇨ Data ⇨

Model ⇨ Analysis

⇨ Results

- results depend on the model

Data Analysis

Confirmatory

- *"How well does my model fit to the data?"*

Problem ⇨ Data ⇨ Model ⇨ Analysis ⇨ Results

- results depend on the model

Exploratory

- *"Is there anything interesting in the data?"*

Problem ⇨ Data ⇨ Analysis ⇨ Model ⇨ Results

- can give unexpected results

EDA techniques

- try to ‘explain’ / represent the data
  - by calculating quantities that summarise the data
  - by extracting underlying ‘hidden’ features that are ‘interesting’

EDA techniques

- try to ‘explain’ / represent the data
  - by calculating quantities that summarise the data
  - by extracting underlying ‘hidden’ features that are ‘interesting’
- differ in what is considered ‘interesting’
  - are localised in time and/or space (Clustering)
  - explain observed data variance (PCA, FDA, FA)
  - are maximally independent (ICA)

EDA techniques

- try to ‘explain’ / represent the data
  - by calculating quantities that summarise the data
  - by extracting underlying ‘hidden’ features that are ‘interesting’
- differ in what is considered ‘interesting’
  - are localised in time and/or space (Clustering)
  - explain observed data variance (PCA, FDA, FA)
  - are maximally independent (ICA)
- typically are multivariate and linear

EDA techniques for FMRI

- are mostly multivariate
- often provide a multivariate linear decomposition:

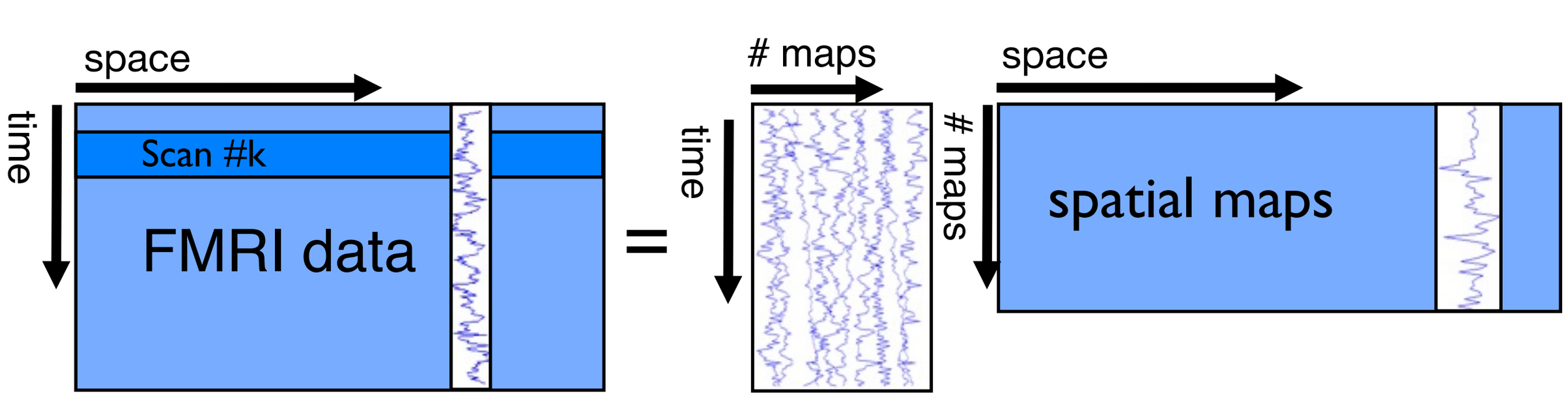

Data is represented as a 2D matrix and decomposed into factor matrices (or modes)

Spatial ICA for FMRI

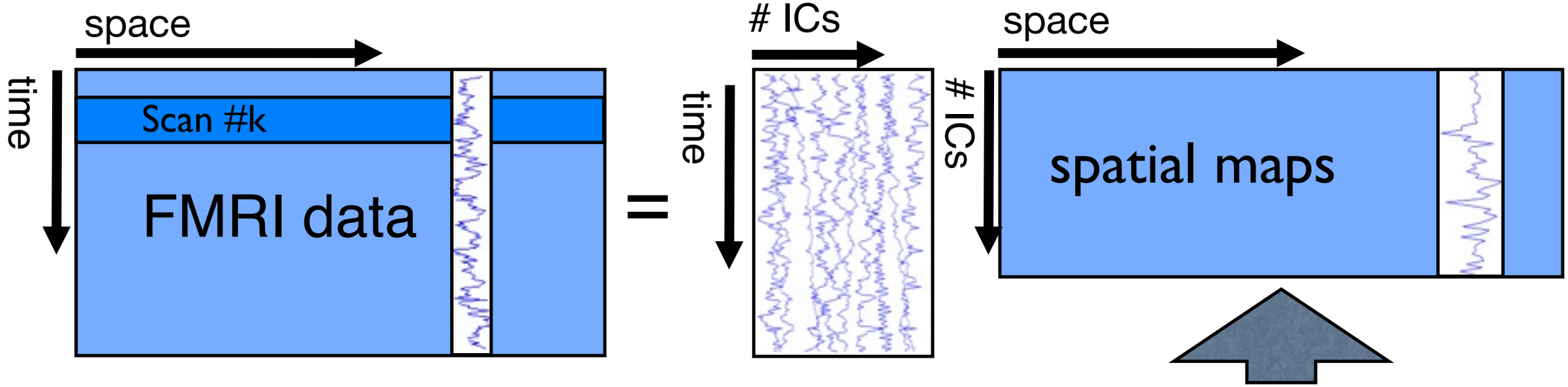

- data is decomposed into a set of spatially independent maps and a set of time-courses

McKeown et al. HBM 1998

PCA vs. ICA ?

Simulated Data

(2 components, slightly different timecourses)

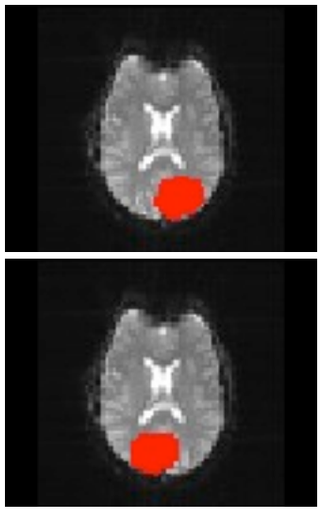

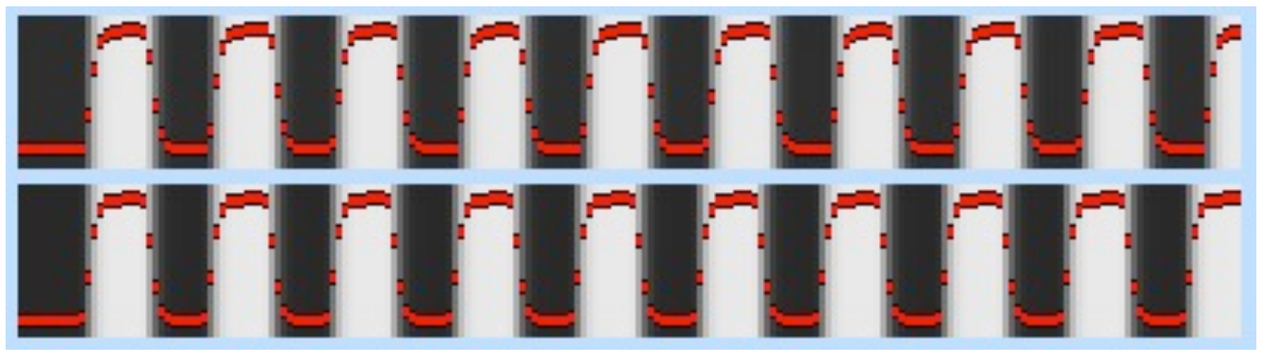

PCA vs. ICA ?

Simulated Data

(2 components, slightly different timecourses)

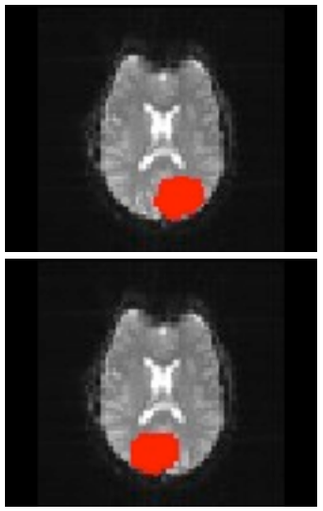

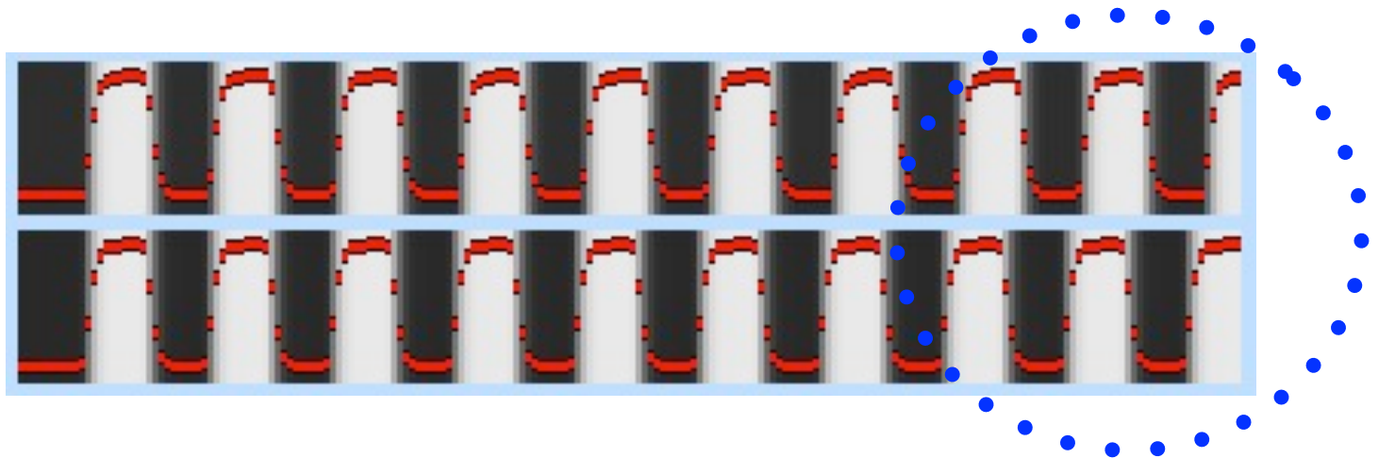

PCA vs. ICA ?

Simulated Data

(2 components, slightly different timecourses)

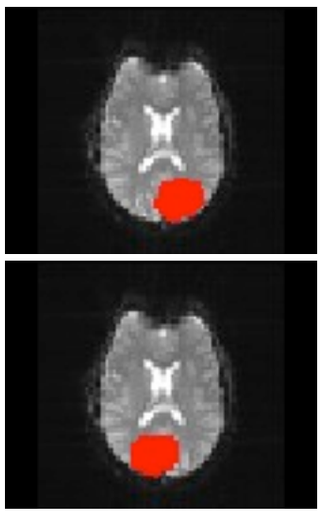

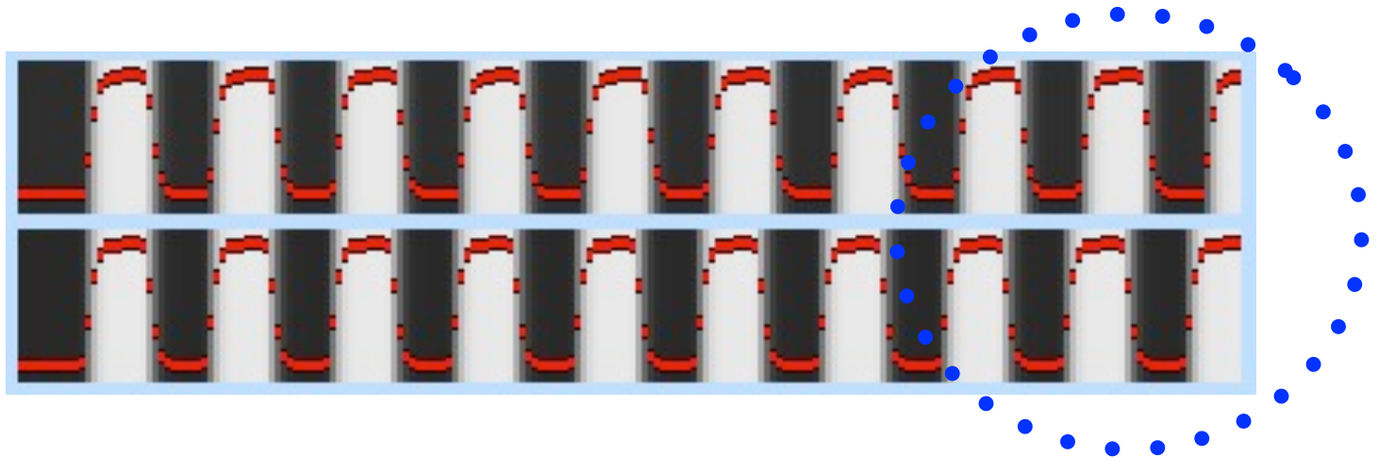

PCA

- Timecourses orthogonal
- Spatial maps and timecourses "wrong"

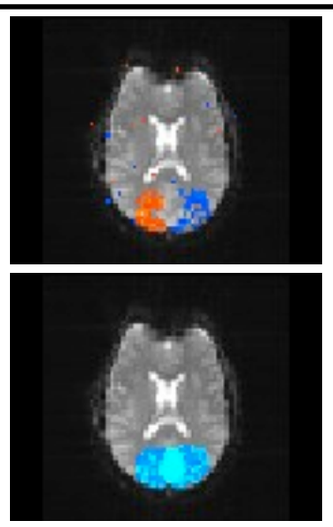

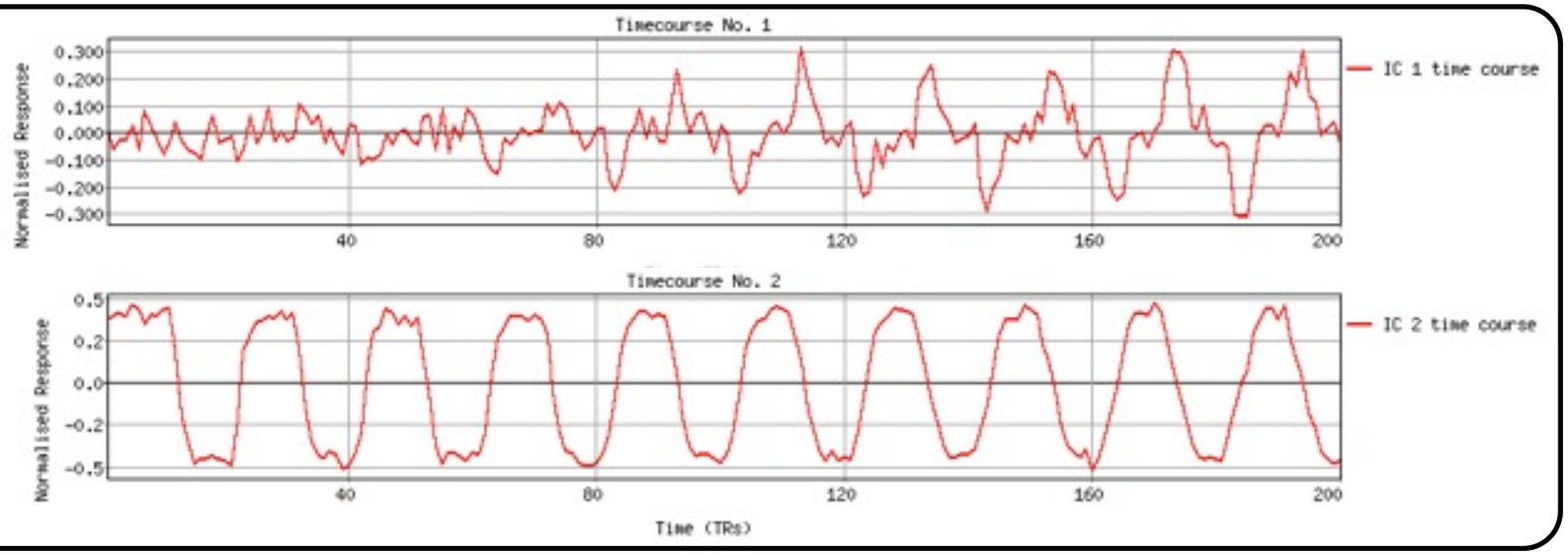

PCA vs. ICA ?

Simulated Data

(2 components, slightly different timecourses)

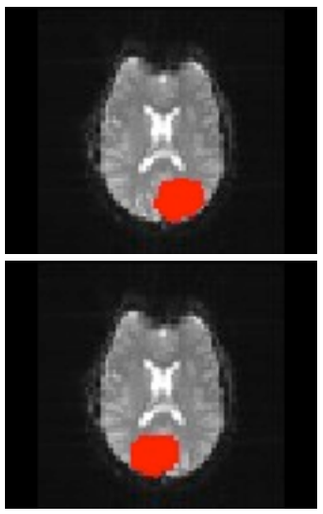

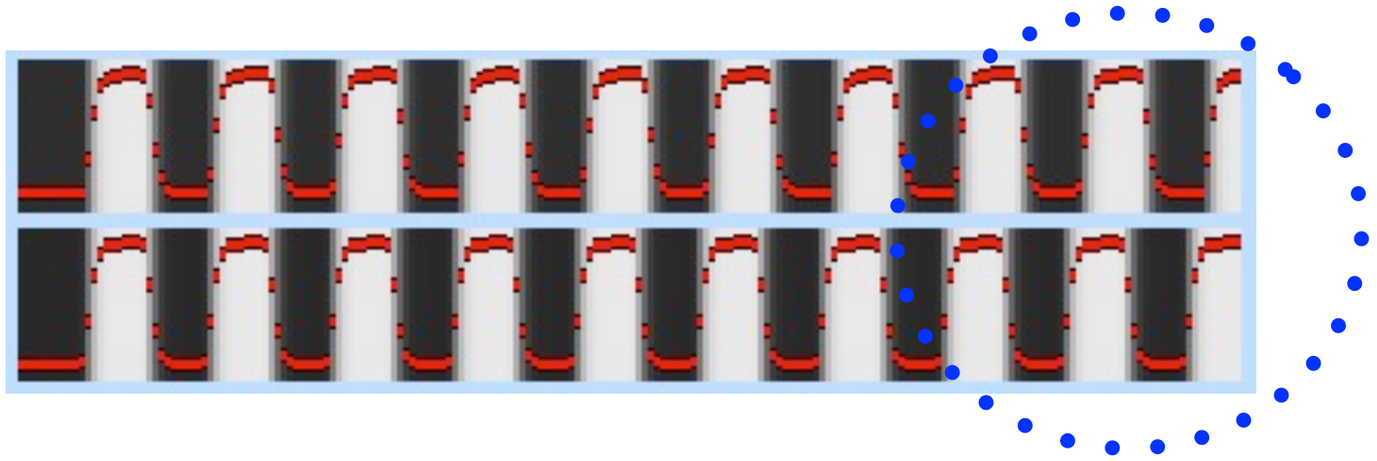

PCA

- Timecourses orthogonal
- Spatial maps and timecourses "wrong"

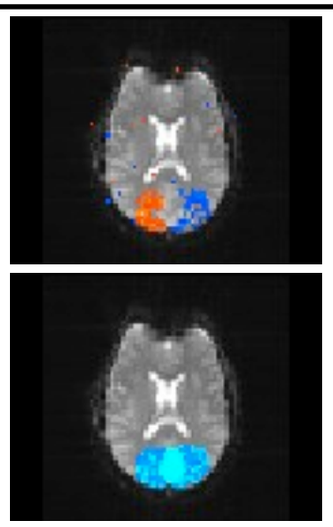

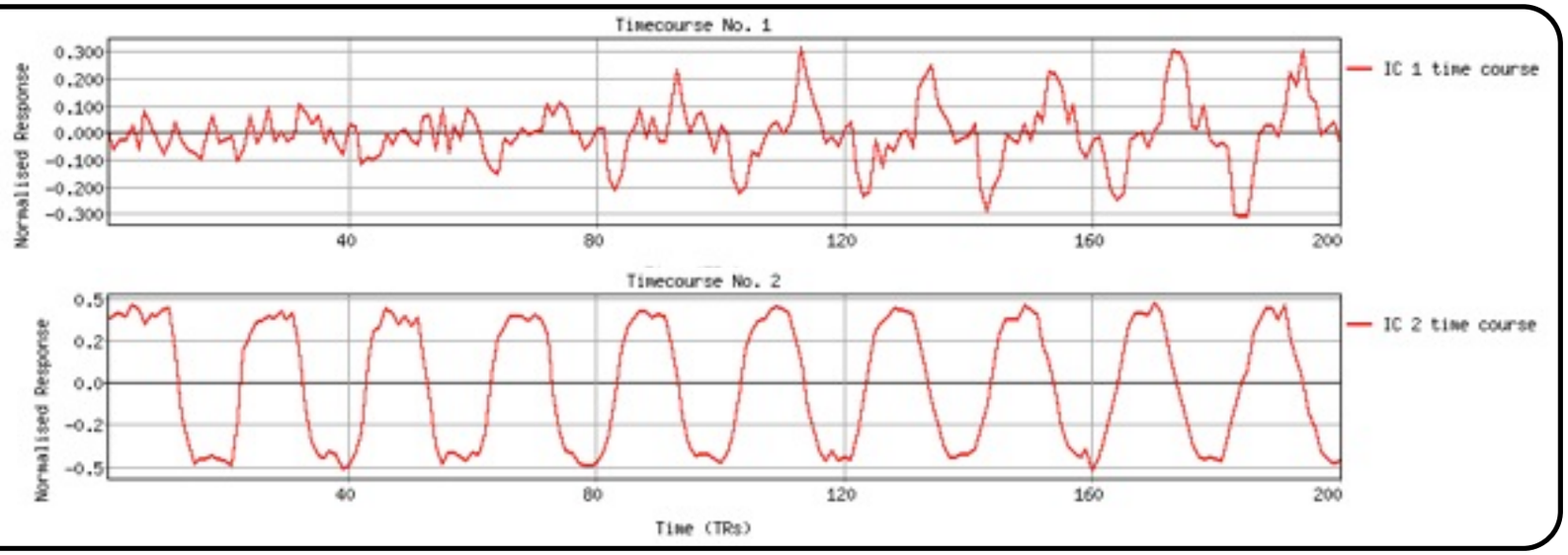

ICA

- Timecourses non-co-linear
- Spatial maps and timecourses "right"

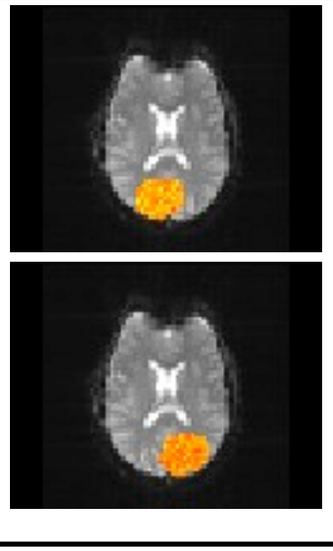

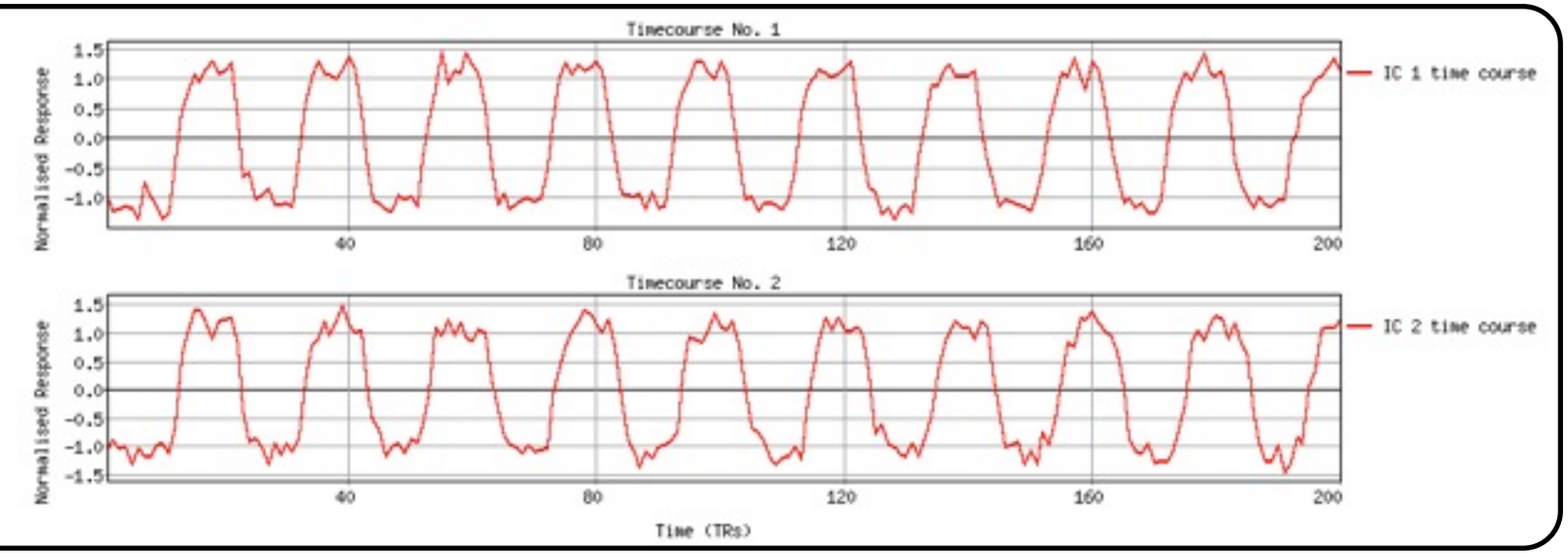

PCA vs. ICA

- PCA finds projections of maximum amount of variance in Gaussian data (uses 2nd order statistics only)
- Independent Component Analysis (ICA) finds projections of maximal independence in non-Gaussian data (using higher-order statistics)

PCA vs. ICA

- PCA finds projections of maximum amount of variance in Gaussian data (uses 2nd order statistics only)
- Independent Component Analysis (ICA) finds projections of maximal independence in non-Gaussian data (using higher-order statistics)

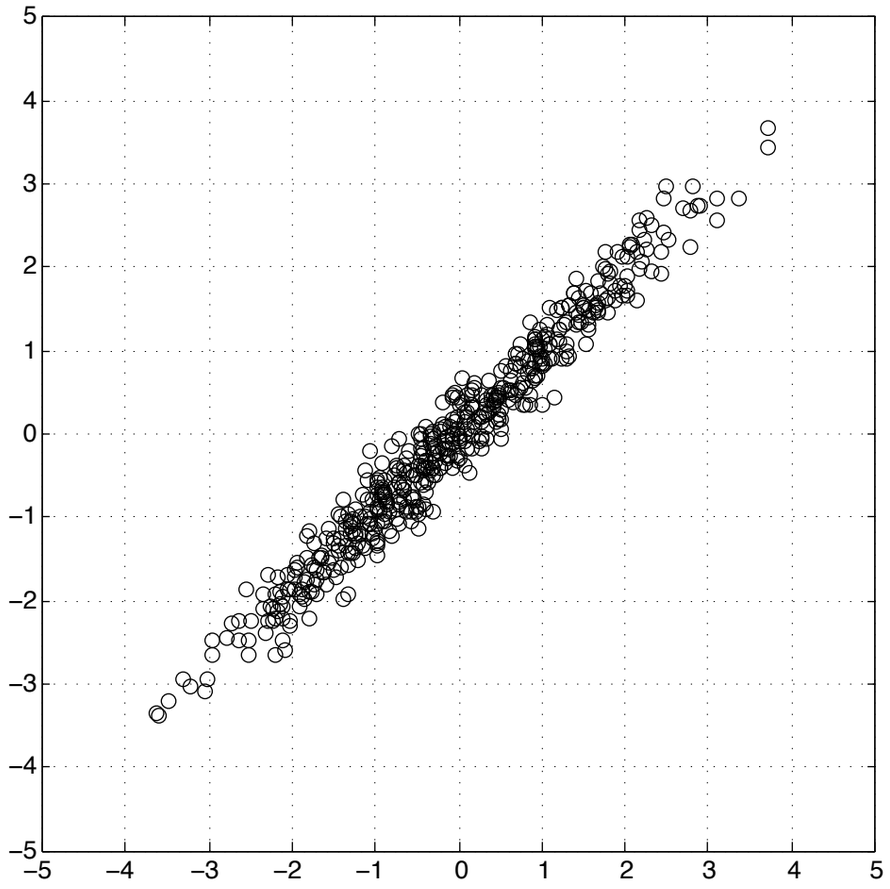

Gaussian data

PCA vs. ICA

- PCA finds projections of maximum amount of variance in Gaussian data (uses 2nd order statistics only)
- Independent Component Analysis (ICA) finds projections of maximal independence in non-Gaussian data (using higher-order statistics)

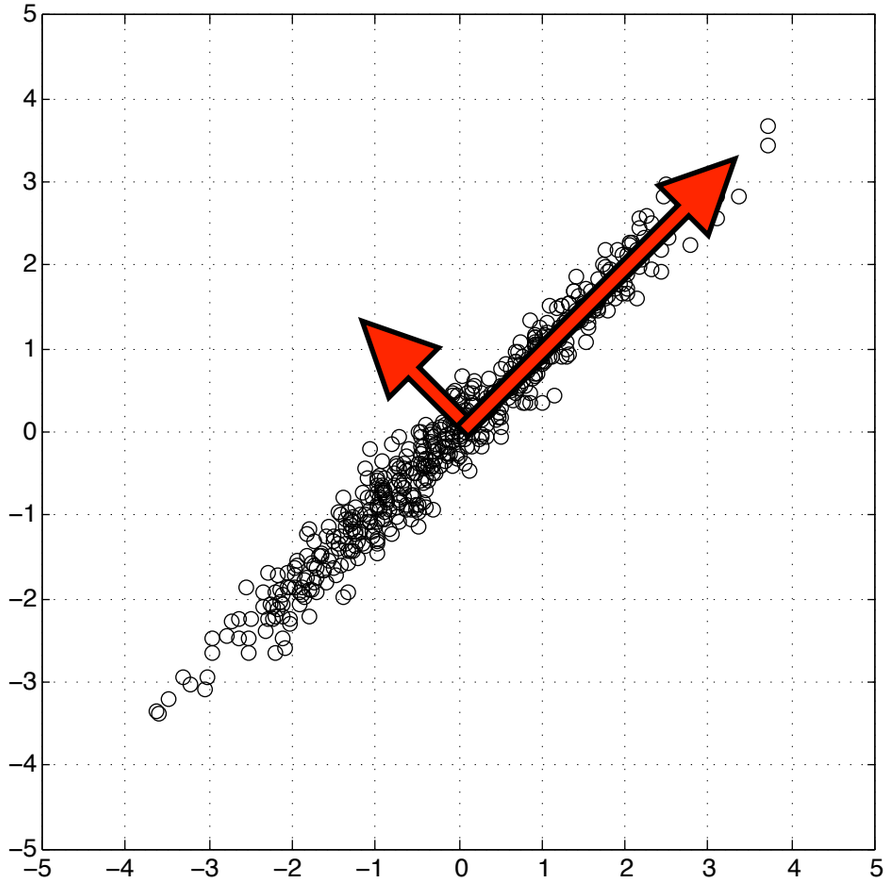

Gaussian data

PCA vs. ICA

- PCA finds projections of maximum amount of variance in Gaussian data (uses 2nd order statistics only)
- Independent Component Analysis (ICA) finds projections of maximal independence in non-Gaussian data (using higher-order statistics)

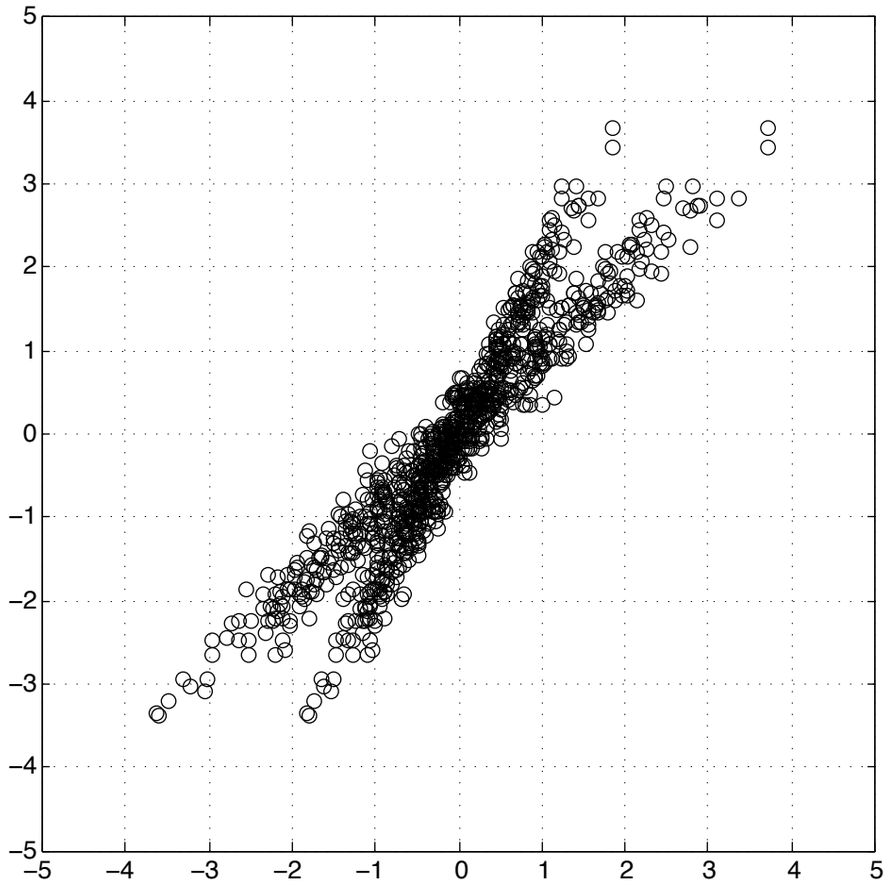

non-Gaussian data

PCA vs. ICA

- PCA finds projections of maximum amount of variance in Gaussian data (uses 2nd order statistics only)
- Independent Component Analysis (ICA) finds projections of maximal independence in non-Gaussian data (using higher-order statistics)

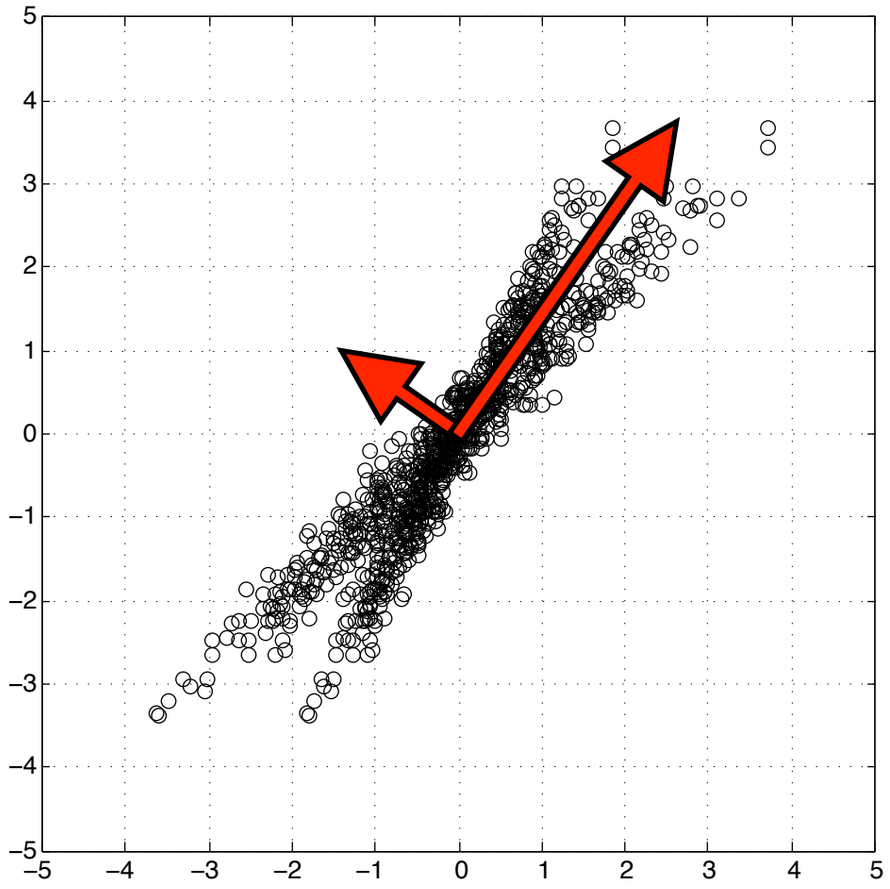

non-Gaussian data

PCA vs. ICA

- PCA finds projections of maximum amount of variance in Gaussian data (uses 2nd order statistics only)
- Independent Component Analysis (ICA) finds projections of maximal independence in non-Gaussian data (using higher-order statistics)

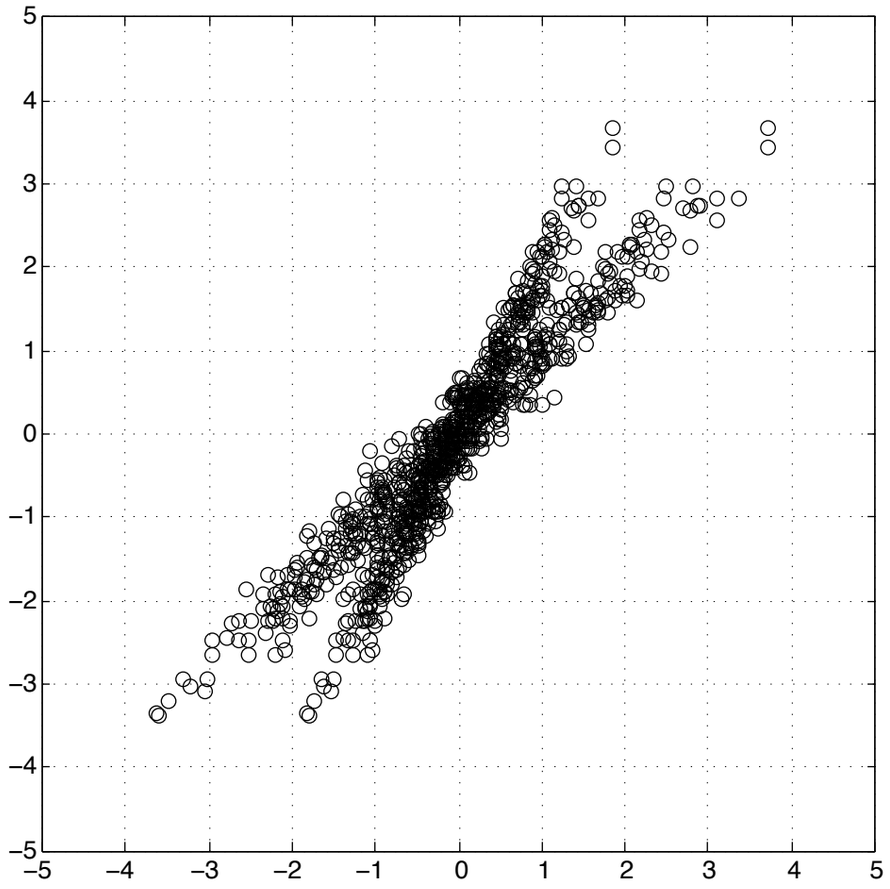

non-Gaussian data

PCA vs. ICA

- PCA finds projections of maximum amount of variance in Gaussian data (uses 2nd order statistics only)
- Independent Component Analysis (ICA) finds projections of maximal independence in non-Gaussian data (using higher-order statistics)

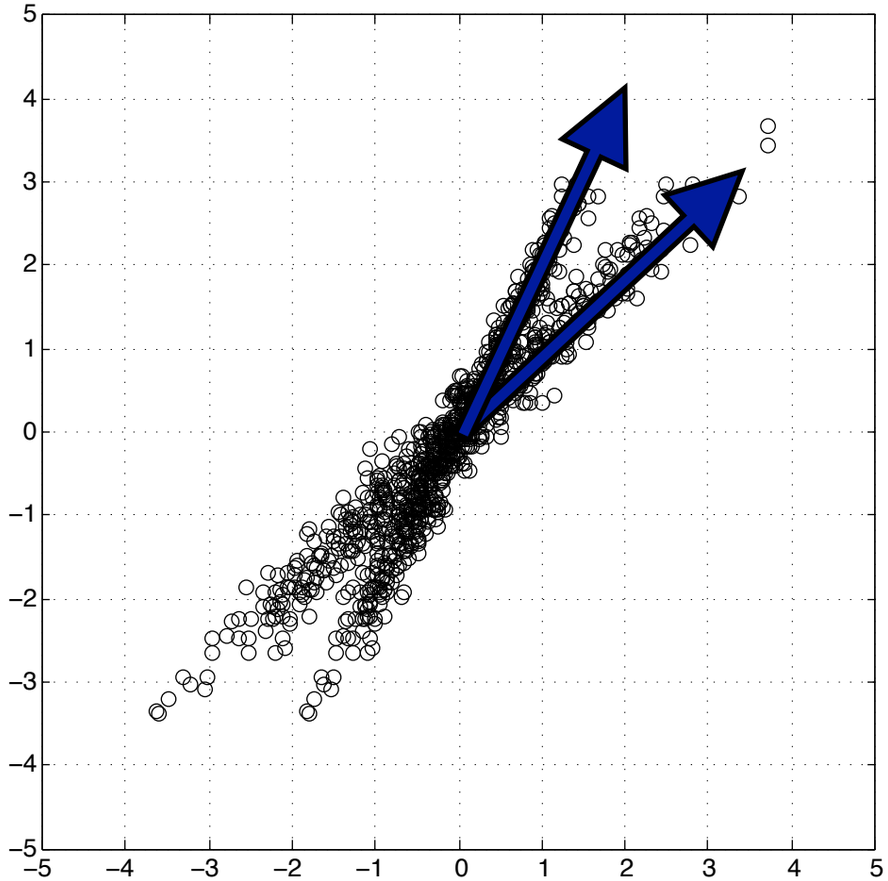

non-Gaussian data

Correlation vs. independece

- de-correlated signals can still be dependent

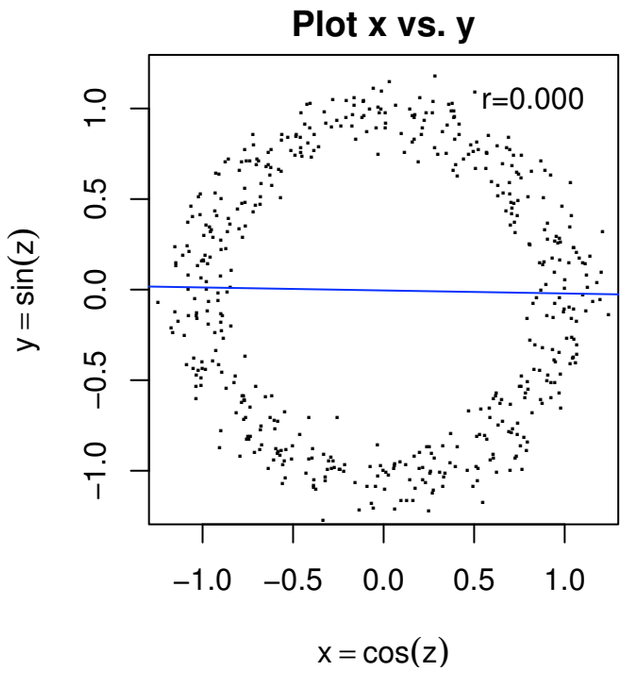

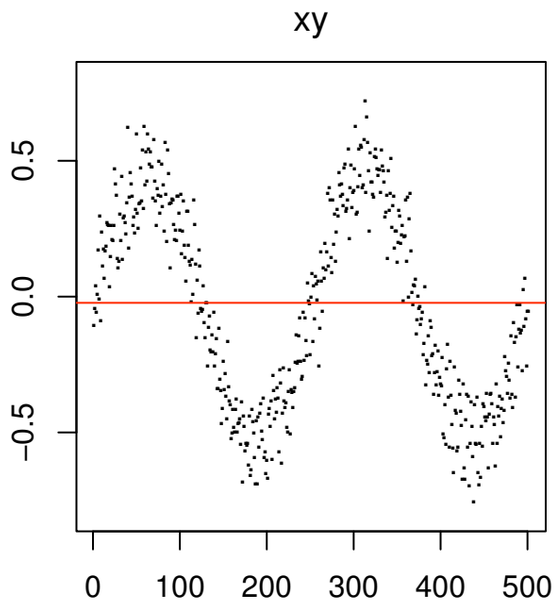

Correlation vs. independece

- de-correlated signals can still be dependent

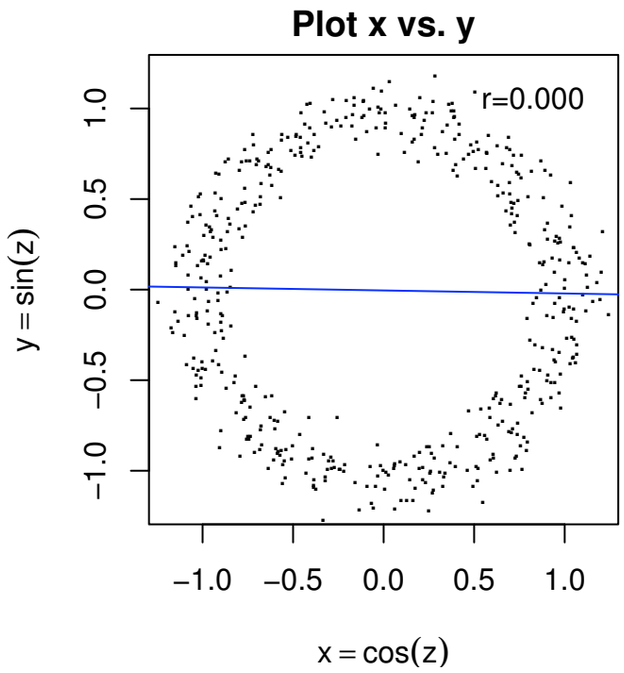

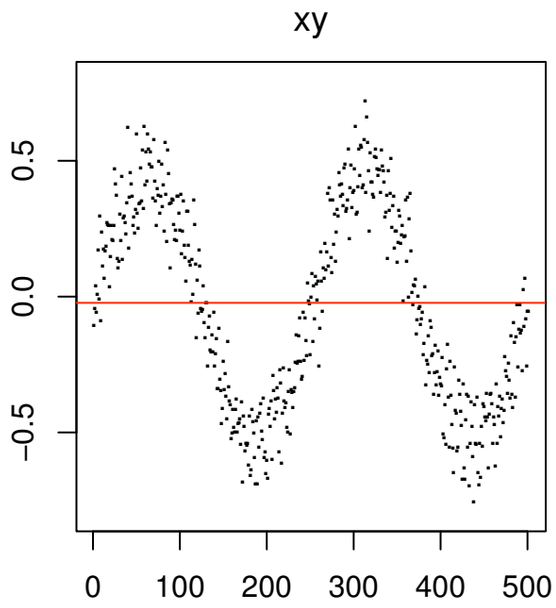

Correlation vs. independece

- de-correlated signals can still be dependent

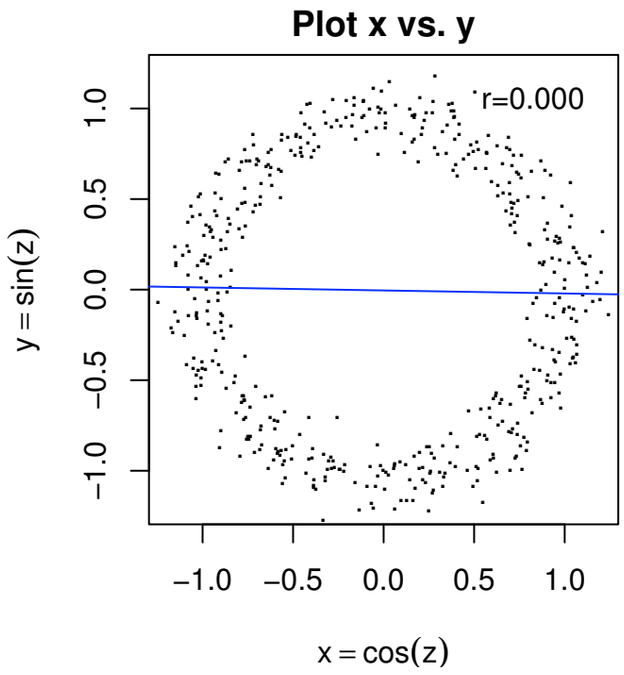

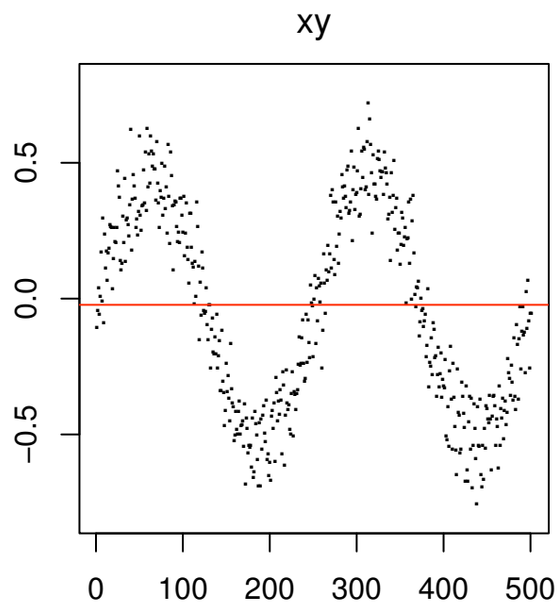

- higher-order statistics (beyond mean and variance) can reveal these dependencies

Stone et al. 2002

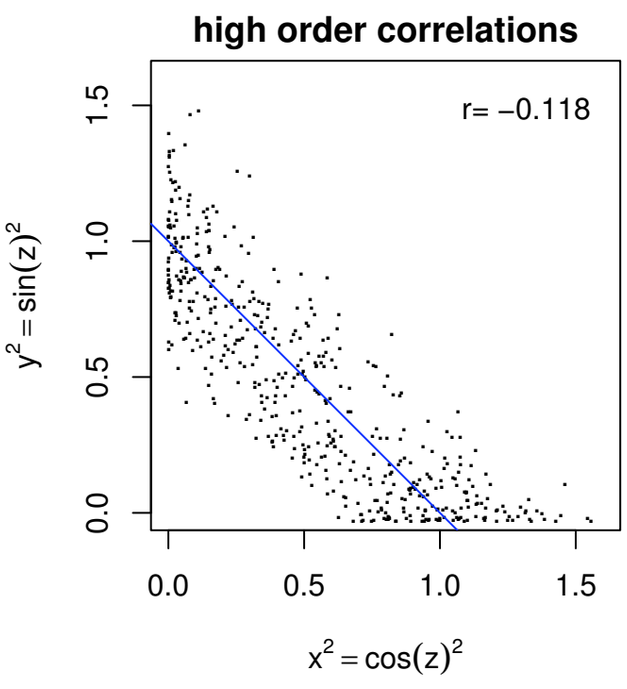

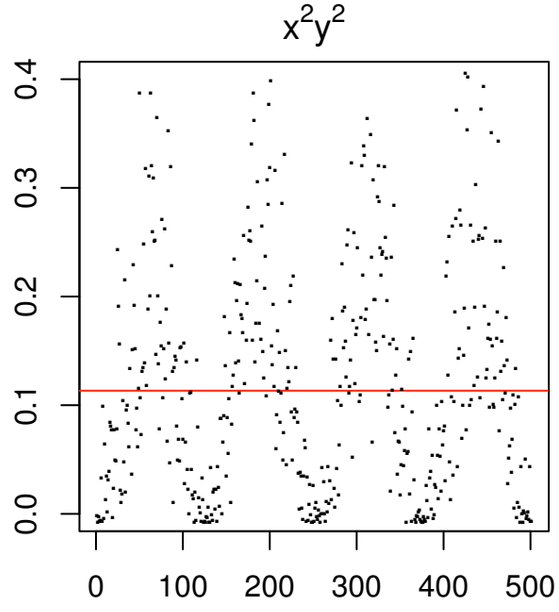

The ‘overfitting’ problem

- fitting a noise-free model to noisy observations:
  - no control over signal vs. noise (non-interpretable results)
  - statistical significance testing not possible

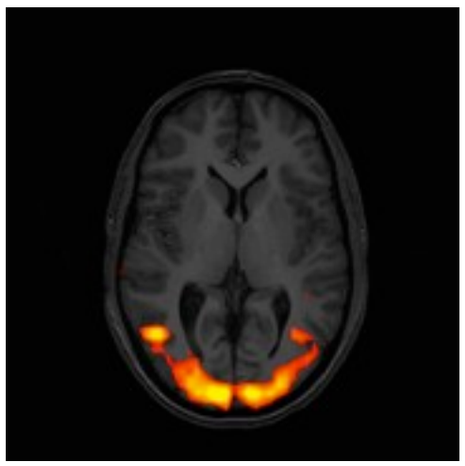

GLM analysis

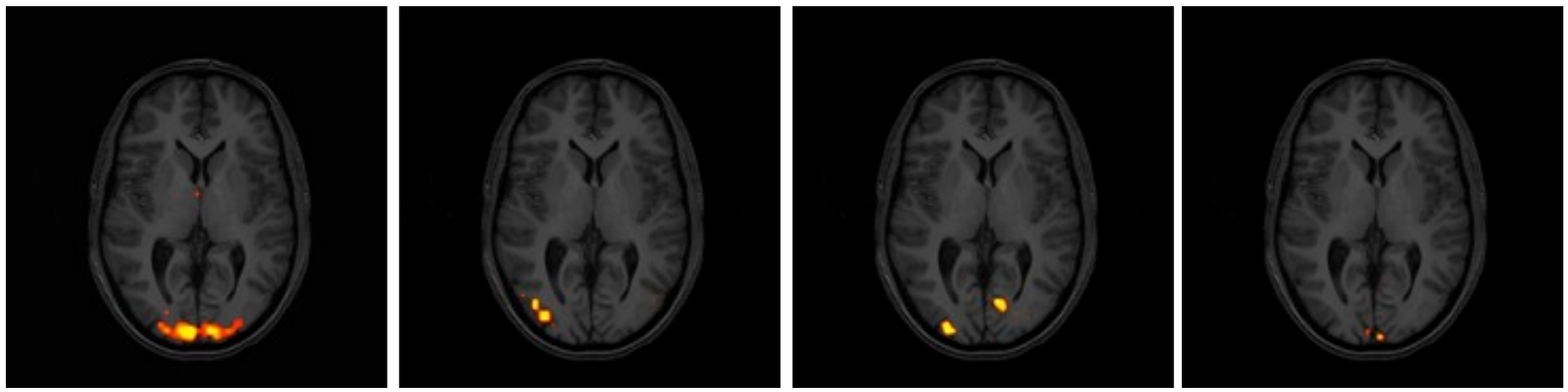

standard ICA (unconstrained)

Probabilistic ICA model

- statistical "latent variables" model: we observe linear mixtures of hidden sources in the presence of Gaussian noise

$$Y = XB + E$$

Probabilistic ICA model

- statistical "latent variables" model: we observe linear mixtures of hidden sources in the presence of Gaussian noise

$$Y = XB + E$$

- Issues:
  - Model Order Selection: how many components?
  - Component estimation: how to find ICs?
  - Inference: how to threshold ICs?

Model Order Selection

- The sample covariance matrix has a Wishart distribution and we can calculate the empirical distribution function for the eigenvalues

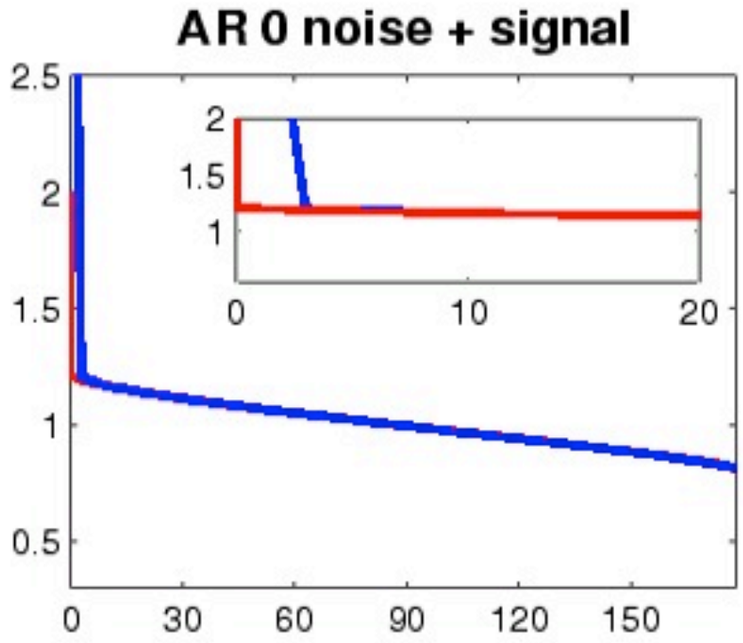

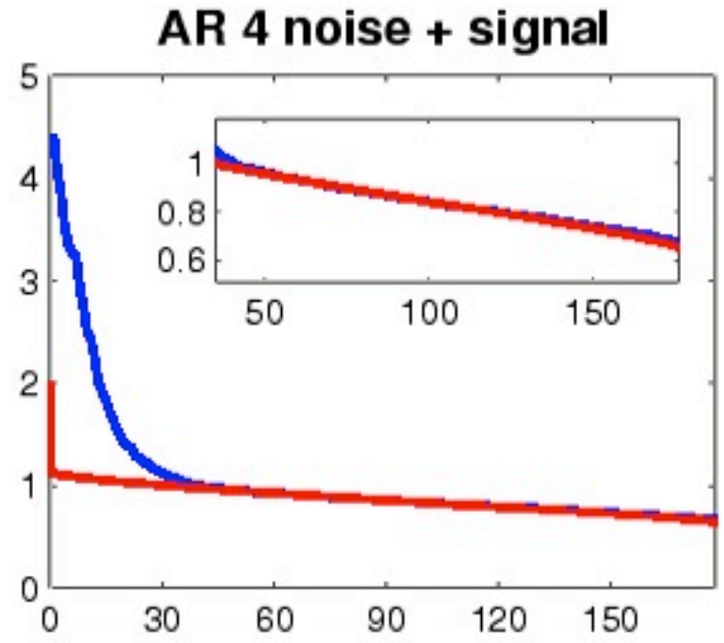

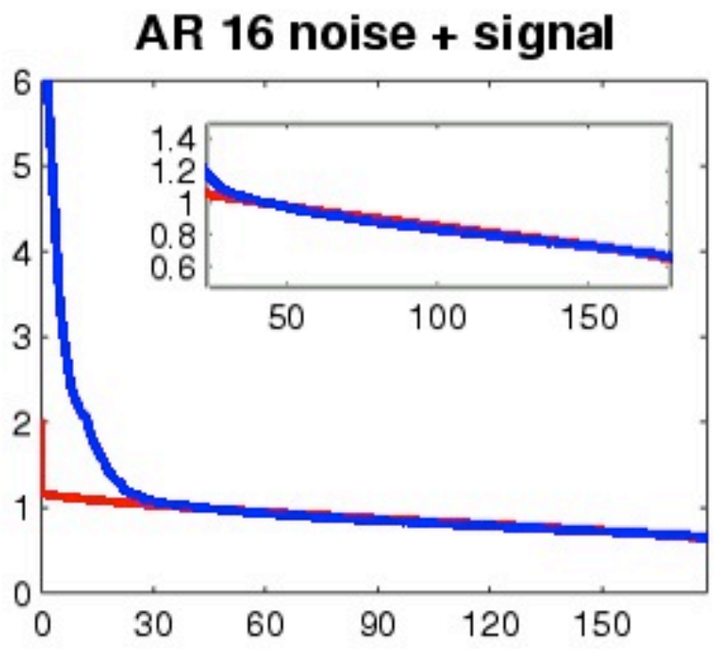

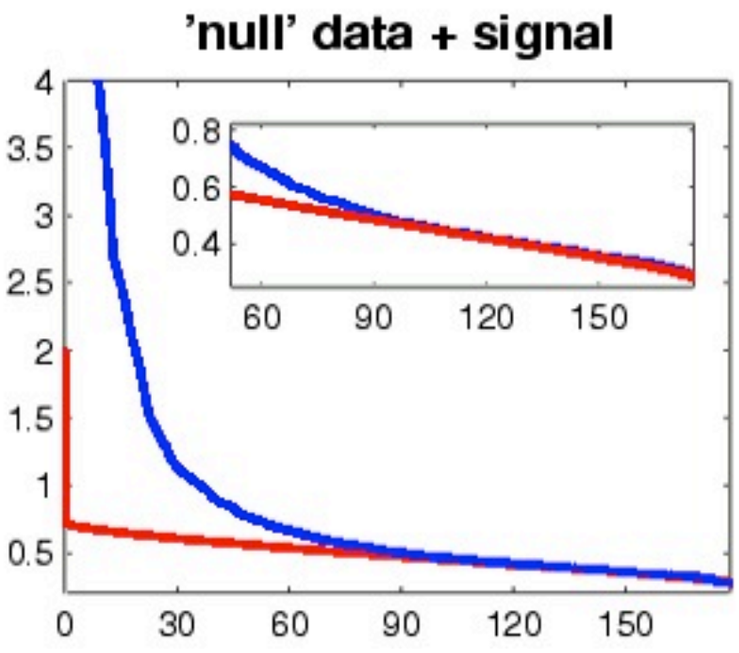

Empirical distribution function

observed Eigenspectrum

Everson & Roberts, IEEE Trans. Sig. Proc. 48(7), 2000

Model Order Selection

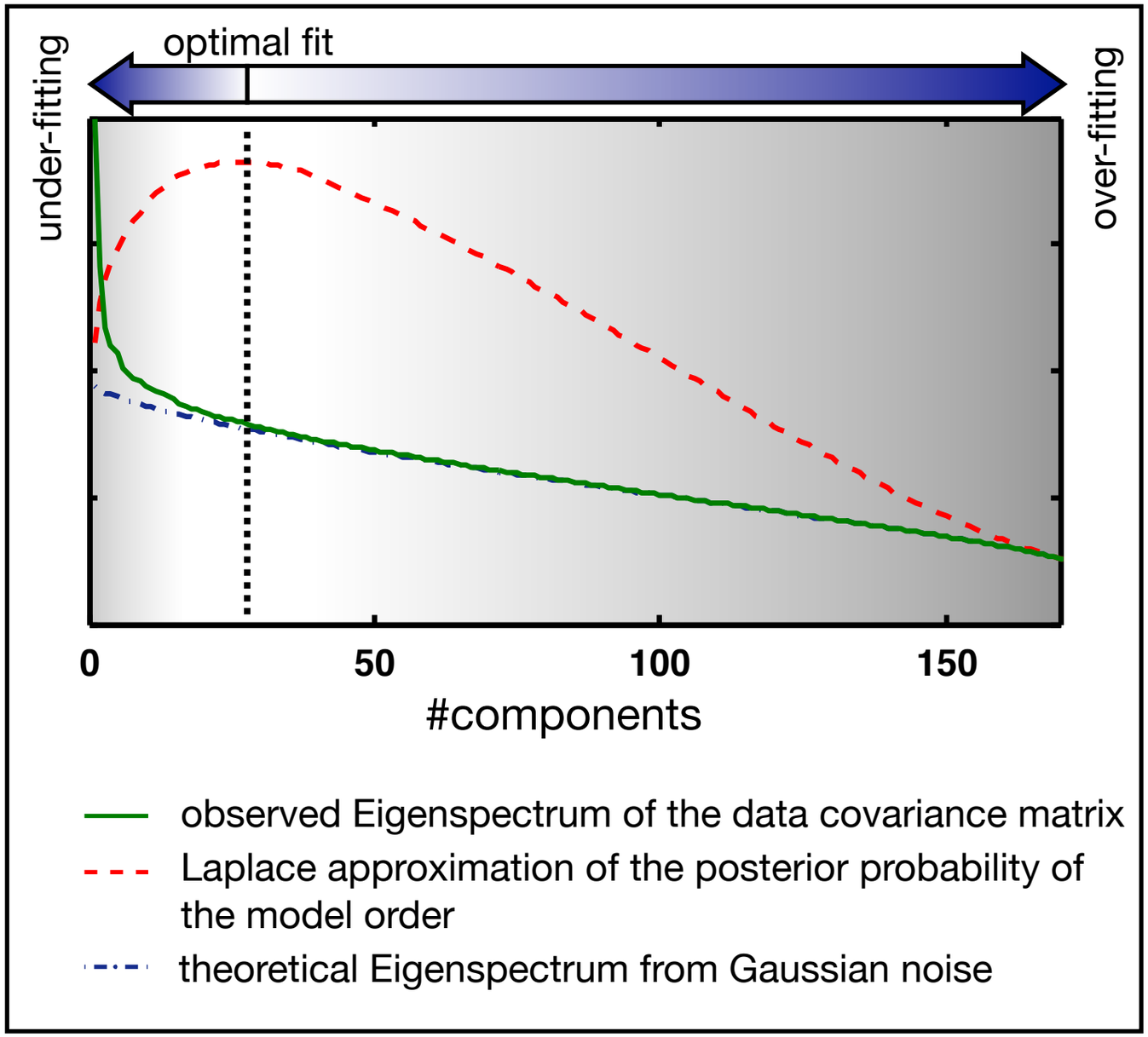

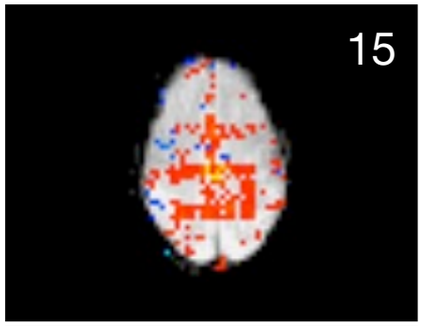

under-fitting: the amount of explained data variance is insufficient to obtain good estimates of the signals

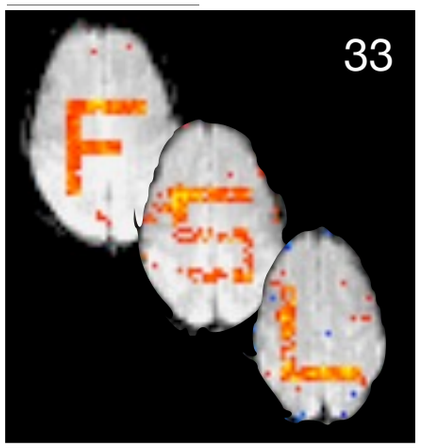

optimal fitting: the amount of explained data variance is sufficient to obtain good estimates of the signals while preventing further splits into spurious components

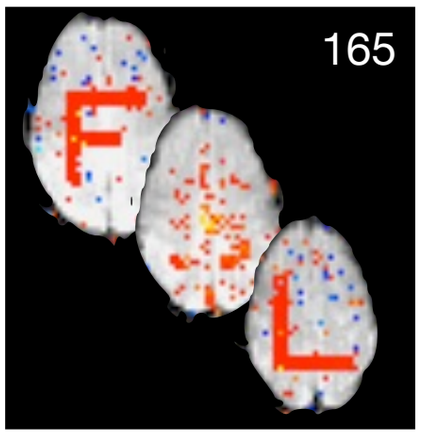

over-fitting: the inclusion of too many components leads to fragmentation of signal across multiple component maps, reducing the ability to identify the signals of interest

Variance Normalisation

- we *might* choose to ignore temporal auto-correlation in the EPI time-series but:
- *generally* need to normalise by the voxel-wise variance

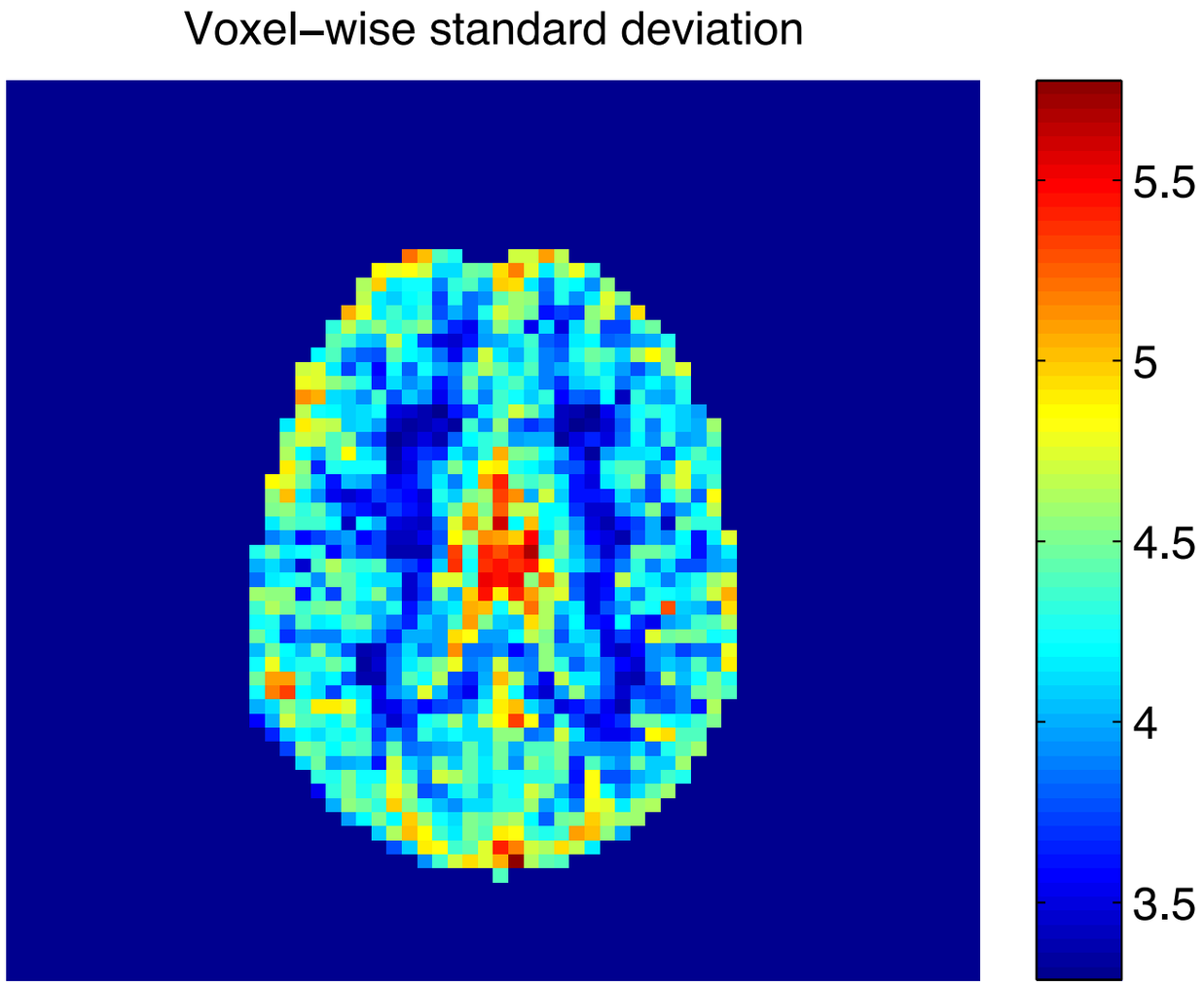

Estimated voxel-wise std. deviation (log-scale) from FMRI data obtained under rest condition.

ICA estimation

- need to find an *unmixing matrix* such that the dependency between estimated sources is minimised
- need (i) a *contrast (objective/cost) function* to drive the unmixing which measures statistical independence and (ii) an *optimisation technique*:
  - kurtosis or cumulants & gradient descent (Jade)
  - maximum entropy & gradient descent (Infomax)
  - neg-entropy & fixed point iteration (FastICA)

Non-Gaussianity

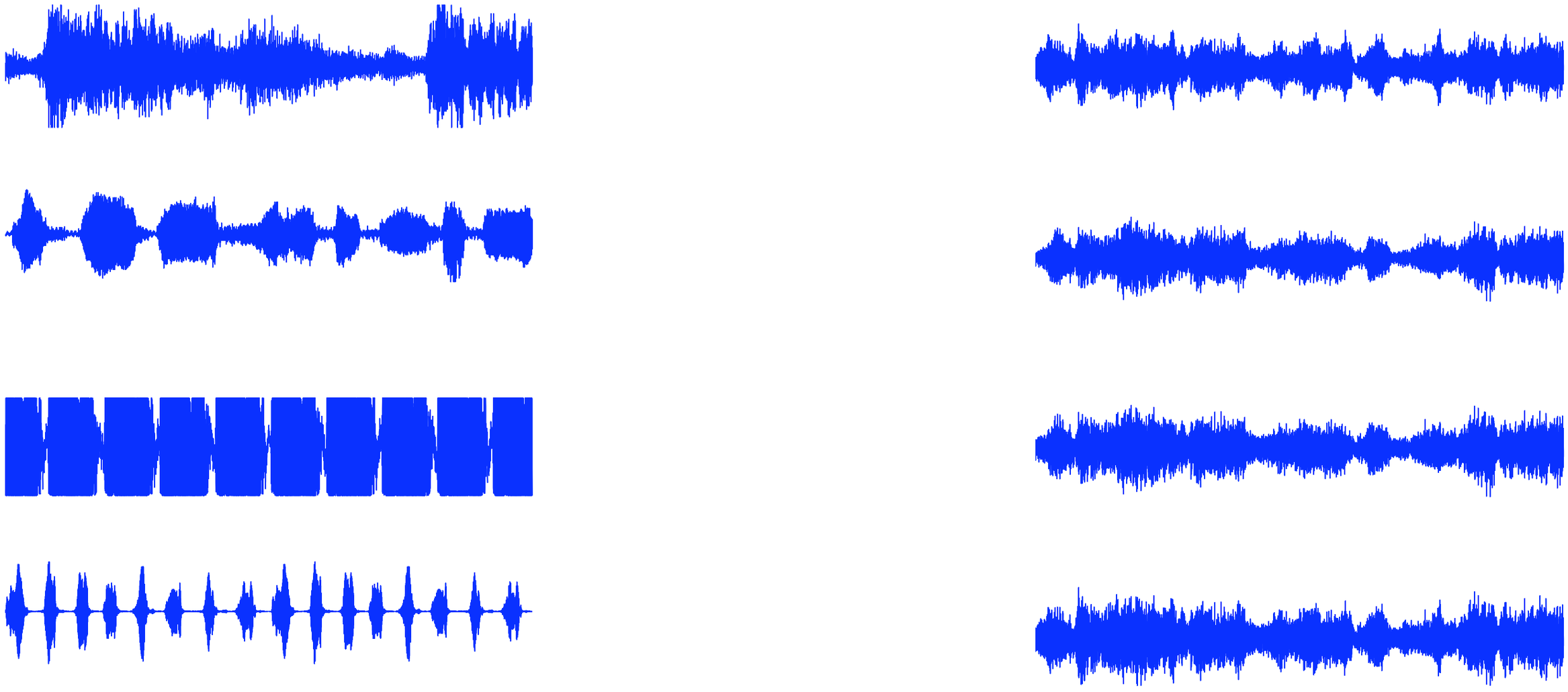

Non-Gaussianity

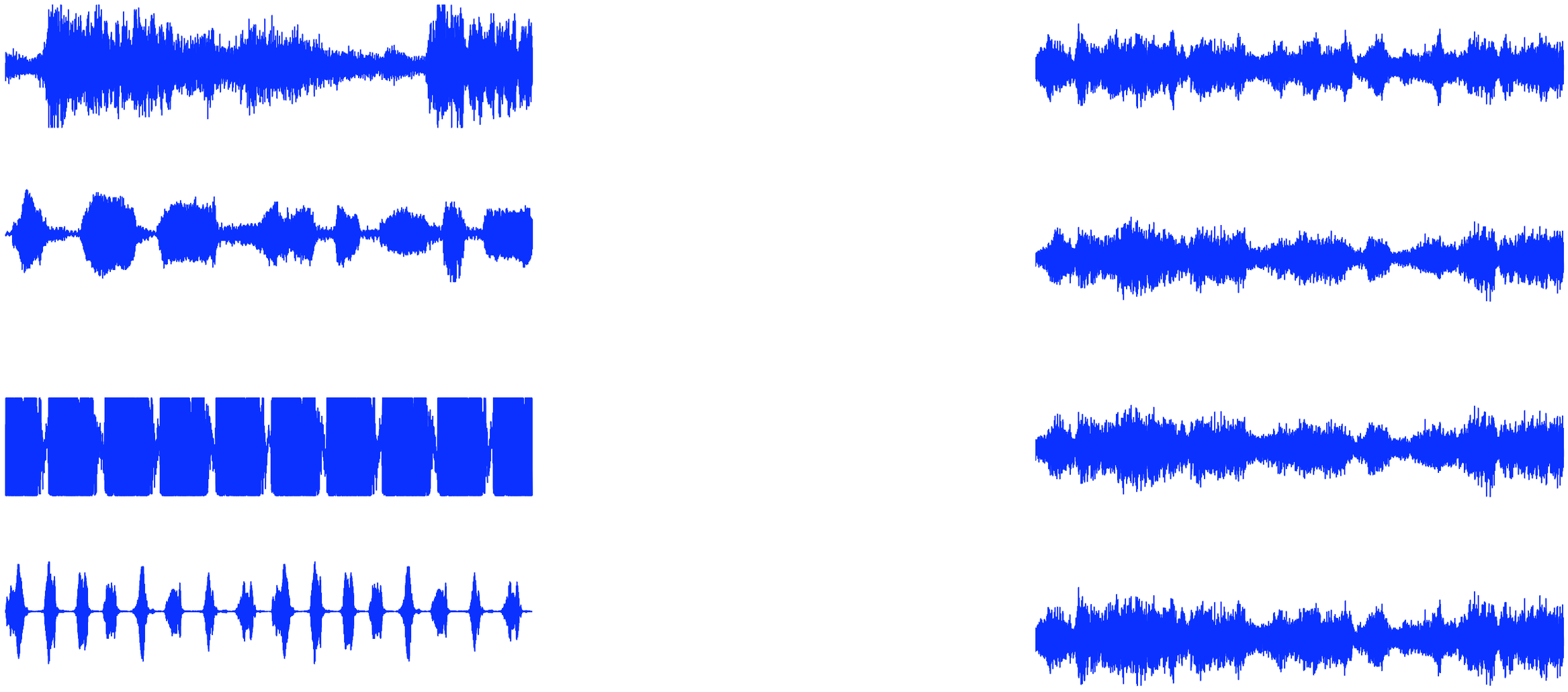

Non-Gaussianity

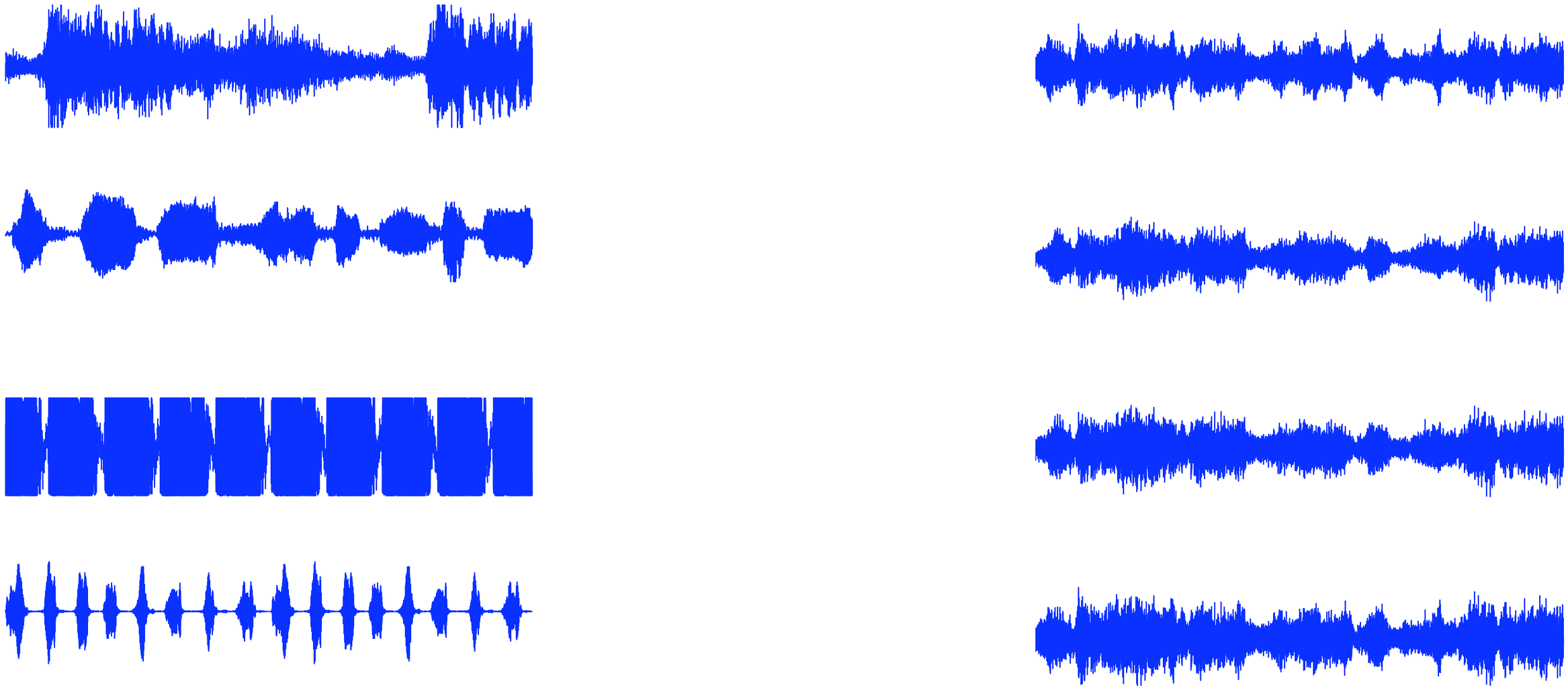

Non-Gaussianity

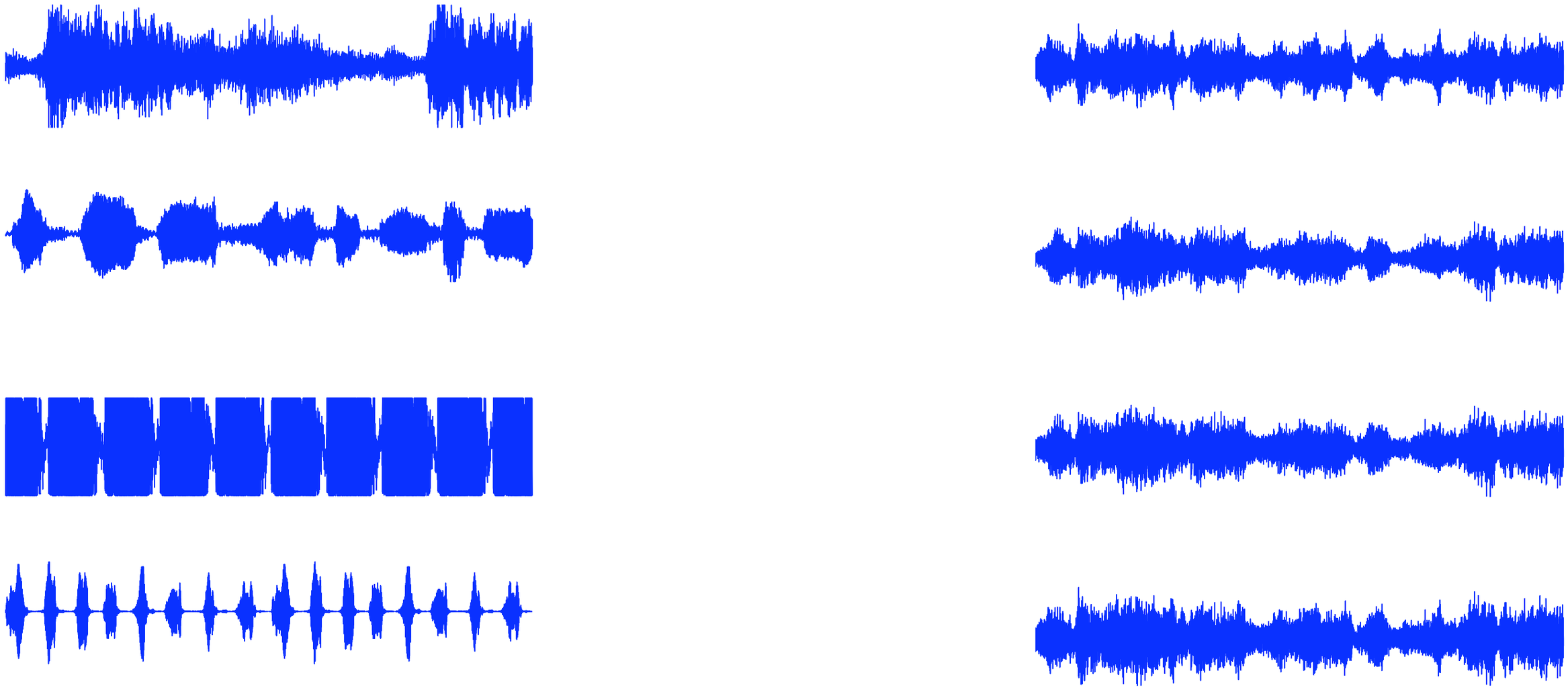

Non-Gaussianity

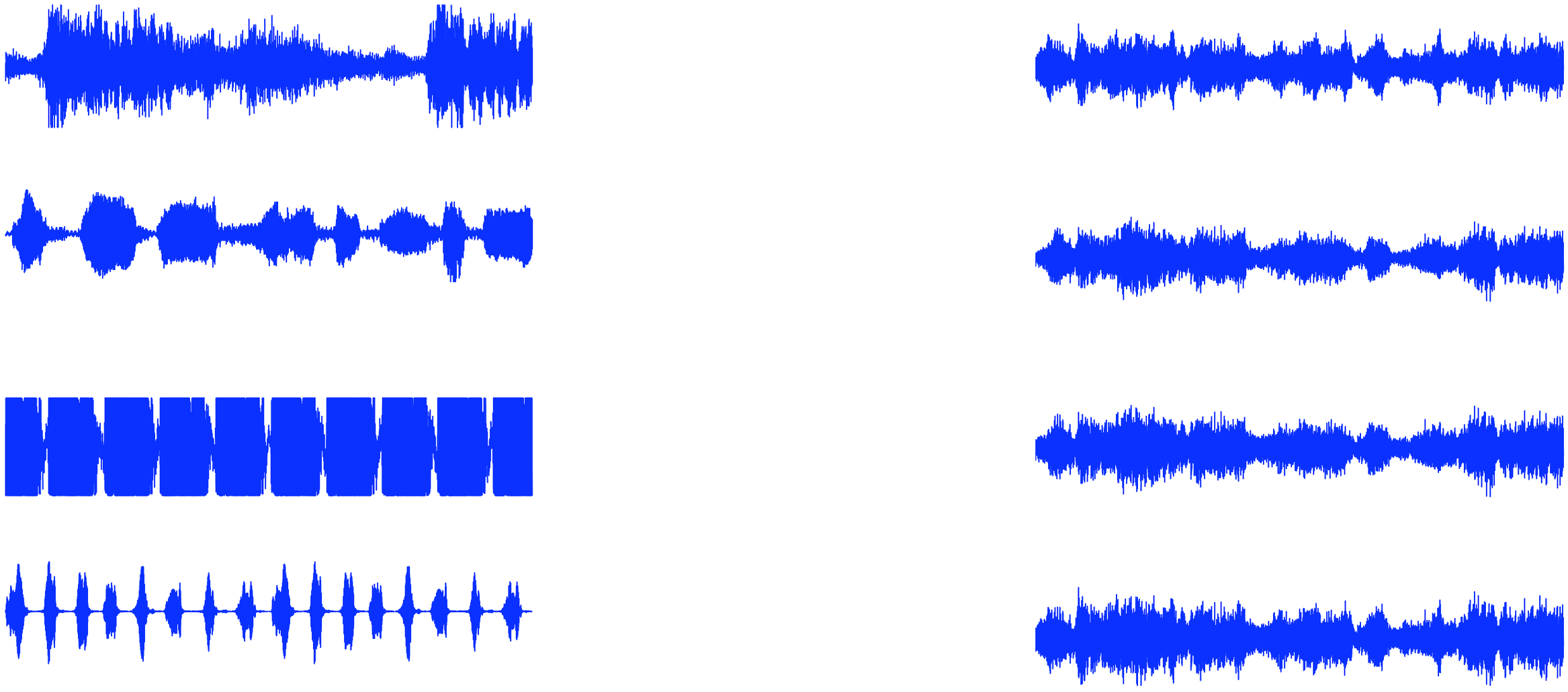

Non-Gaussianity

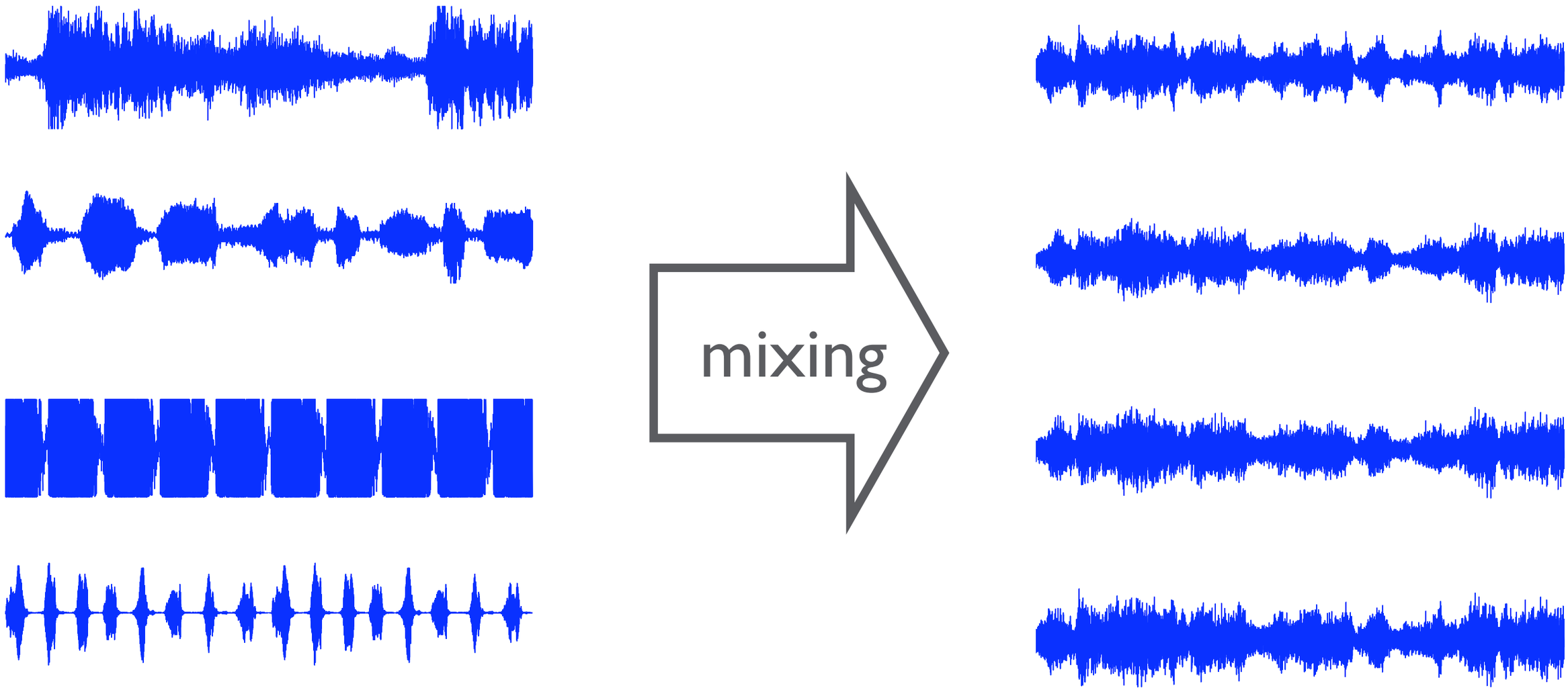

Non-Gaussianity

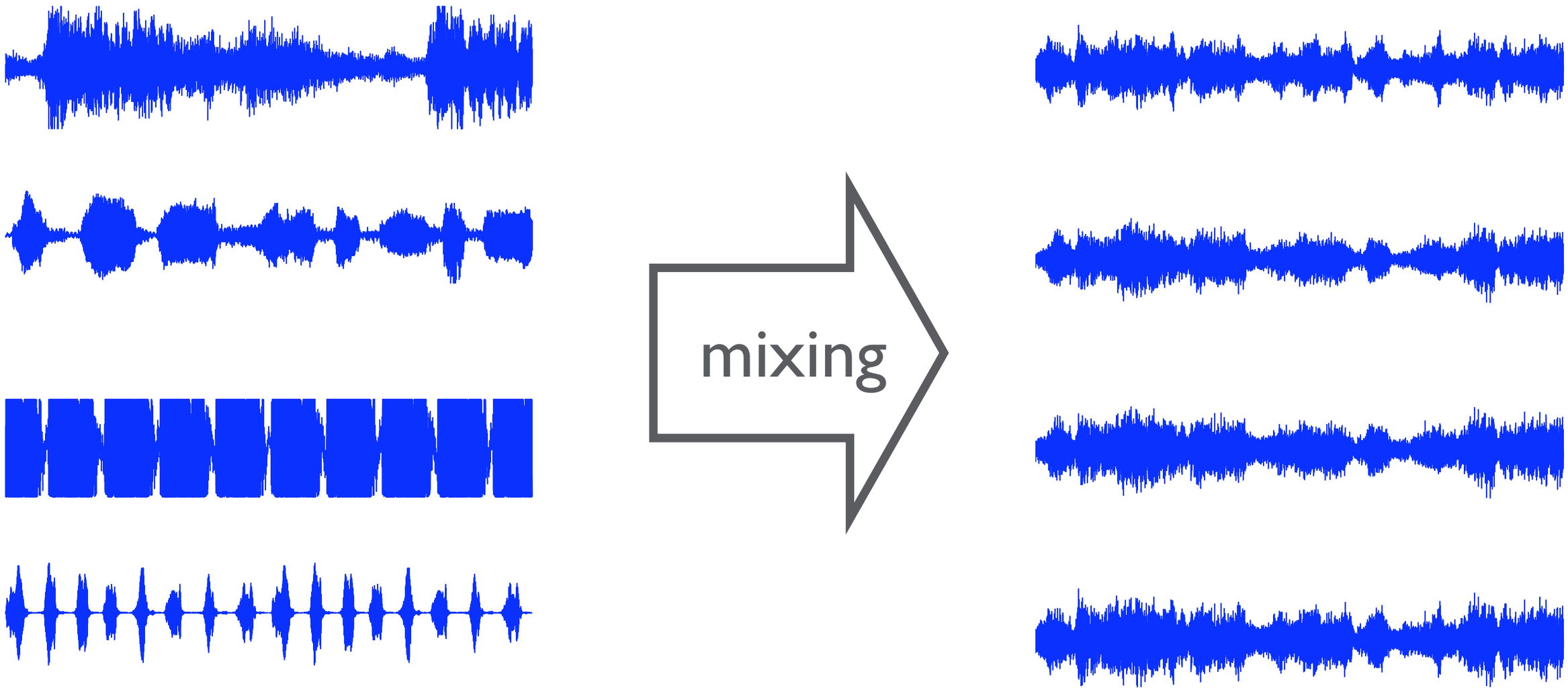

Non-Gaussianity

Non-Gaussianity

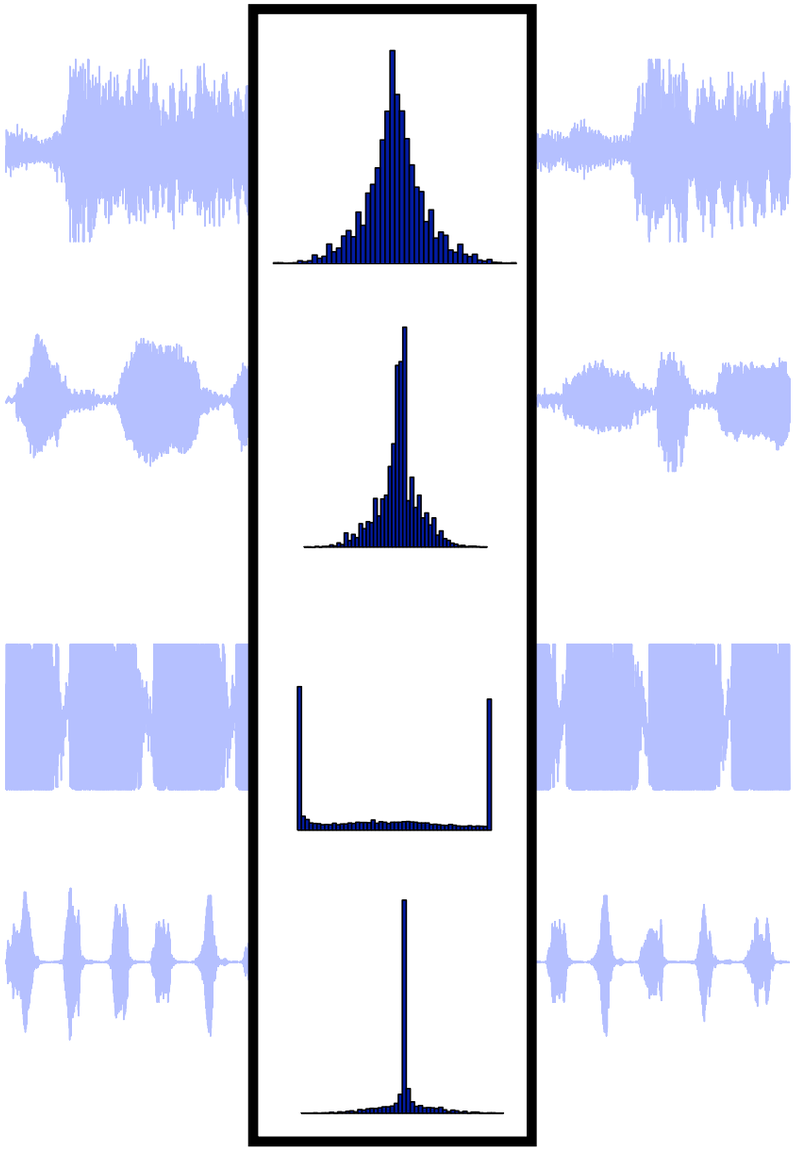

non-Gaussian

Non-Gaussianity

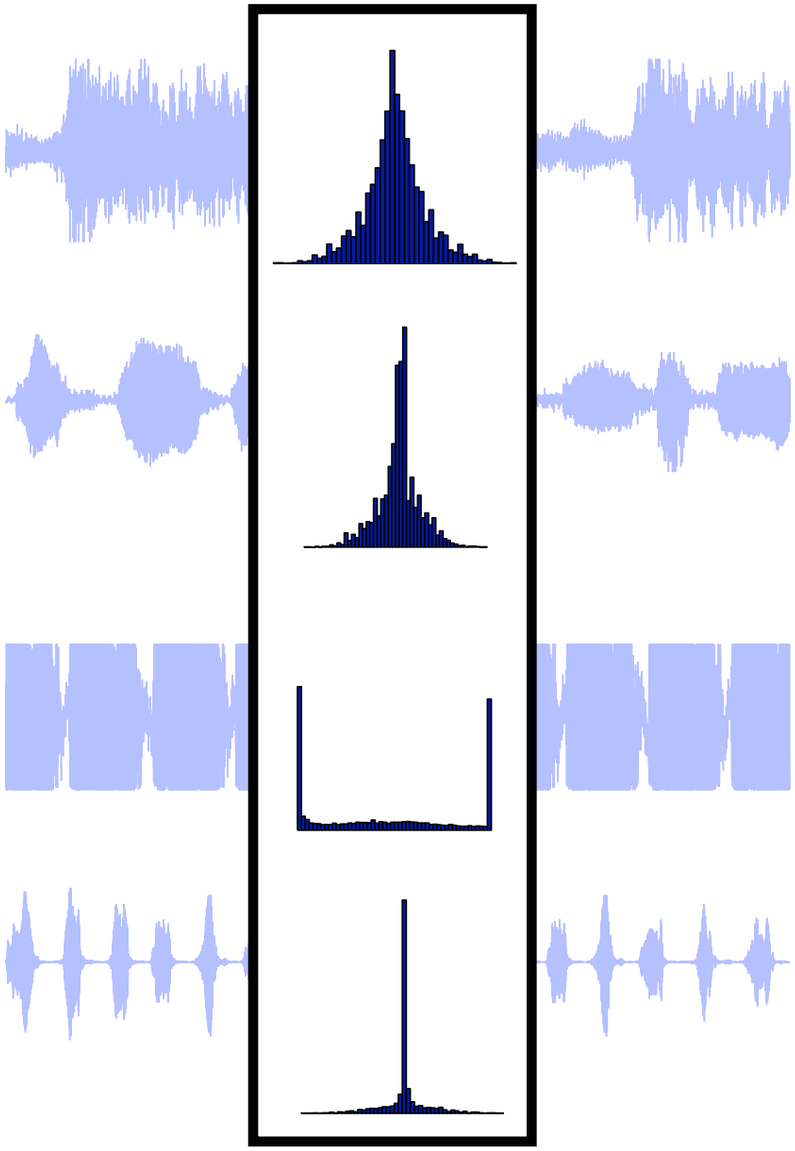

non-Gaussian

mixing

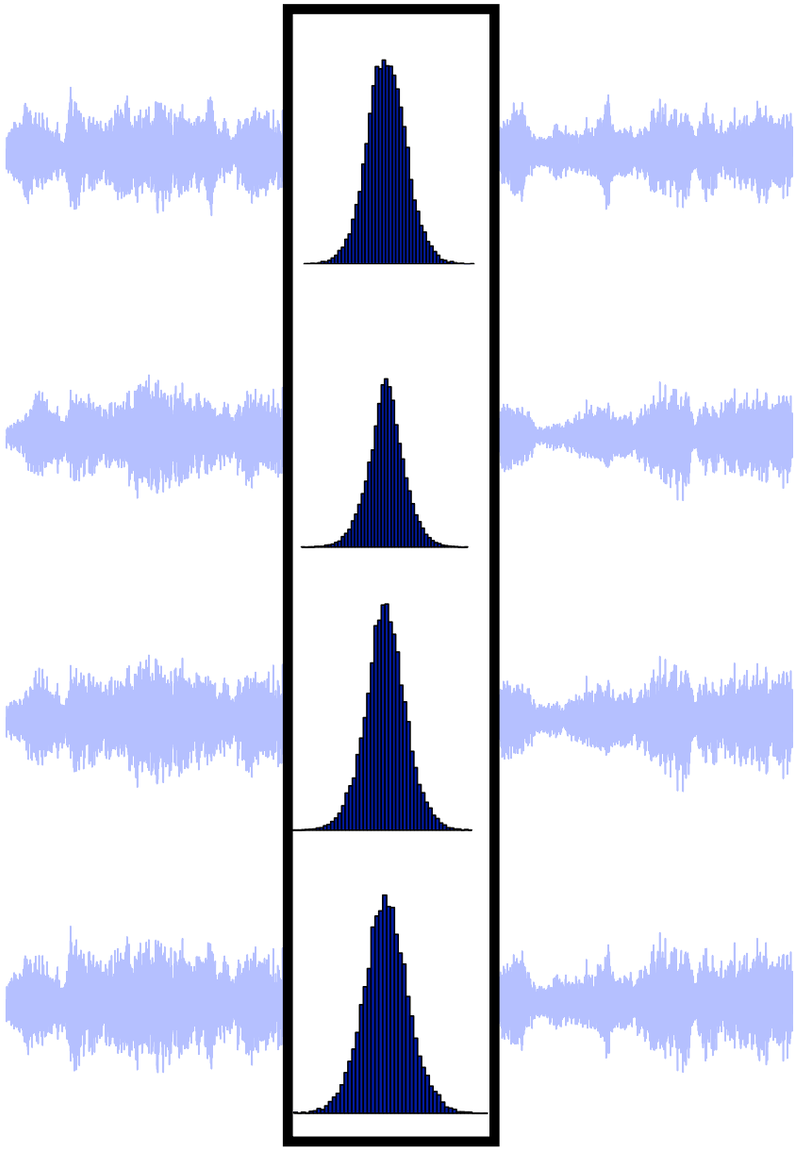

Gaussian

ICA estimation

- *Random* mixing results in more Gaussian-shaped PDFs (Central Limit Theorem)

ICA estimation

- *Random* mixing results in more Gaussian-shaped PDFs (Central Limit Theorem)

- conversely:

if mixing matrix produces *less* Gaussian-shaped PDFs this is unlikely to be a random result

➡ measure non-Gaussianity

ICA estimation

- *Random* mixing results in more Gaussian-shaped PDFs (Central Limit Theorem)

- conversely:

  if mixing matrix produces *less* Gaussian-shaped PDFs this is unlikely to be a random result

  ➡ measure non-Gaussianity

- can use neg-entropy as a measure of non-Gaussianity  Hyvärinen & Oja 1997

Thresholding

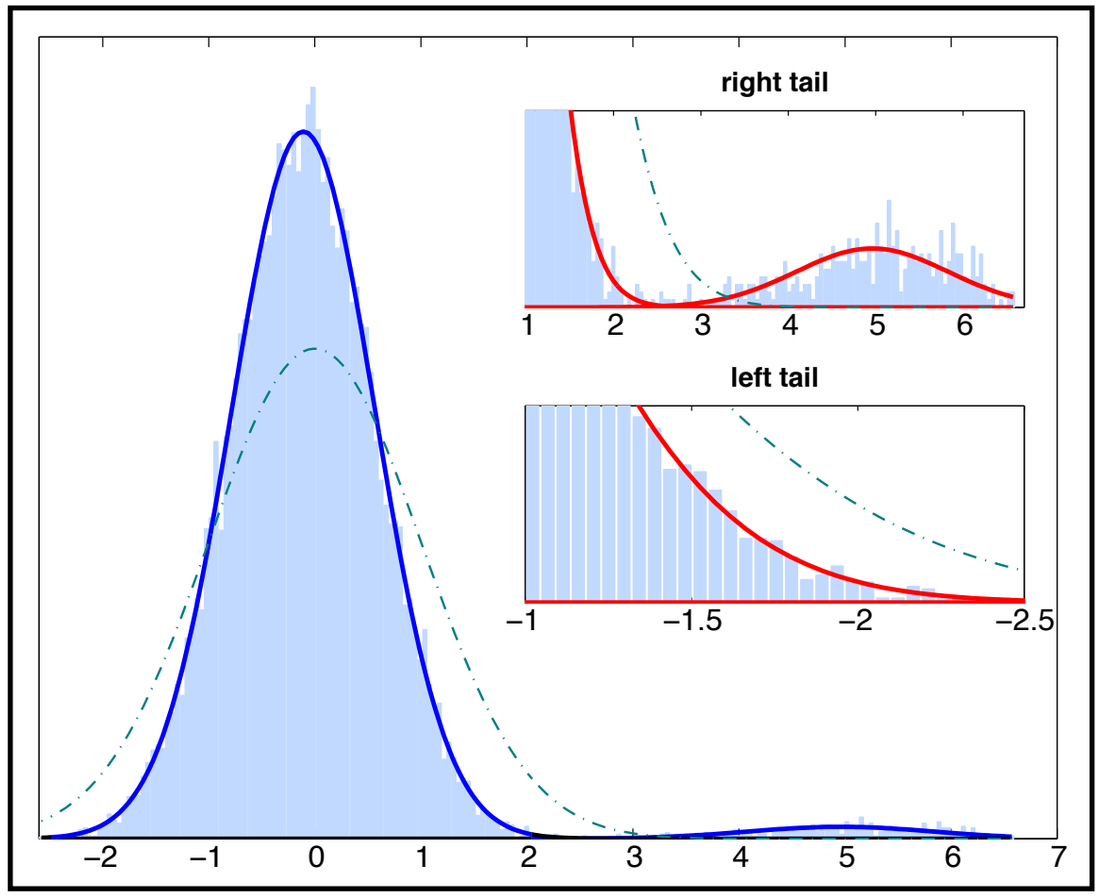

Thresholding

- classical null-hypothesis testing is invalid

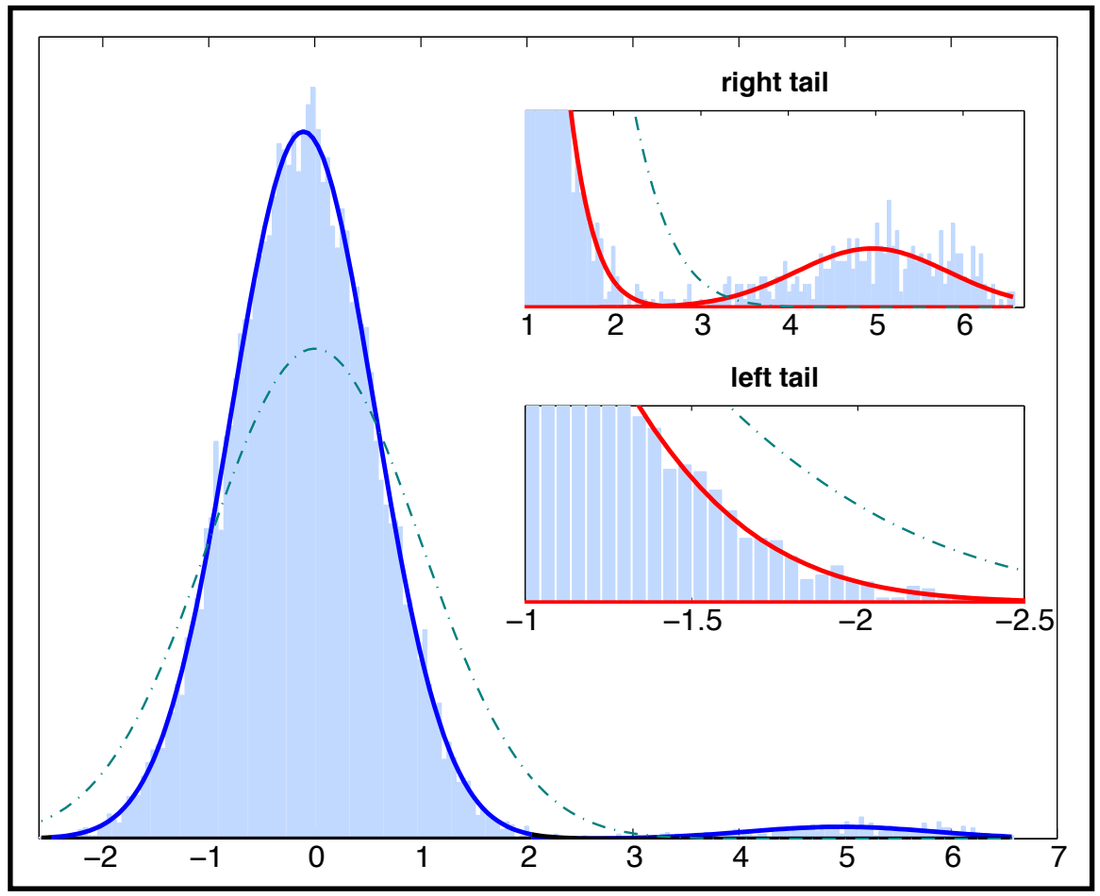

Thresholding

- classical null-hypothesis testing is invalid
- After estimation, the spatial maps are a projection of data on to the ‘unmixing matrix’

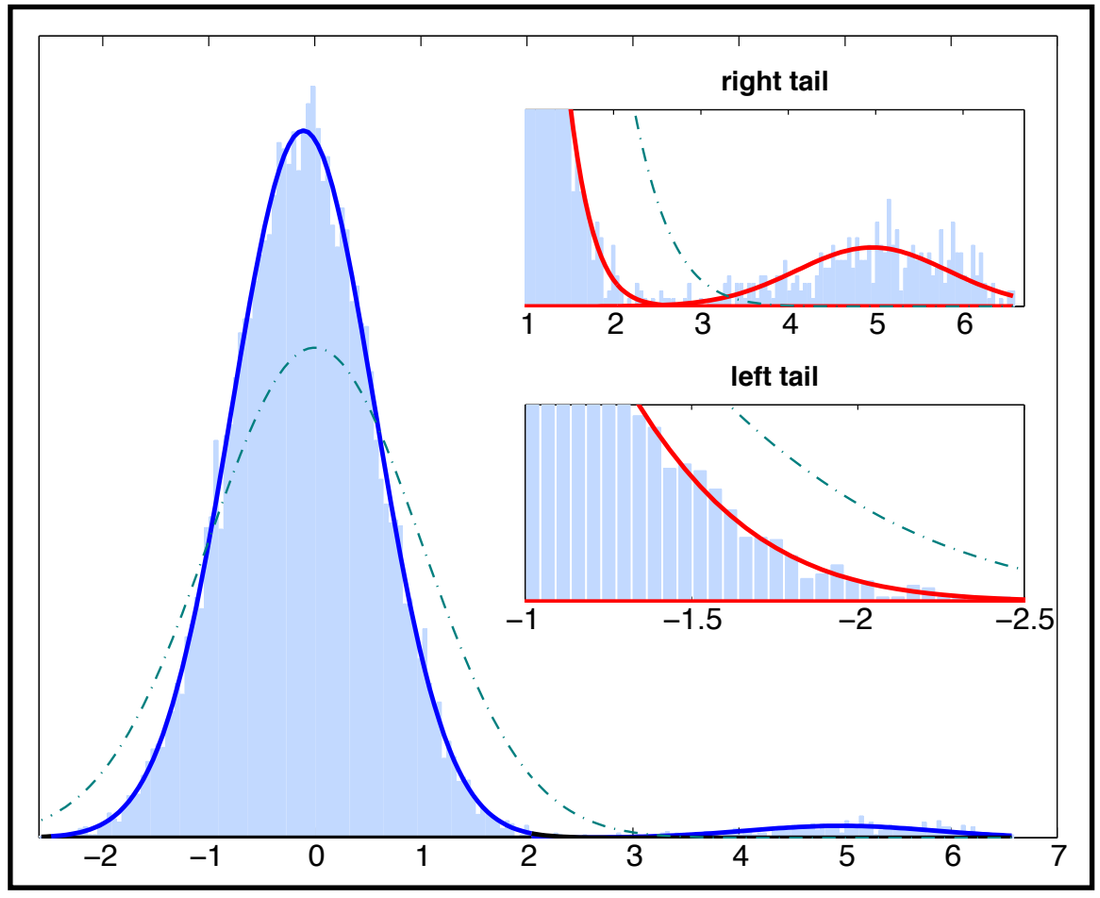

Thresholding

- classical null-hypothesis testing is invalid
- After estimation, the spatial maps are a projection of data on to the 'unmixing matrix'
- data is assumed to be a linear combination of signals and noise

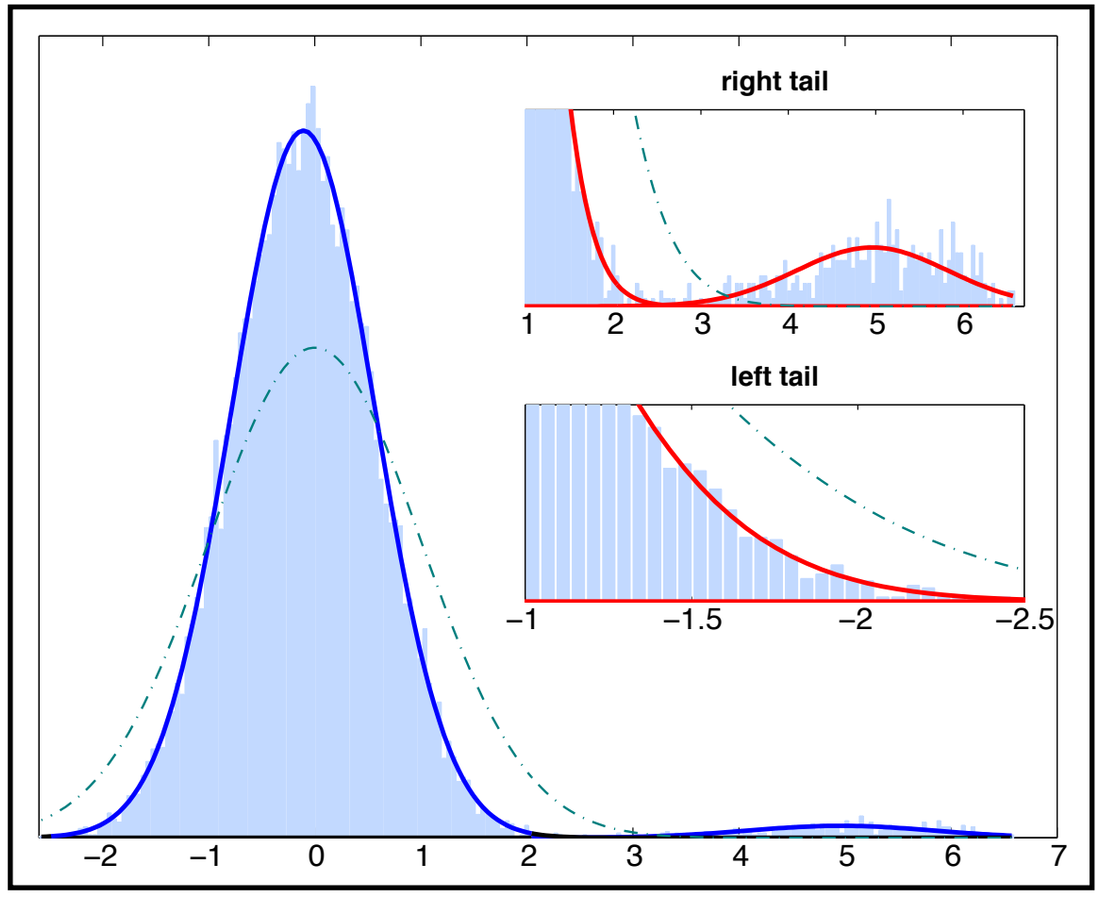

Thresholding

- classical null-hypothesis testing is invalid
- After estimation, the spatial maps are a projection of data on to the 'unmixing matrix'
- data is assumed to be a linear combination of signals and noise
- the distribution of the estimated spatial maps is a mixture distribution!

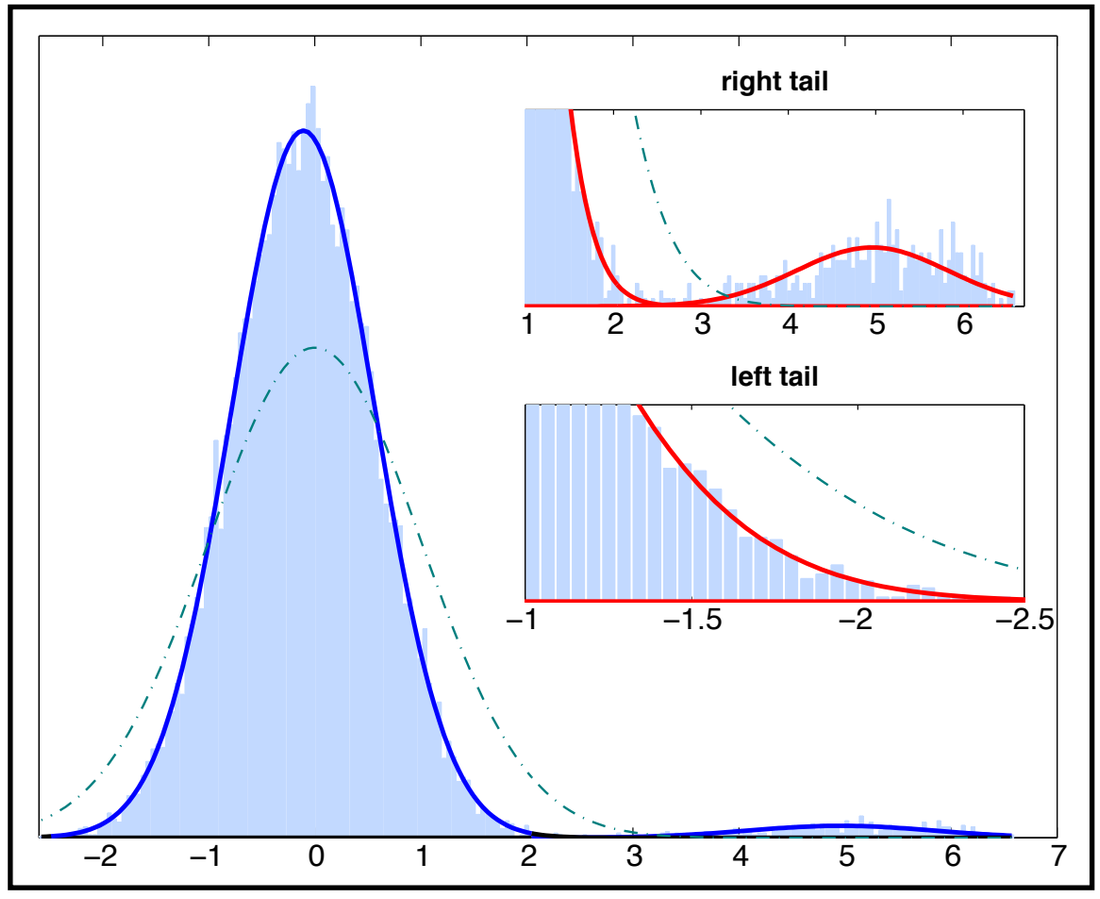

Alternative Hypothesis Test

- use Gaussian/Gamma mixture model fitted to the histogram of intensity values (using EM)

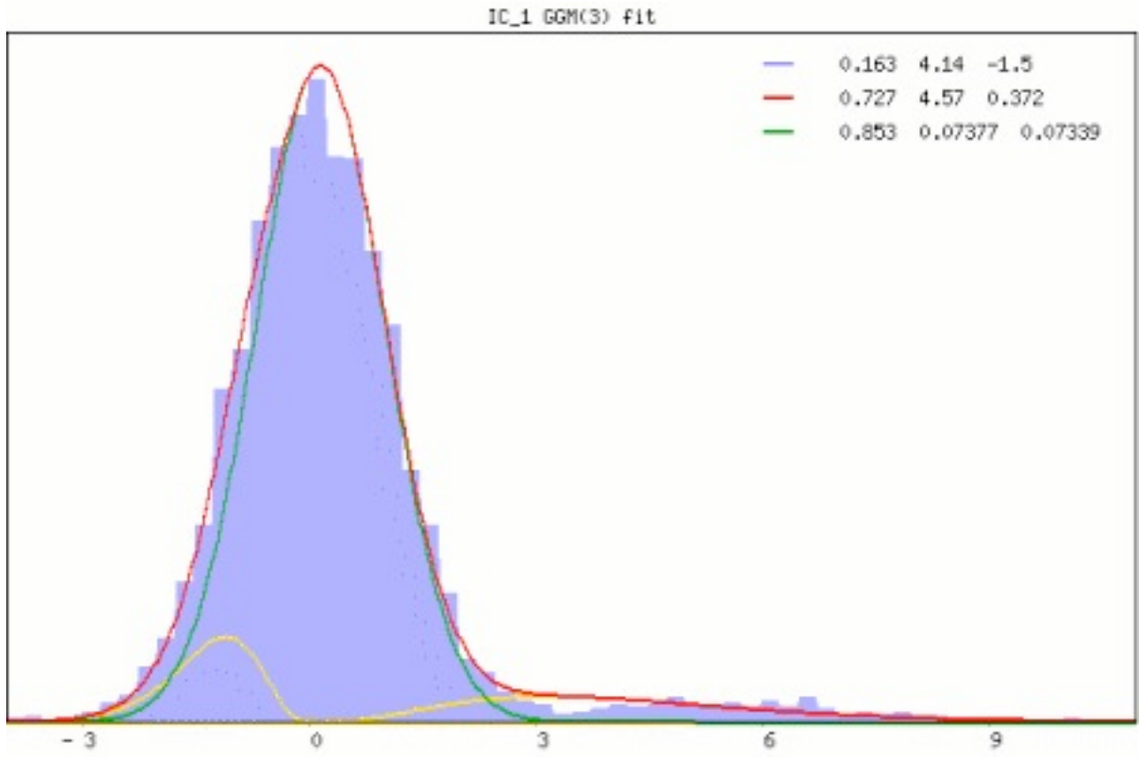

Alternative Hypothesis Test

- use Gaussian/Gamma mixture model fitted to the histogram of intensity values (using EM)

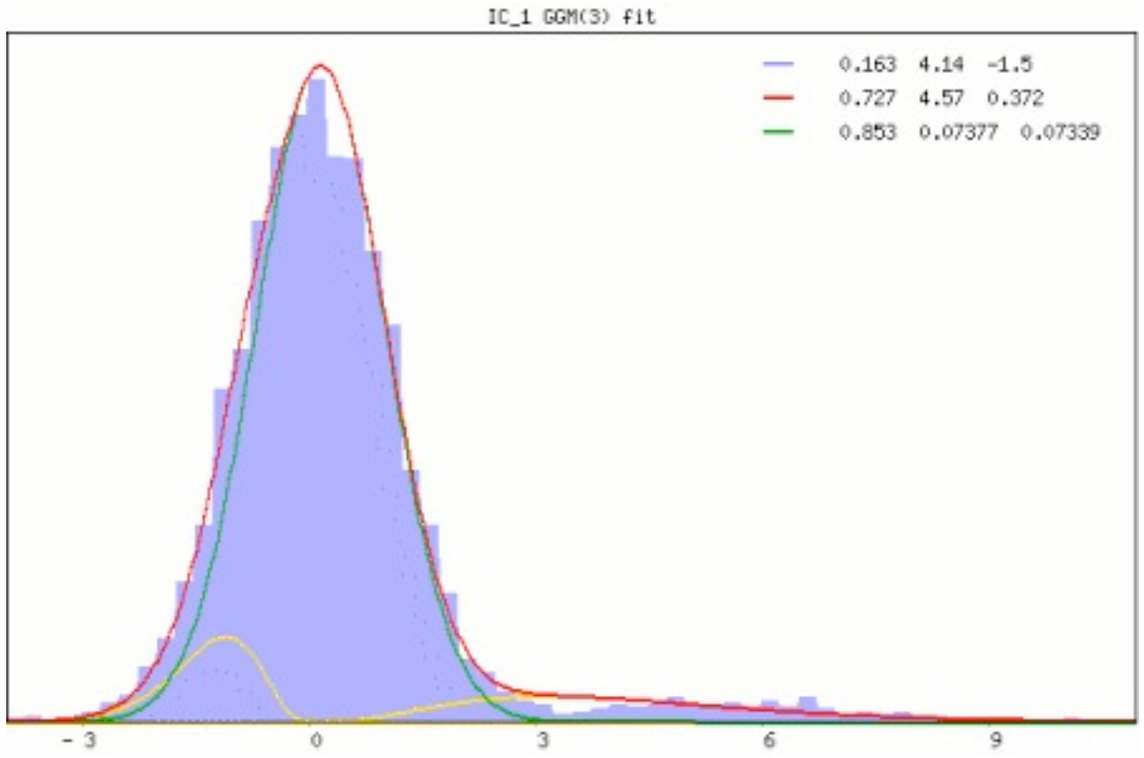

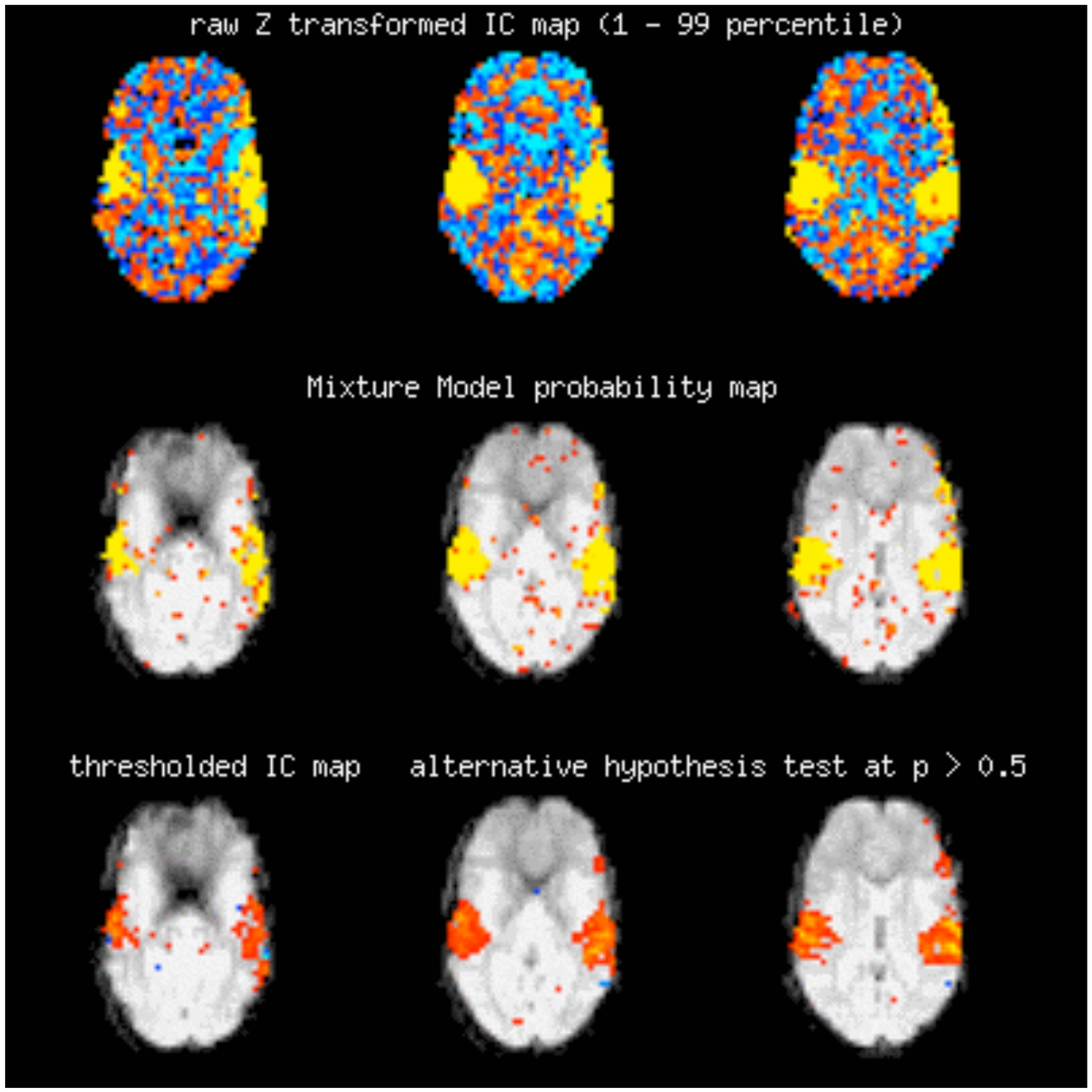

Probabilistic ICA

GLM analysis

standard ICA (unconstrained)

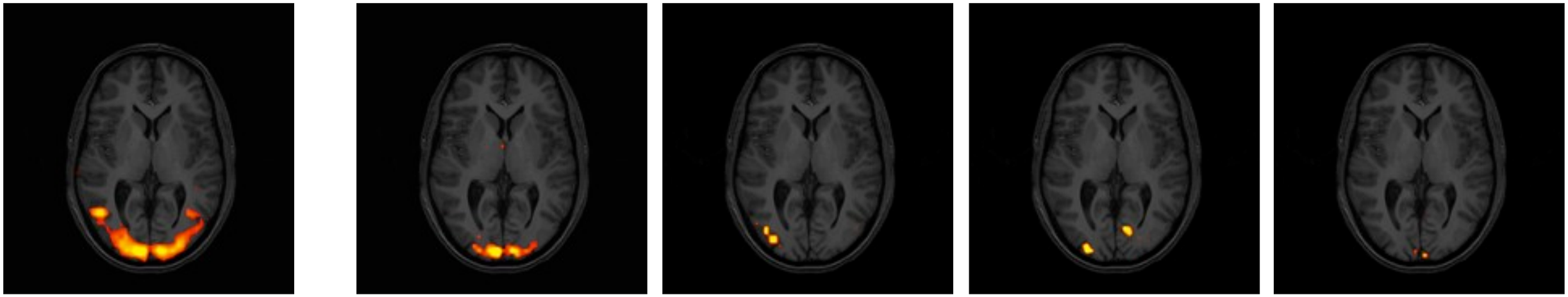

Probabilistic ICA

GLM analysis

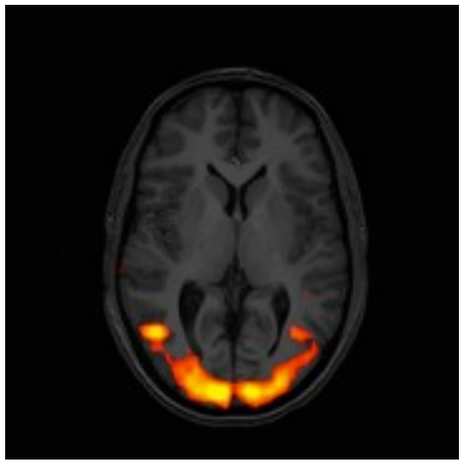

probabilistic ICA

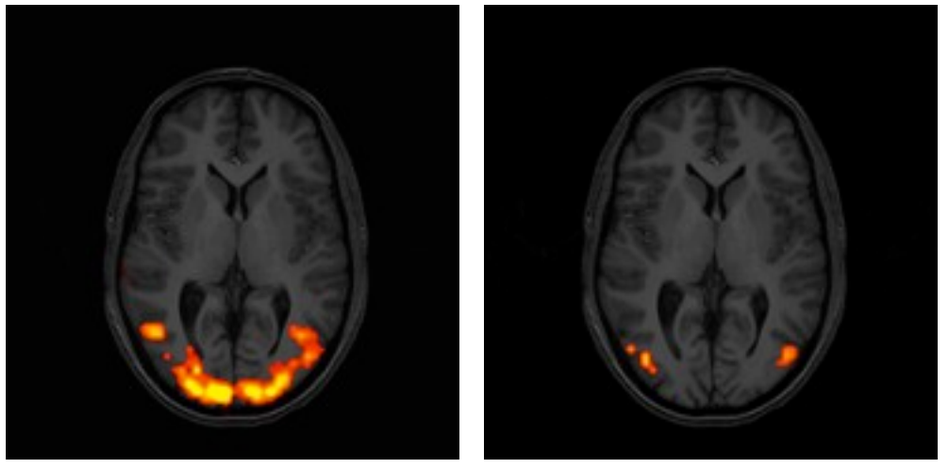

- designed to address the ‘overfitting problem’:
  - tries to avoid generation of ‘spurious’ results
  - high spatial sensitivity and specificity

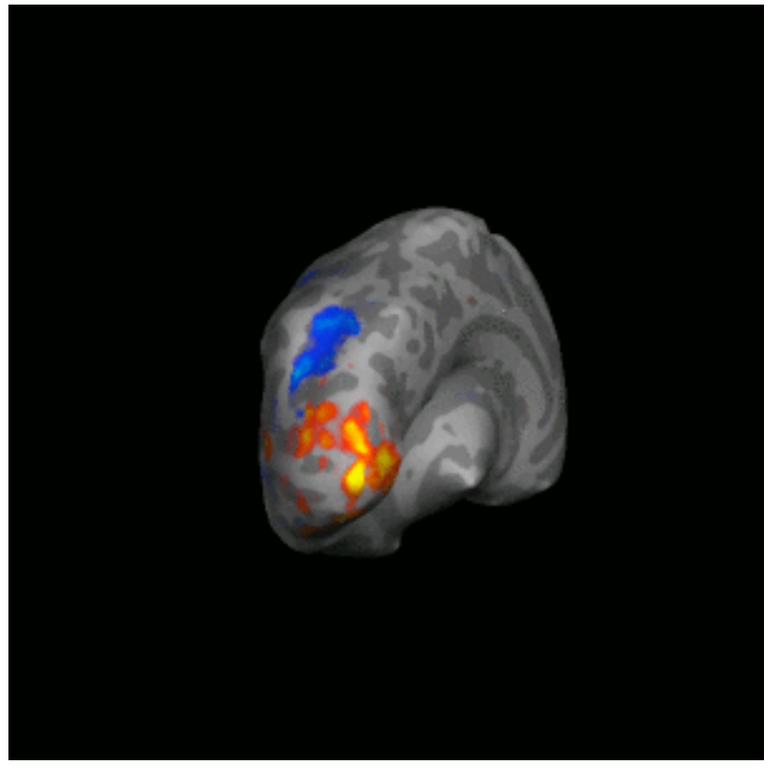

Applications

EDA techniques can be useful to

- investigate the BOLD response
- estimate artefacts in the data
- find areas of ‘activation’ which respond in a non-standard way
- analyse data for which no model of the BOLD response is available

Applications

EDA techniques can be useful to

- investigate the BOLD response
- estimate artefacts in the data
- find areas of 'activation' which respond in a non-standard way
- analyse data for which no model of the BOLD response is available

Investigate BOLD response

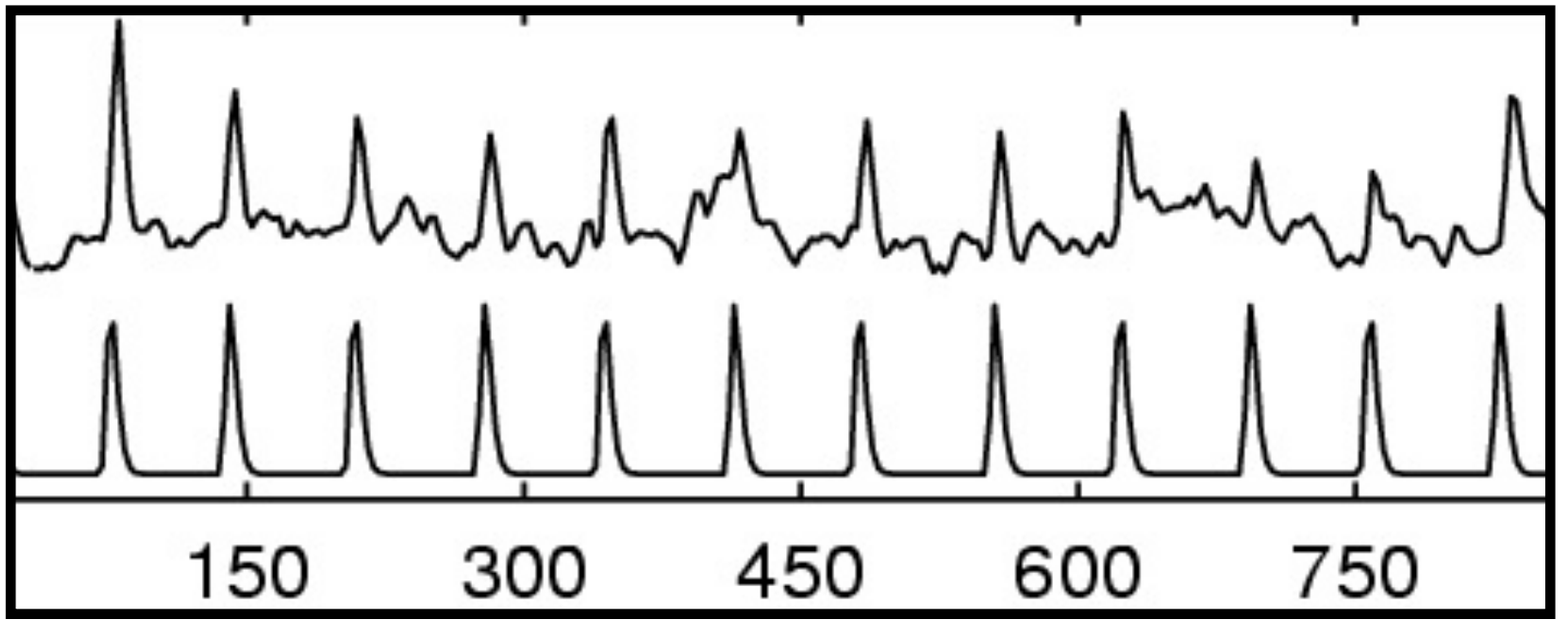

estimated signal time course

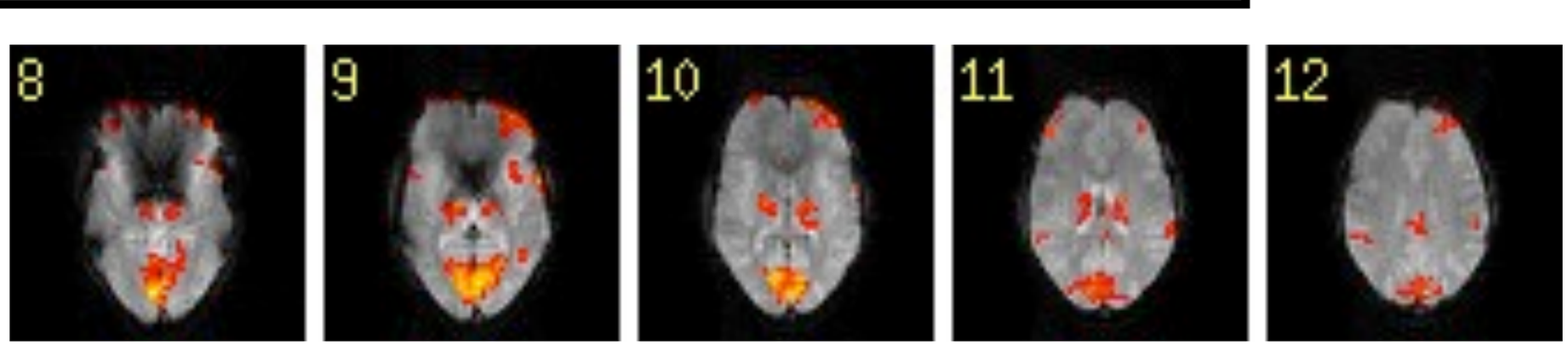

standard hrf model

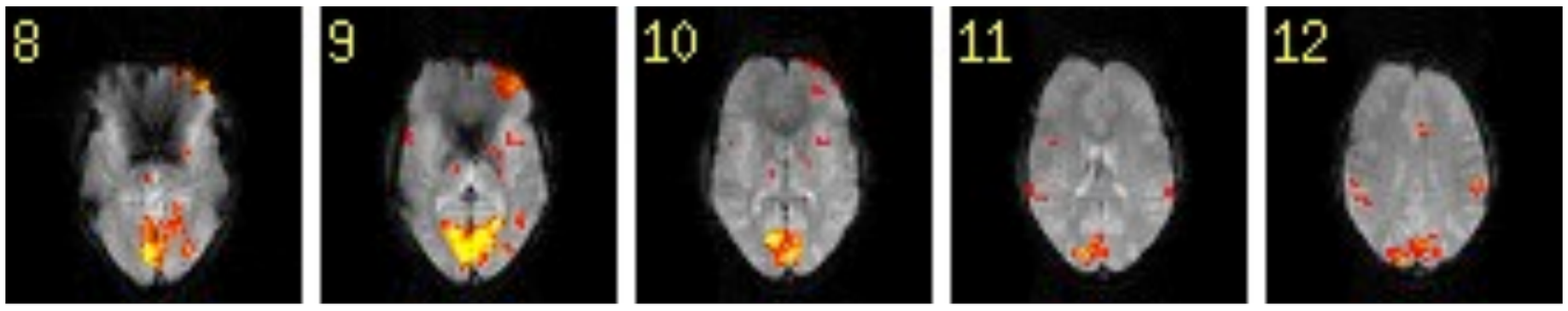

Applications

EDA techniques can be useful to

- investigate the BOLD response
- estimate artefacts in the data
- find areas of 'activation' which respond in a non-standard way
- analyse data for which no model of the BOLD response is available

Artefact detection

- FMRI data contain a variety of source processes
- Artifactual sources typically have unknown spatial and temporal extent and cannot easily be modelled accurately
- Exploratory techniques do not require a priori knowledge of time-courses and spatial maps

slice drop-outs

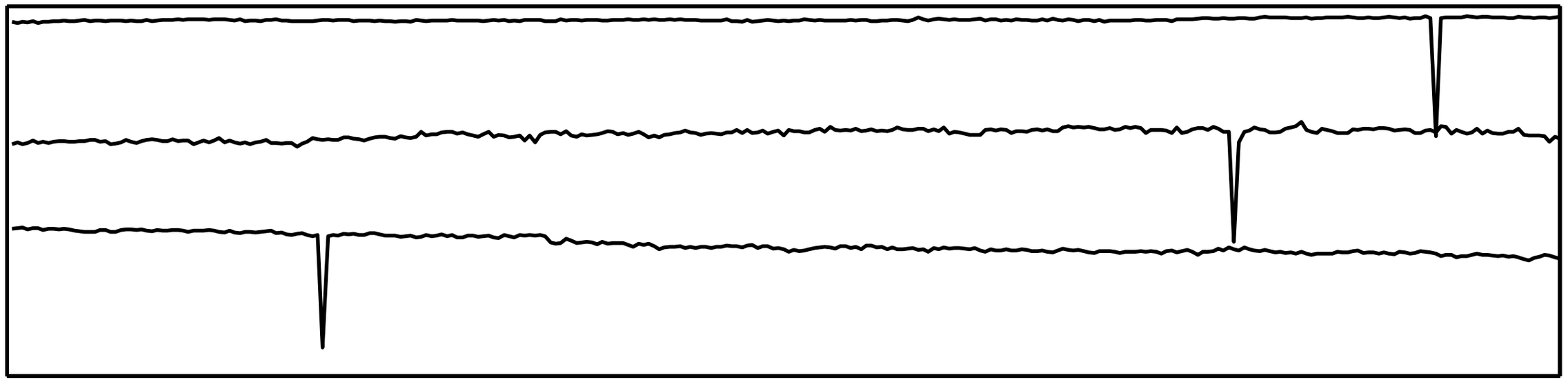

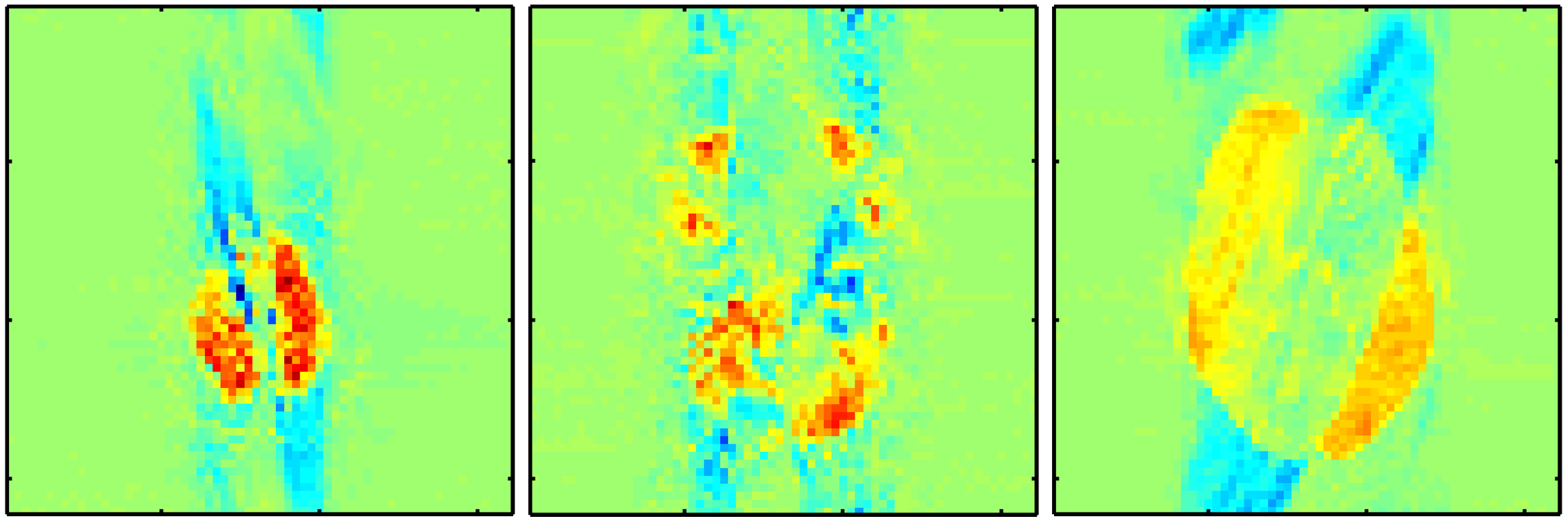

gradient instability

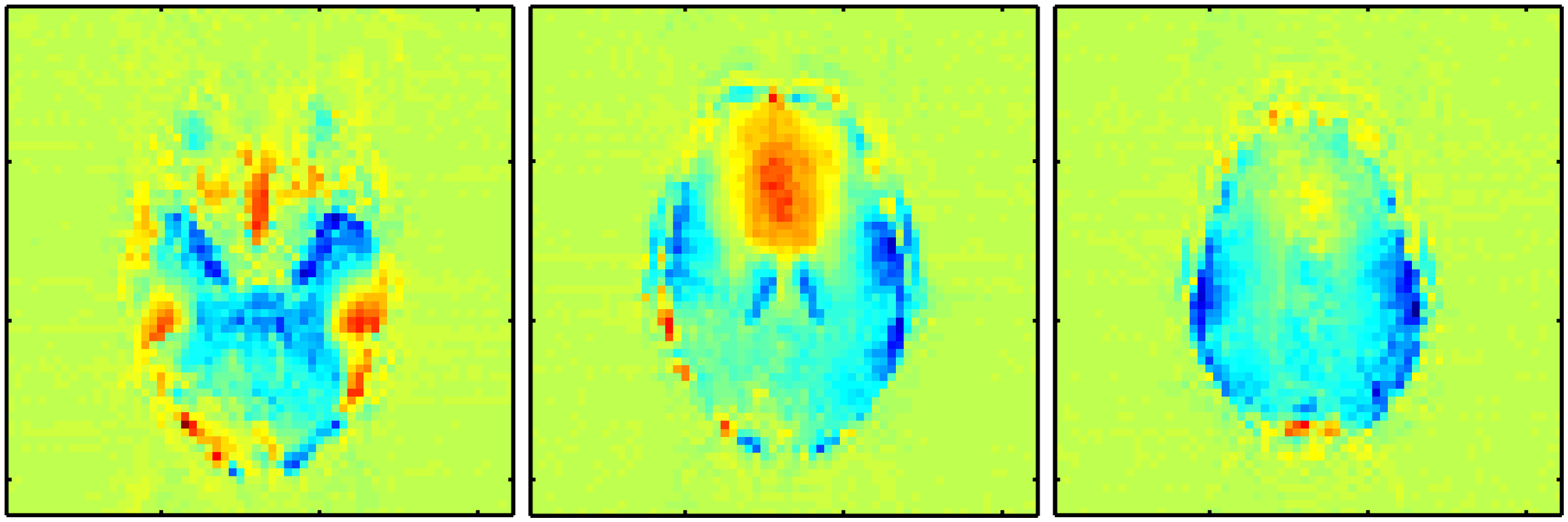

EPI ghost

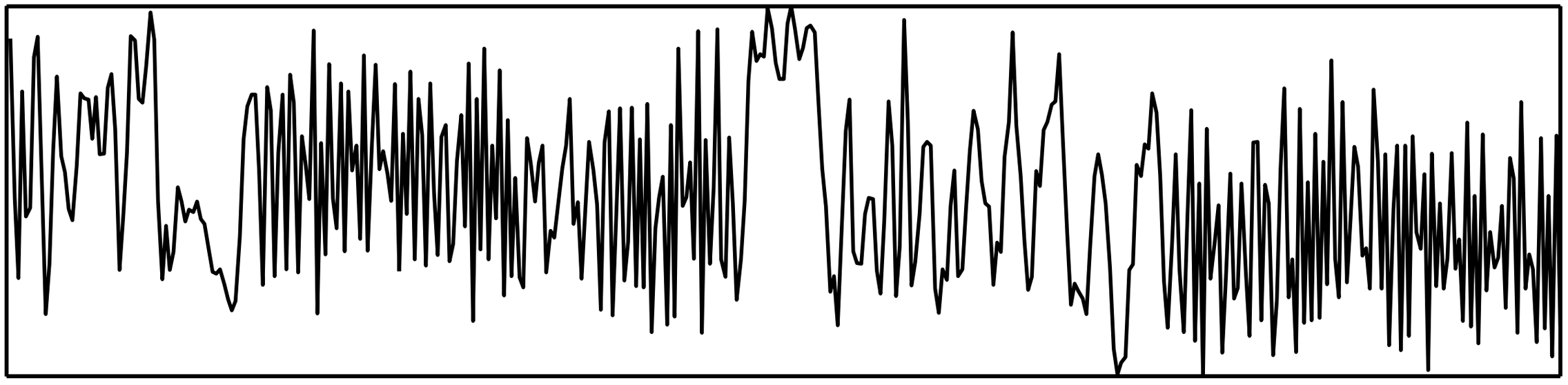

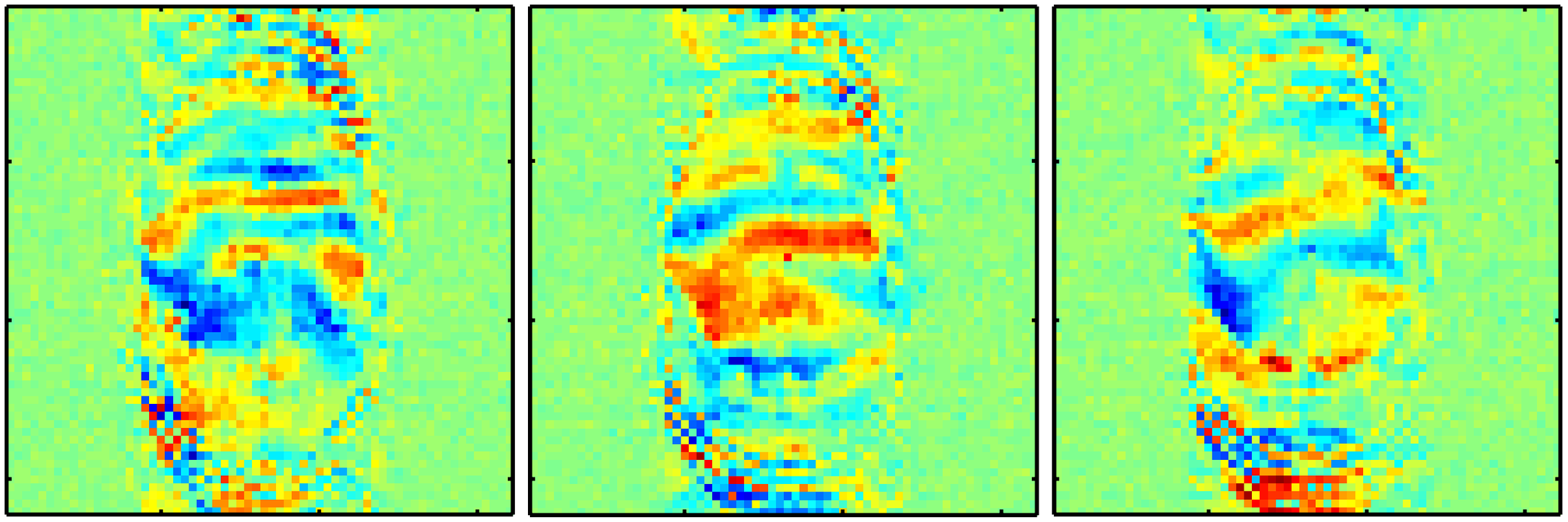

high-frequency noise

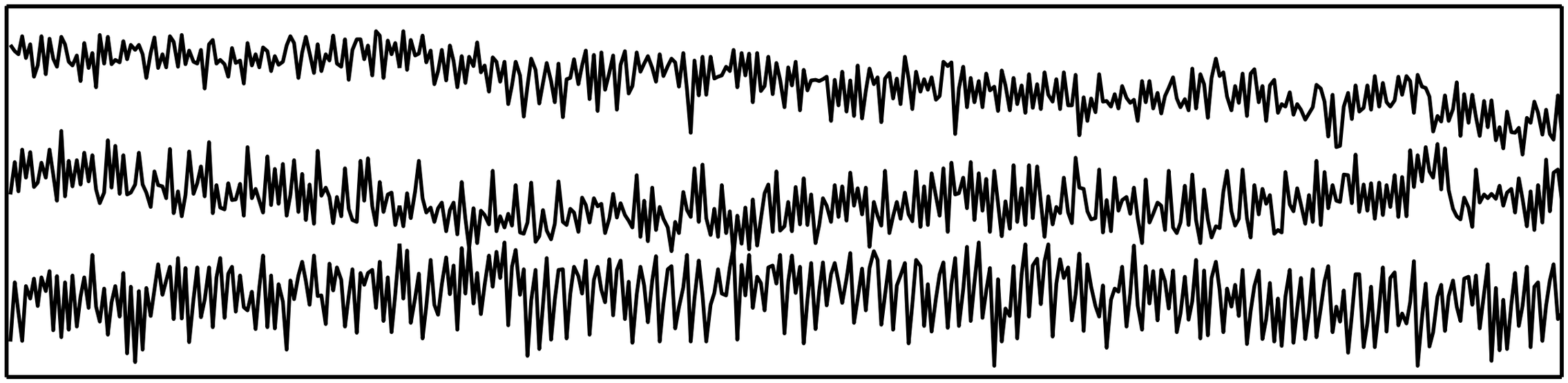

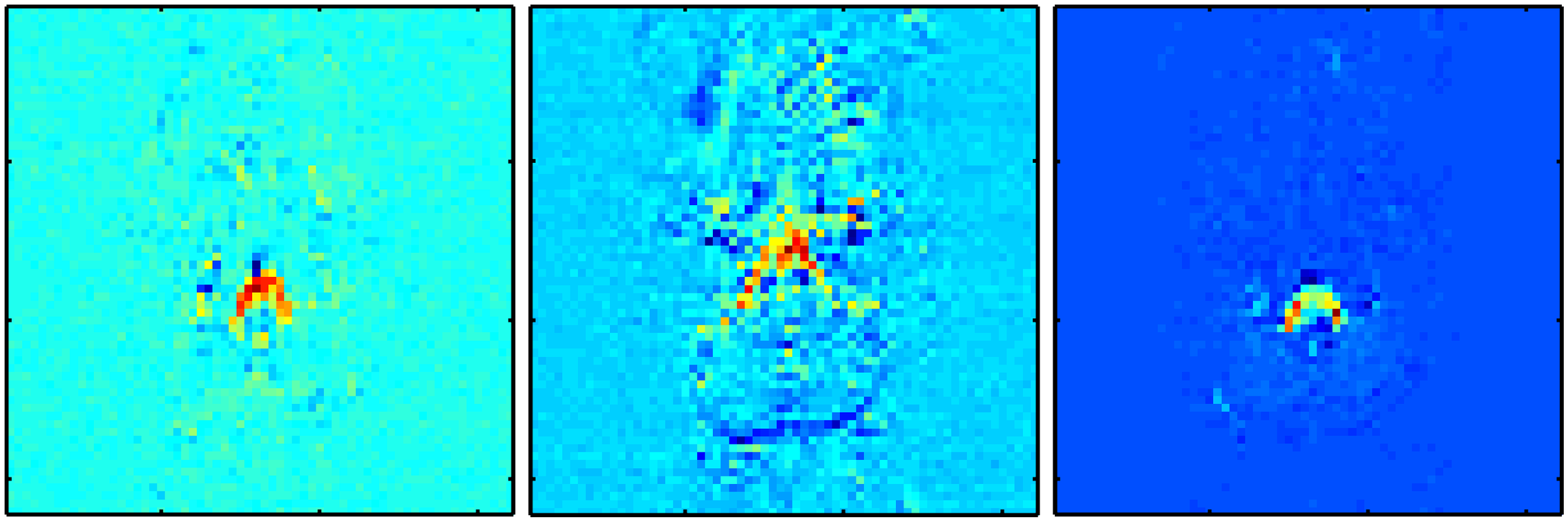

head motion

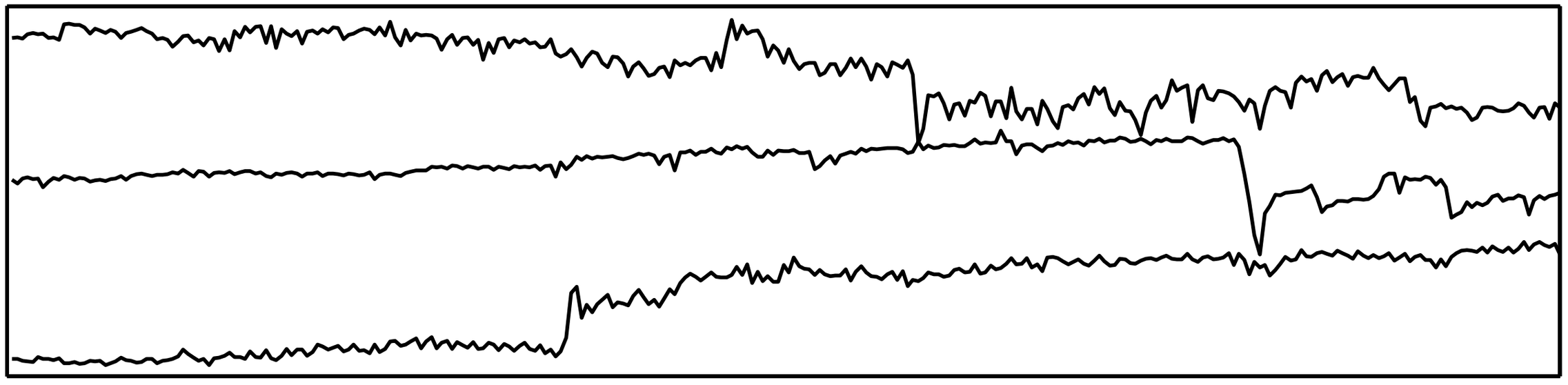

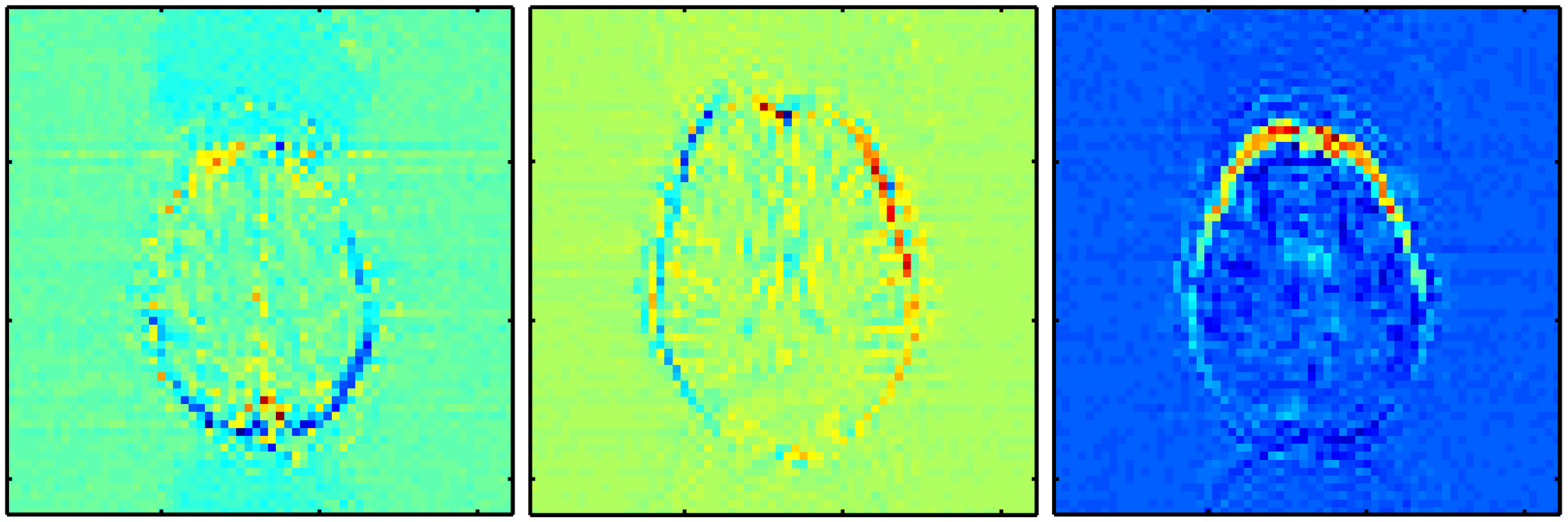

field inhomogeneity

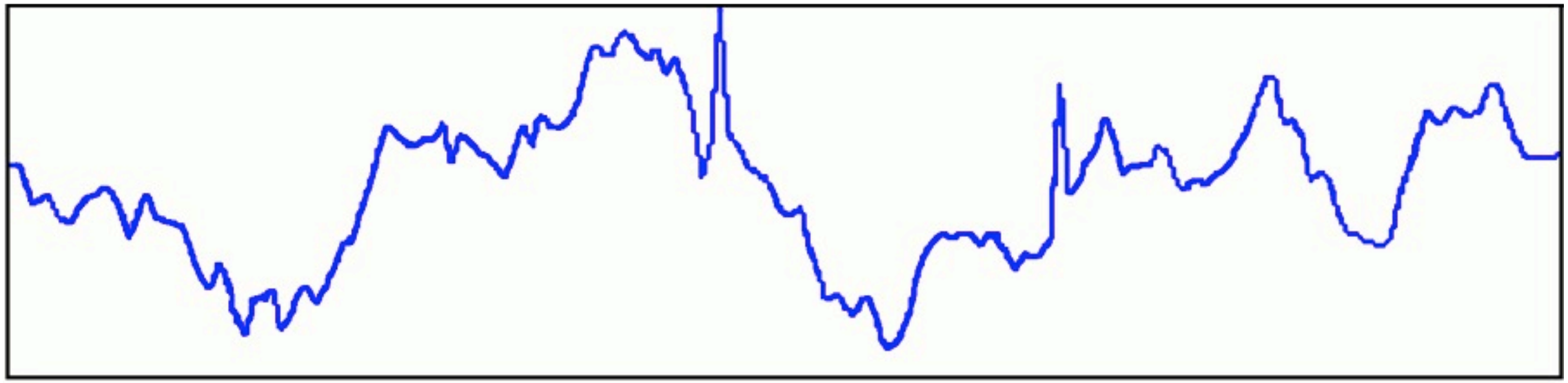

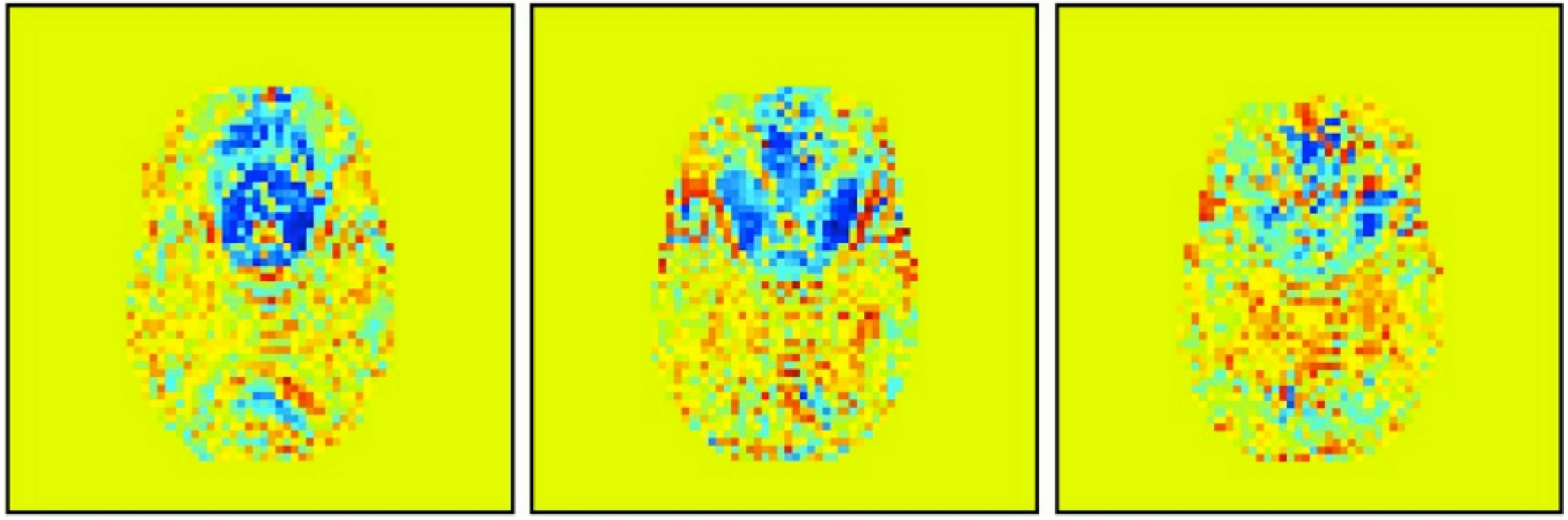

eye-related artefacts

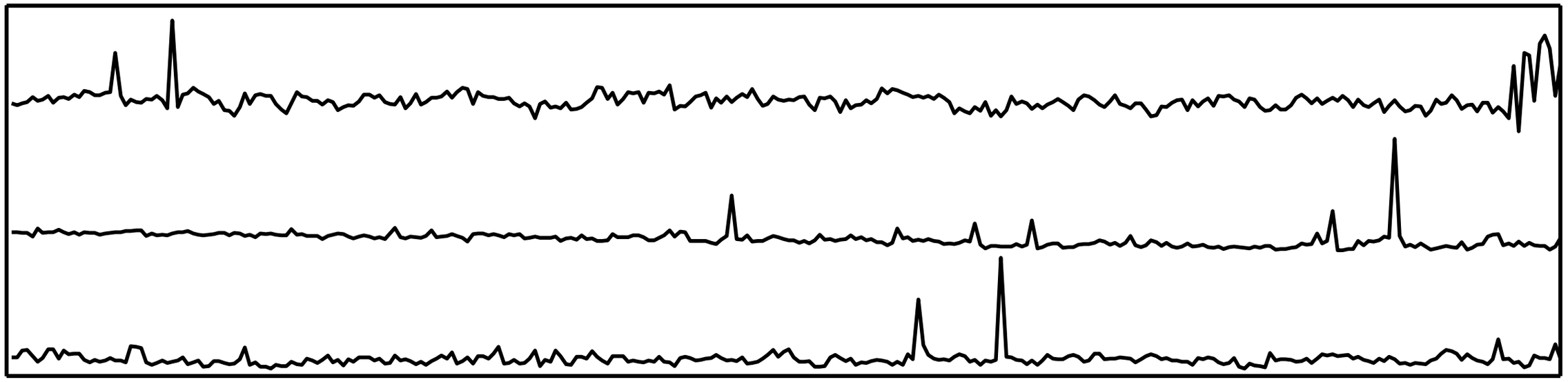

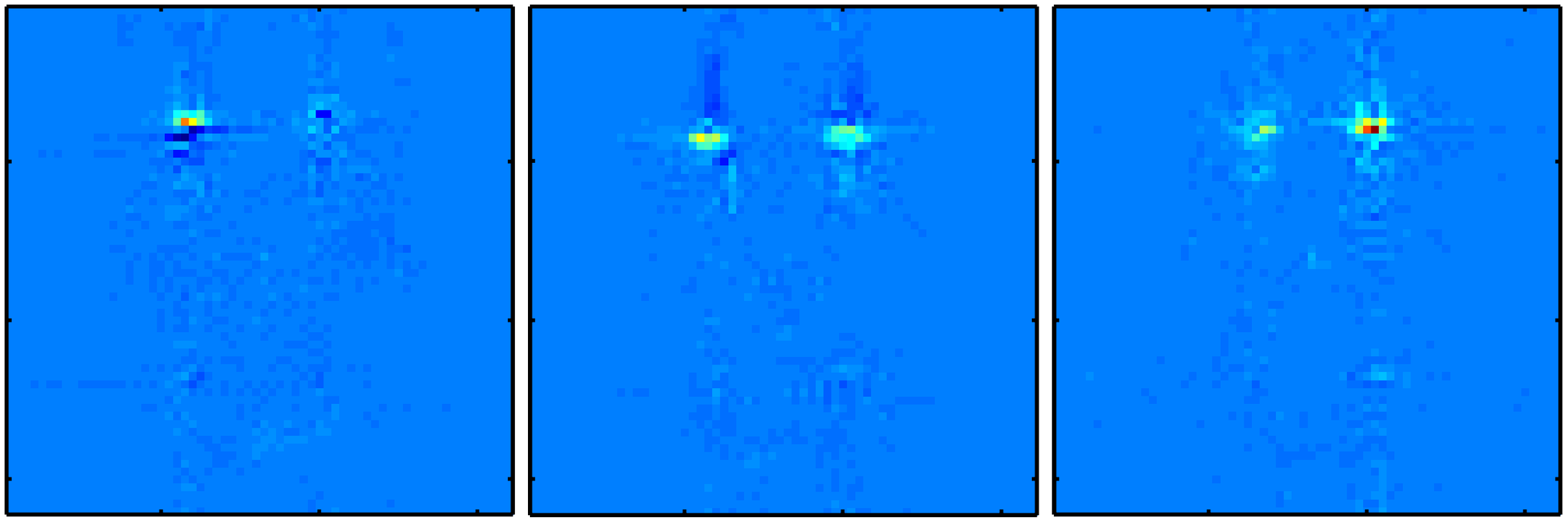

eye-related artefacts

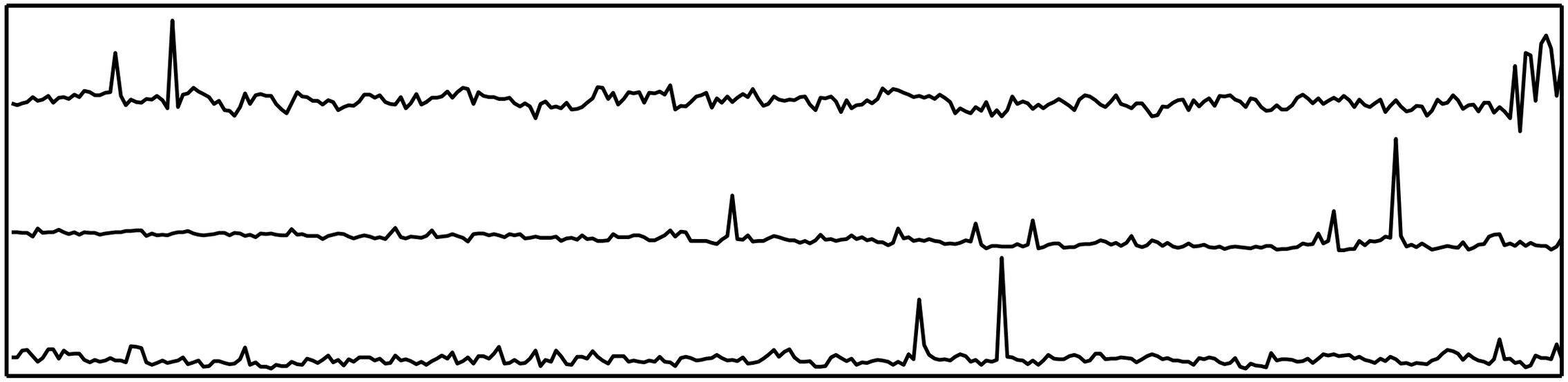

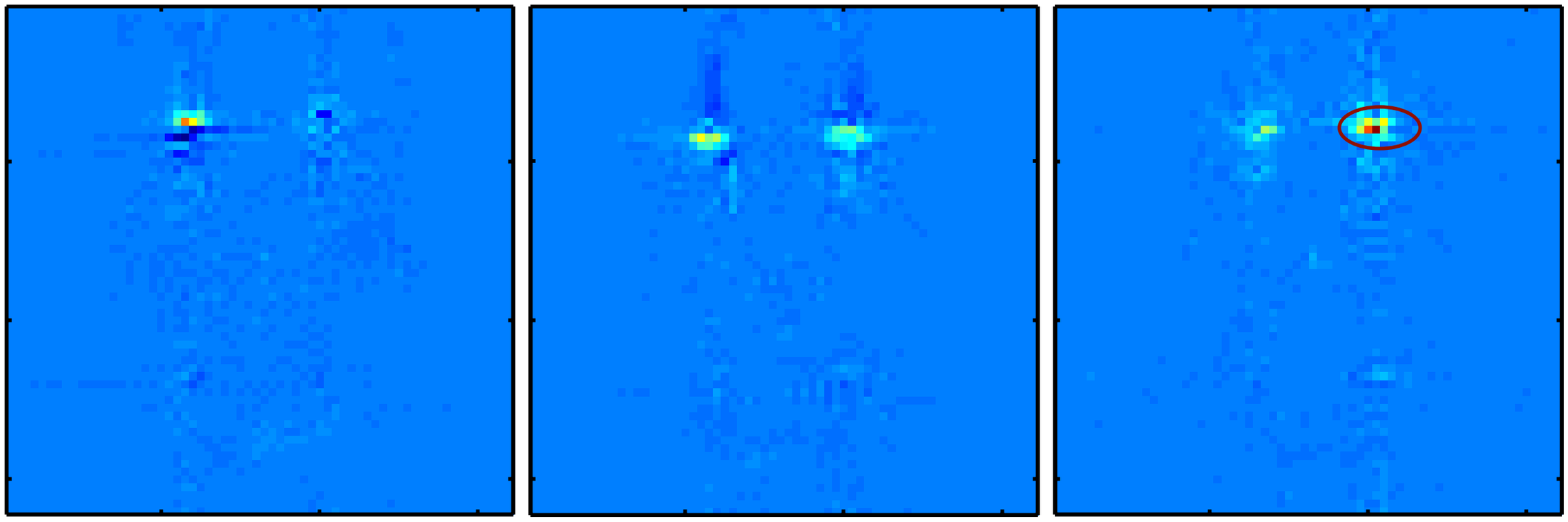

eye-related artefacts

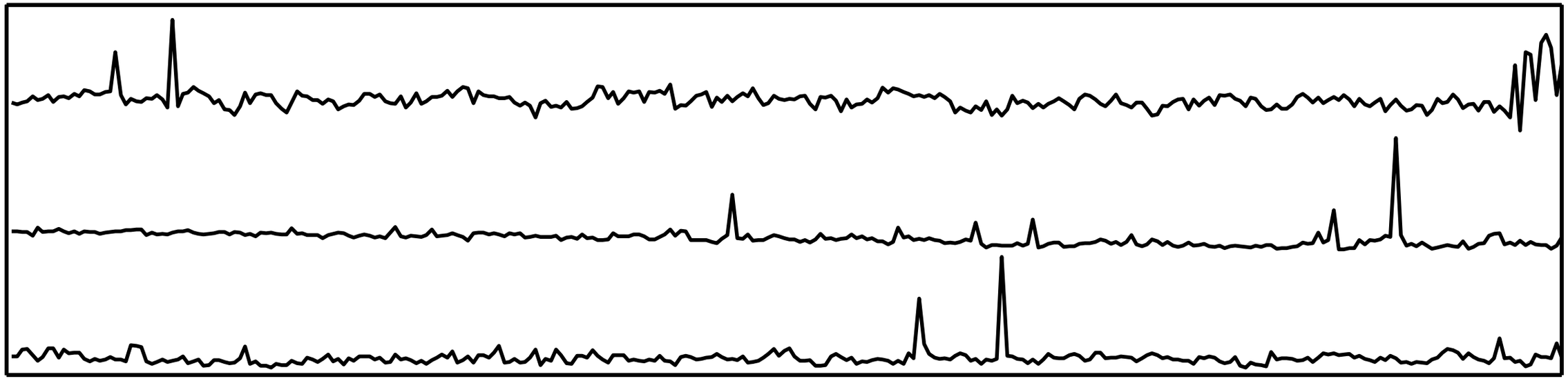

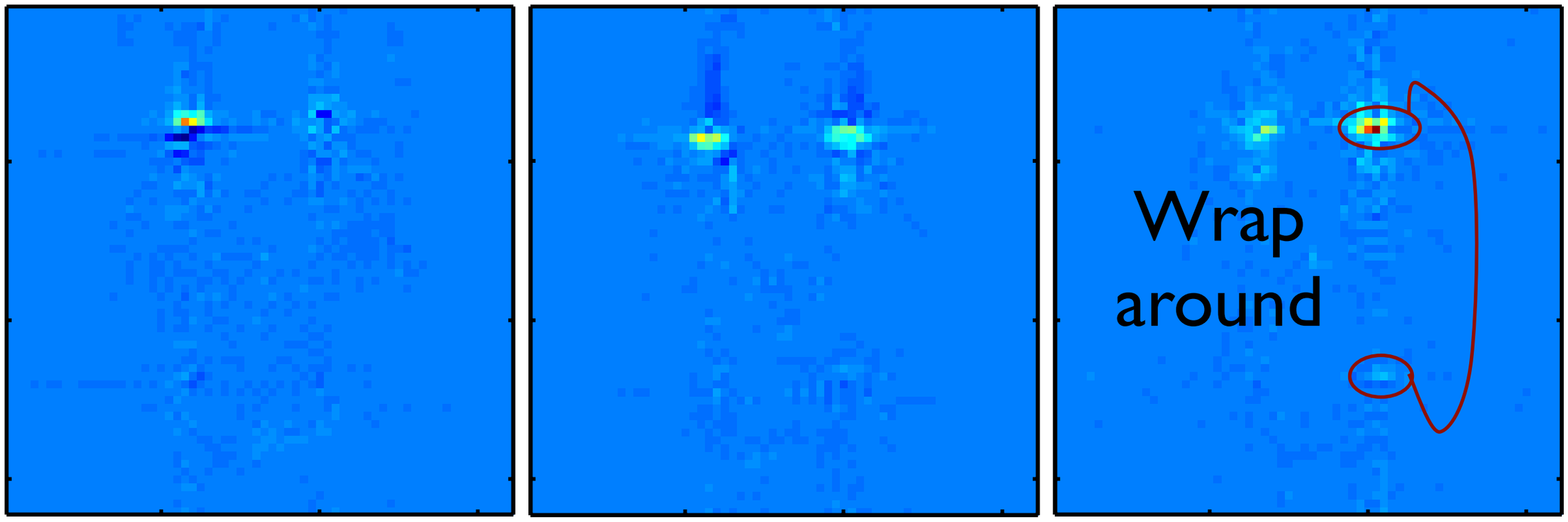

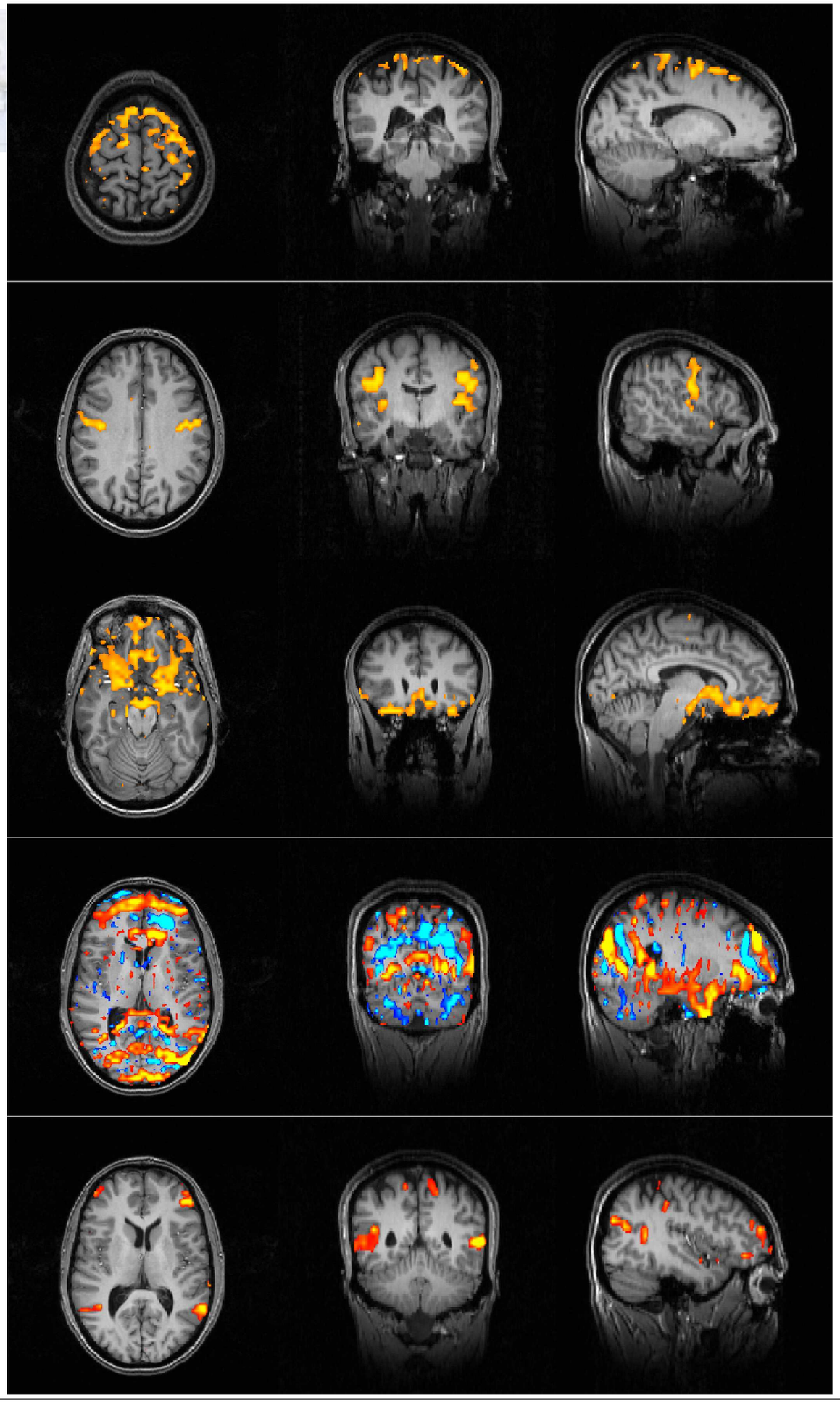

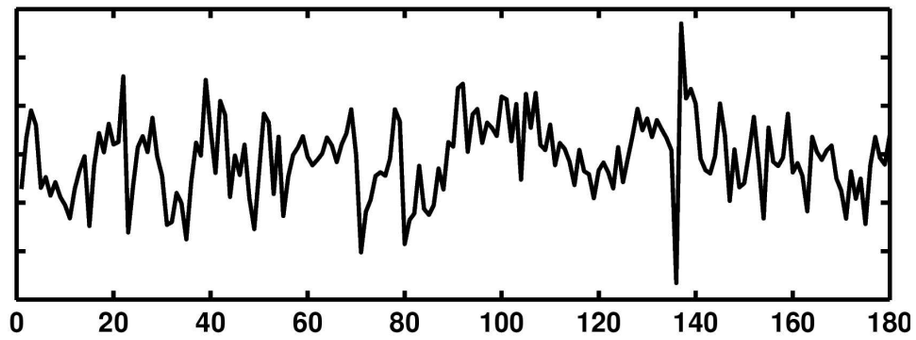
0
20
40
60
80
100
120
140
160
180

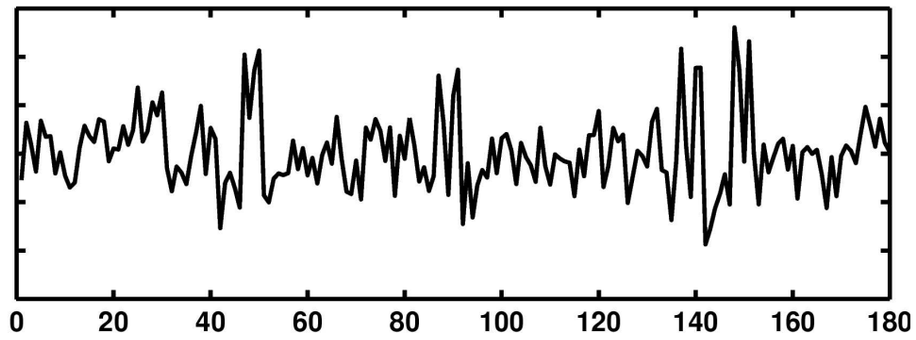
0
20
40
60
80
100
120
140
160
180

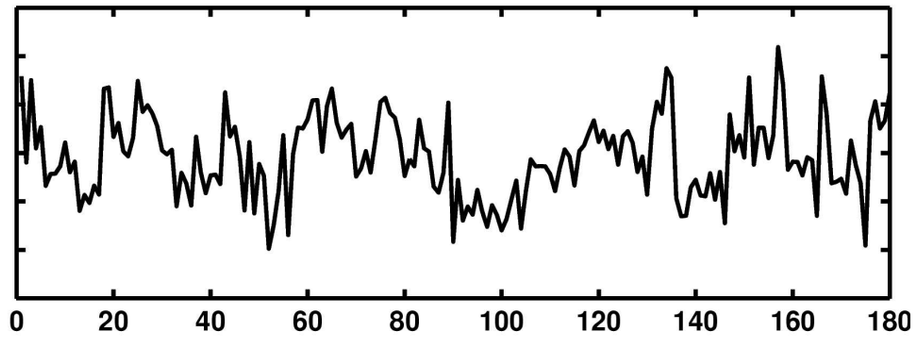
0
20
40
60
80
100
120
140
160
180

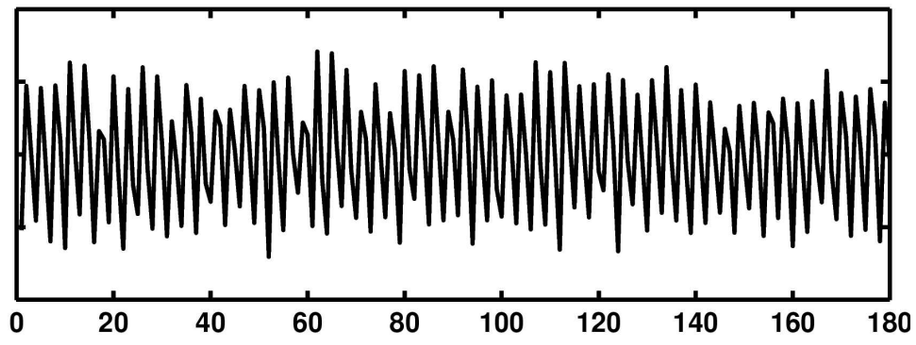
0
20
40
60
80
100
120
140
160
180

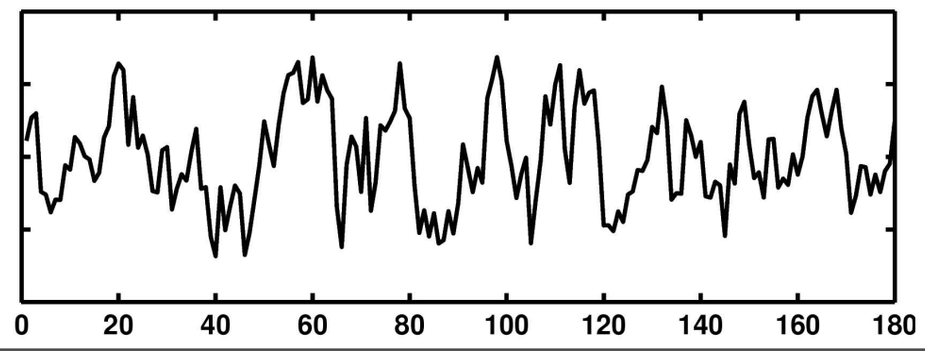
0
20
40
60
80
100
120
140
160
180

Structured Noise and the GLM

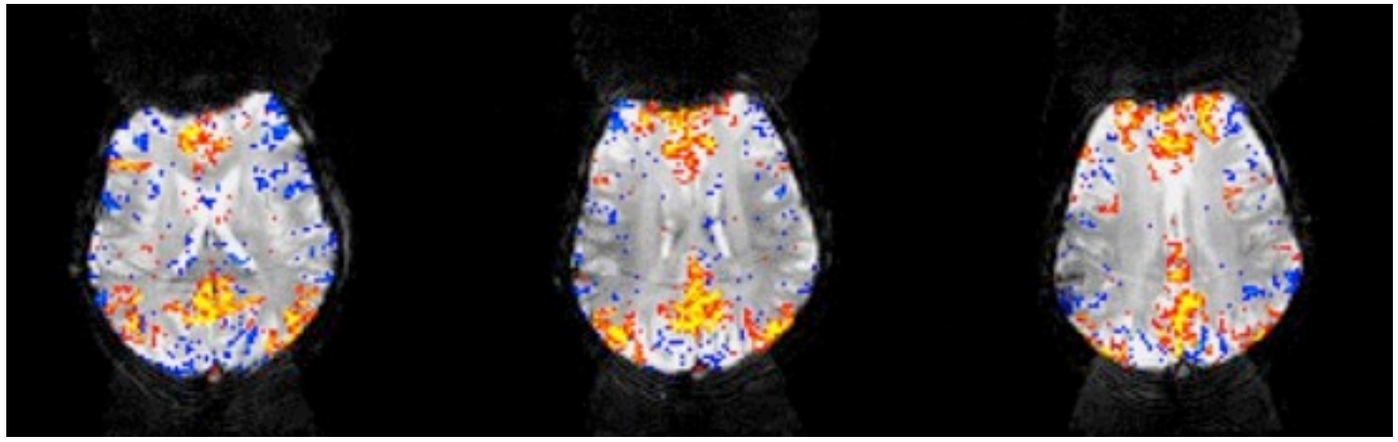

- ‘structured noise’ appears:
  - in the GLM residuals - inflates variance estimates *(more false negatives)*
  - in the parameter estimates *(more false positives and/or false negatives)*
- In either case leads to suboptimal estimates and wrong inference!

Structured noise and GLM Z-stats bias

- Correlations of the noise time courses with 'typical' FMRI regressors can cause a shift in the histogram of the Z-statistics
- Thresholded maps will have wrong false-positive rate

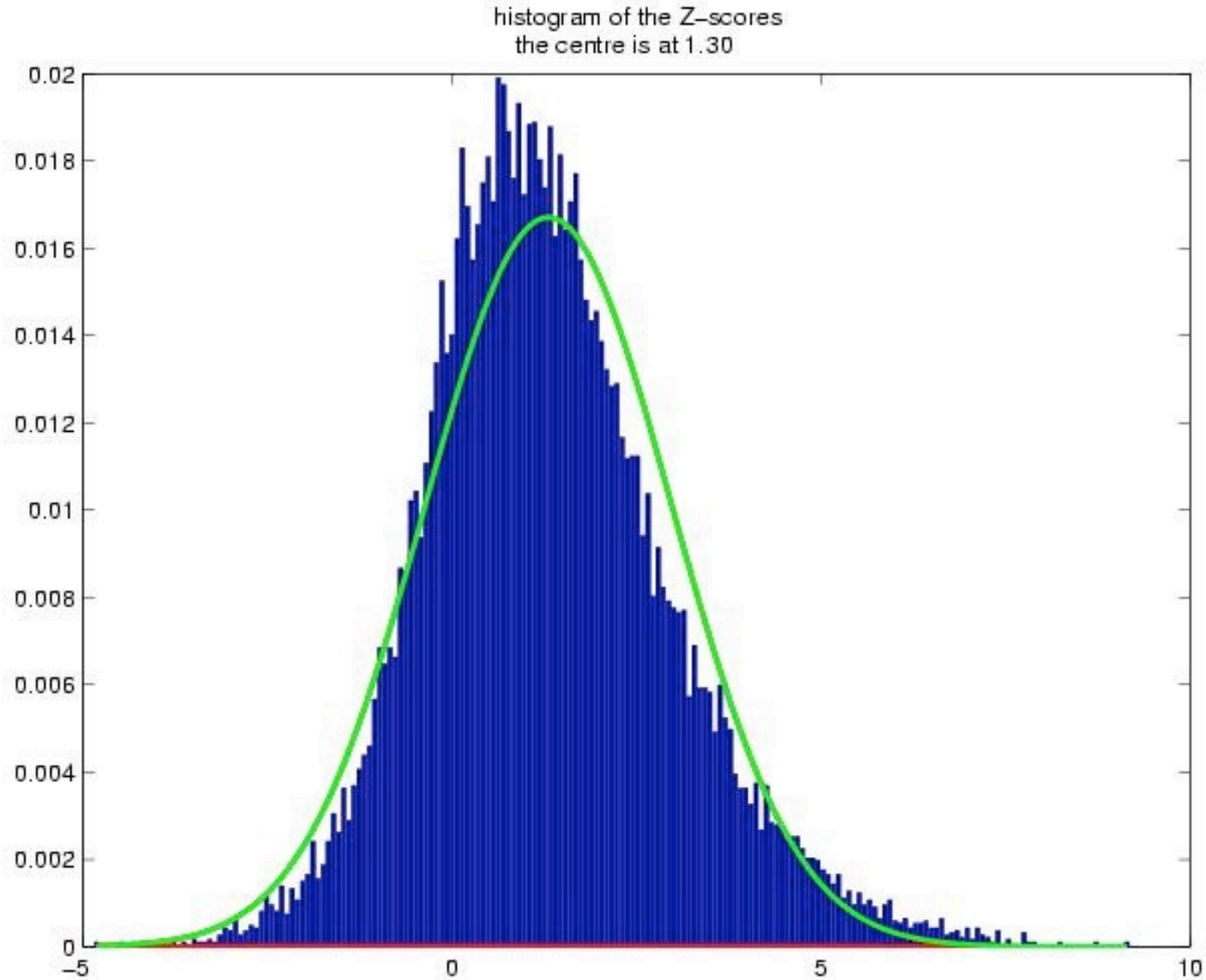

Denoising FMRI

- Example: left vs right hand finger tapping

before denoising

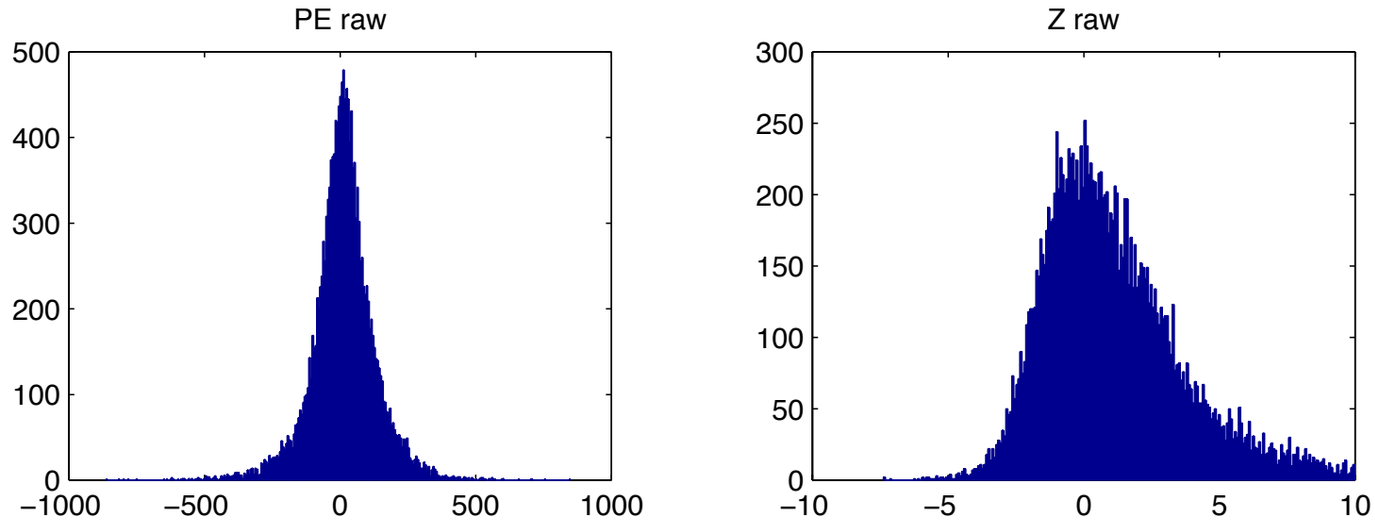

RIGHT

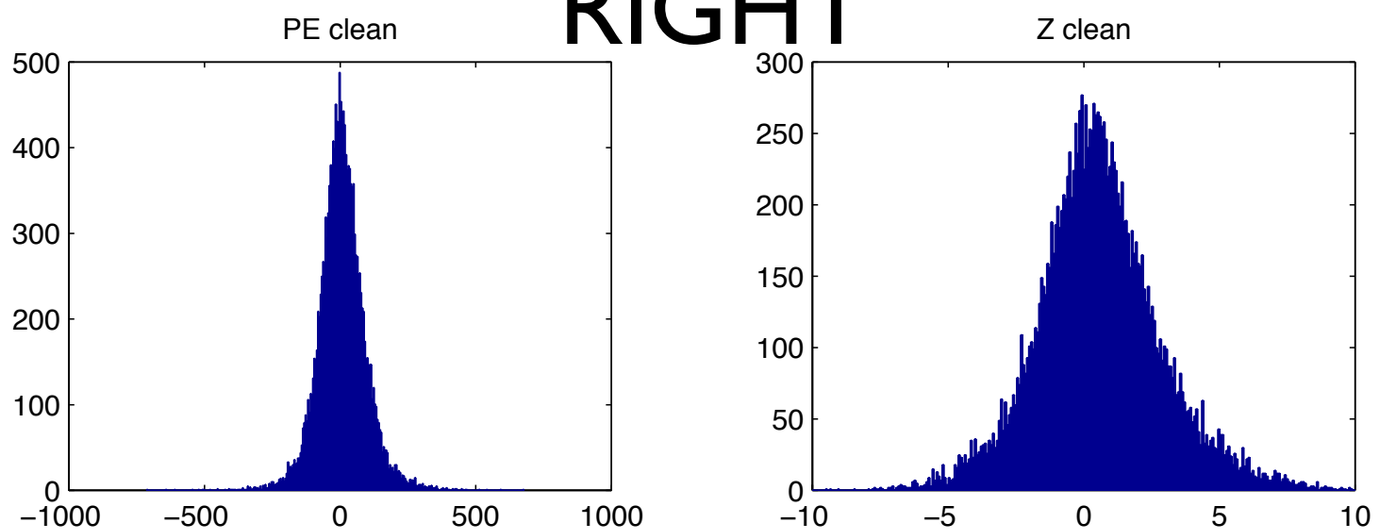

after denoising

Denoising FMRI

- Example: left vs right hand finger tapping

before denoising

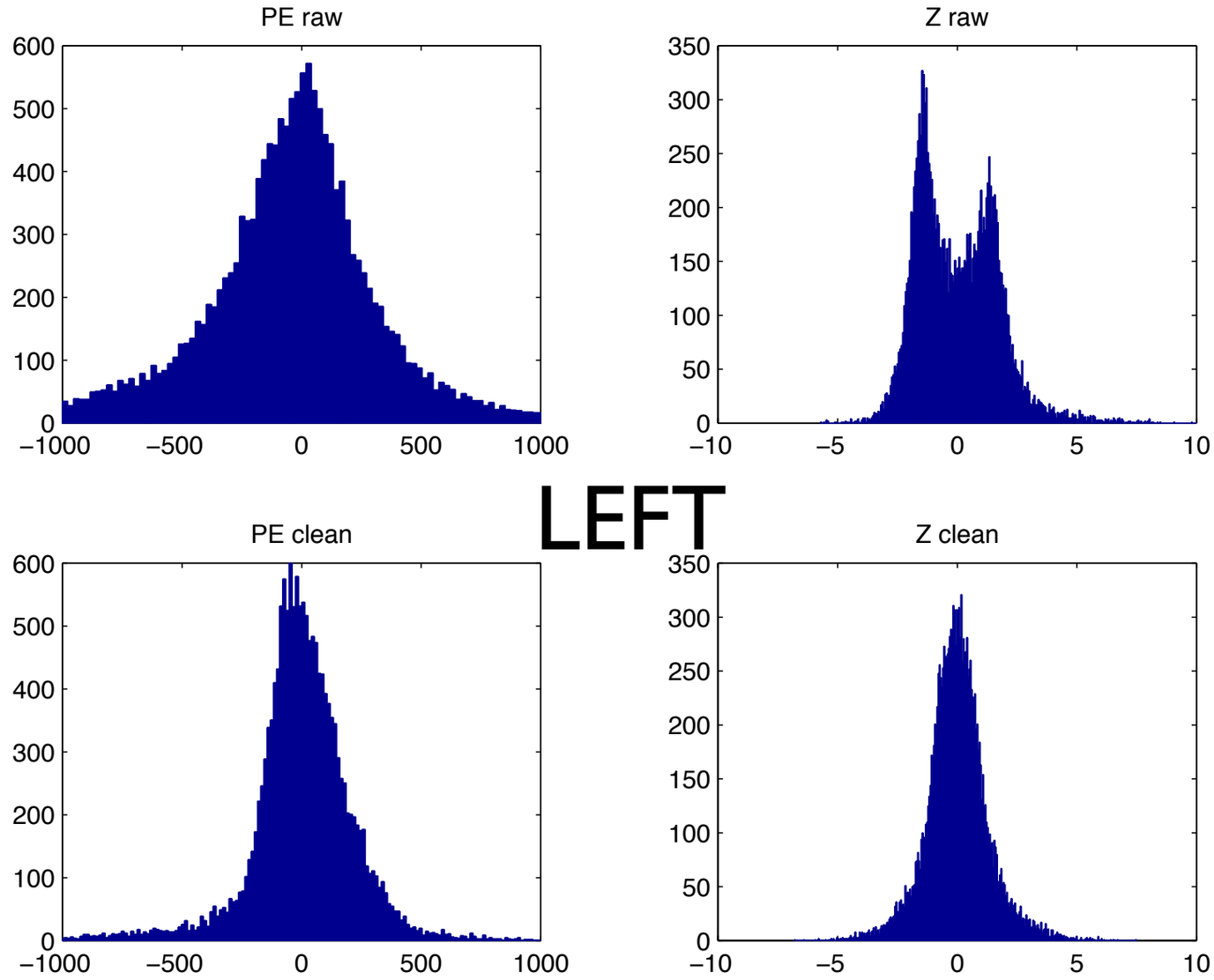

after denoising

Denoising FMRI

- Example: left vs right hand finger tapping

before denoising

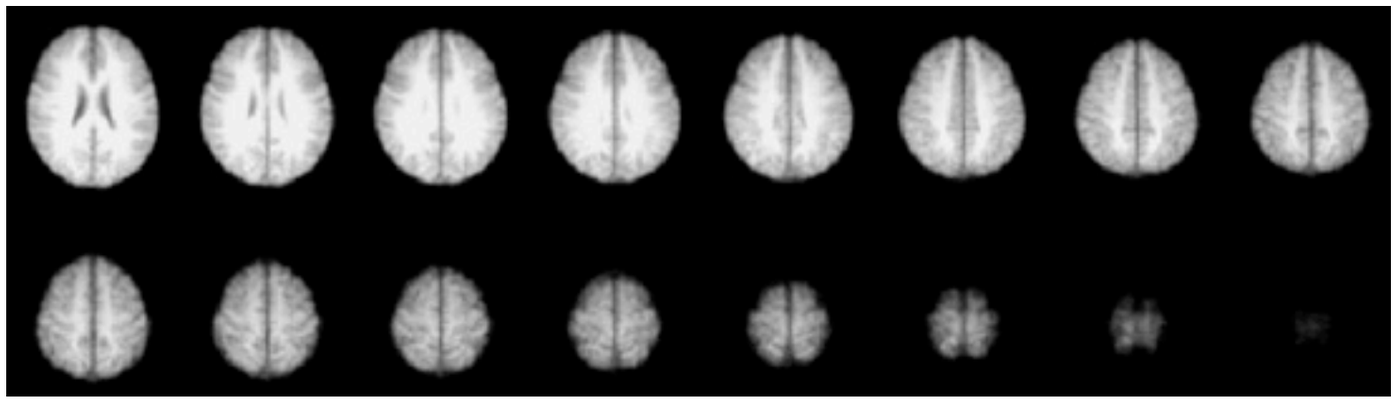

LEFT - RIGHT contrast

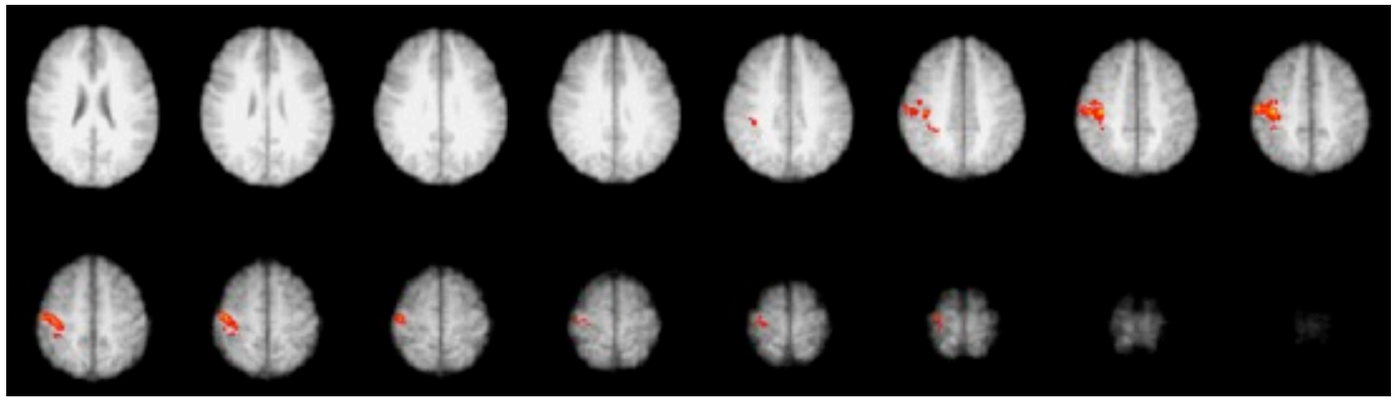

after denoising

Apparent variability

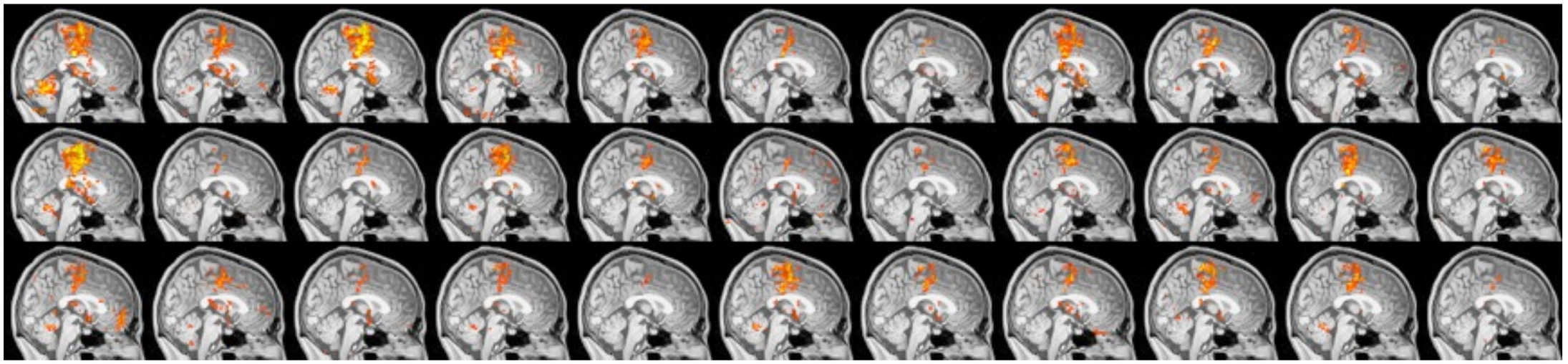

McGonigle et al.: 33 Sessions under motor paradigm

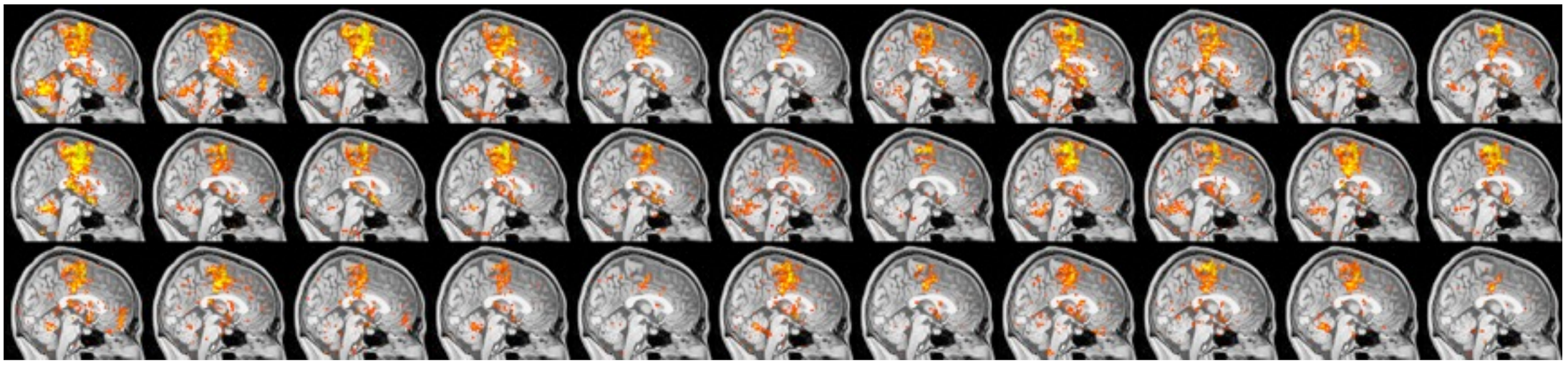

‘de-noising’ data by regressing out noise:
reduced ‘apparent’ session variability

Applications

EDA techniques can be useful to

- investigate the BOLD response
- estimate artefacts in the data
- find areas of 'activation' which respond in a non-standard way
- analyse data for which no model of the BOLD response is available

Example of nonstandard temporal response

- use EPI readout gradient noise to evoke auditory responses in patients before cochlear implant surgery

MODIFIED EPI GRADIENT-TRAIN WITH READ-OUT OMISSIONS & EXPECTED AUDITORY BOLD SIGNAL MODULATIONS:

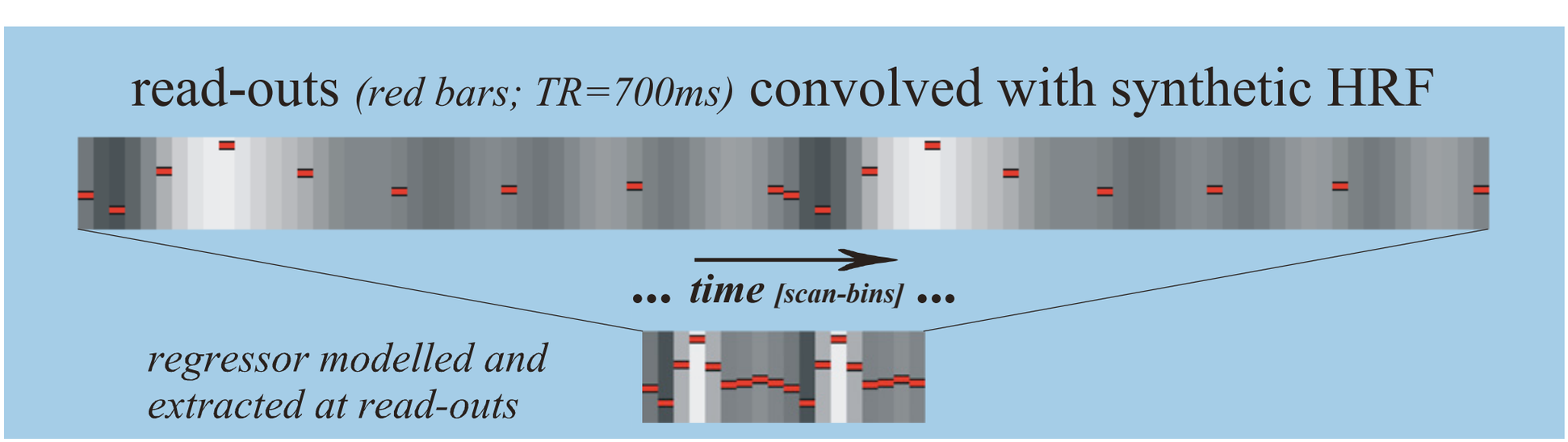

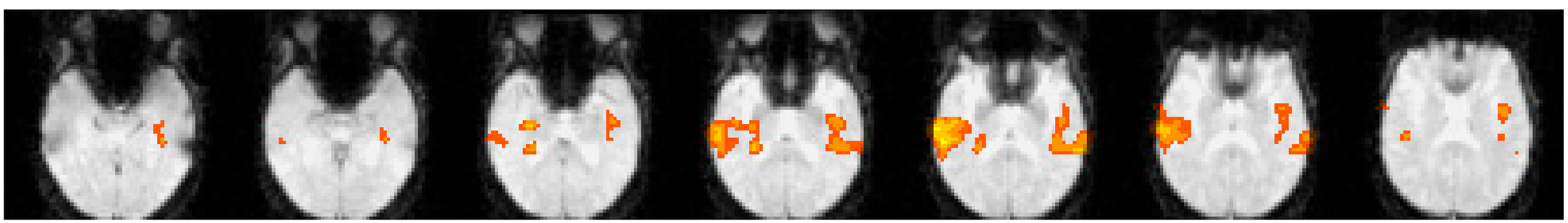

Bartsch et al. HBM 2004

Example of nonstandard temporal response

- use EPI readout gradient noise to evoke auditory responses in patients before cochlear implant surgery

MODIFIED EPI GRADIENT-TRAIN WITH READ-OUT OMISSIONS & EXPECTED AUDITORY BOLD SIGNAL MODULATIONS:

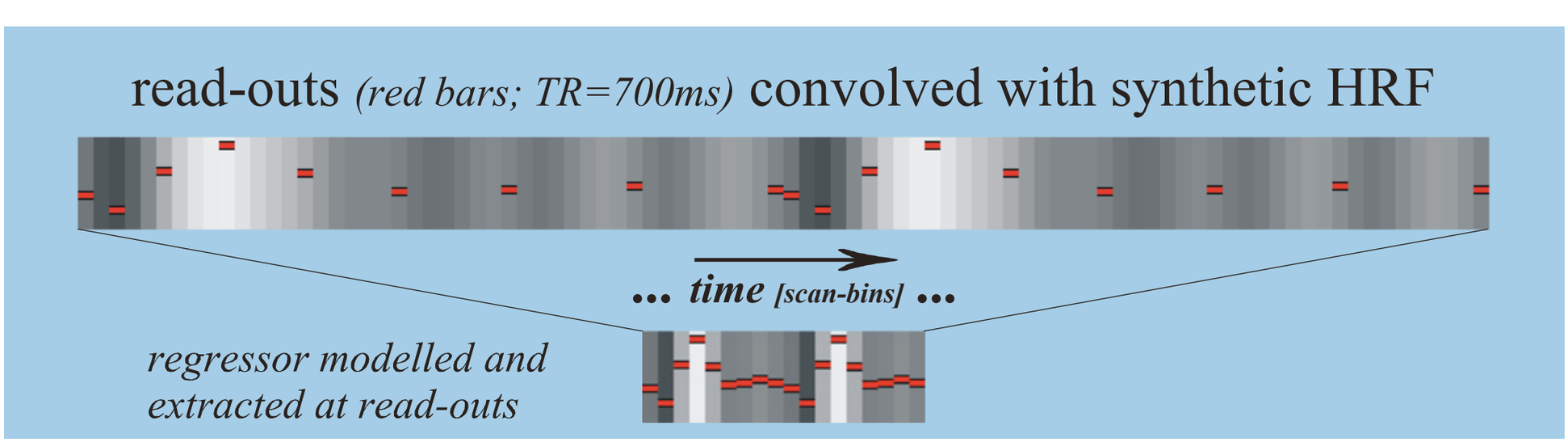

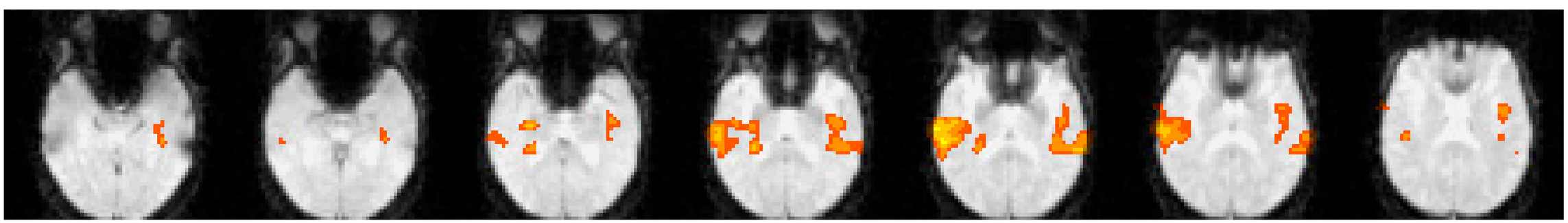

Bartsch et al. HBM 2004

Applications

EDA techniques can be useful to

- investigate the BOLD response
- estimate artefacts in the data
- find areas of 'activation' which respond in a non-standard way
- analyse data for which no model of the BOLD response is available

PICA on resting data

- perform ICA on null data and compare spatial maps between subjects/scans
- ICA maps depict spatially localised and temporally coherent signal changes

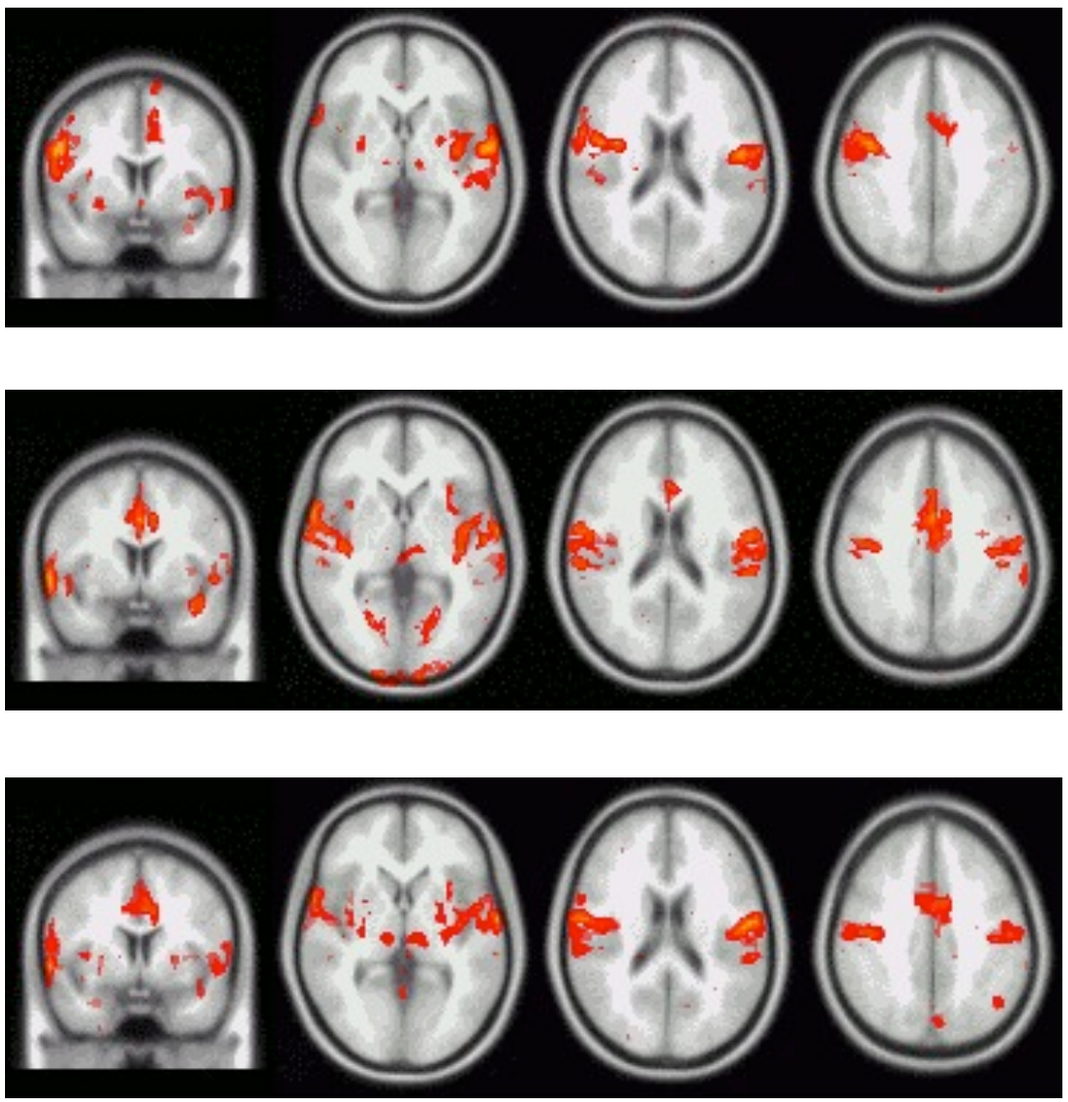

Example: ICA maps - 1 subject at 3 different sessions

Multi-Subject ICA

Different ICA models

Single-Session ICA

each ICA component comprises:

spatial map & timecourse

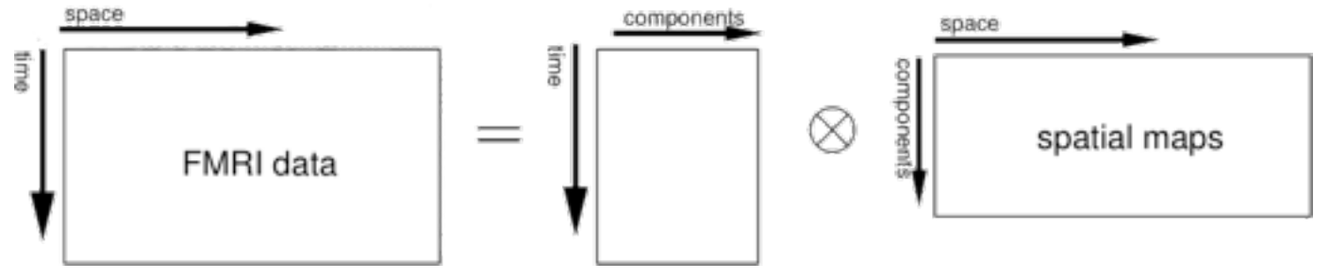

Different ICA models

Single-Session ICA

each ICA component comprises:
spatial map & timecourse

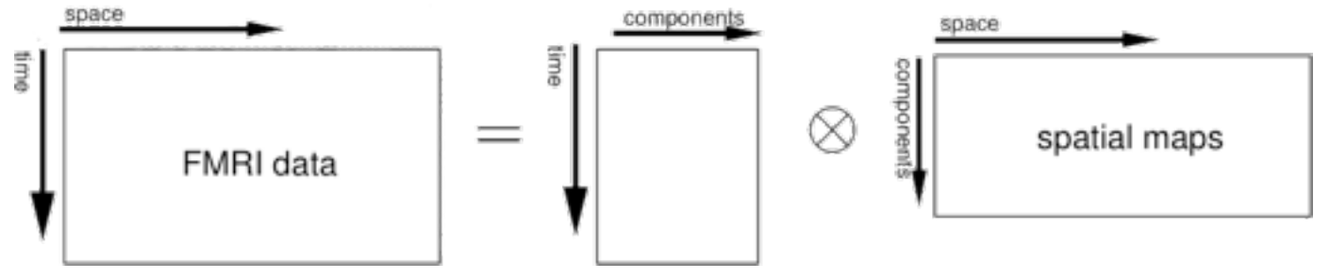

Multi-Session or Multi-Subject ICA: **Concatenation approach**

each ICA component comprises:
spatial map & timecourse
(that can be split up into subject-specific chunks)

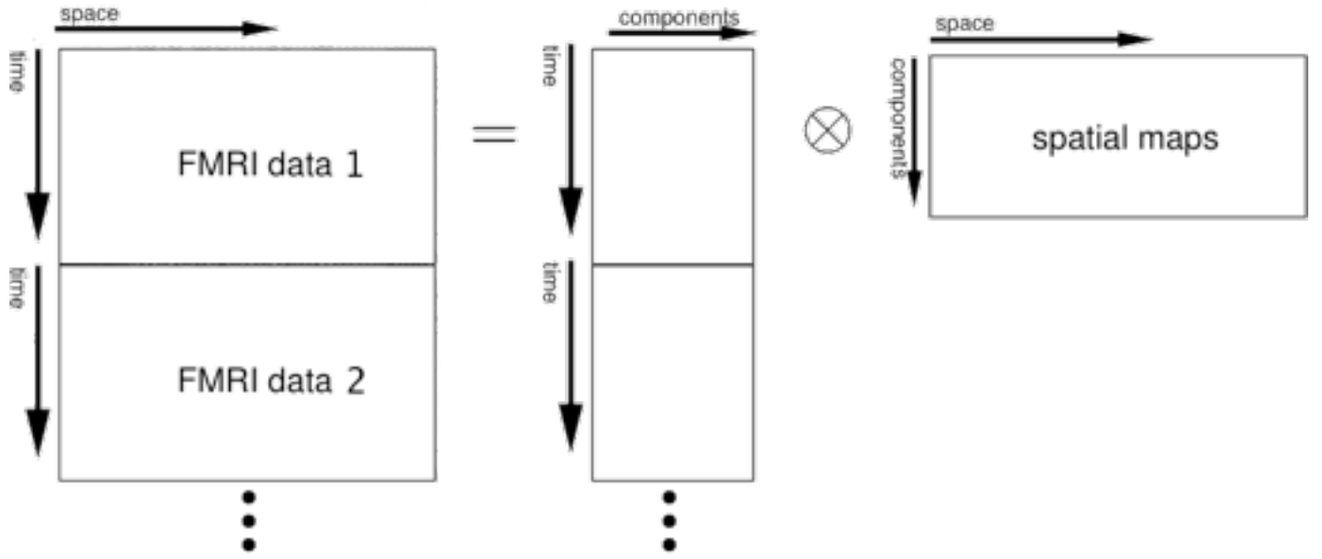

Different ICA models

Single-Session ICA

each ICA component comprises:
spatial map & timecourse

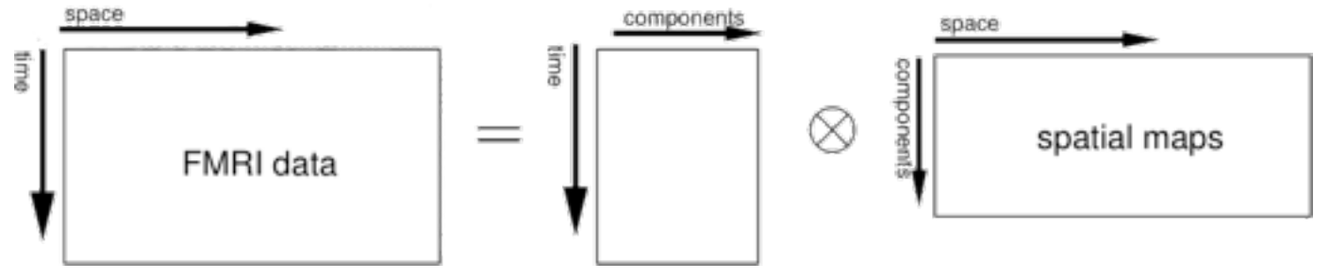

Multi-Session or Multi-Subject ICA:
Concatenation approach

each ICA component comprises:
spatial map & timecourse
(that can be split up into subject-specific chunks)

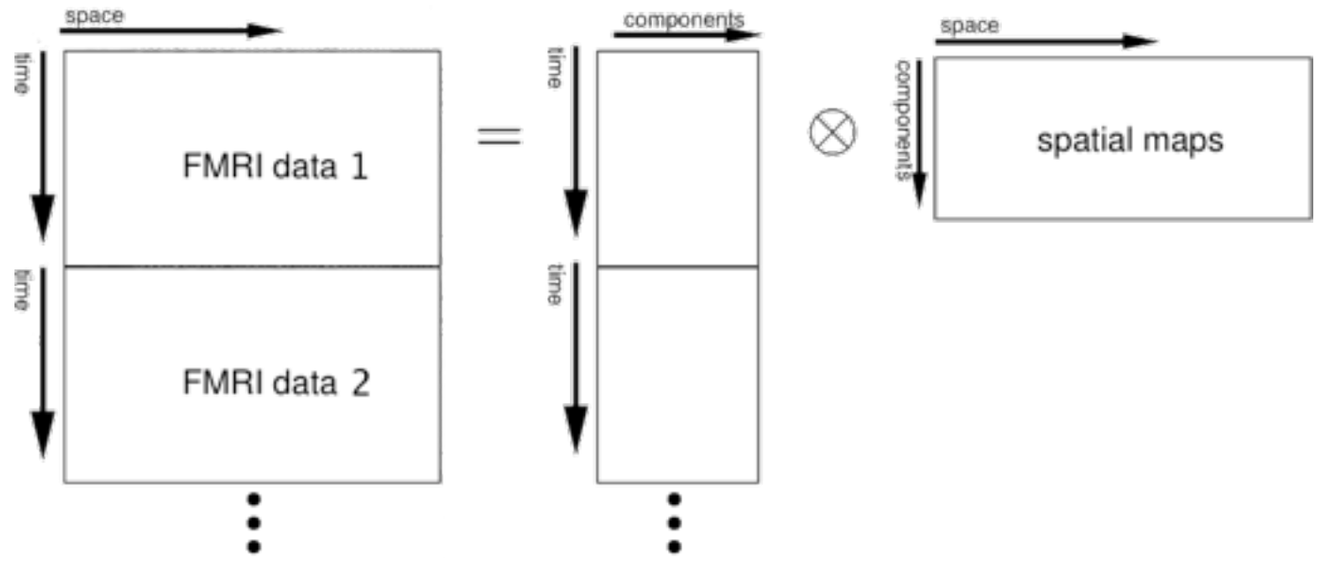

Multi-Session or Multi-Subject ICA:
Tensor-ICA approach

each ICA component comprises:
spatial map, session-long-timecourse
& subject-strength plot

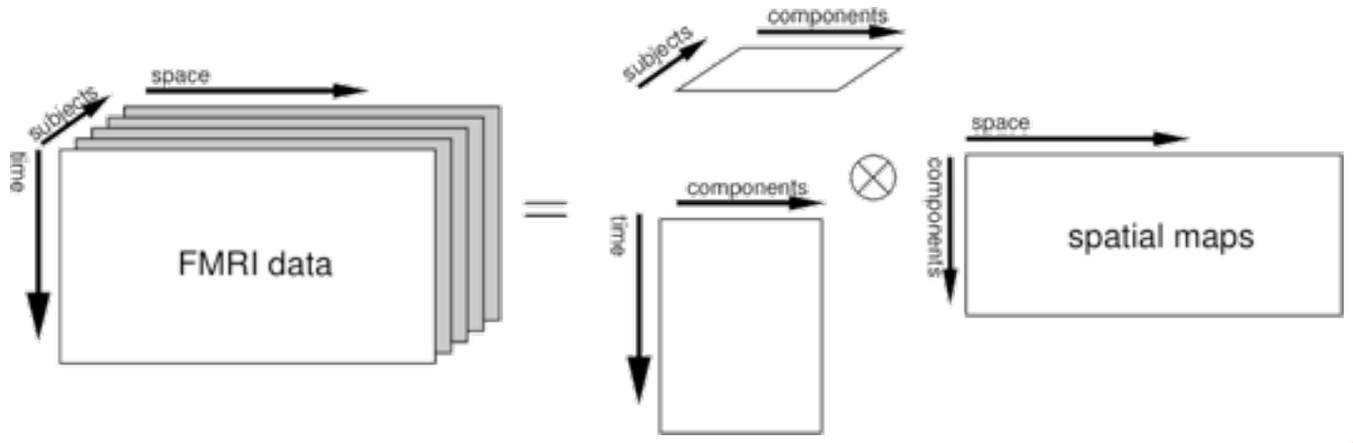

Different ICA models

Single-Session ICA

each ICA component comprises:


spatial map & timecourse
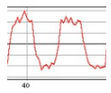

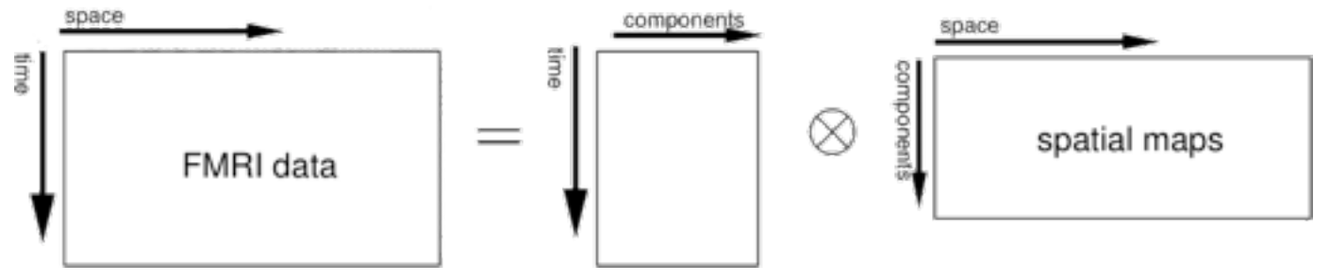

Multi-Session or Multi-Subject ICA: **Concatenation approach**

each ICA component comprises:


spatial map & timecourse
(that can be split up into subject-specific chunks)
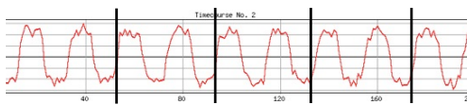

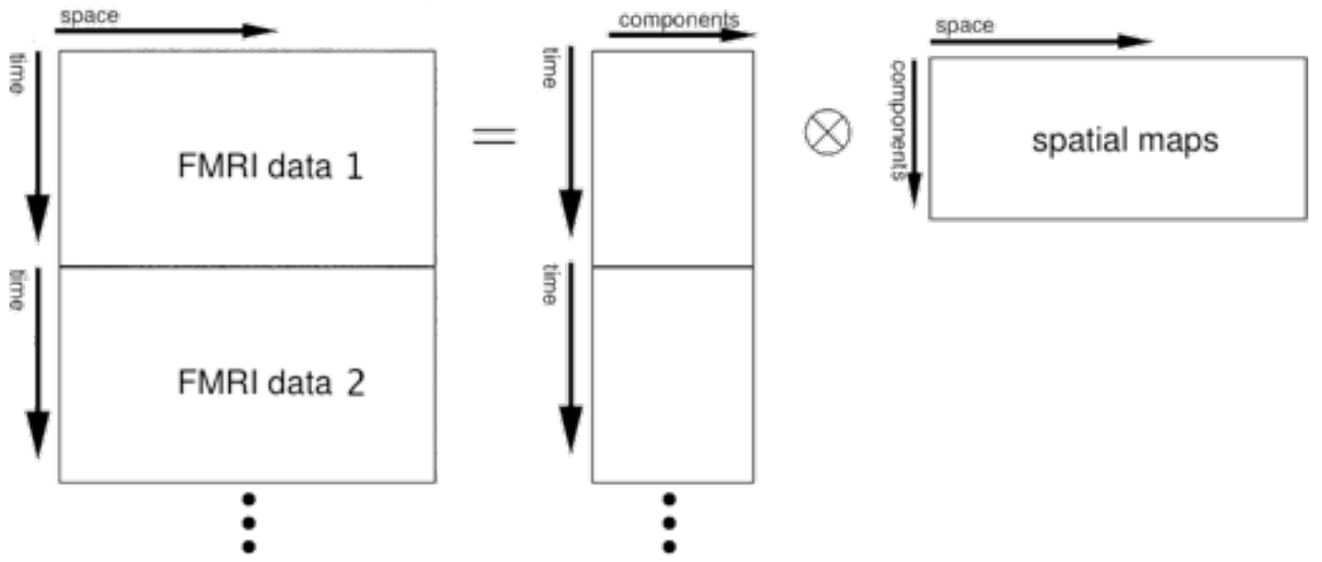

Multi-Session or Multi-Subject ICA: **Tensor-ICA approach**

each ICA component comprises:

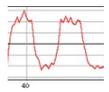

spatial map, session-long-timecourse & subject-strength plot


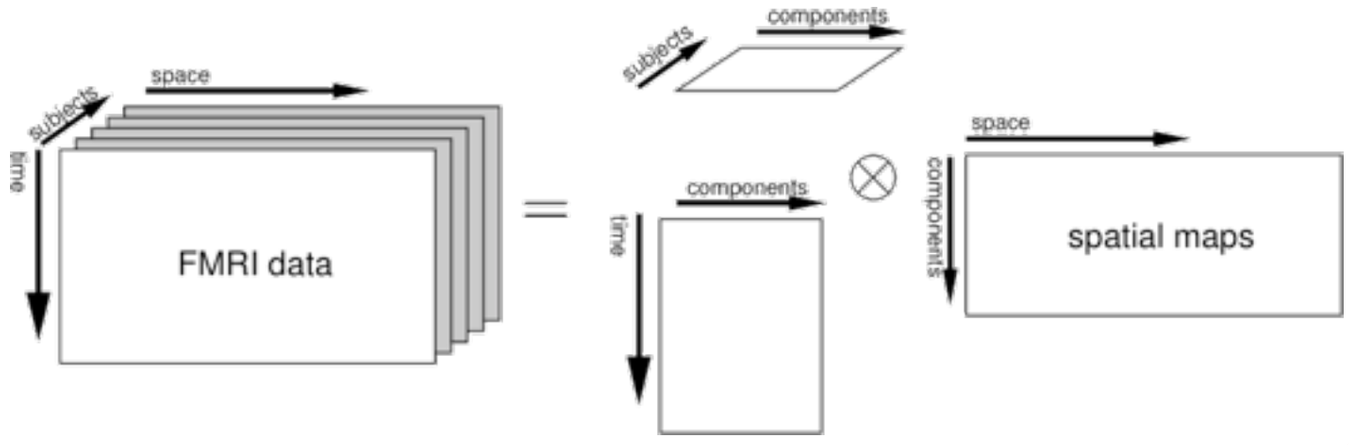

Different ICA models

Single-Session ICA

each ICA component comprises:
spatial map & timecourse

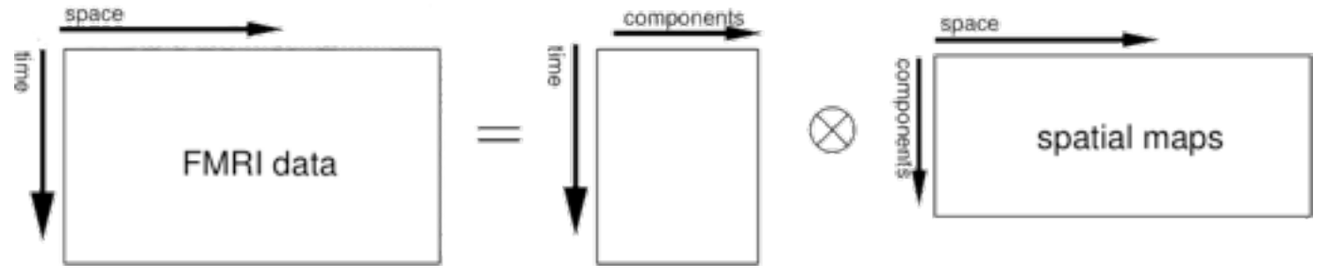

Multi-Session or Multi-Subject ICA:
Concatenation approach

good when:
each subject has DIFFERENT timeseries
e.g. resting-state FMRI

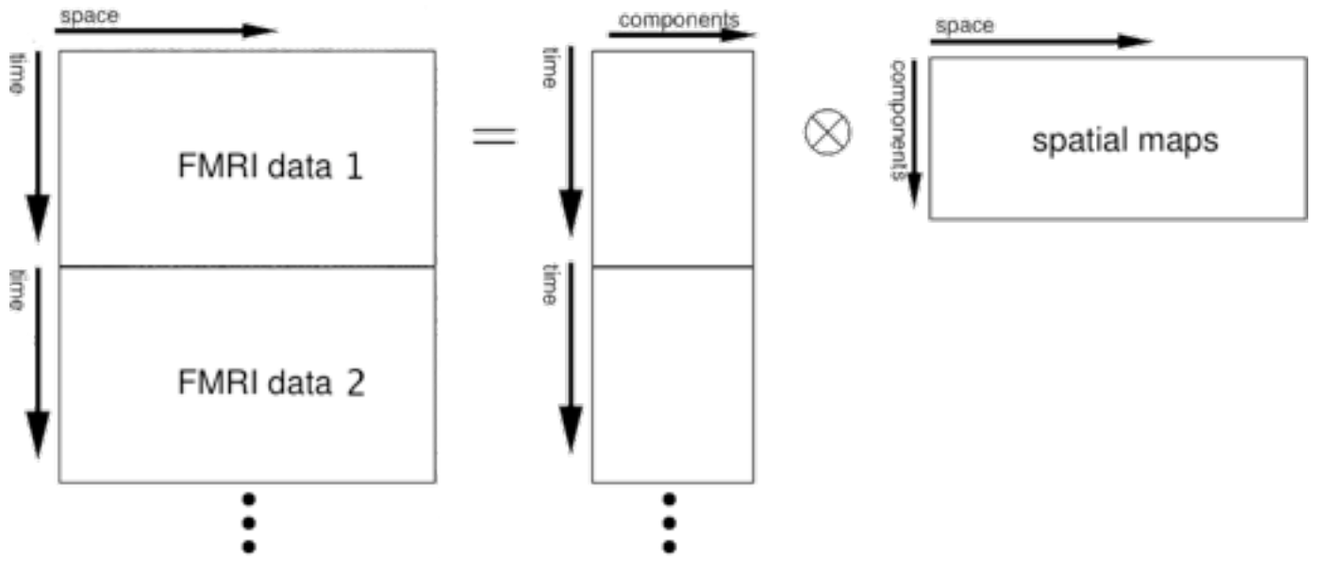

Multi-Session or Multi-Subject ICA:
Tensor-ICA approach

good when:
each subject has SAME timeseries
e.g. activation FMRI

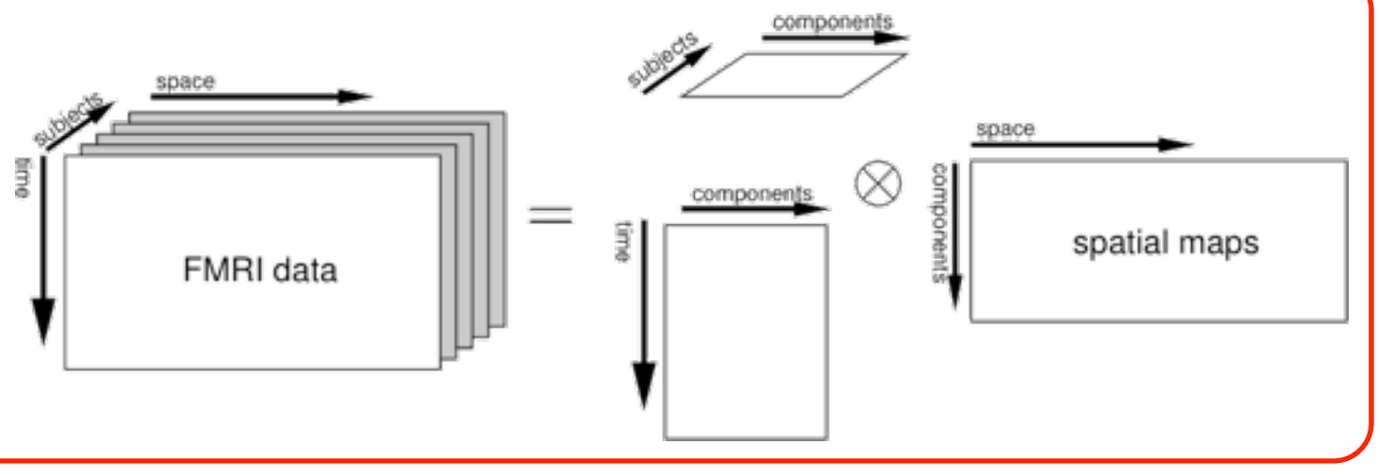

ICA Group analysis

Extend single ICA to higher dimensions

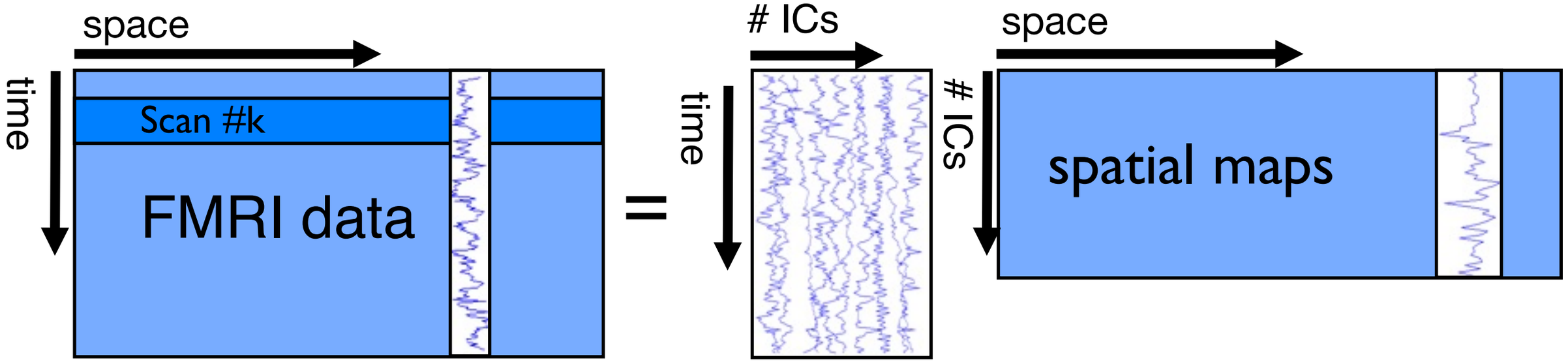

Bi-linear model

ICA Group analysis

Extend single ICA to higher dimensions

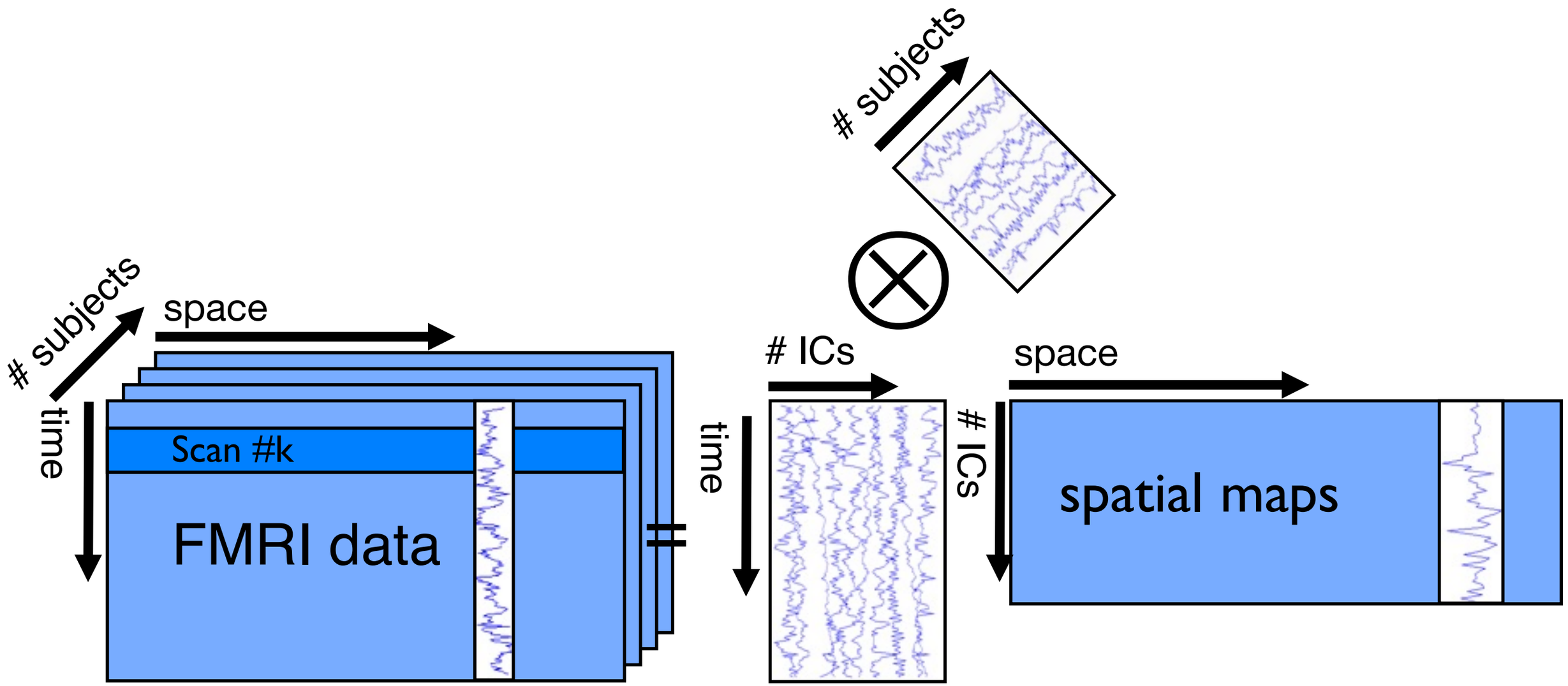

Tri-linear model

Unfolding

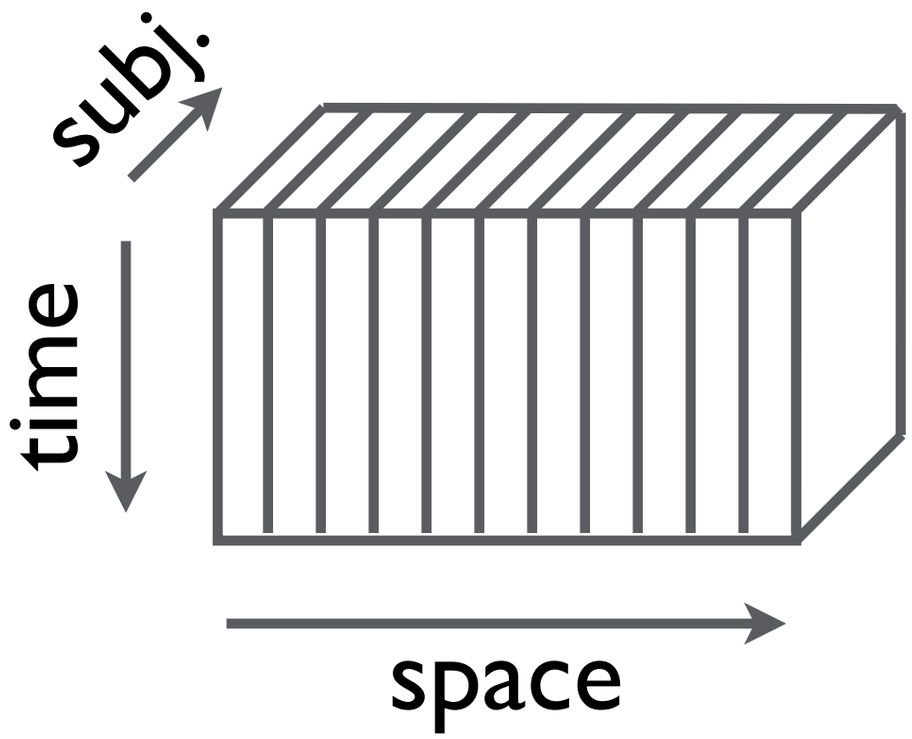

Unfolding

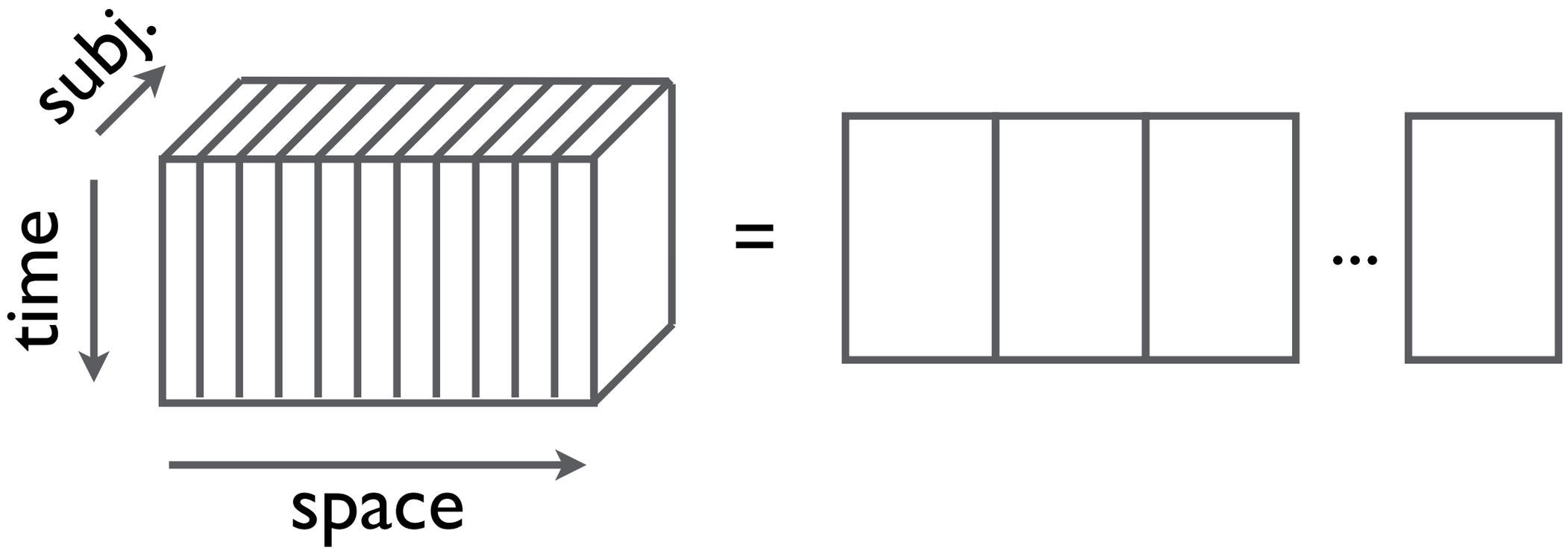

create (#vols × #subj.) matrix for each voxel and concatenate

Unfolding

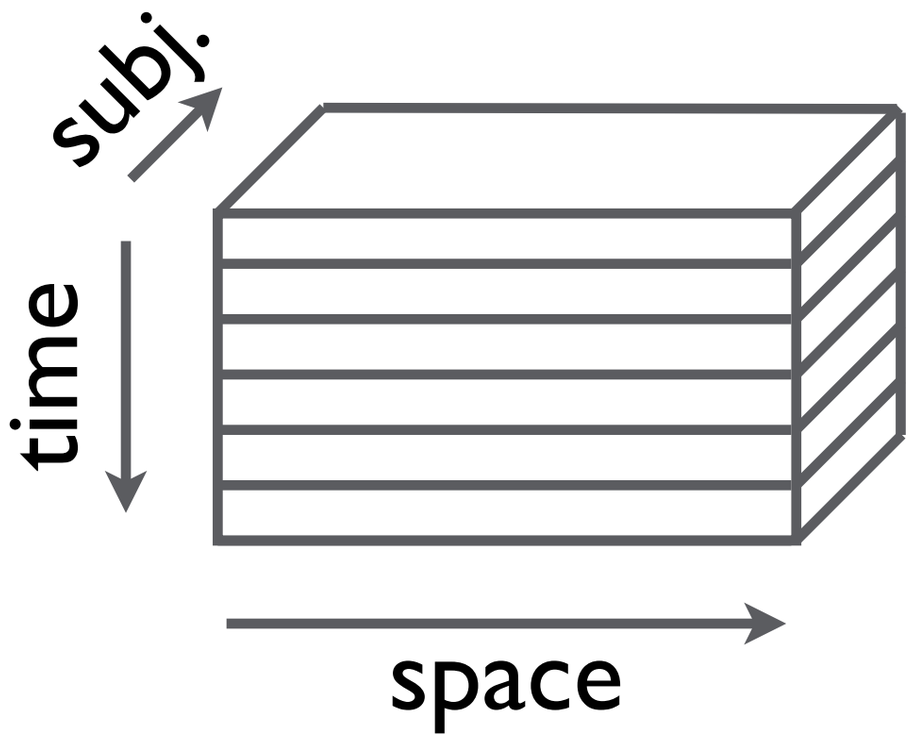

Unfolding

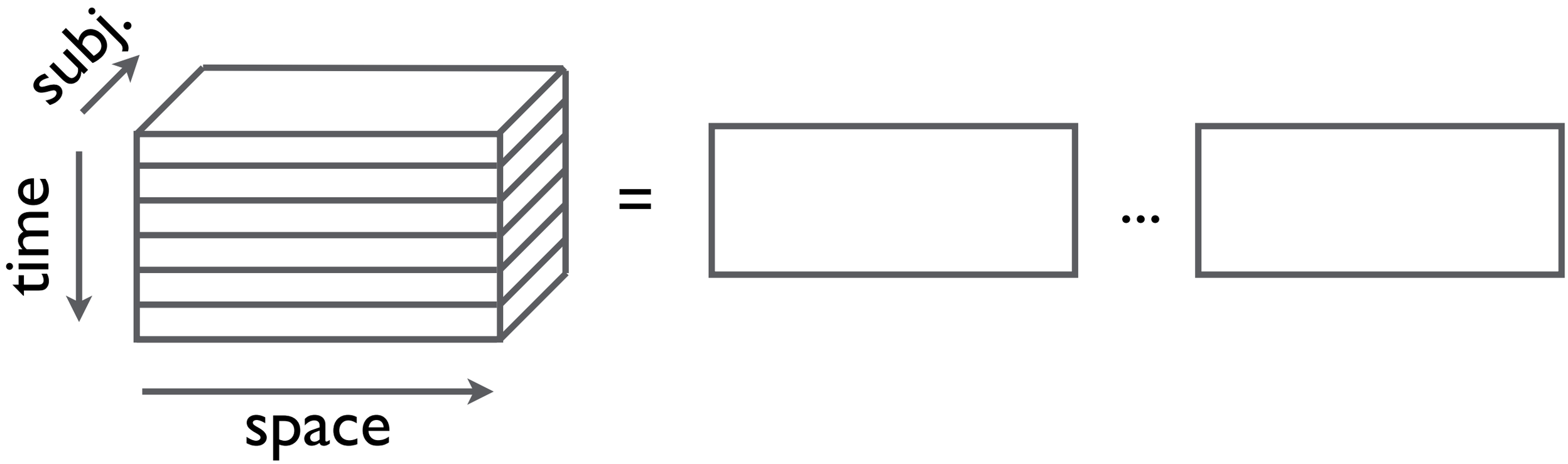

create a (#subj. × #voxels) matrix for each time point and concatenate

Unfolding

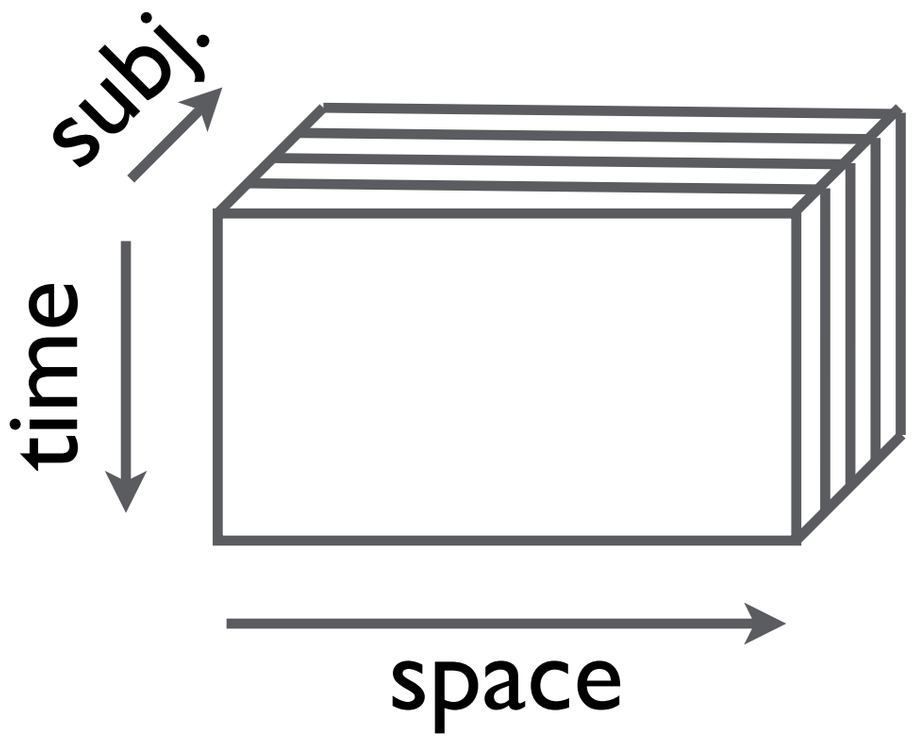

Unfolding

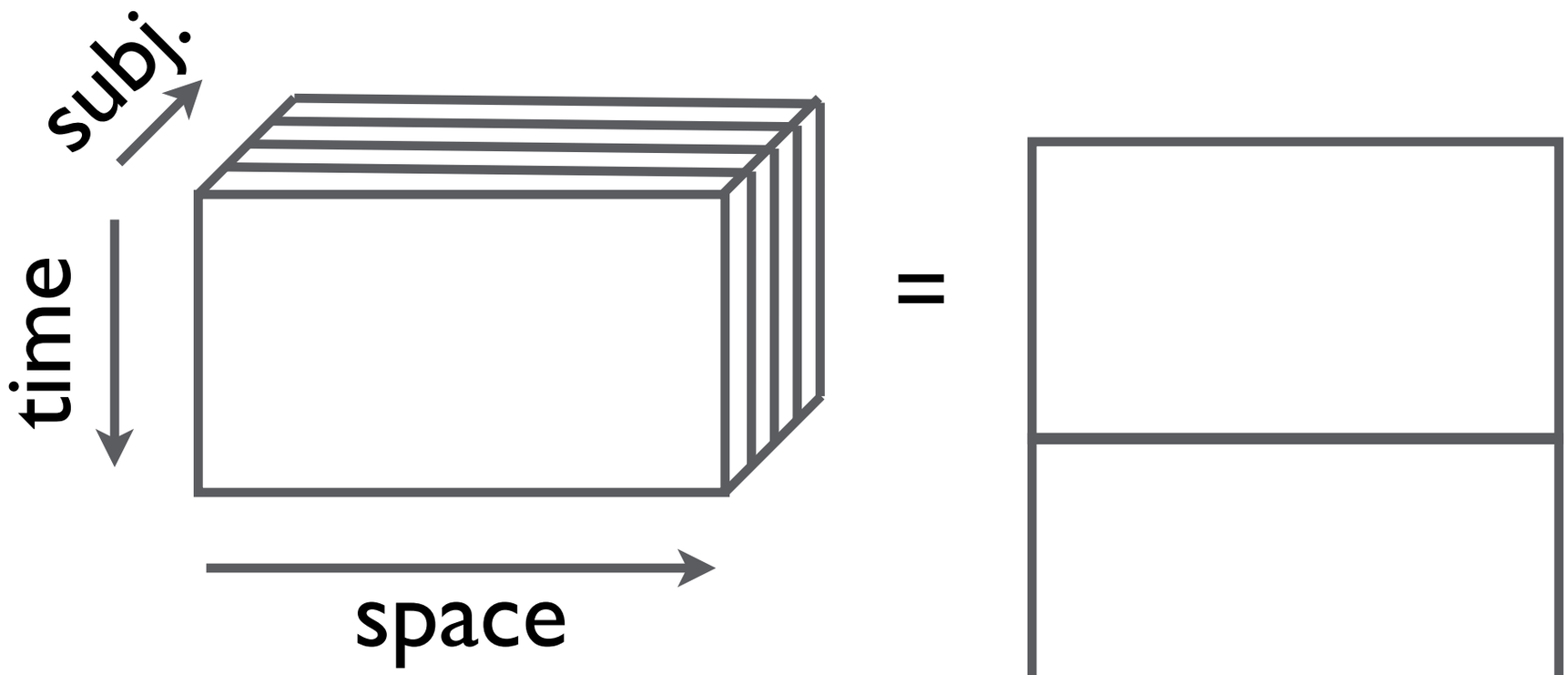

create a (#vols. × #voxels) matrix for each subject and concatenate temporally

PARAFAC

PARAFAC

- as a symmetric least-square problem this is known as *Parallel Factor Analysis*  *Harshman 1970*

PARAFAC

- as a symmetric least-square problem this is known as *Parallel Factor Analysis*  *Harshman 1970*

- can be solved using *Alternating Least Squares (ALS)*, i.e. iterating between least-squares solution for each one of the three different representations

- *Problem:* treats all modes the same

Tensor-PICA

- can be treated as a 2-stage estimation problem

Tensor-PICA

- can be treated as a 2-stage estimation problem

1. (2D) PICA estimation of the spatial maps from the concatenated data (volumes * subjects) × voxels

Tensor-PICA

- can be treated as a 2-stage estimation problem

1. (2D) PICA estimation of the spatial maps from the concatenated data (volumes * subjects) × voxels

2. rank-1 Eigen-decomposition of each column of the mixing matrix, reshaped into a (volumes × subjects) matrix, in order to find underlying factors

Beckmann and Smith NI 2005

Tensor-ICA

Tensor-ICA

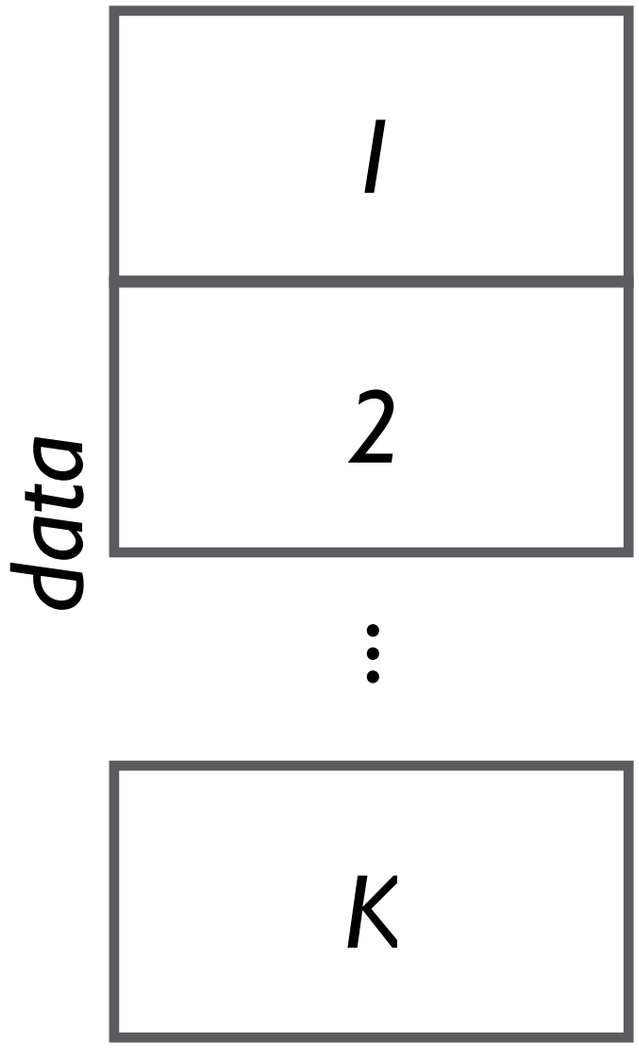

Tensor-ICA

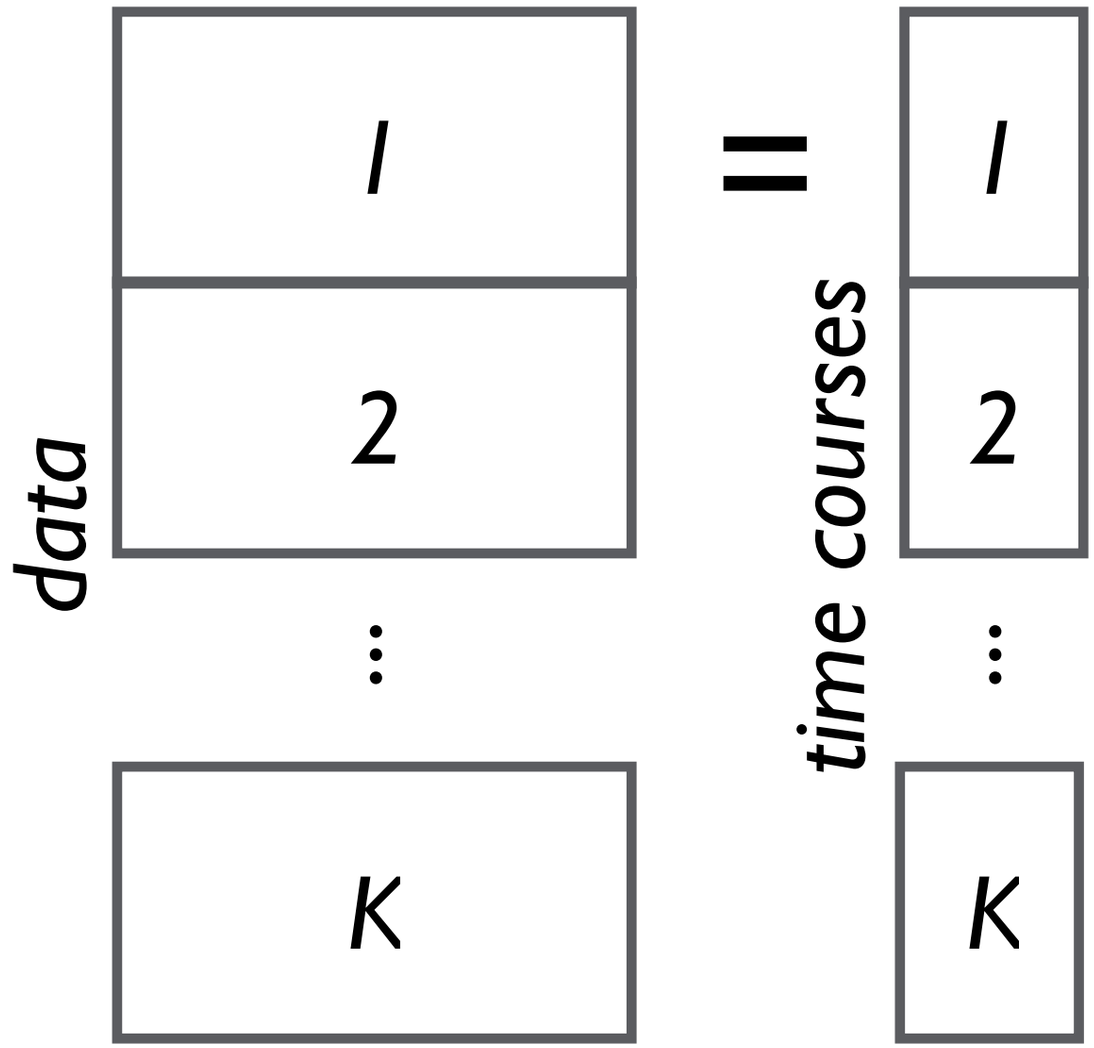

Tensor-ICA

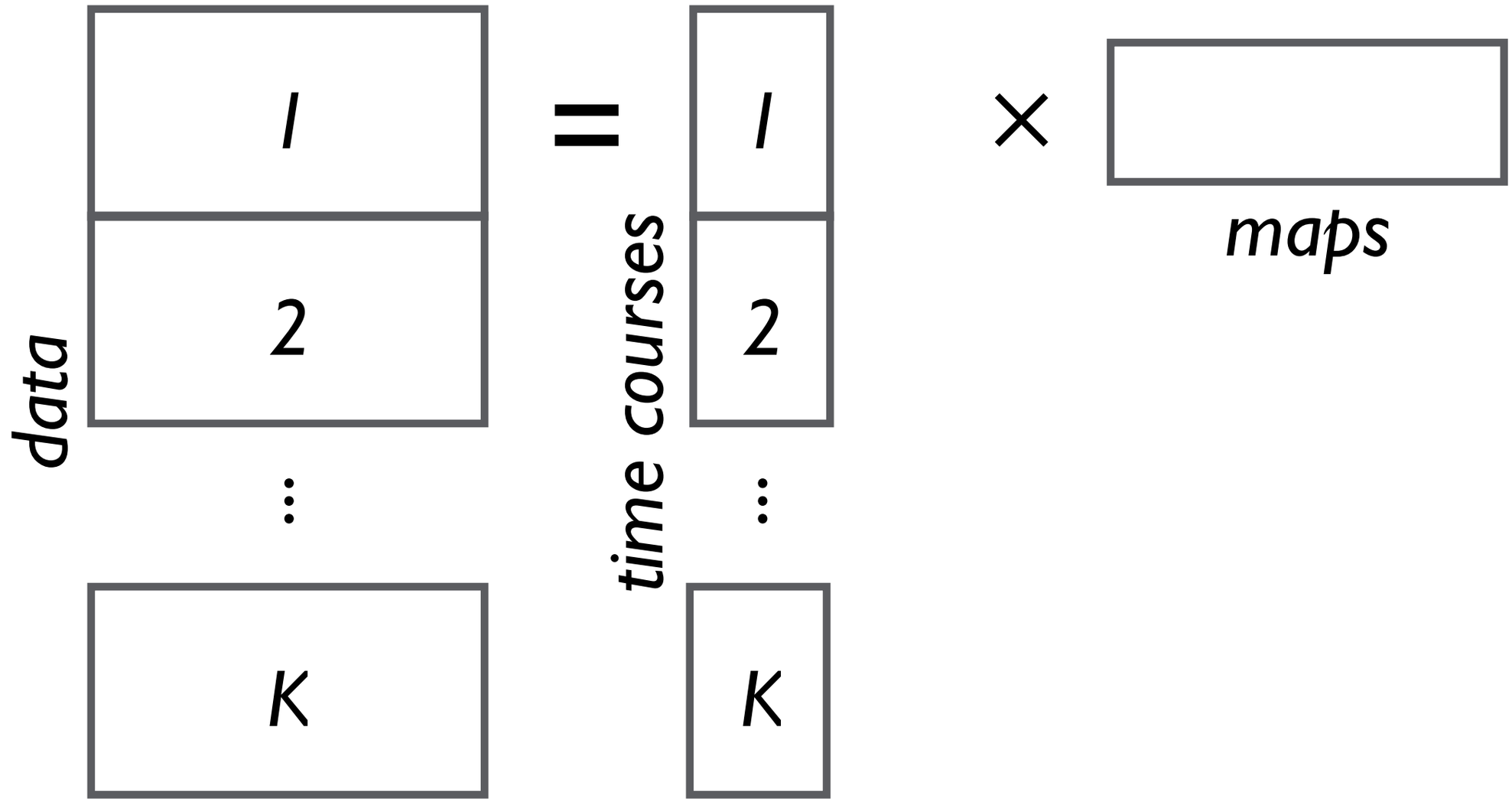

Tensor-ICA

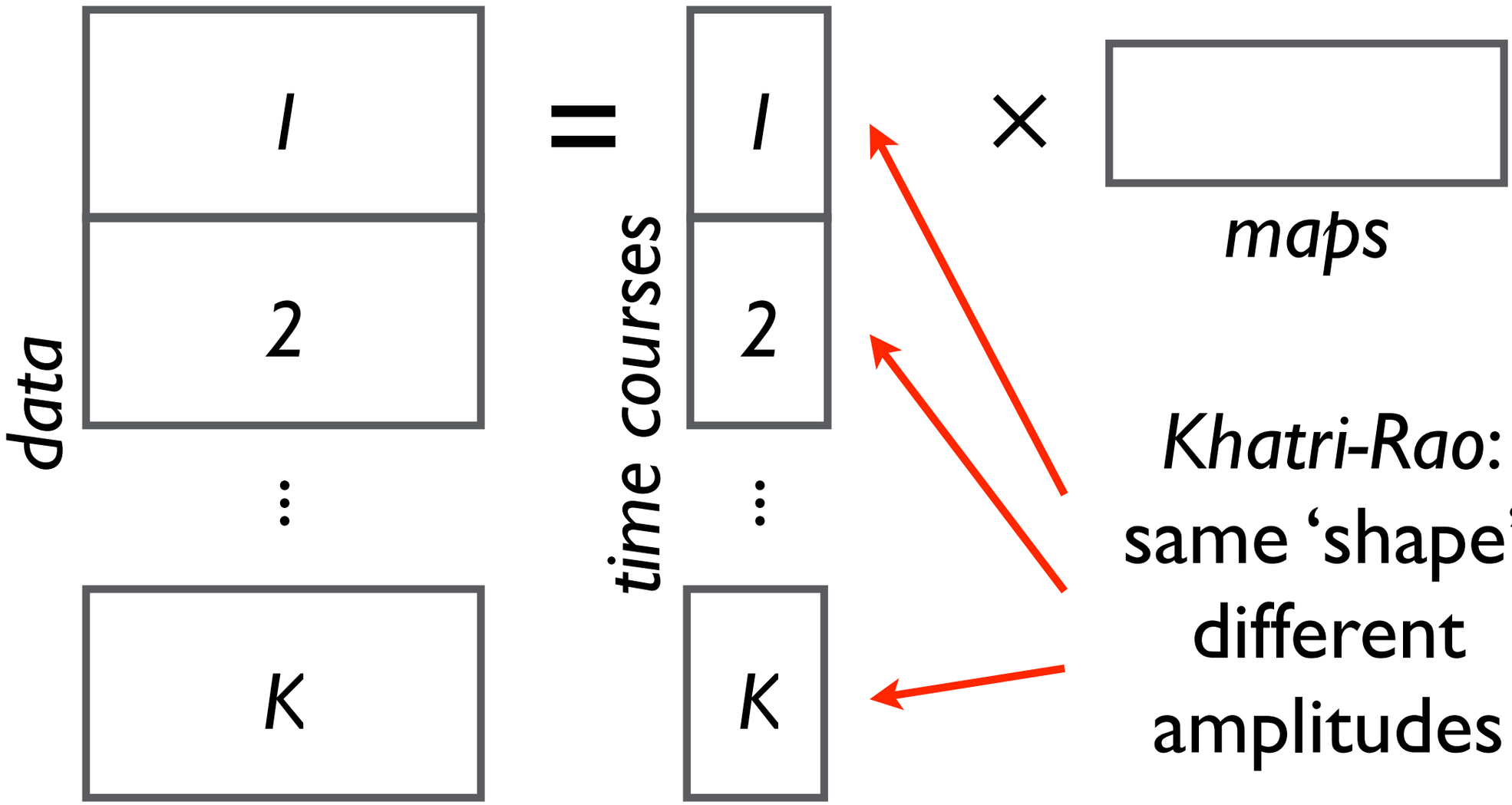
I
=
I
×
maps
data
2
time courses
2
...
...
K
K
Khatri-Rao:
same ‘shape’,
different
amplitudes

Tensor-ICA

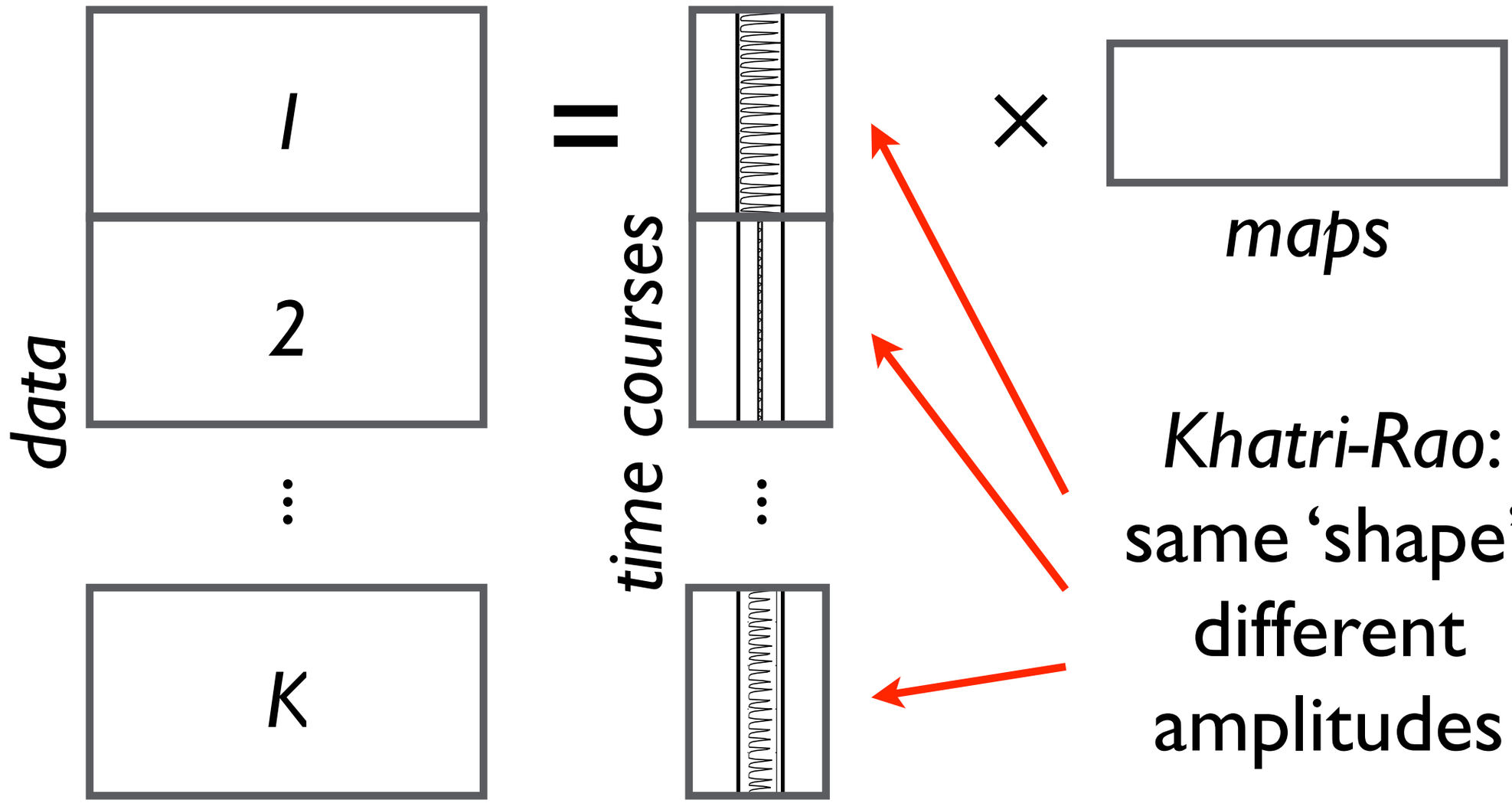
I
data
2
K
=
time courses
×
maps
Khatri-Rao:
same ‘shape’,
different
amplitudes

Tensor-PICA

- can be treated as a 2-stage estimation problem

Tensor-PICA

- can be treated as a 2-stage estimation problem
- jointly estimate modes which describe signal in the temporal/ spatial and subject domain

Tensor-PICA

- can be treated as a 2-stage estimation problem
- jointly estimate modes which describe signal in the temporal/ spatial and subject domain
- provides a mixed-effects model (incorporates within-session and between session variations)

Tensor-ICA

- ‘robust’ statistics: can estimate common activation pattern in the presence of subject-specific processes

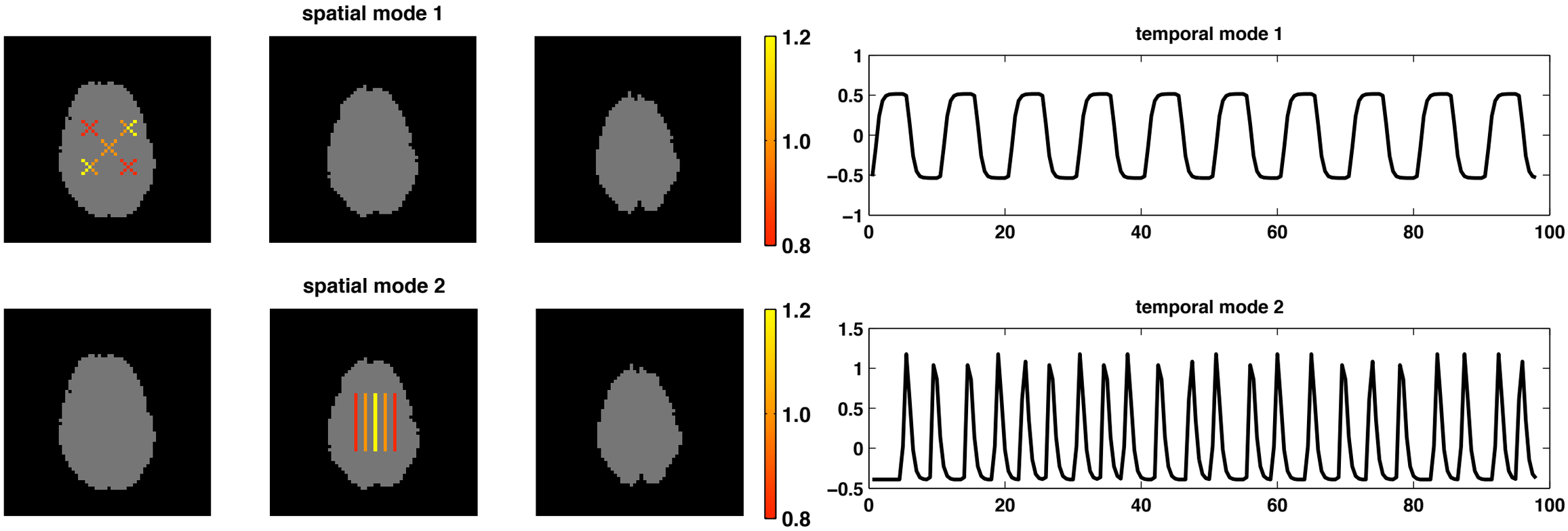

Tensor-ICA

- ‘robust’ statistics: can estimate common activation pattern in the presence of subject-specific processes

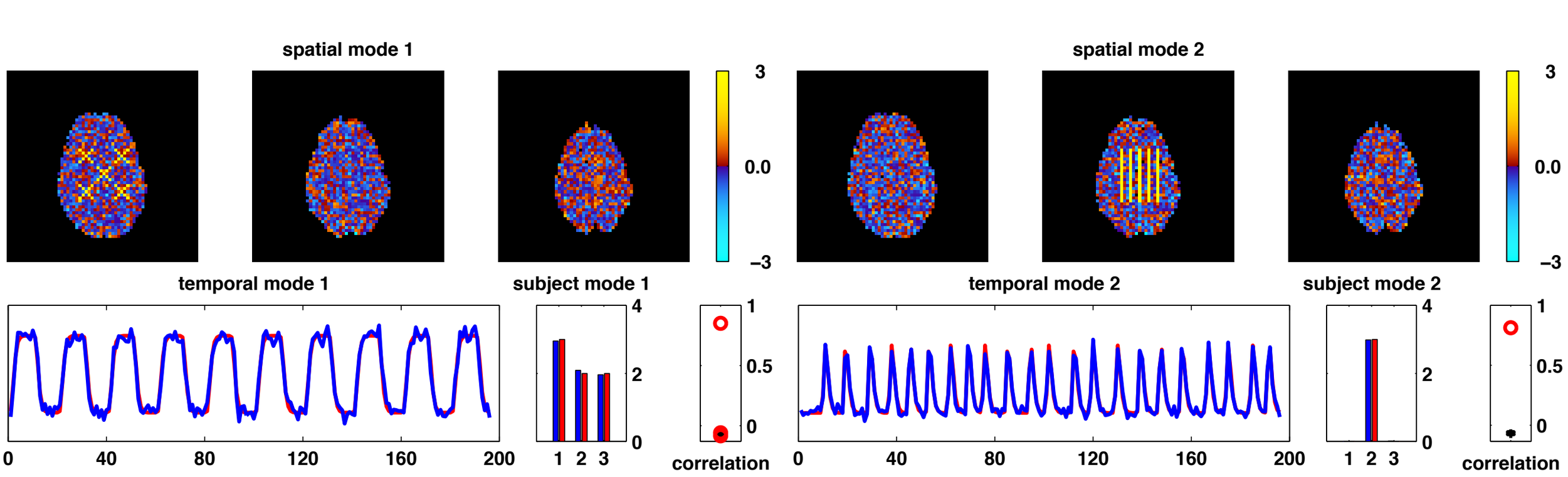

Tensor-ICA vs. PARAFAC

- more accurate (lower RMSE; less cross-talk)

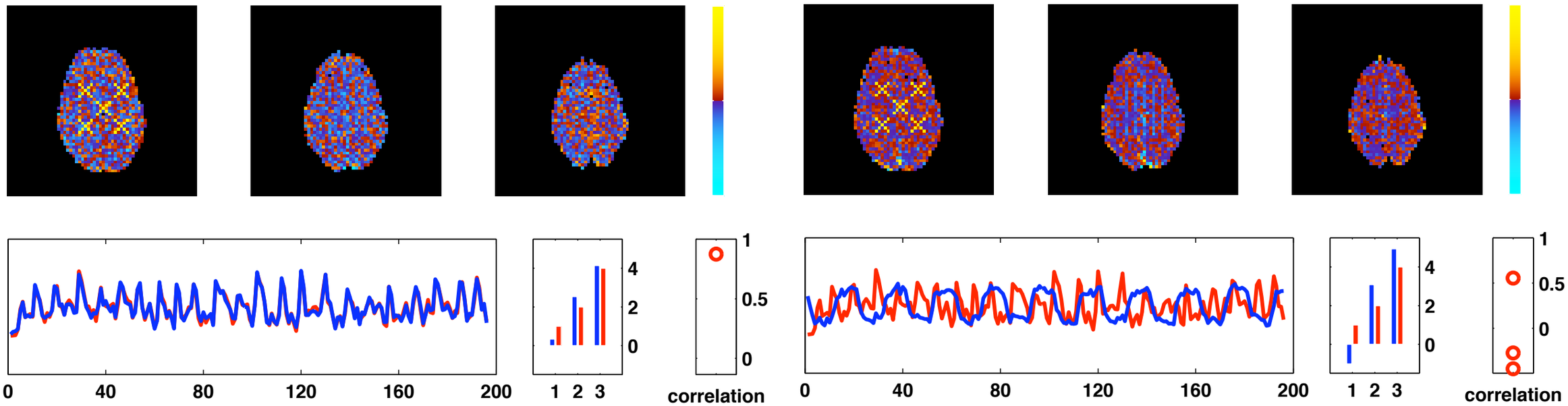

Tensor-ICA

PARAFAC

Tensor-ICA vs. PARAFAC

- more accurate (lower RMSE; less cross-talk)
- more robust against overfitting (less sensitive to model order selection)

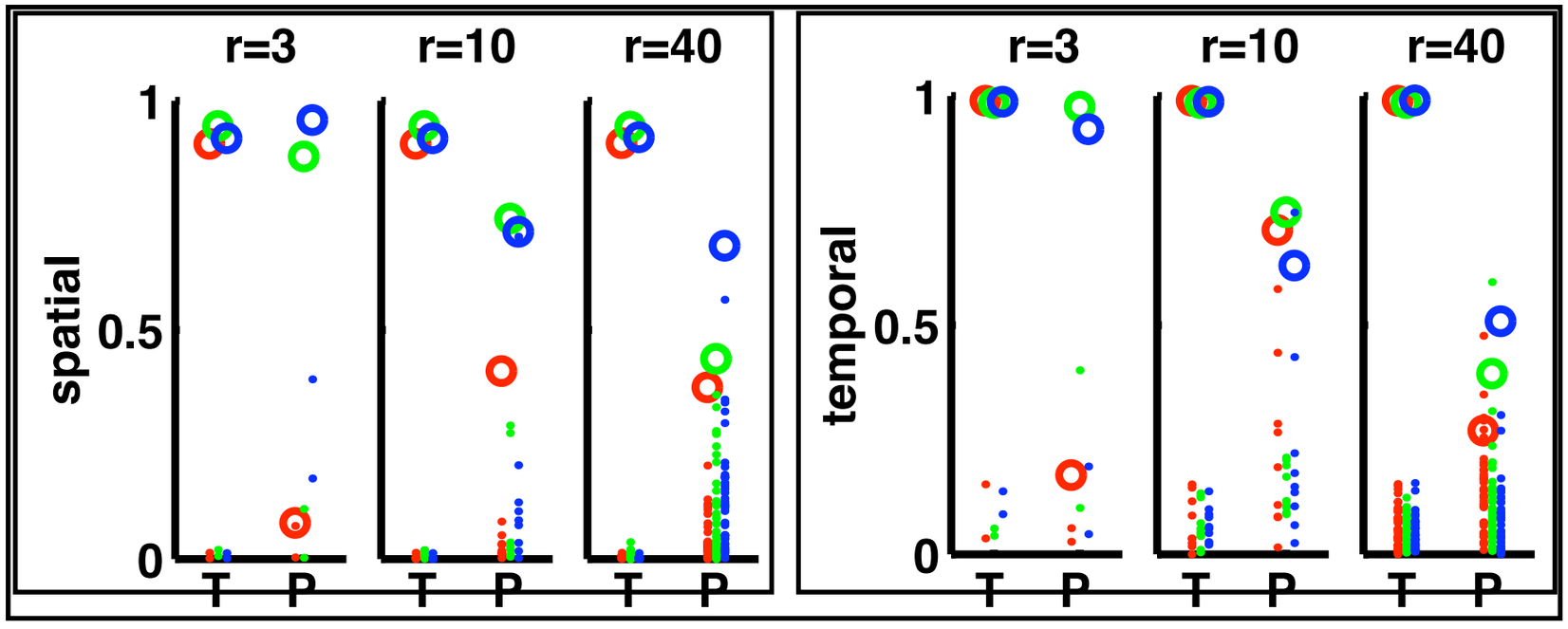

Tensor-ICA vs. PARAFAC

- more accurate (lower RMSE; less cross-talk)
- more robust against overfitting (less sensitive to model order selection)
- less computationally demanding

Tensor-ICA multi-session example

- 10 sessions under motor paradigm (right index finger tapping)
- Group-level GLM results (mixed-effects)

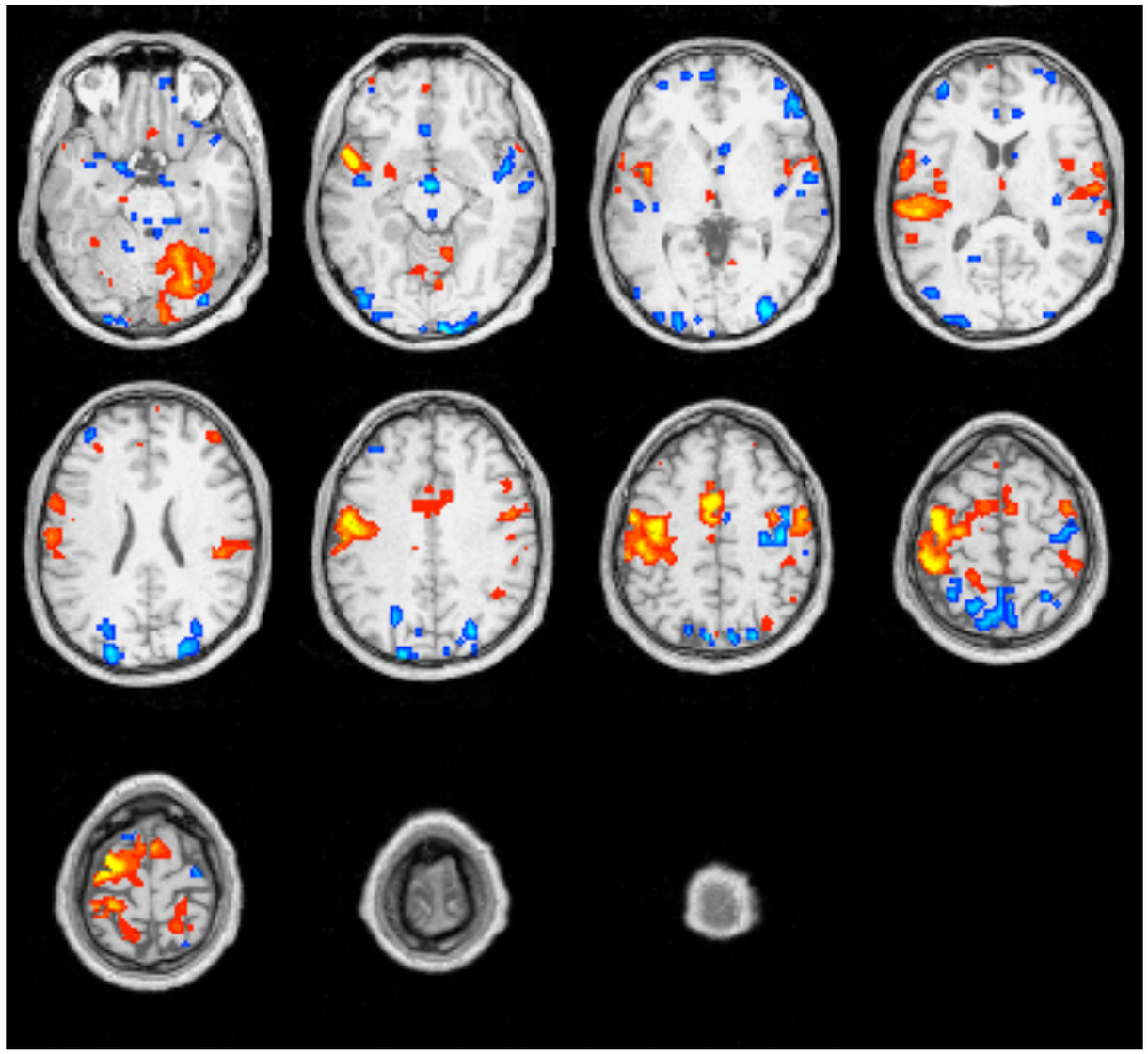

McGonigle et al. NI 2000

Tensor-ICA multi-session example

- tensor-ICA map

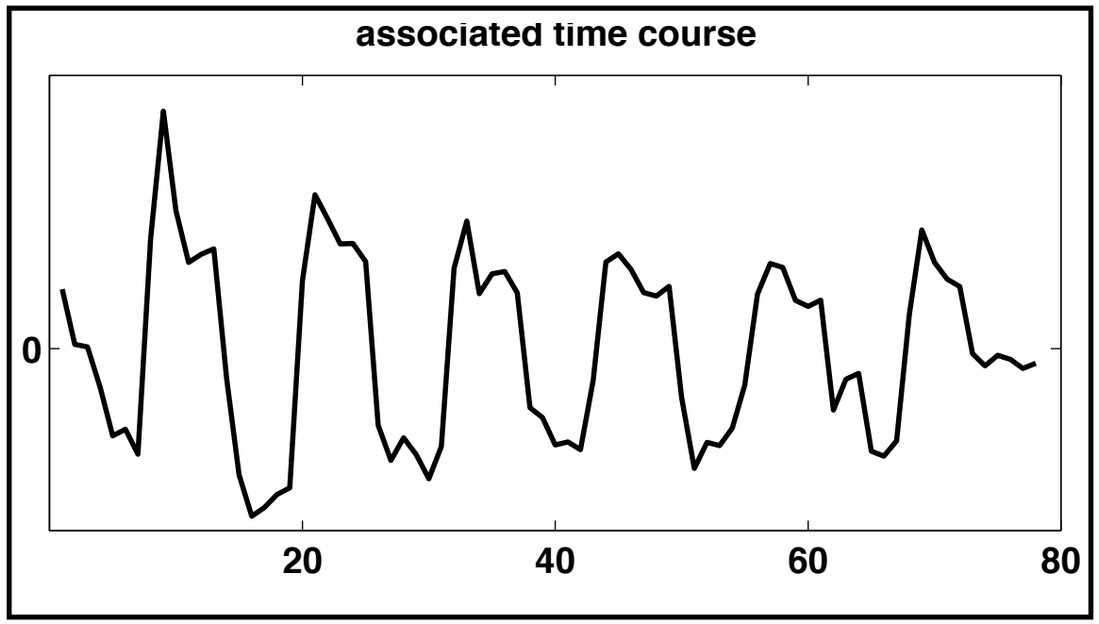

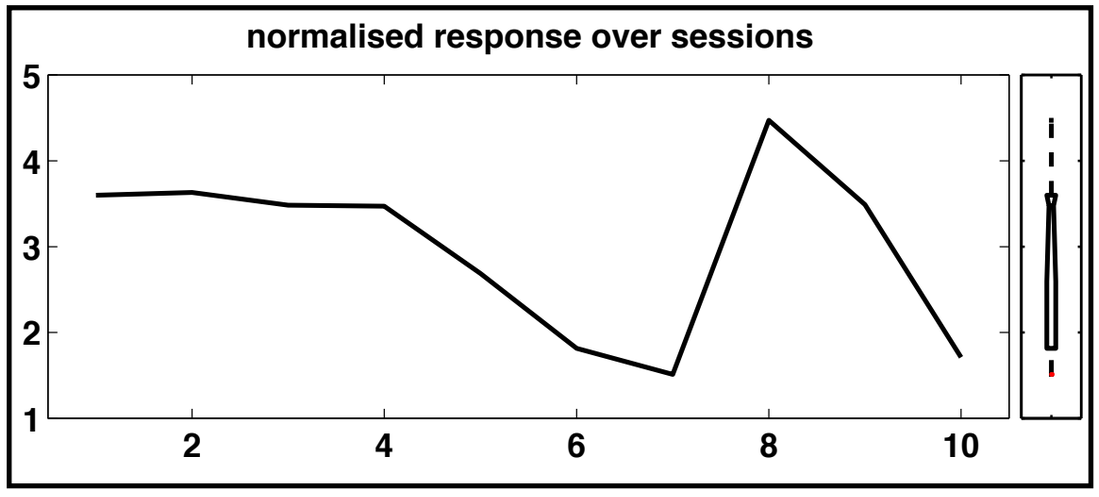

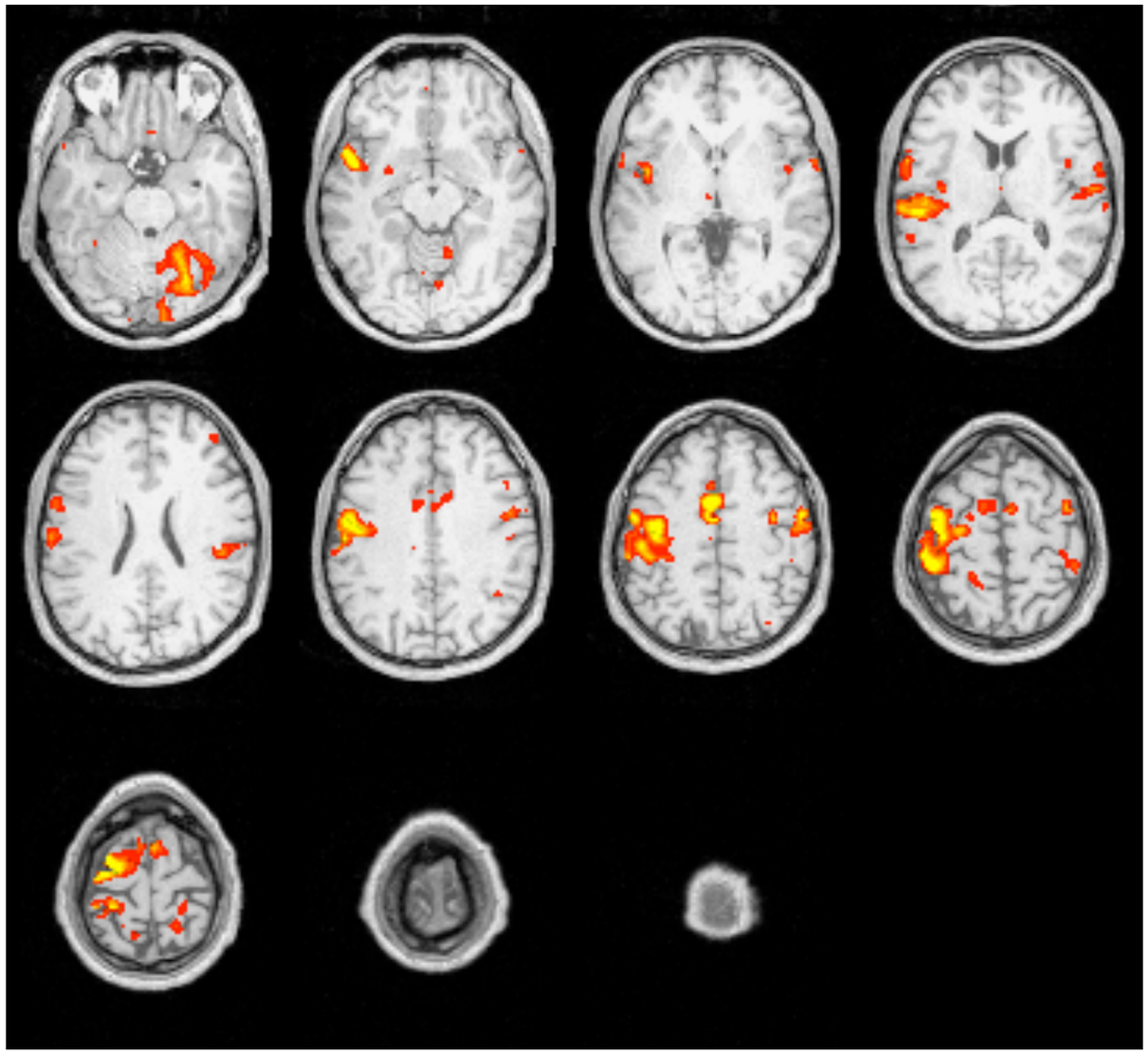

Tensor-ICA multi-session example

- estimated ‘de-activation’

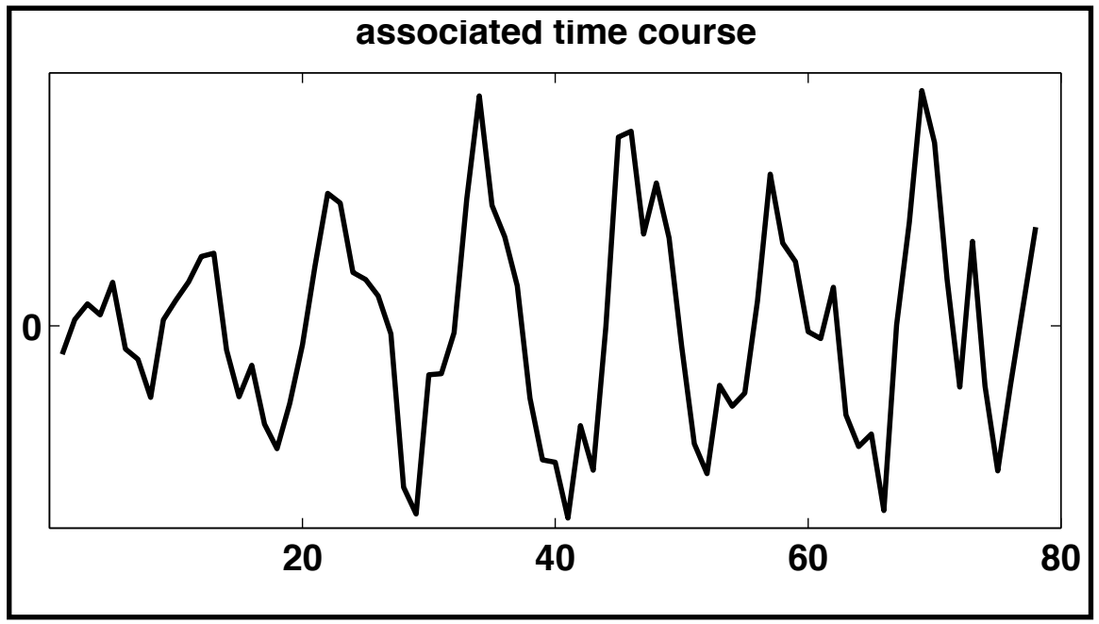

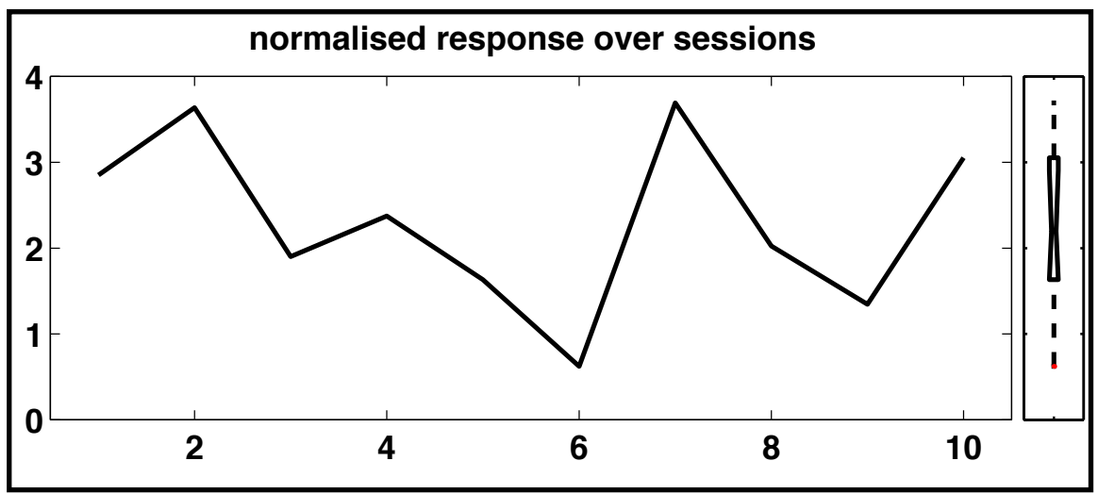

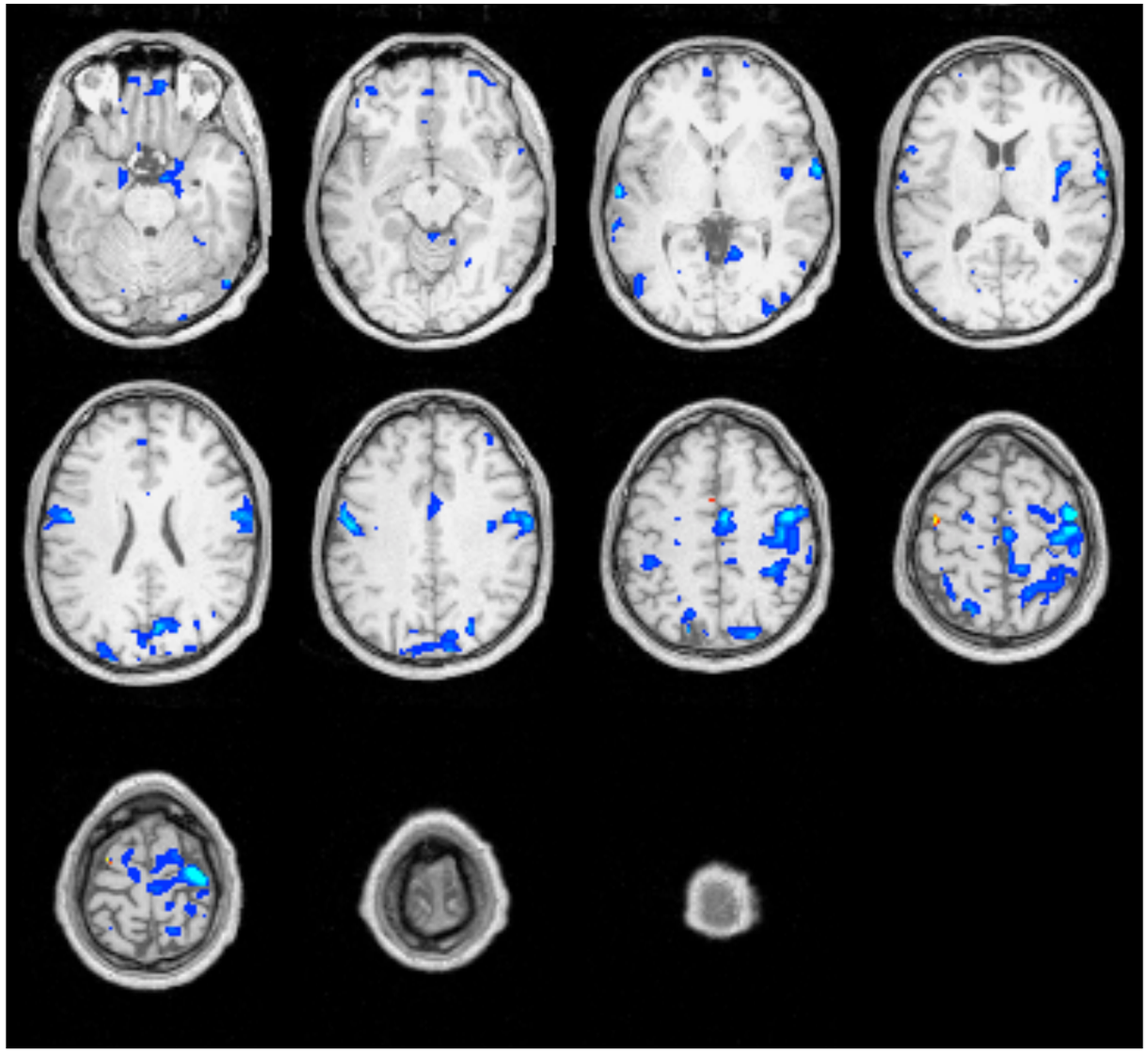

Tensor-ICA multi-session example

- residual stimulus correlated motion

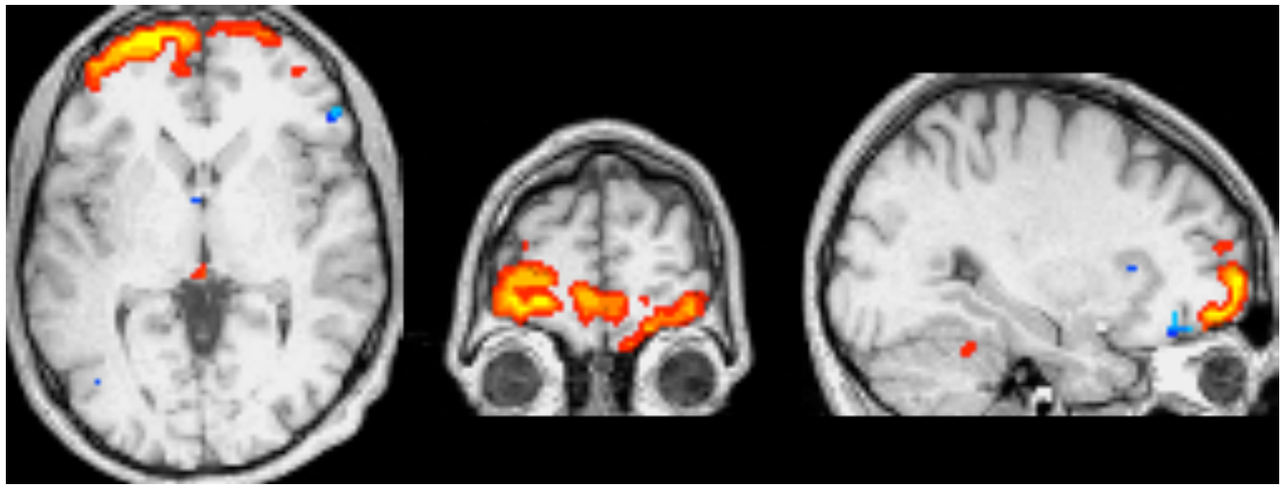

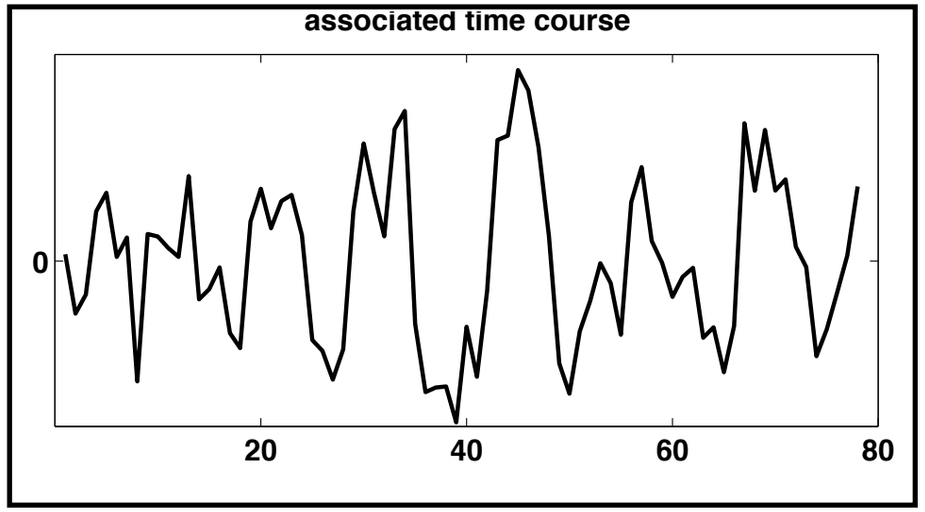

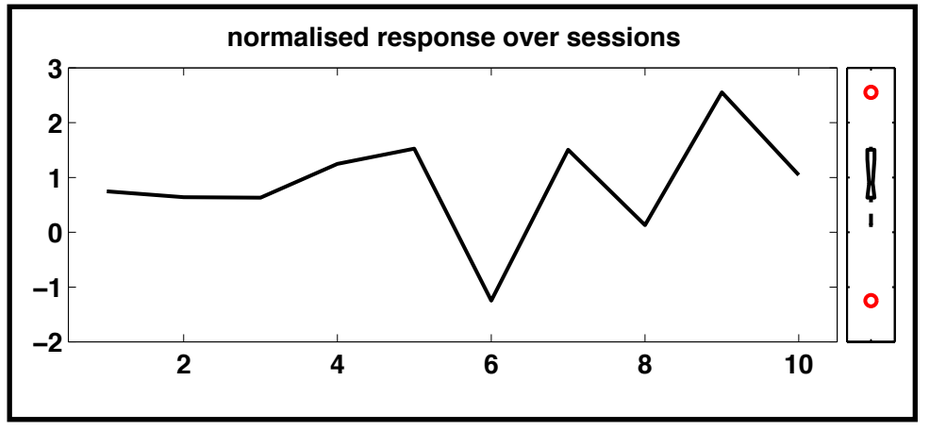

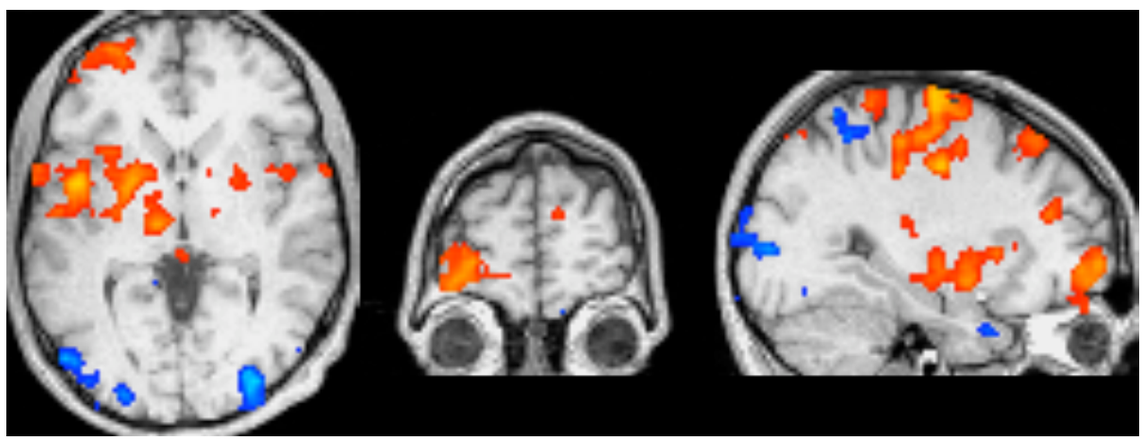

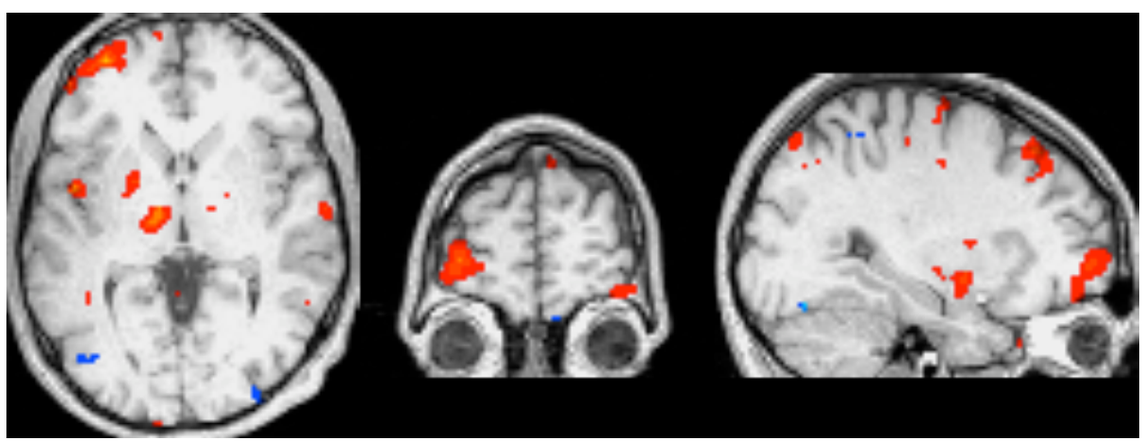

Tensor-ICA multi-subject example

- reaction-time task (index vs. sequential vs. random finger movement

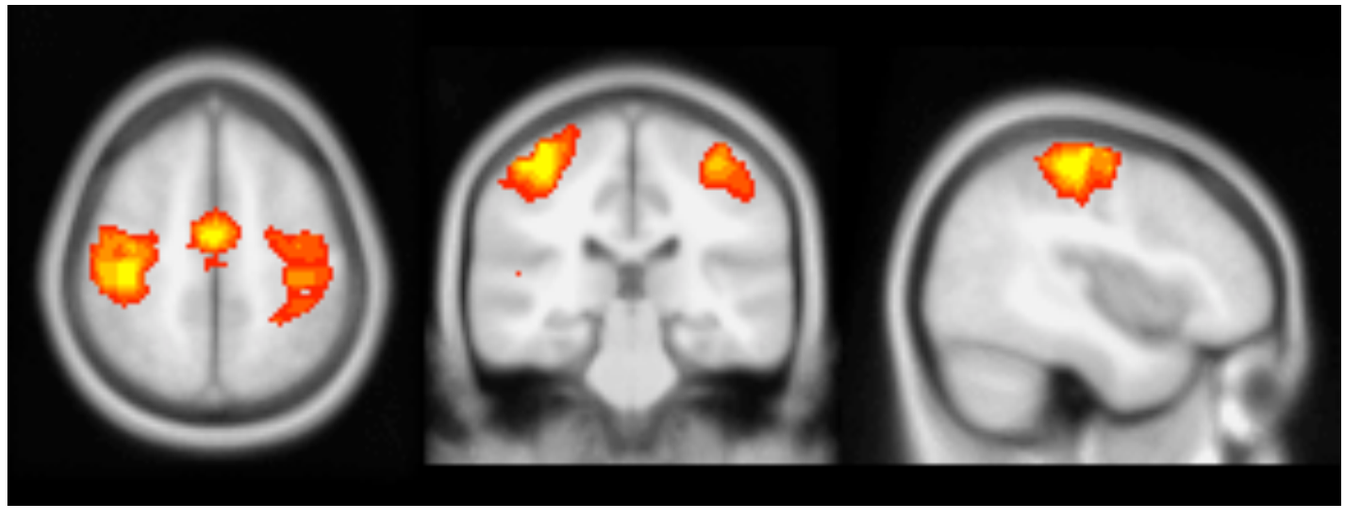

Tensor-ICA multi-subject example

- reaction-time task (index vs. sequential vs. random finger movement

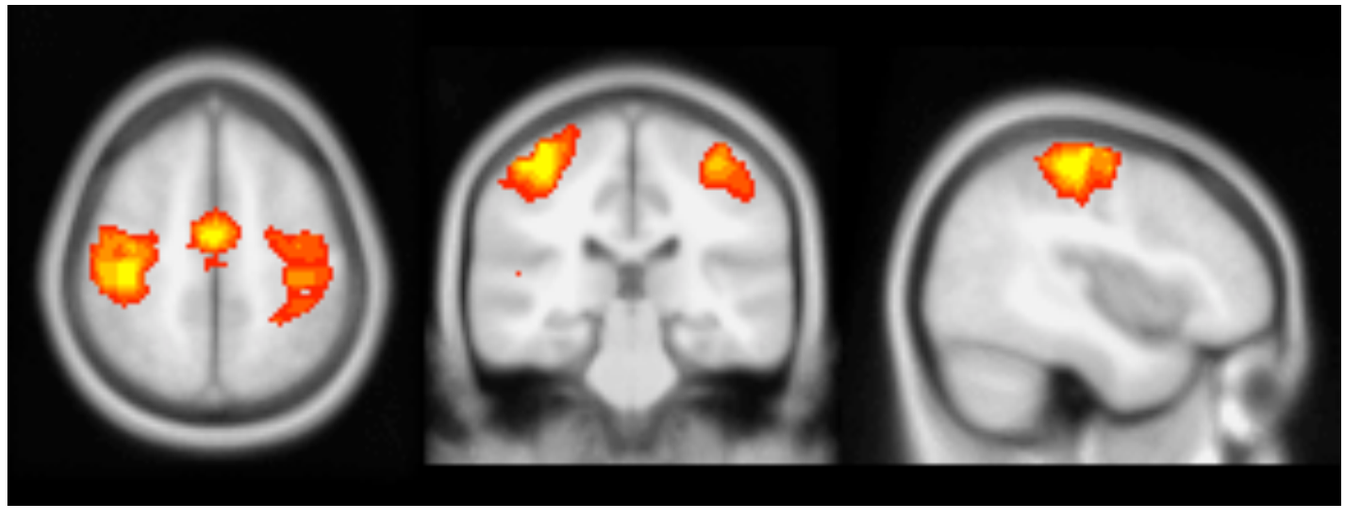

- r > 0.84 regression fit of GLM model against time course

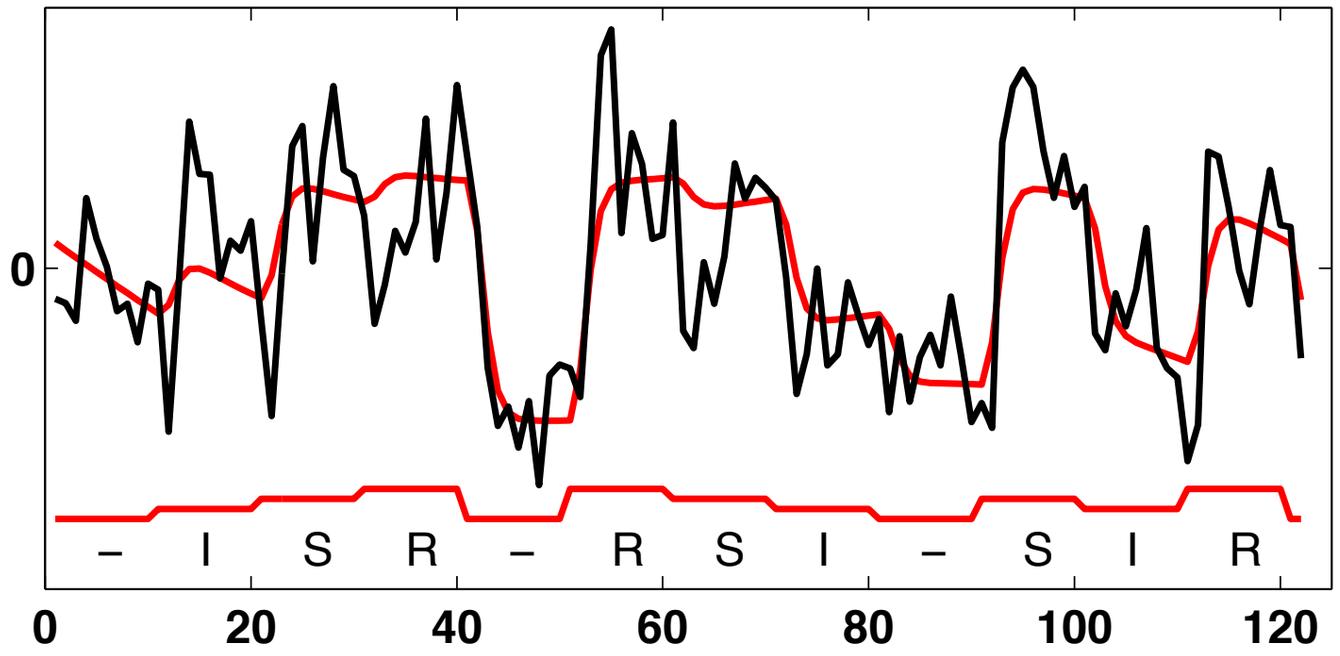

Tensor-ICA multi-subject example

- reaction-time task (index vs. sequential vs. random finger movement

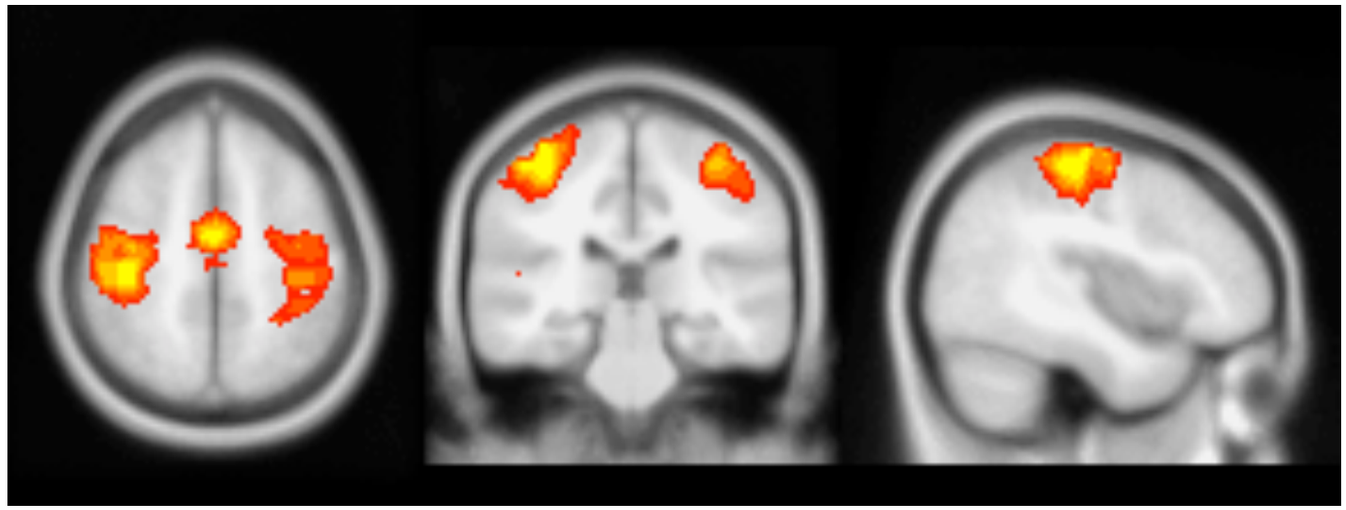

- r > 0.84 regression fit of GLM model against time course
- GLM on associated time-course shows significant ($p<0.01$) differences: I < S < R

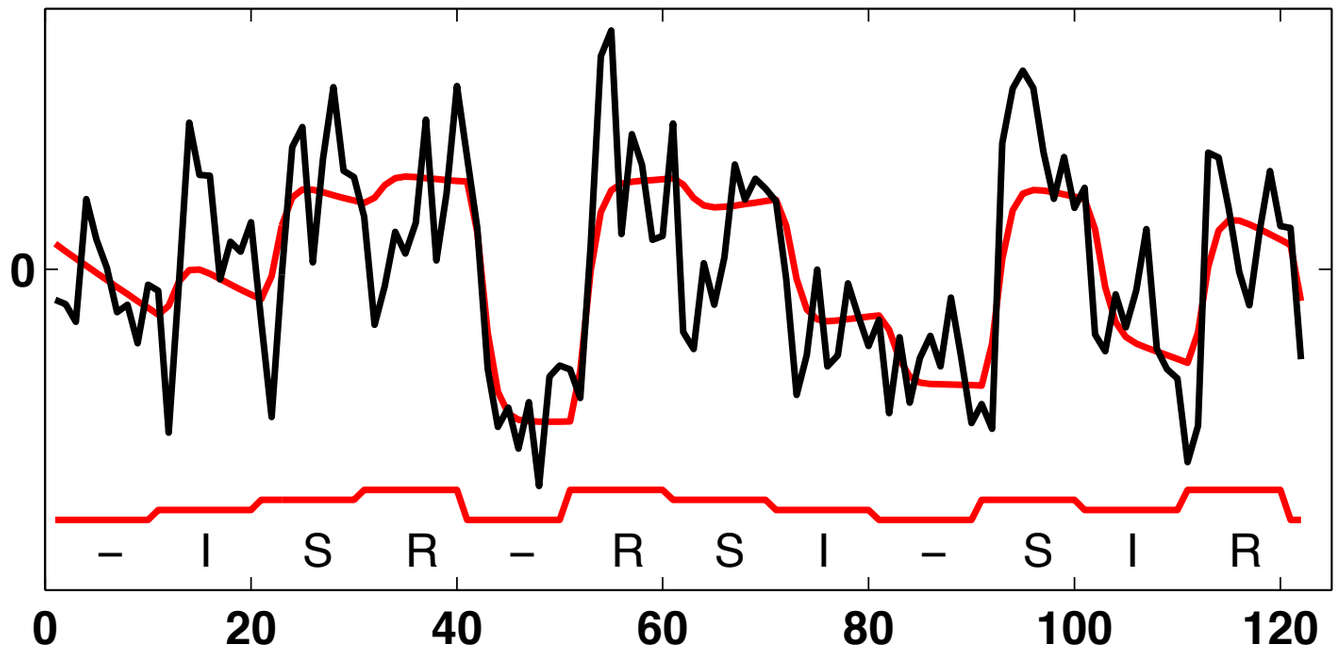

Tensor-ICA

Tensor-ICA

- *simultaneously* estimates processes in the temporal & spatial & session/subject domain

Tensor-ICA

- *simultaneously* estimates processes in the temporal & spatial & session/subject domain
- full mixed-effects model

Tensor-ICA

- *simultaneously* estimates processes in the temporal & spatial & session/subject domain
- full mixed-effects model
- can use parametric stats on estimated time courses and session/subject modes

Tensor-ICA

- *simultaneously* estimates processes in the temporal & spatial & session/subject domain
- full mixed-effects model
- can use parametric stats on estimated time courses and session/subject modes
- robust statistics: can deal with outlier processes

Tensor-ICA

- *simultaneously* estimates processes in the temporal & spatial & session/subject domain
- full mixed-effects model
- can use parametric stats on estimated time courses and session/subject modes
- robust statistics: can deal with outlier processes
- *MELODIC*^{3}

Resting-State Networks

Multiple spatial patterns of correlated temporal dynamics, resembling activation maps

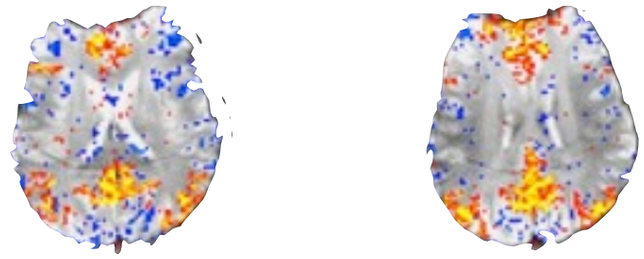

- can be found in FMRI data (BOLD & ASL) obtained at rest *and* in activation data

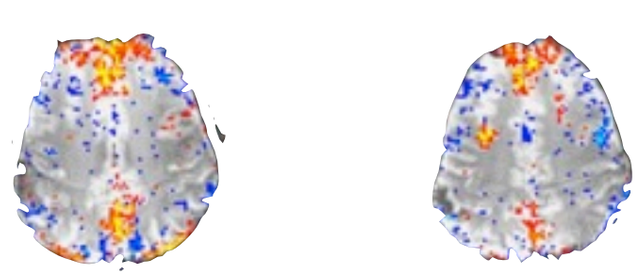

- characterised by (apparent) low frequency power spectra...

- seen when awake/sleep/anaesthesia, human/animals

Also referred to as: “low-frequency correlations”,“default activity”,“default mode”,“spontaneous network correlations”, “intrinsic connectivity networks” ...

Spatial characteristics

- RSNs are grey-matter networks

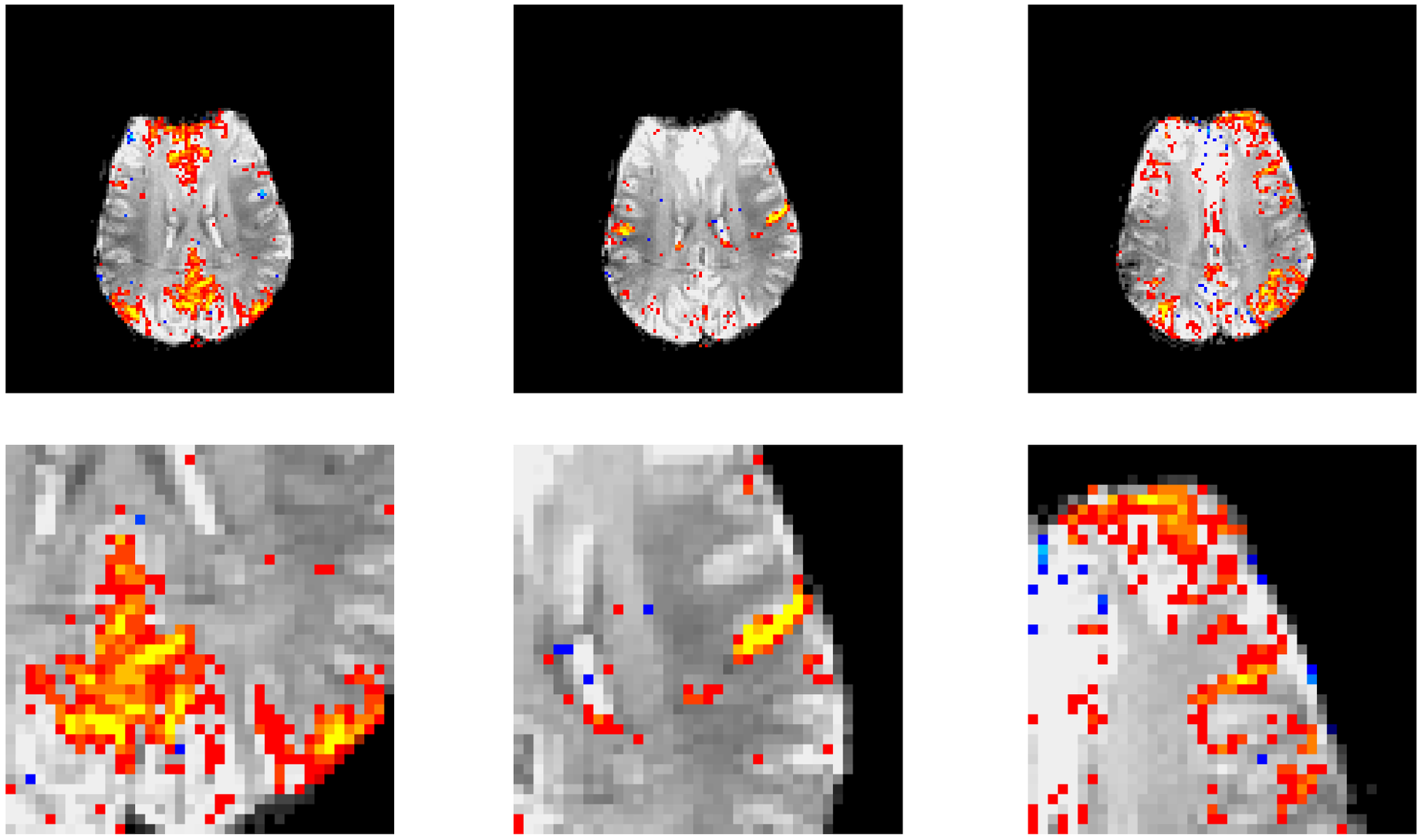

RSNs vs cardiac and respiraton

low TR (120ms)

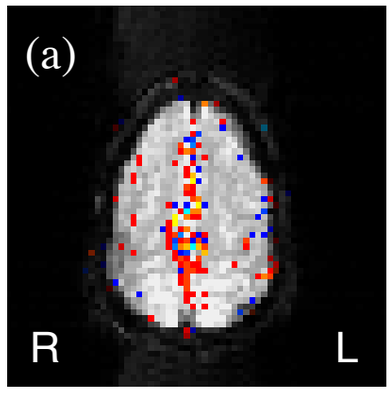

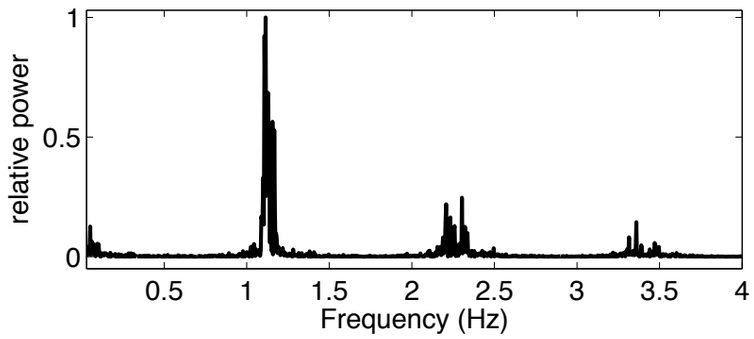

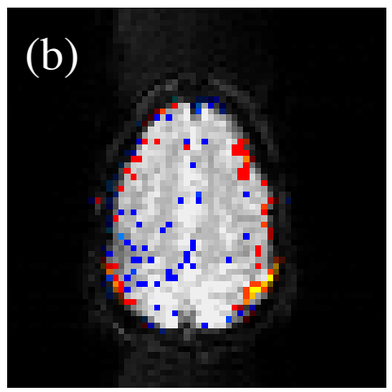

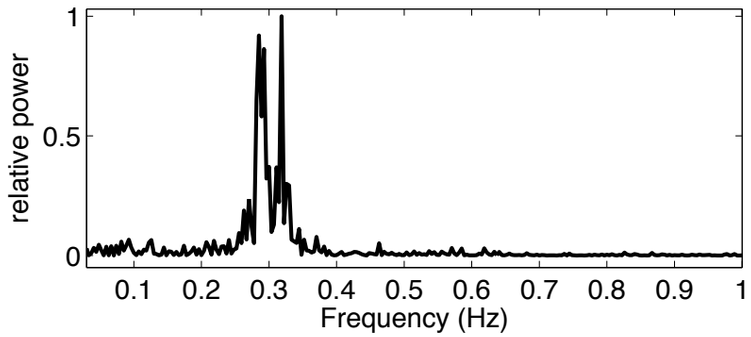

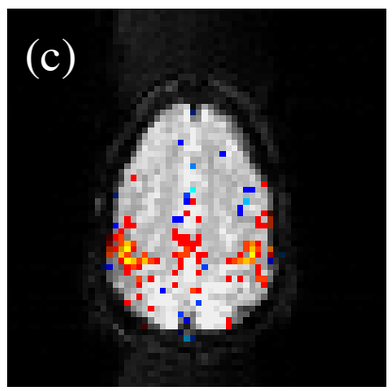

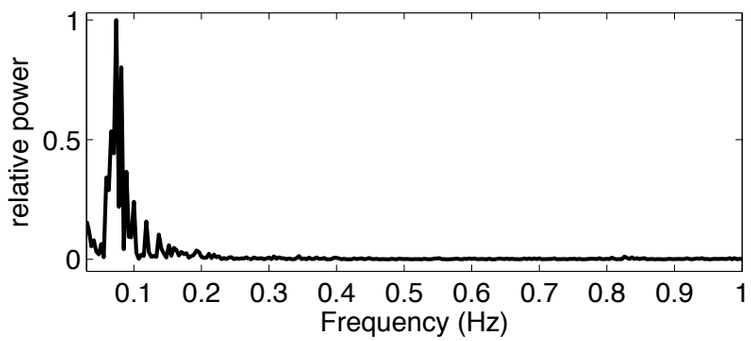

normal TR (3s)

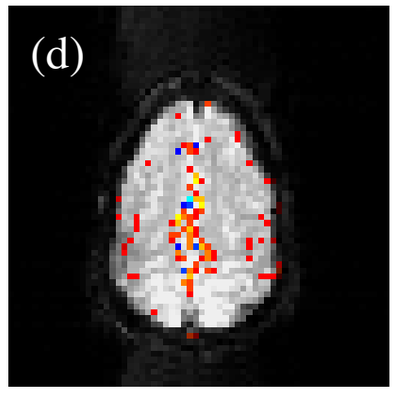

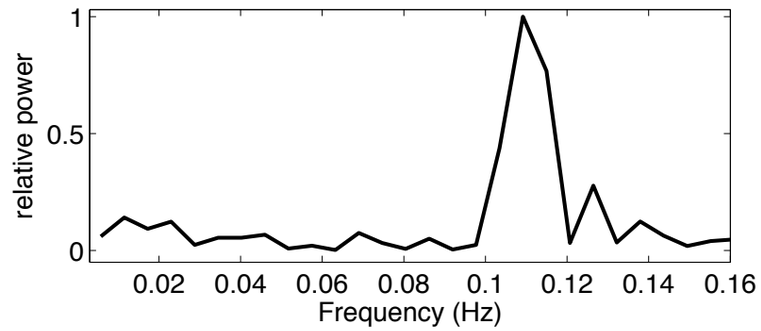

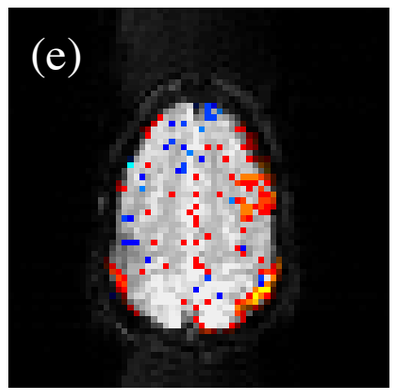

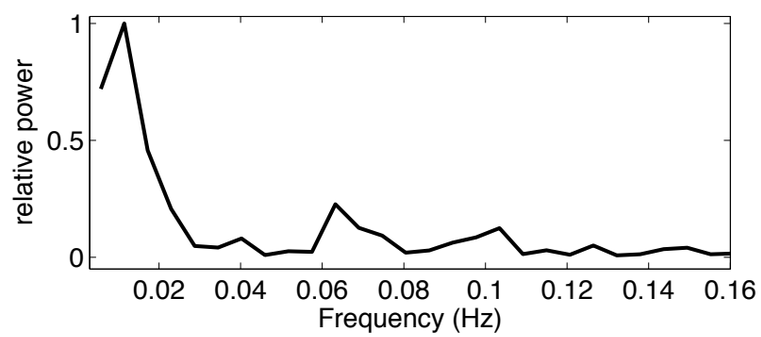

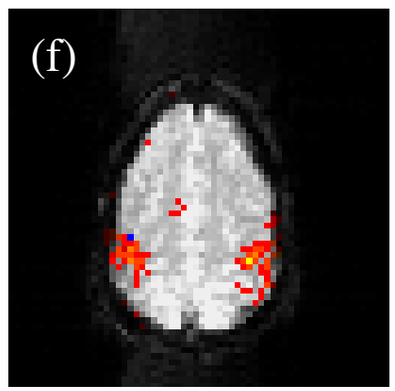

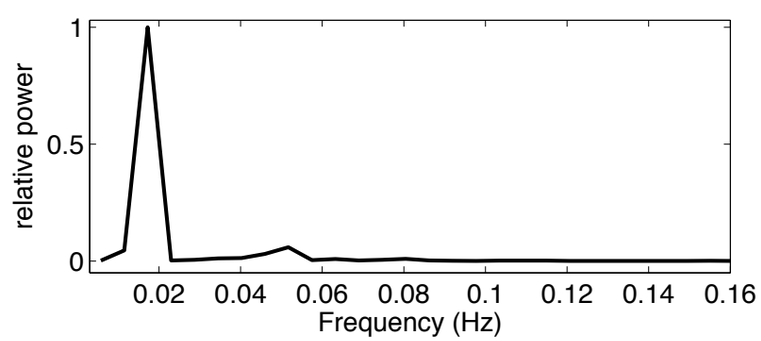

ICA separates RSNs from non-neural physiological and scanner artefacts (also see Birn, Human Brain Mapping, 2007)

Spatial characteristics

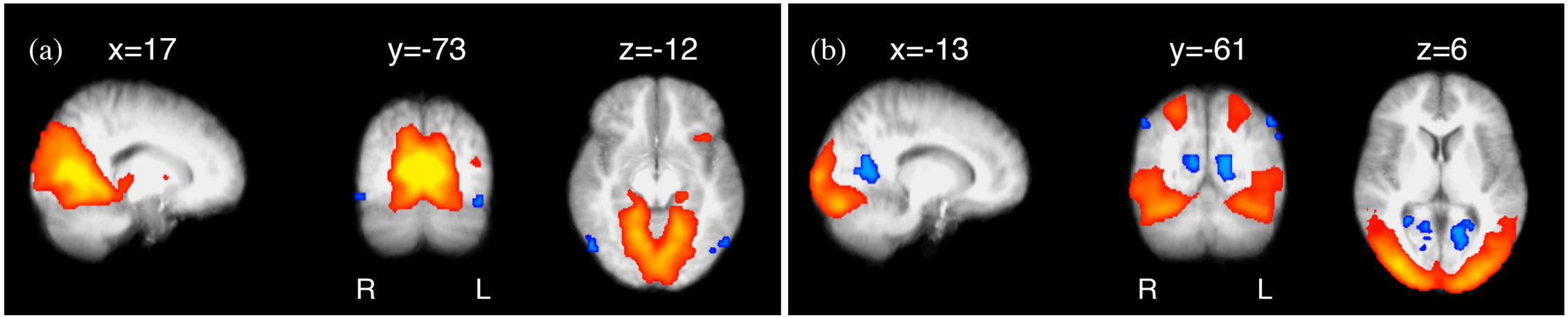

Medial visual cortex

Lateral Visual Cortex

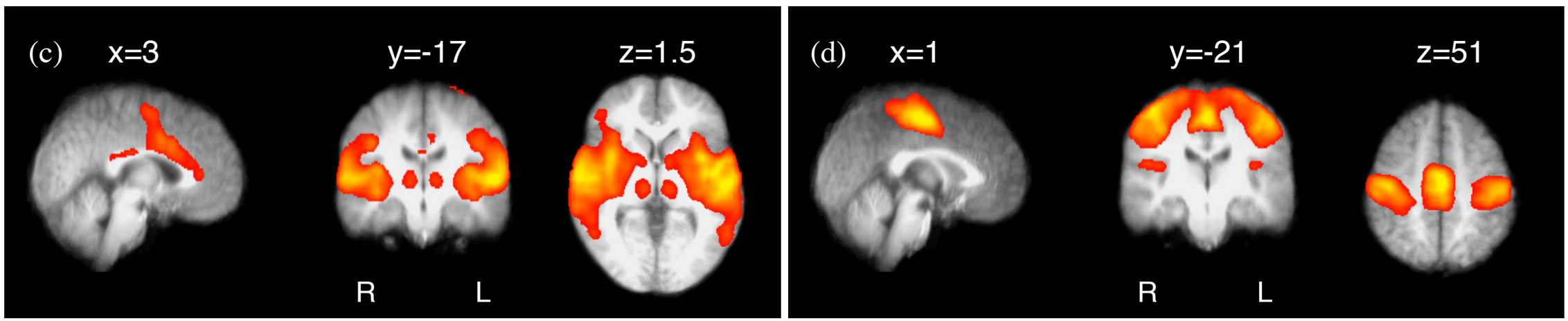

Auditory system

Sensori-motor system

Spatial characteristics

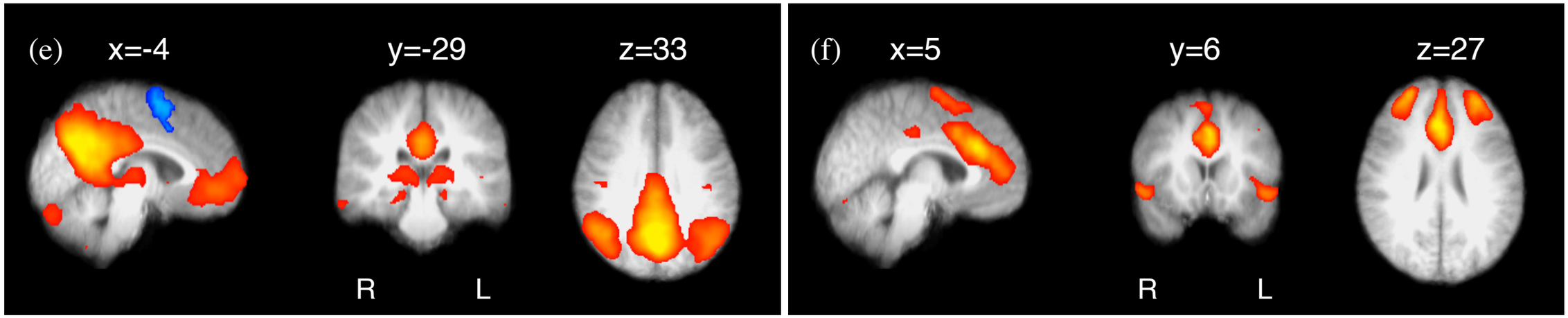

‘default mode network’ Executive control

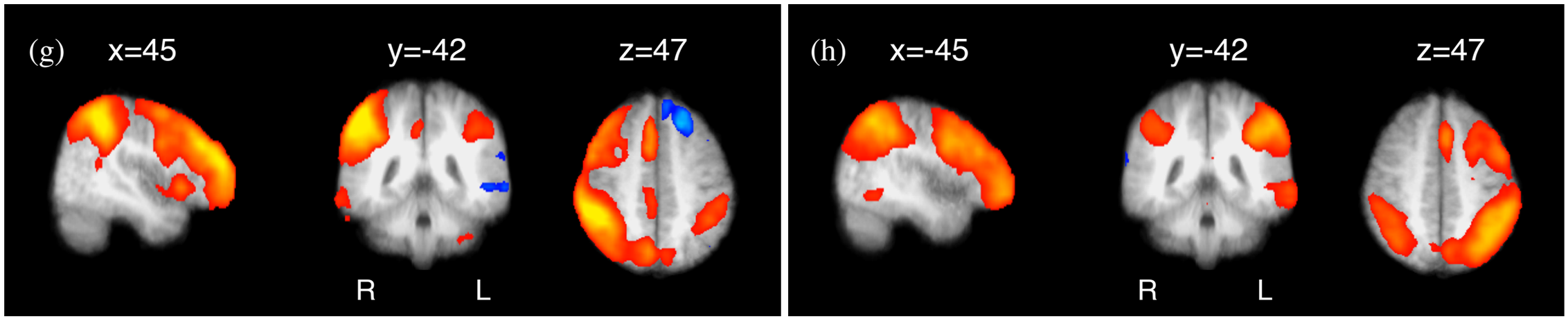

fronto-parietal

RSN consistency

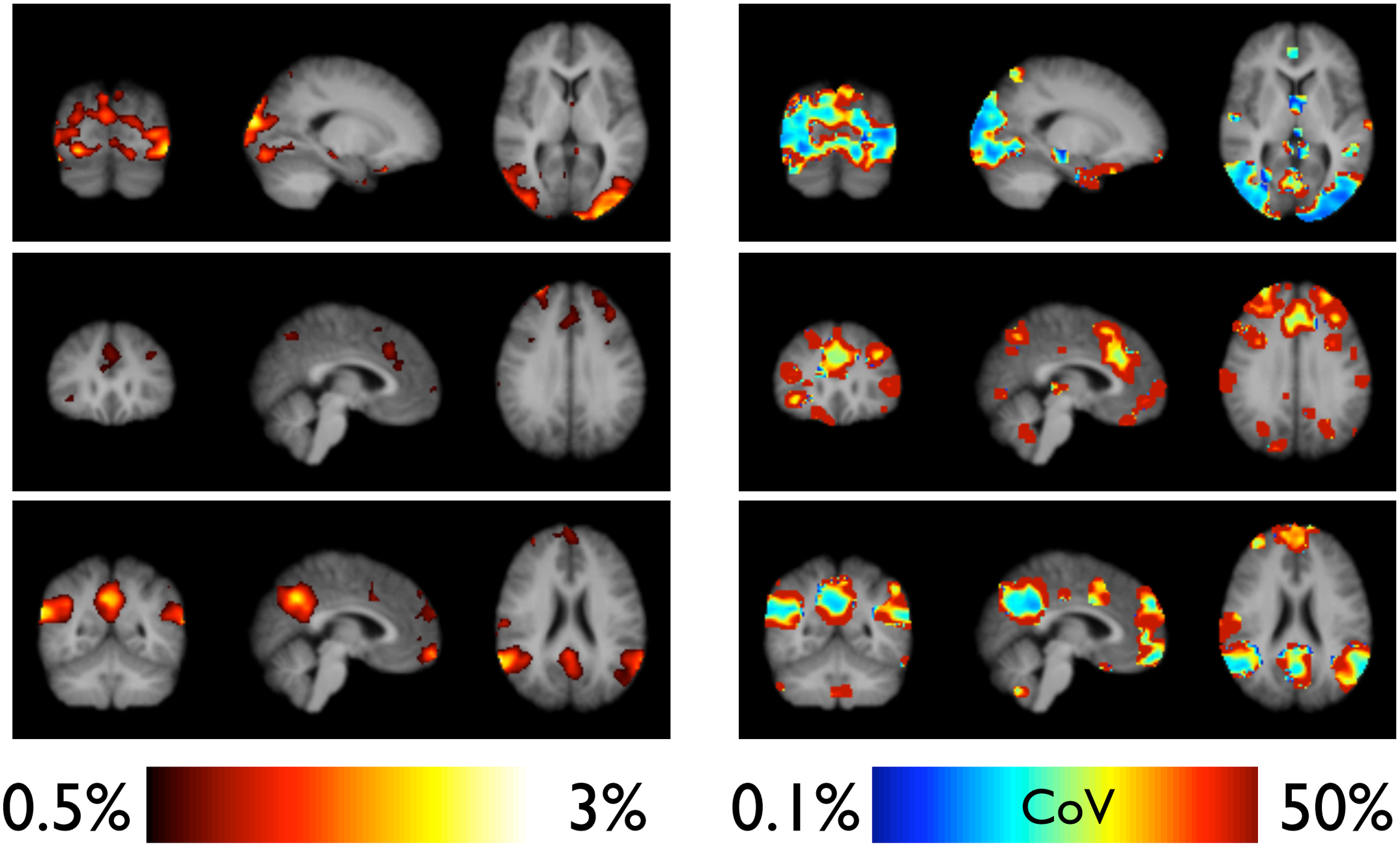

0.5% 3% 0.1% CoV 50%

Damoiseaux et al., PNAS 2006

functional & structural conn.

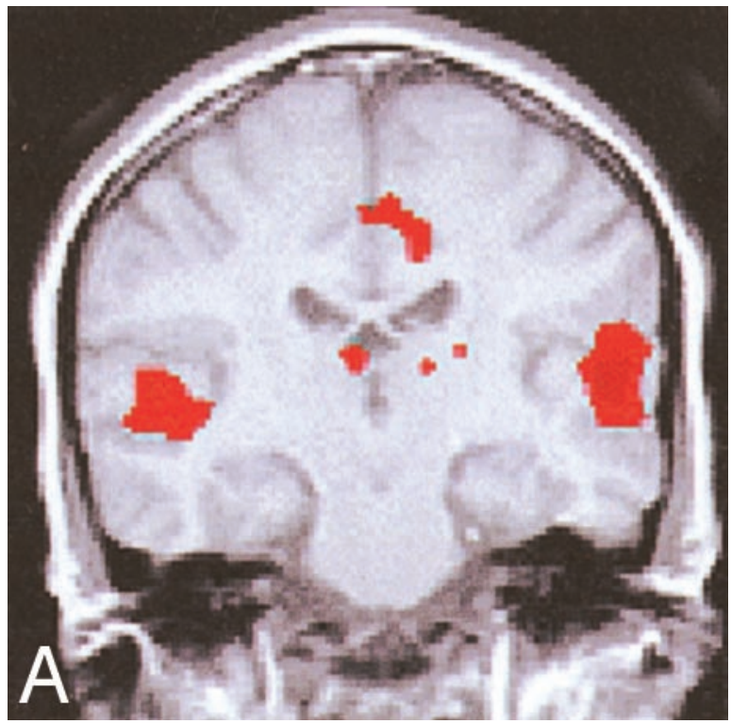

control

- absent contra-lateral connectivity in agenesis of CC

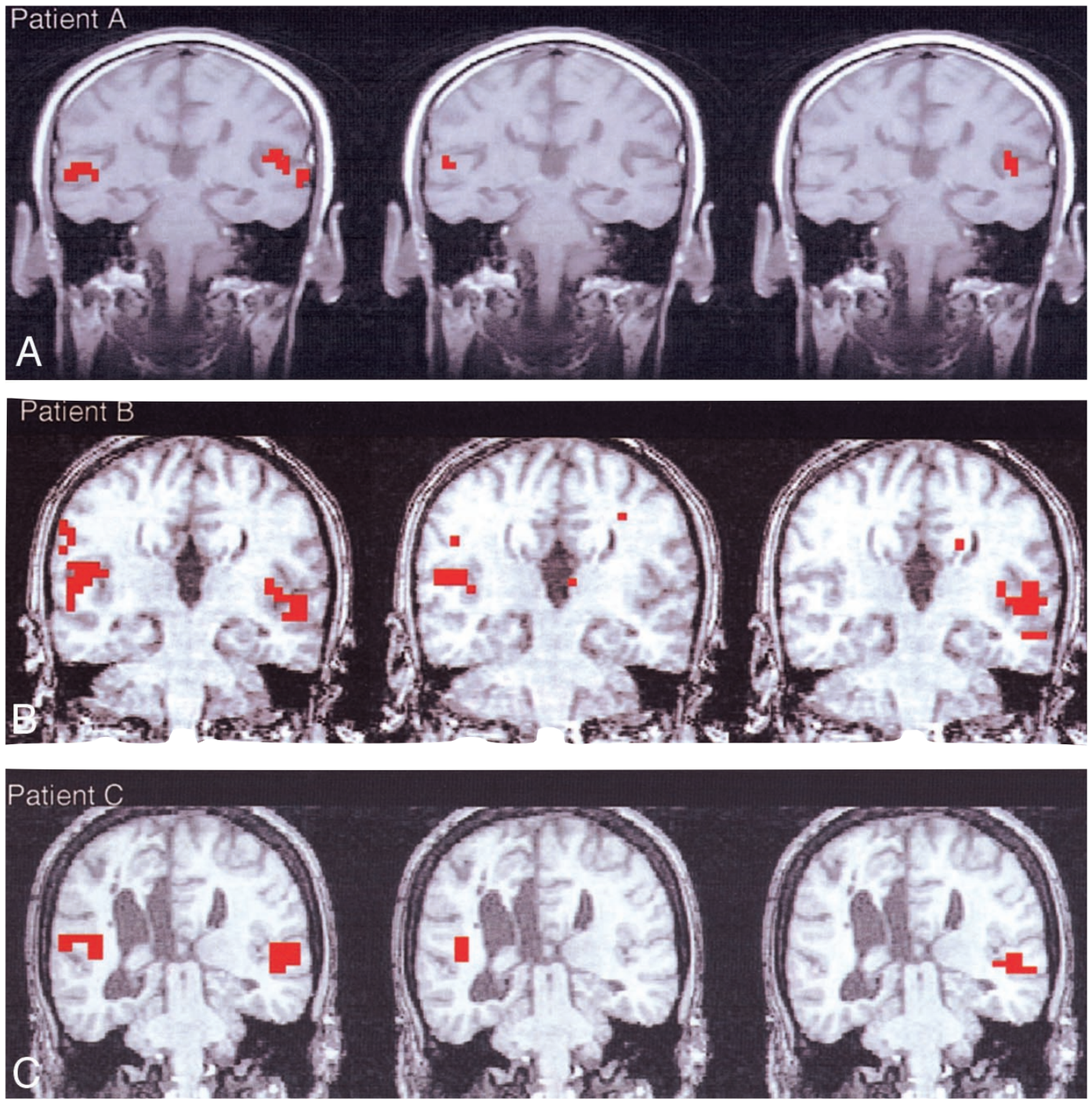

task seed R seed L

Quigley et al., Am J Neuroradiol, 2003

Parcellation of Cerebellum

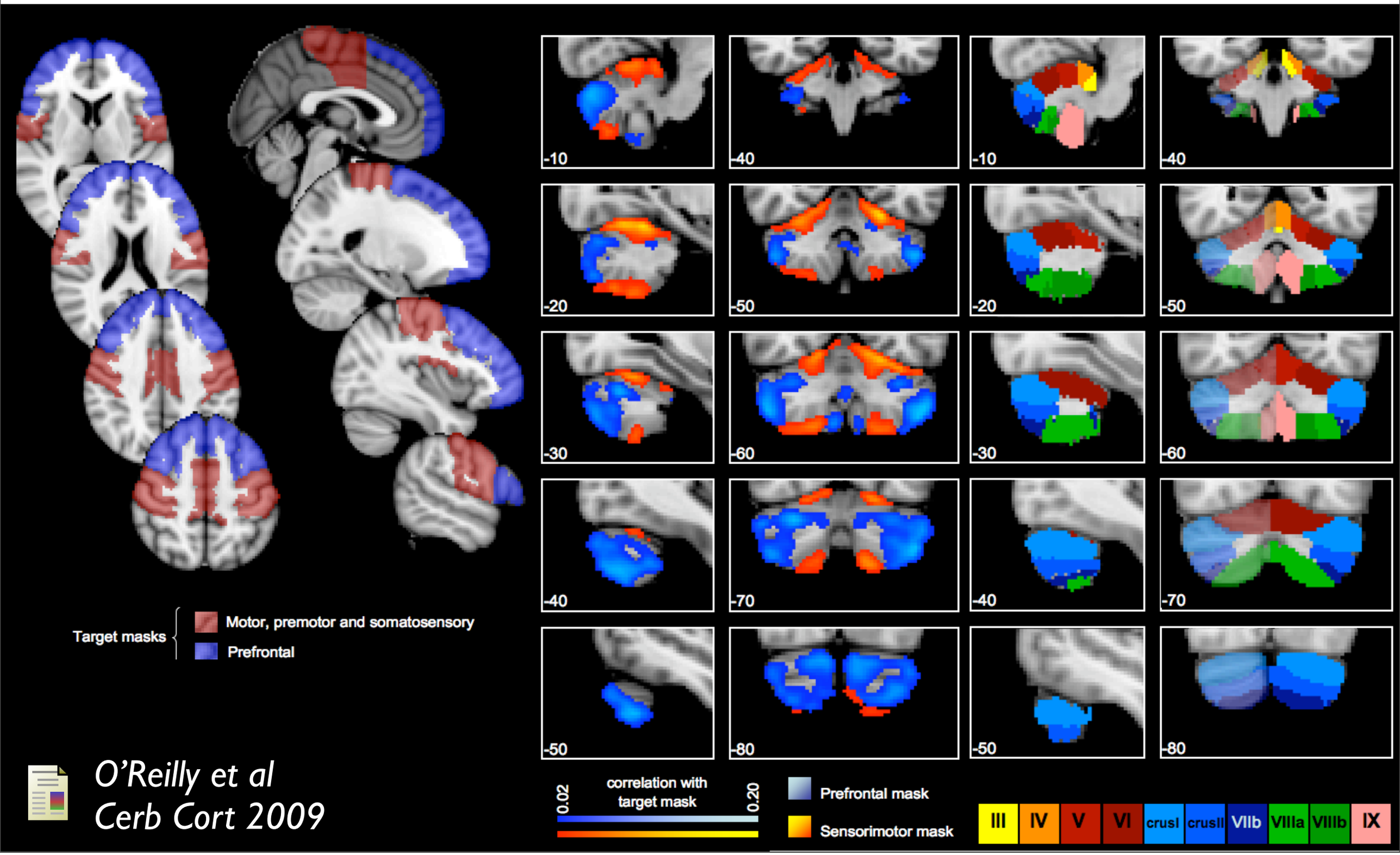

O'Reilly et al
Cerb Cort 2009

RSNs are 'low-frequency oscillations'?

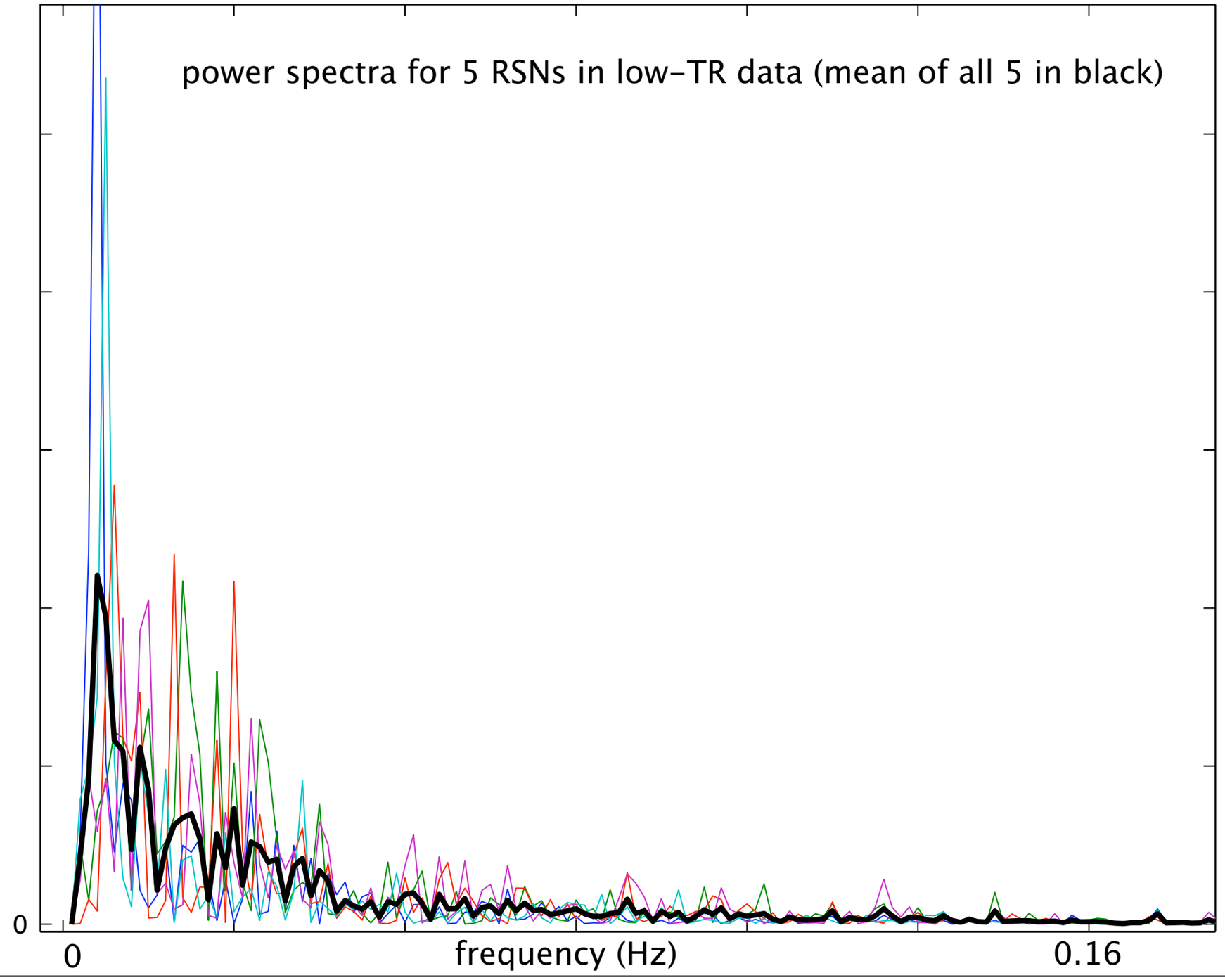

Temporal characteristics

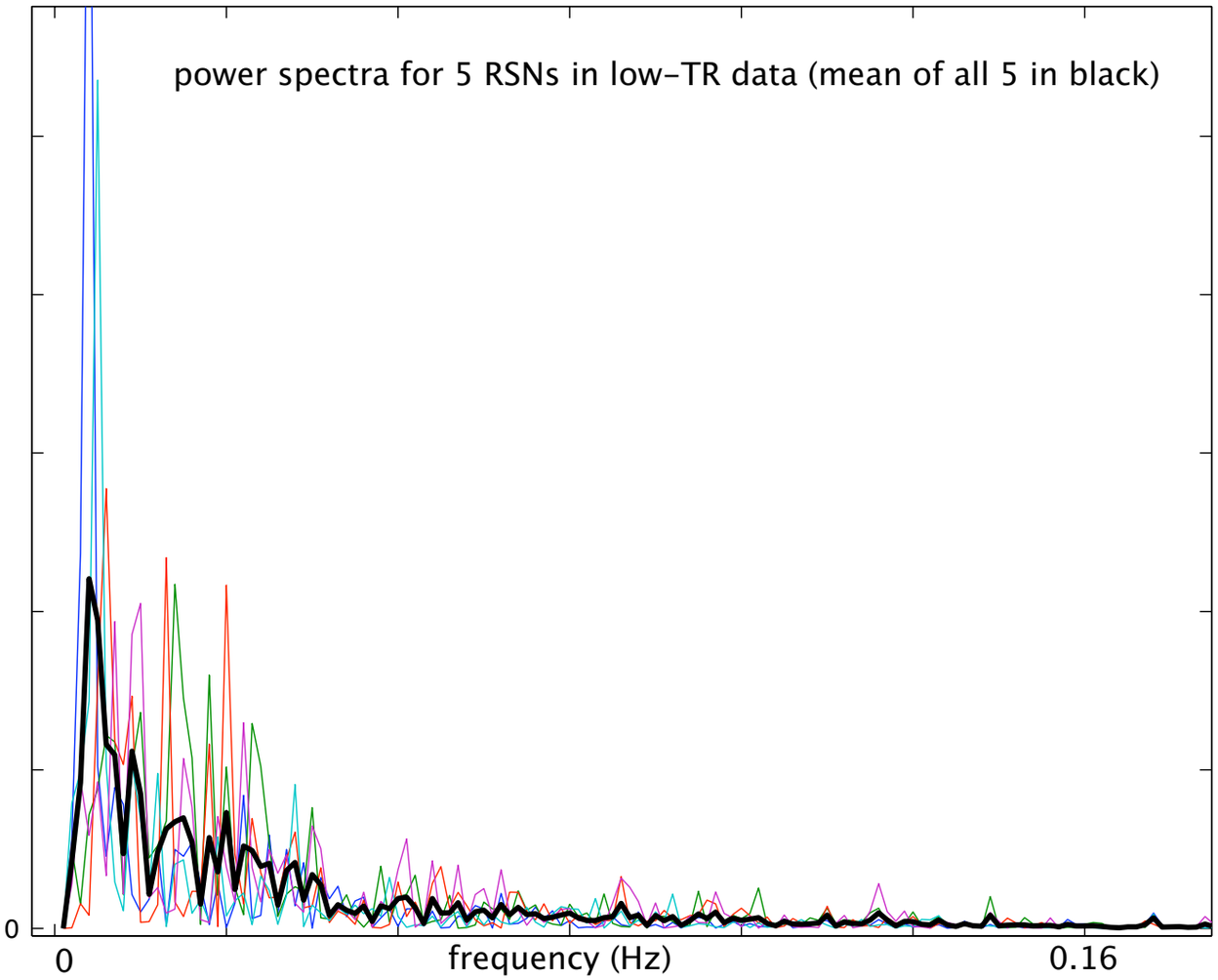

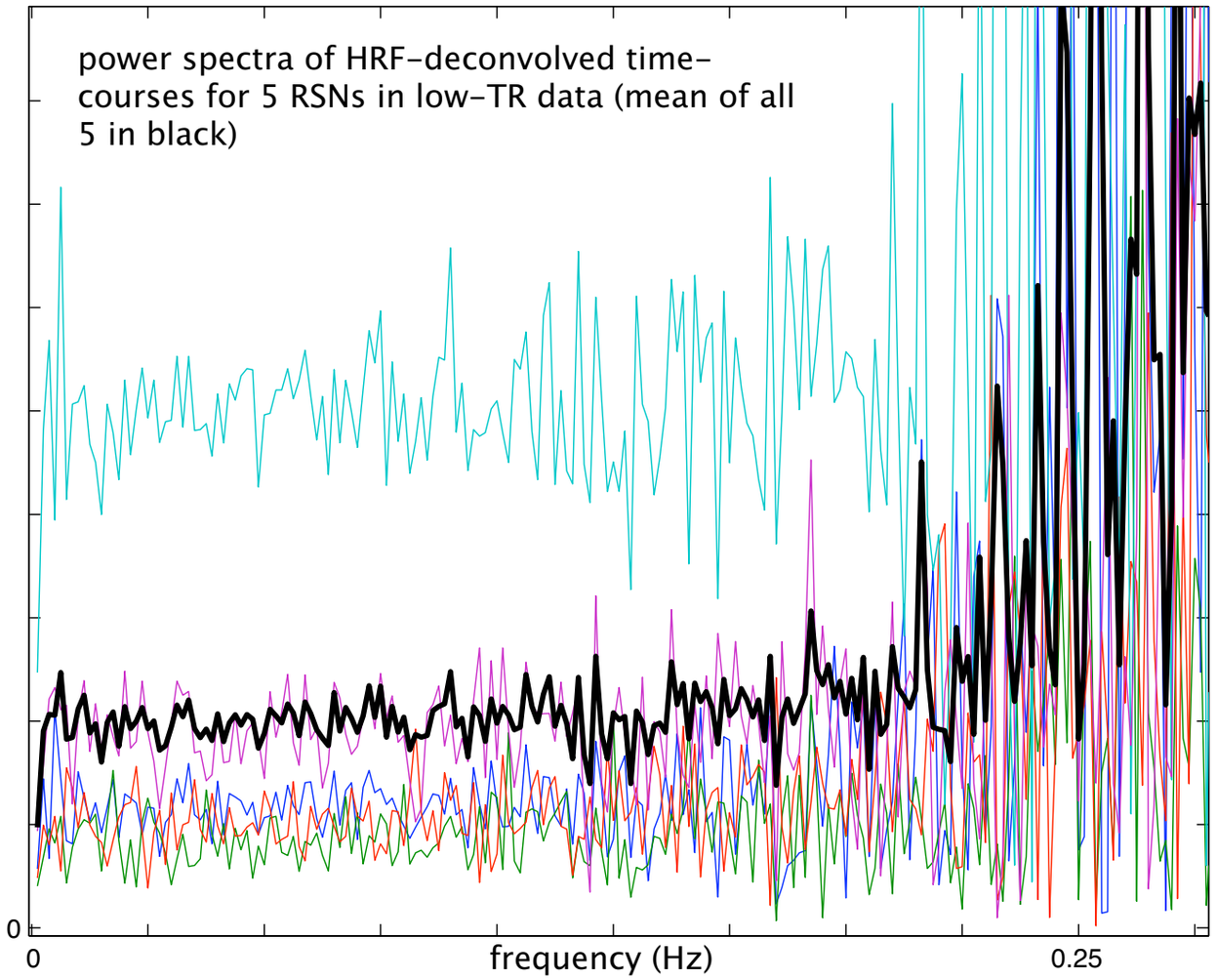

- Resting-state Networks are broadband processes!
- no 1/f characteristics!

Niazy, R et al. (2011)

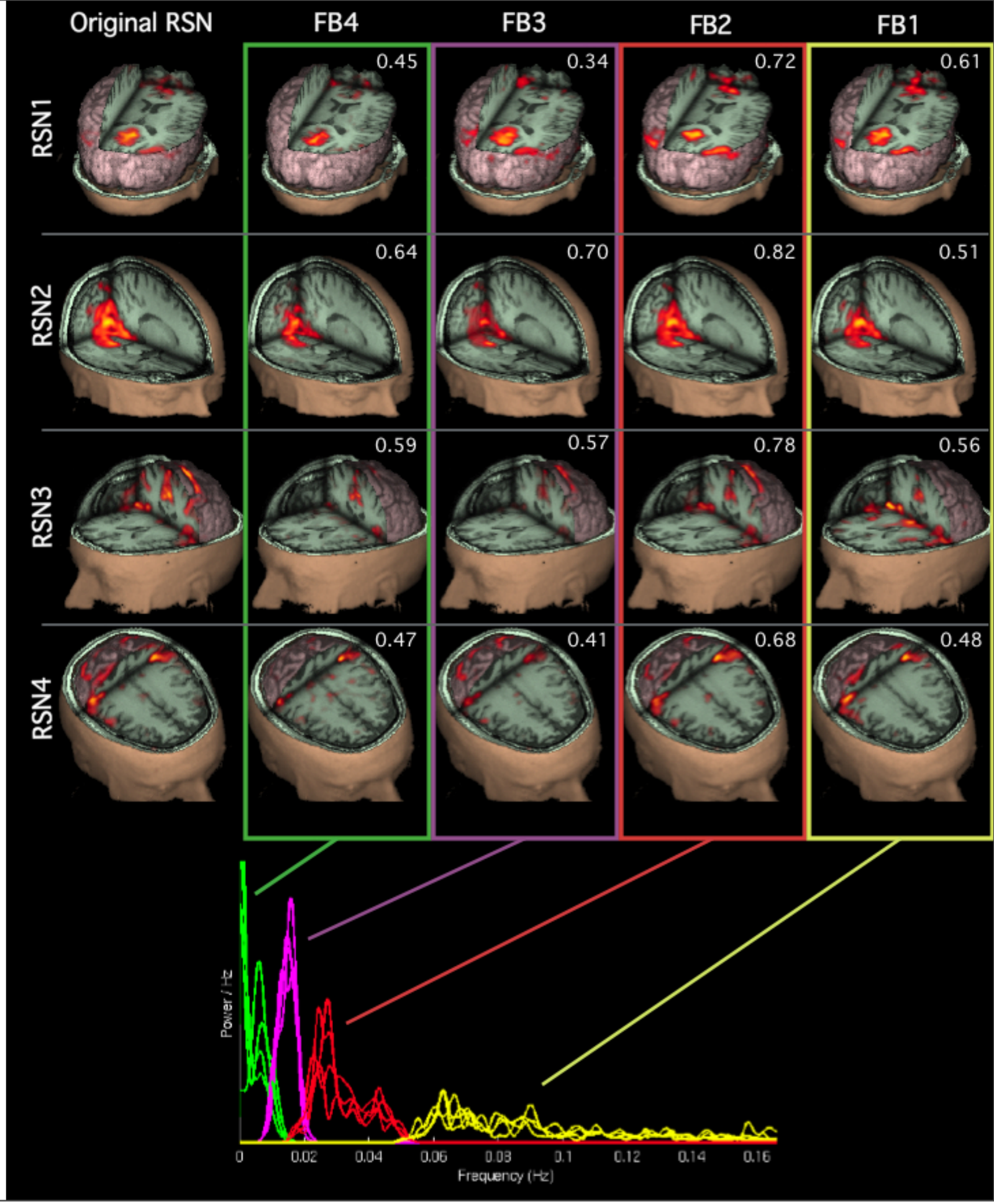

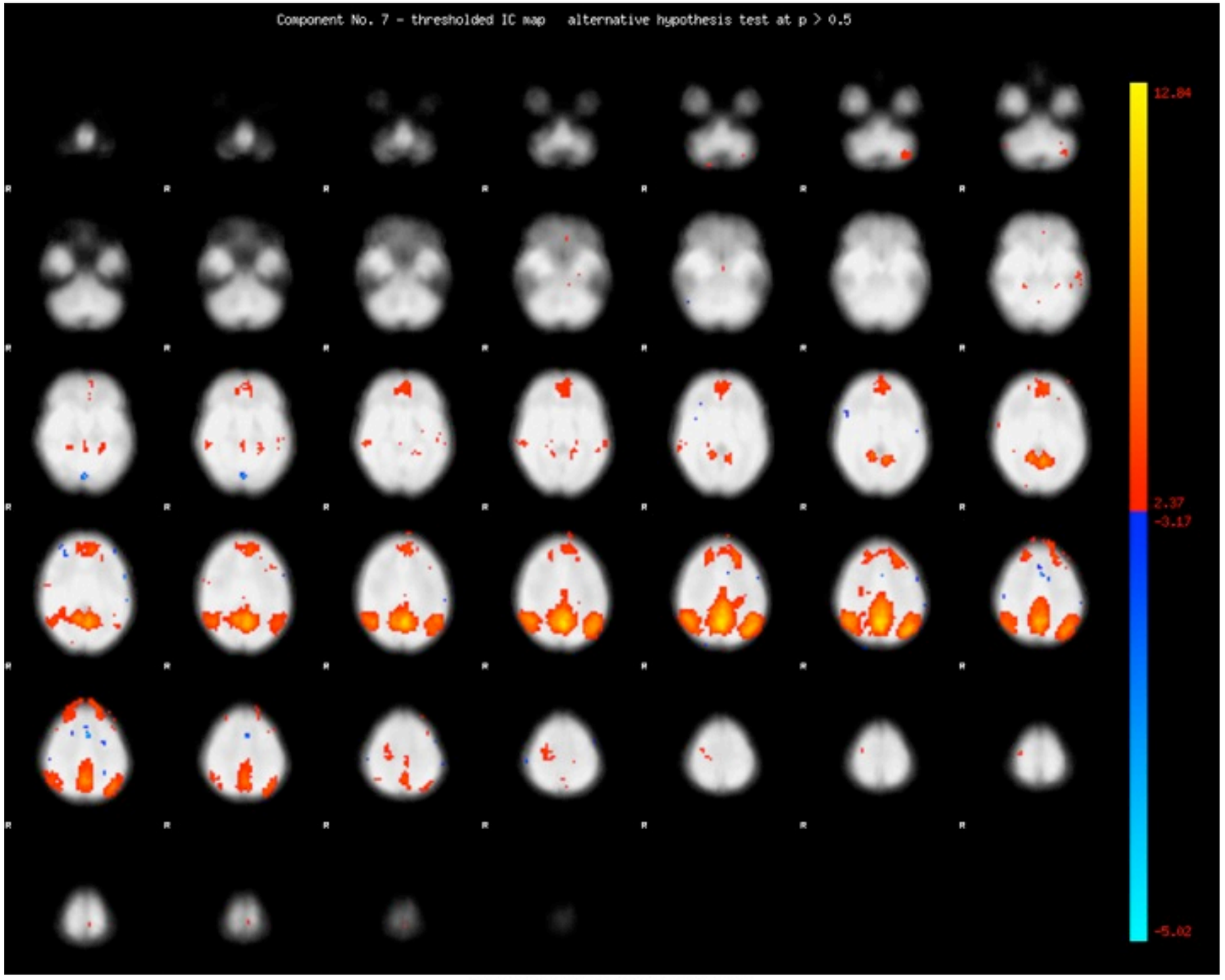
Component No. 7 - thresholded IC map alternative hypothesis test at p > 0.5
12.84
2.37
-3.17
-5.02

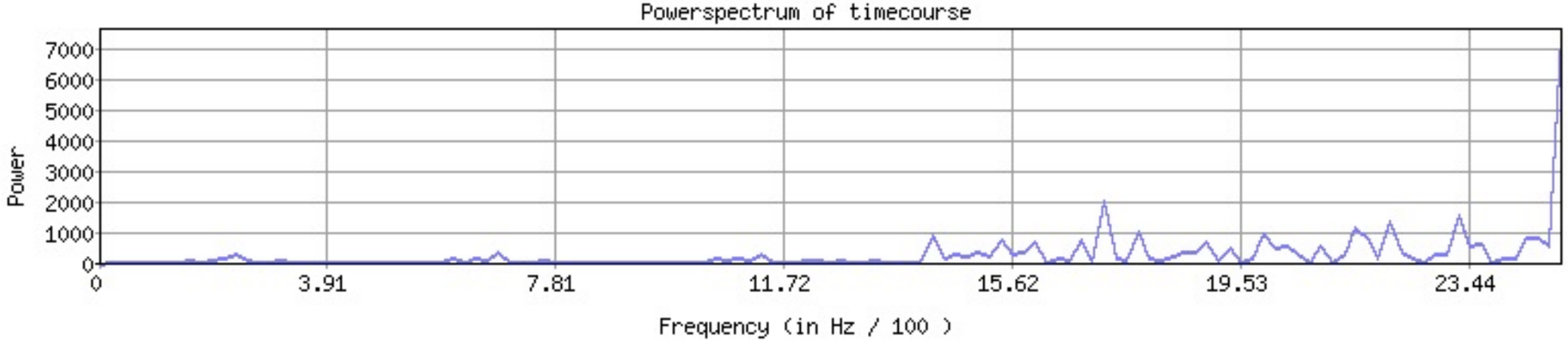
Powerspectrum of timecourse
Power
7000
6000
5000
4000
3000
2000
1000
0
0
3.91
7.81
11.72
15.62
19.53
23.44
Frequency (in Hz / 100)

RSN analysis

Need to estimate whole-brain temporal correlations...

Two popular approaches for RSN analysis:

- Seed-based correlation (Biswal, Raichle/Fox)
- ICA-based analysis (Kiviniemi, Beckmann, Calhoun)

Need to define consistent methods for group analysis

Seed-based analysis

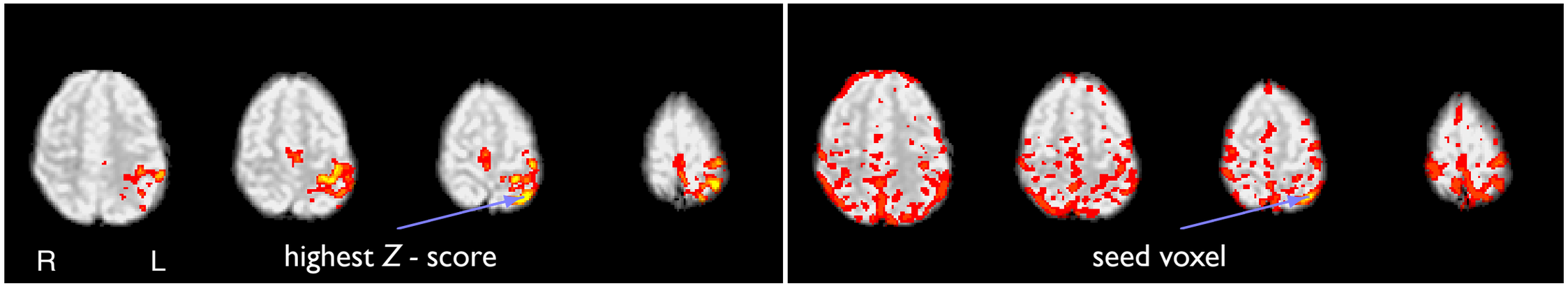

Activation maps from a finger tapping experiment

Correlation maps from a resting state experiment

- Biswal (1995) first studied resting correlations through reference time course:

Functional Connectivity maps

Biswal et al. (1995) MRM

... and the seed-selection bias

- models only effect of interest
  - potentially ignoring secondary effect and/or nuisance effects
- analysis becomes conditional on the specific seed location
  - need to define *consistent* way of defining seed within and across subjects

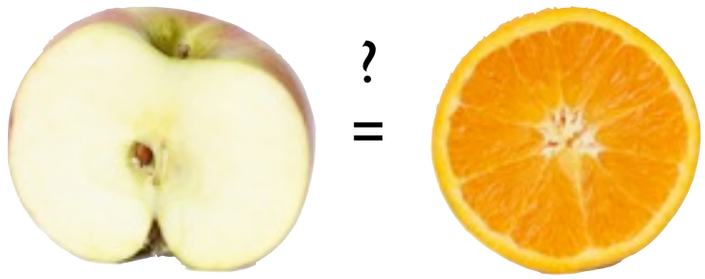

Seed-selection

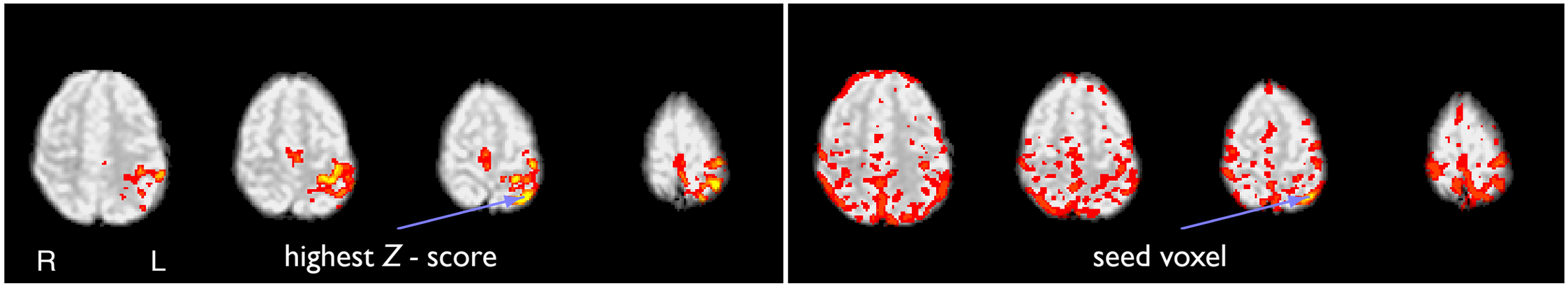

Activation maps from a
finger tapping experiment

Correlation maps from a
resting state experiment

Beckmann et al (2005)
Philos Trans R Soc Lond, B, Biol Sci

Seed-selection

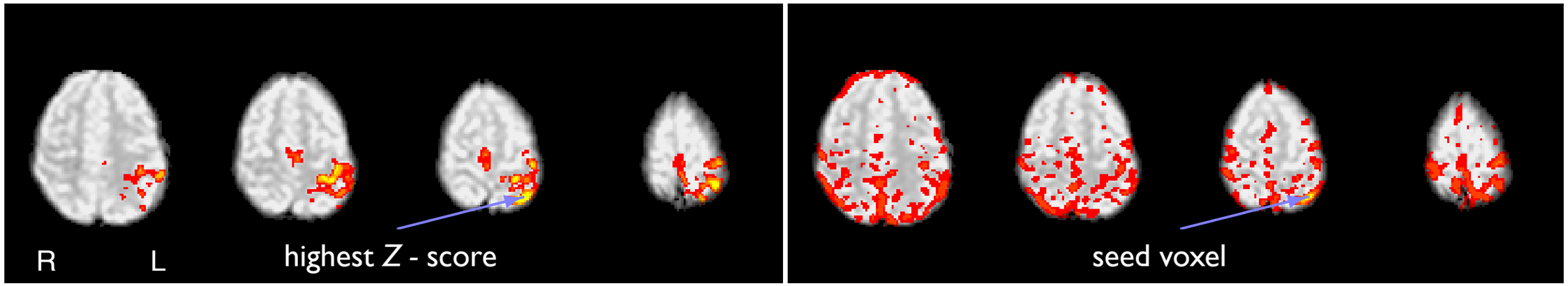

Activation maps from a finger tapping experiment

Correlation maps from a resting state experiment

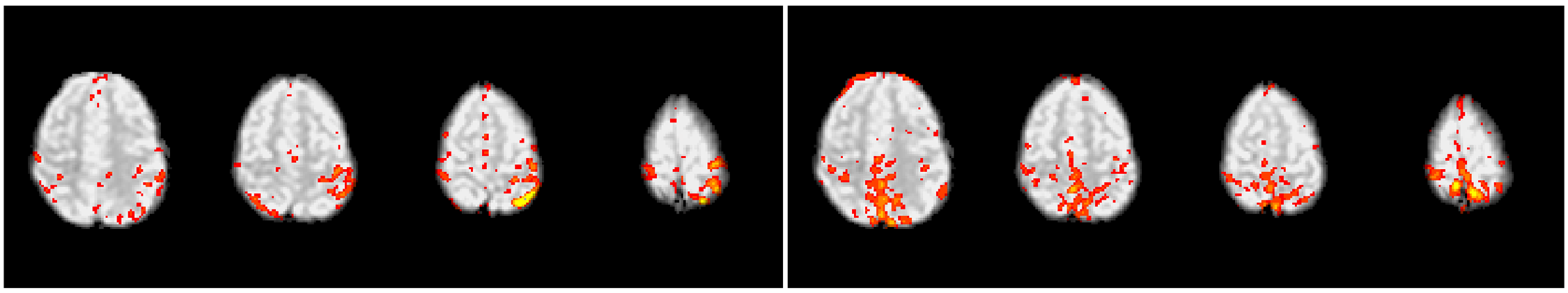

Spatial maps from an ICA decomposition

Beckmann et al (2005)
Philos Trans R Soc Lond, B, Biol Sci

Seed-selection bias

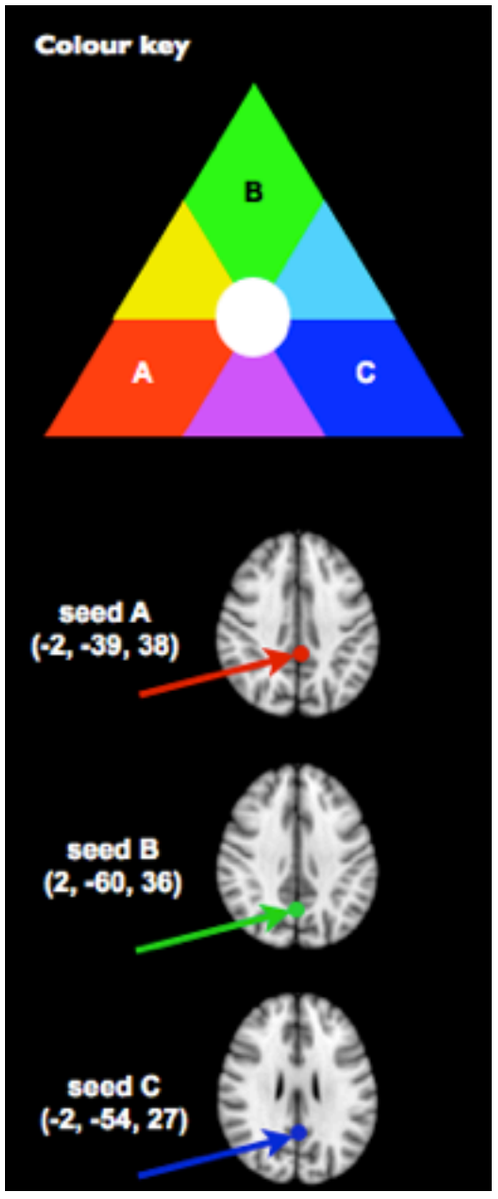

Cole et al (2010)
Front Syst Neurosci

Seed-selection bias

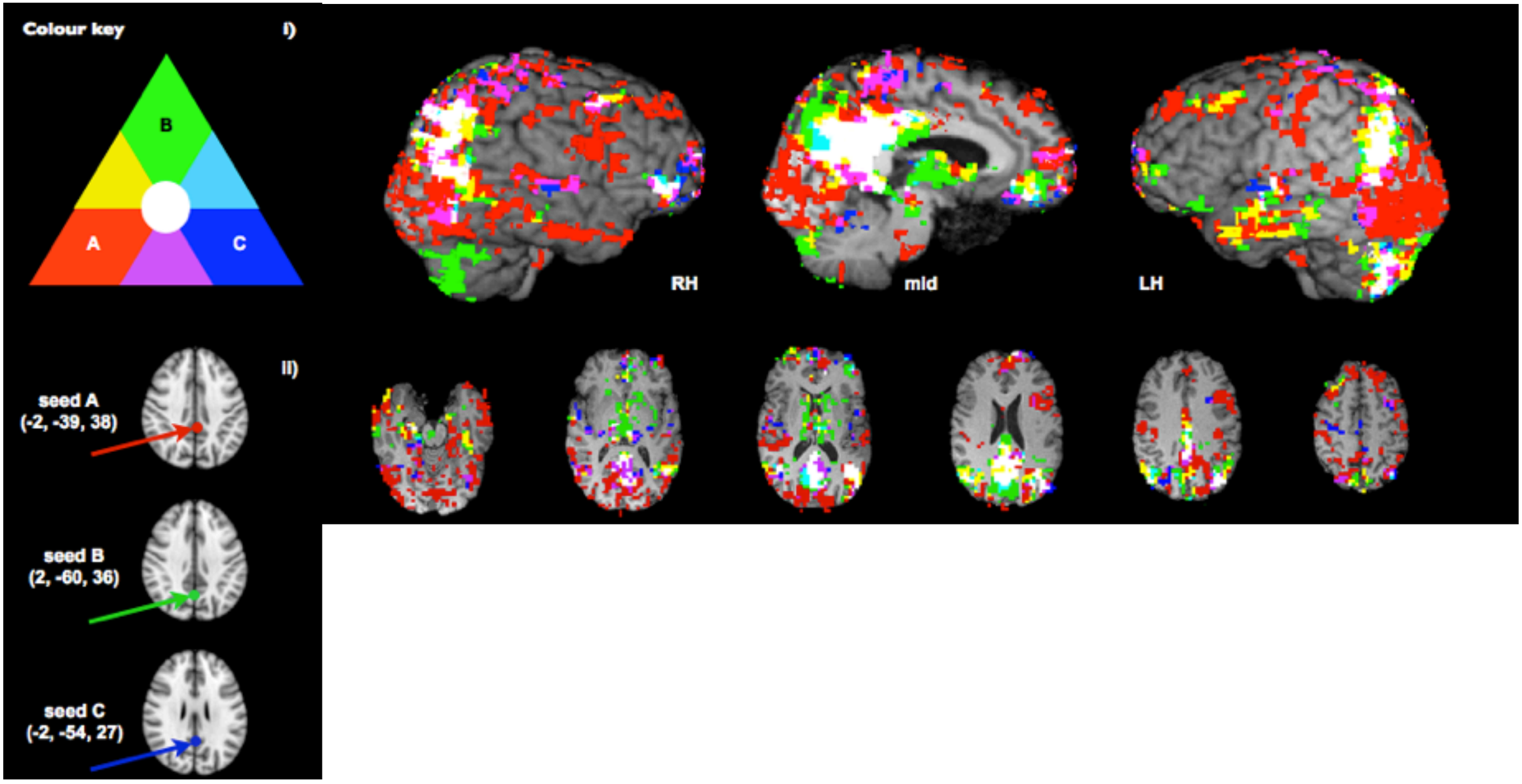

Cole et al (2010)
Front Syst Neurosci

Seed-selection bias

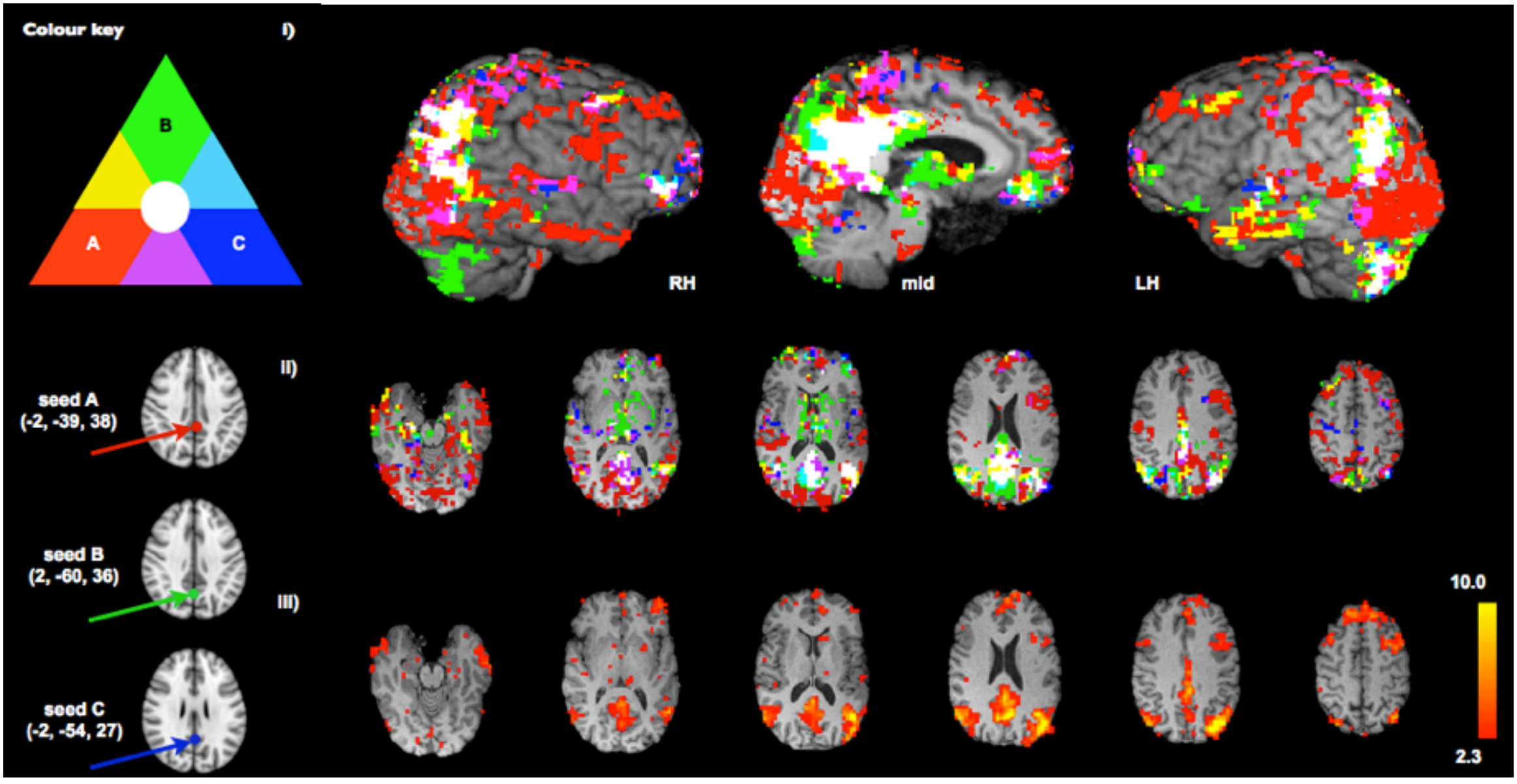

Cole et al (2010) Front Syst Neurosci

ICA bias & dimensionality reduction

- FMRI data are large...
- ...particularly at the group level
- common to reduce dimensionality by means of a *Principal Component Analysis*

Principal Component Analysis

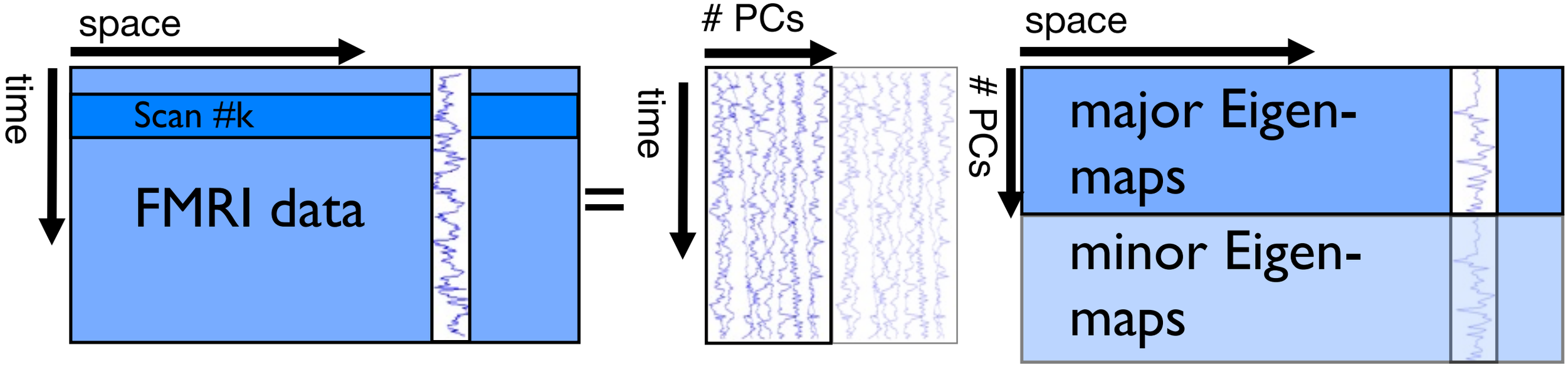

- PCA: data is decomposed into a set of uncorrelated spatial maps and uncorrelated time courses such that a *maximal amount of variance* is retained
- *lossy process!*

Detour: primary vs. differential contrasts

- Even when primary effects are large... *(express loads of variance)*

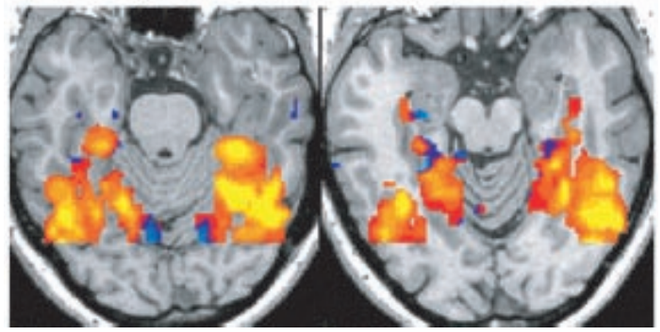

mean across conditions

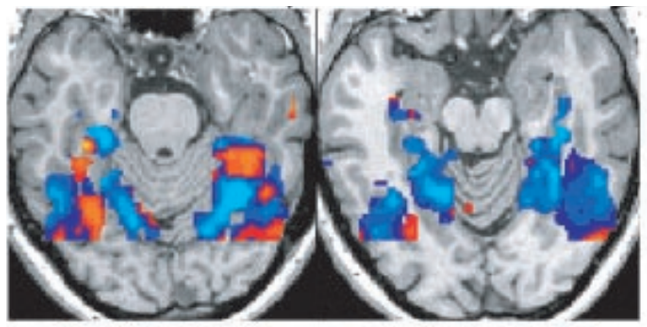

Faces 

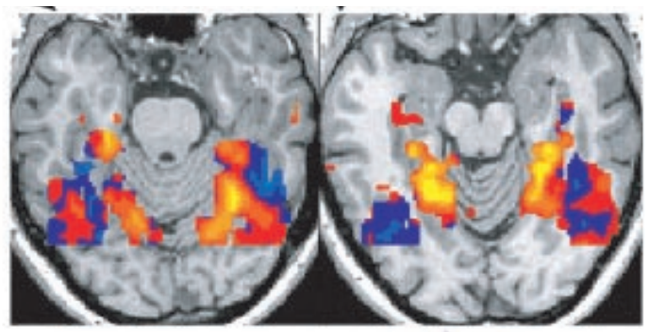

Houses 

Haxby et al. (2001) Science

Detour: primary vs. differential contrasts

- Even when primary effects are large... *(express loads of variance)*

- ... *differential* effects can be very small *(express little variance)*

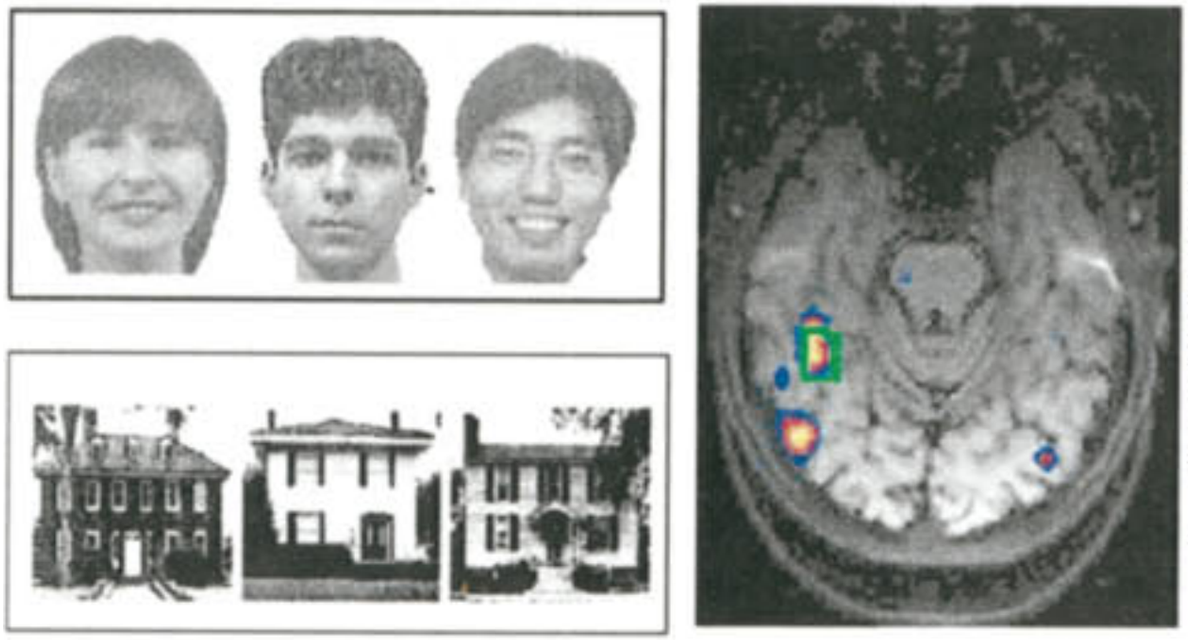

Faces > Houses

Kanwisher et al. (1997) J NeuroSci

Detour: primary vs. differential contrasts

- Even when primary effects are large... *(express loads of variance)*

- ... *differential* effects can be very small *(express little variance)*

- PCA suitable for the former, less suitable for the latter!

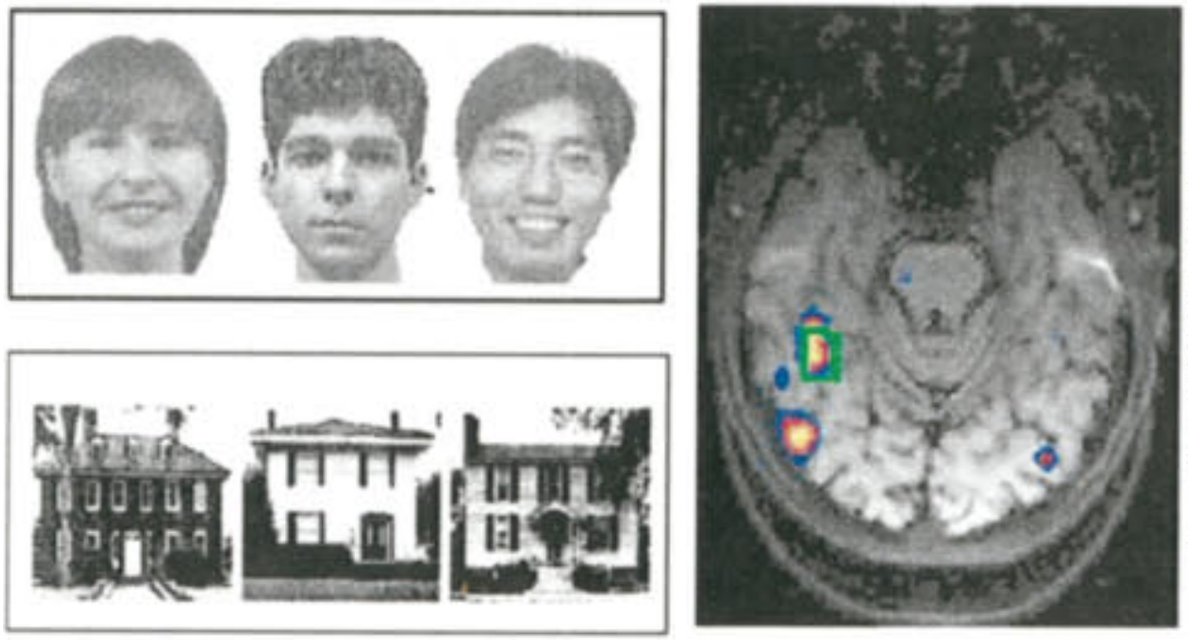

Faces > Houses

Kanwisher et al. (1997) J NeuroSci

PCA bias

- within-subject bias:
  - *tissue-type bias & variance normalisation*
- between-subject bias:
  - *between major & minor subspace*
  - *within the major subspace*

PCA tissue-type bias

voxel-wise temporal standard deviations

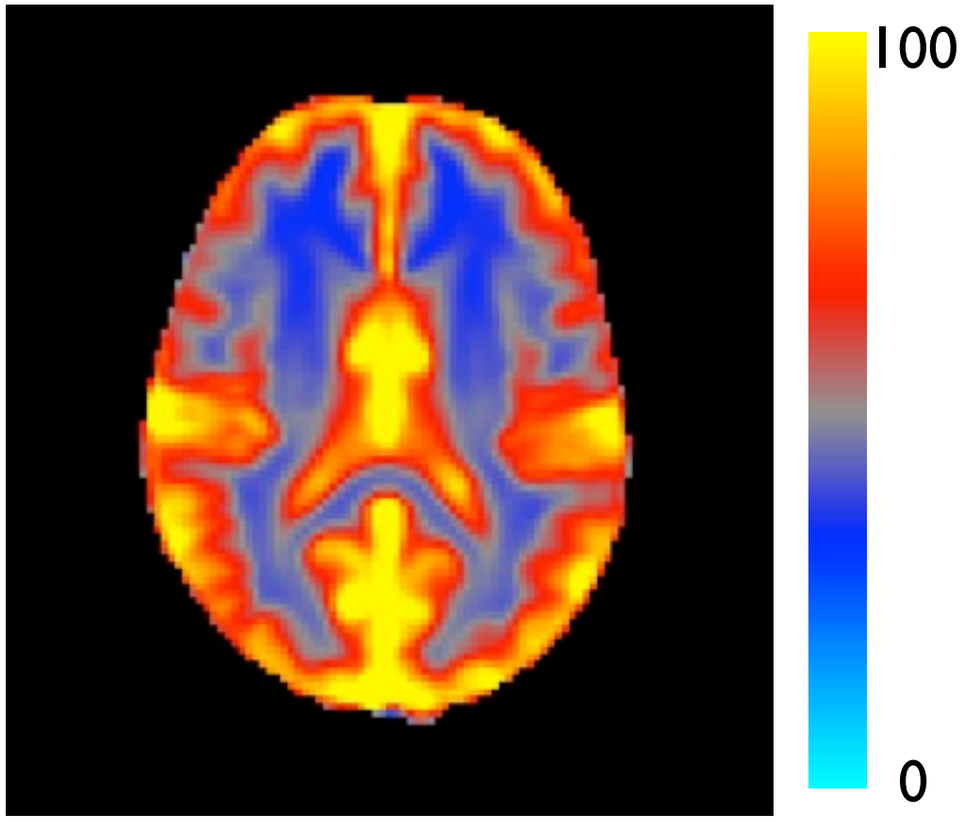

(log) - frequency of voxels appearing in major PCA space

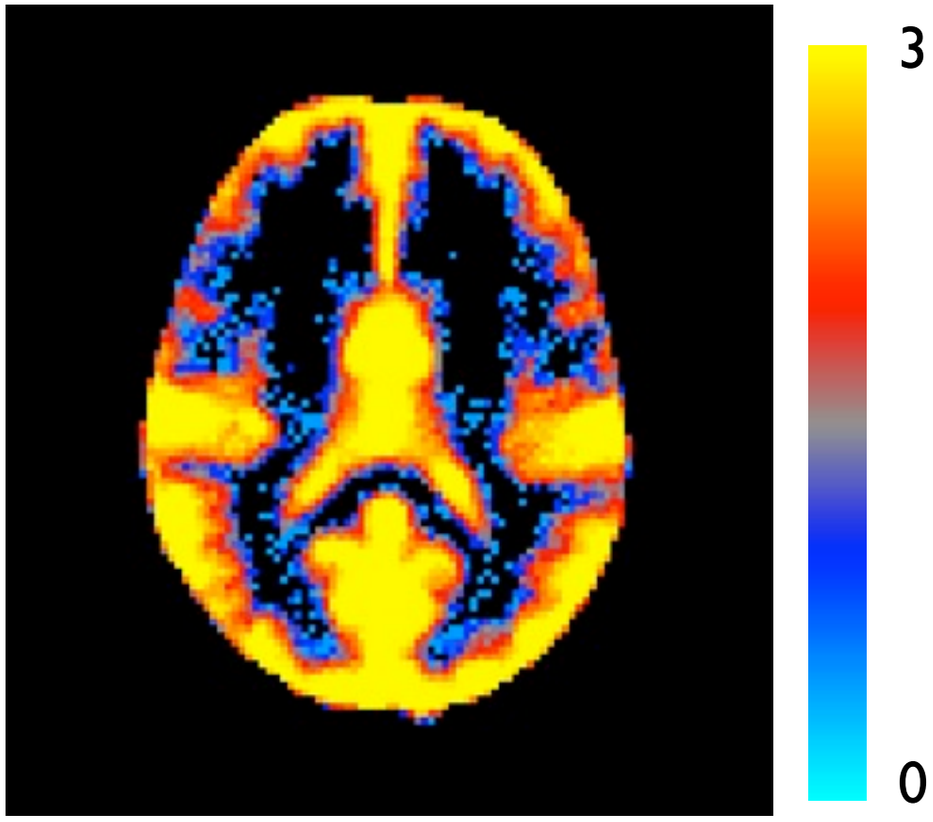

- Without normalisation PCA is biased towards tissue exhibiting strong temporal variation
- use variance-normalisation to obtain uniform specificity

between major & minor subspace

- 2 subjects, only a single (identical) RSN

A

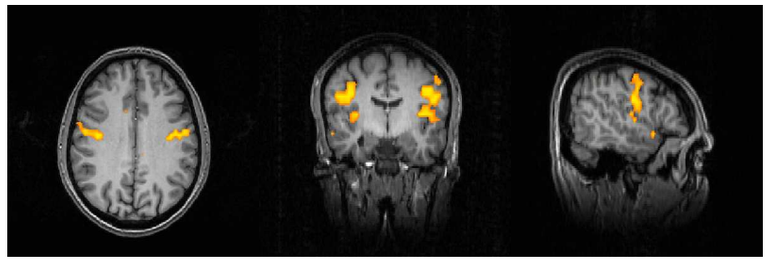

B

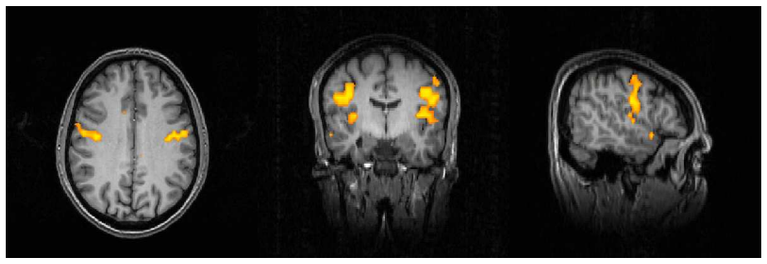

between major & minor subspace

- 2 subjects, only a single (identical) RSN
- one of the subjects has strong motion

A

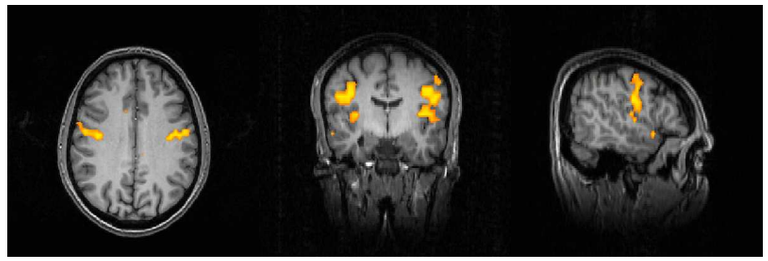

B

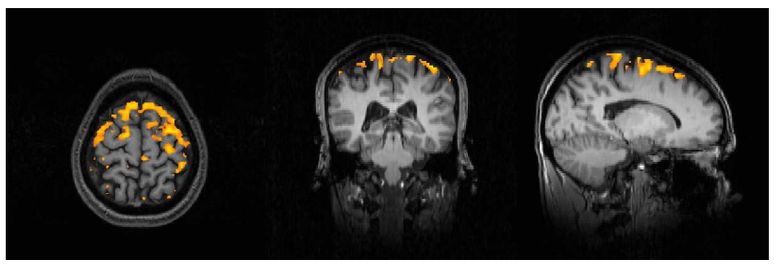

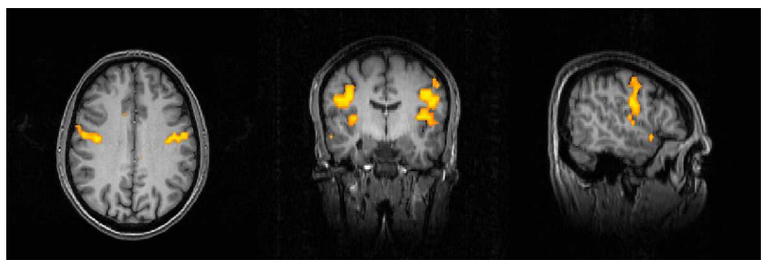

between major & minor subspace

- 2 subjects, only a single (identical) RSN
- one of the subjects has strong motion

A

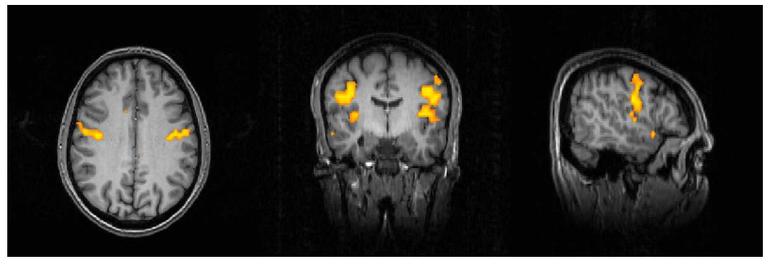

B

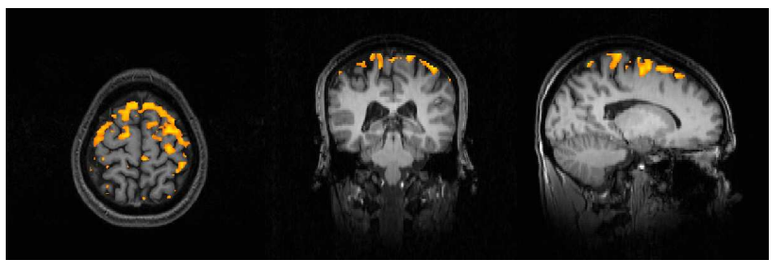

PCA cut-off

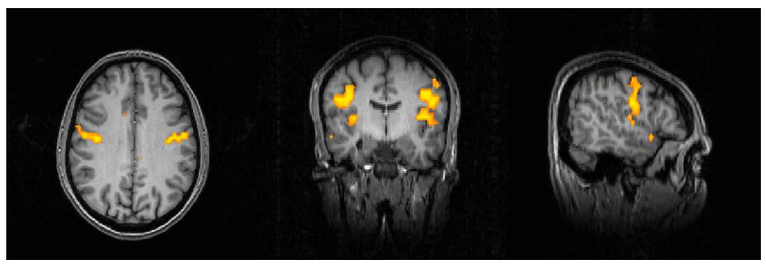

between major & minor subspace

- 2 subjects, only a single (identical) RSN
- one of the subjects has strong motion

A

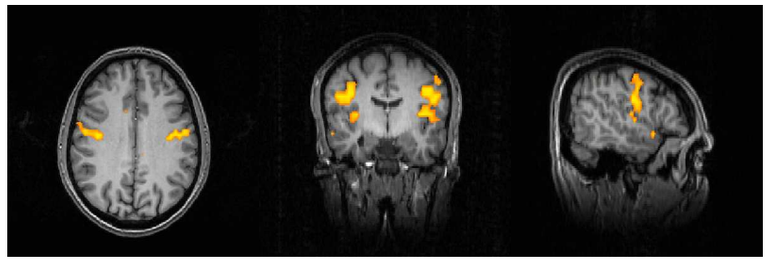

PCA cut-off

B

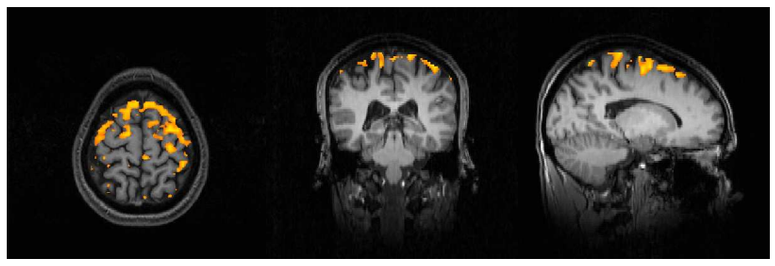

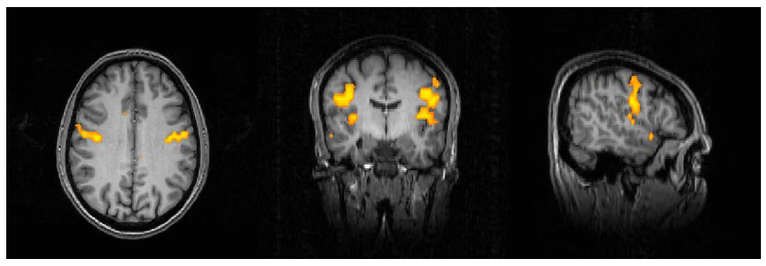

- Inverting PCA will find significant difference wrt RSN

False-positive detection!

within the major subspace

$r_A^{12} \simeq 0$

A

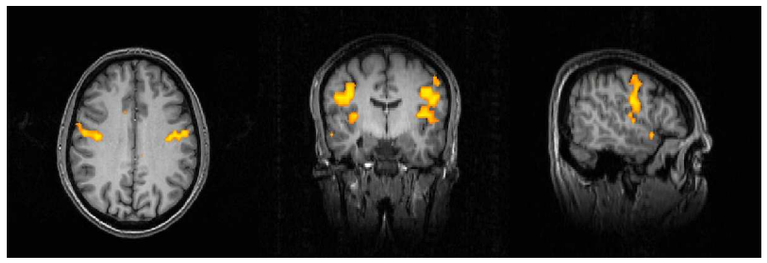

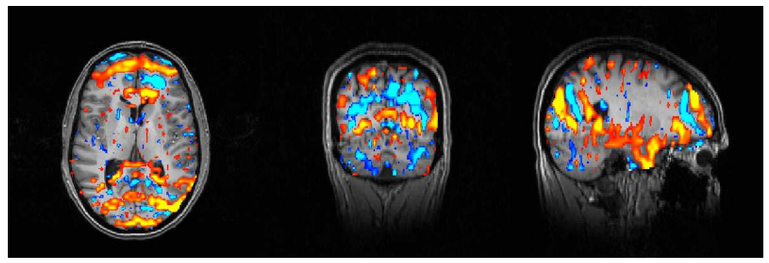

B

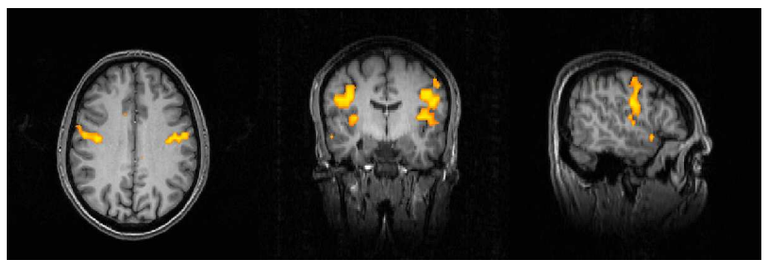

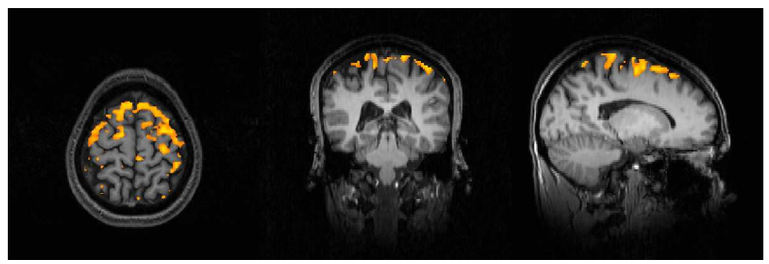

PCA cut-off

$r_B^{12} \simeq 0.3$

within the major subspace

- 2 subjects, 2 effects, different degree of temporal correlation

$r_A^{12} \simeq 0$

A

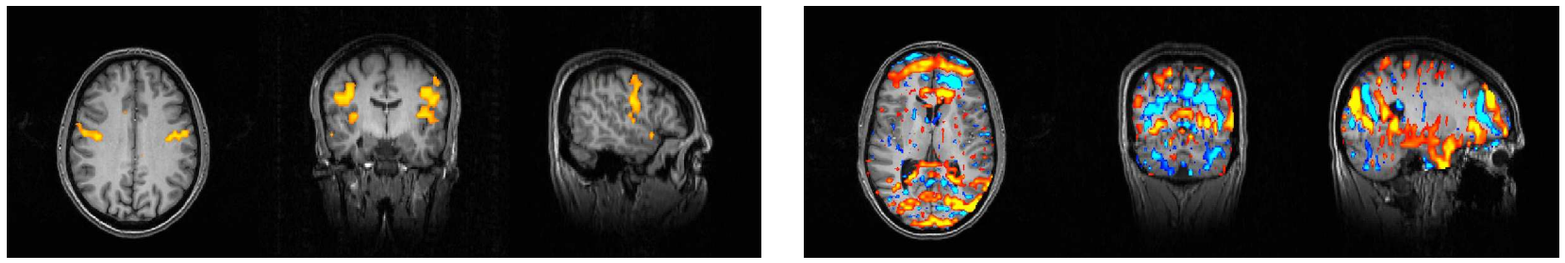

B

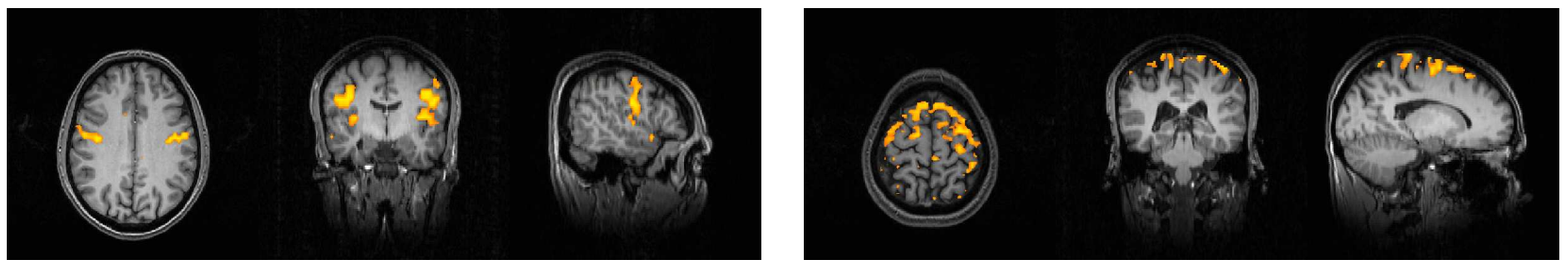

$r_B^{12} \simeq 0.3$

PCA cut-off

within the major subspace

- 2 subjects, 2 effects, different degree of temporal correlation

$r_A^{12} \simeq 0$

A

B

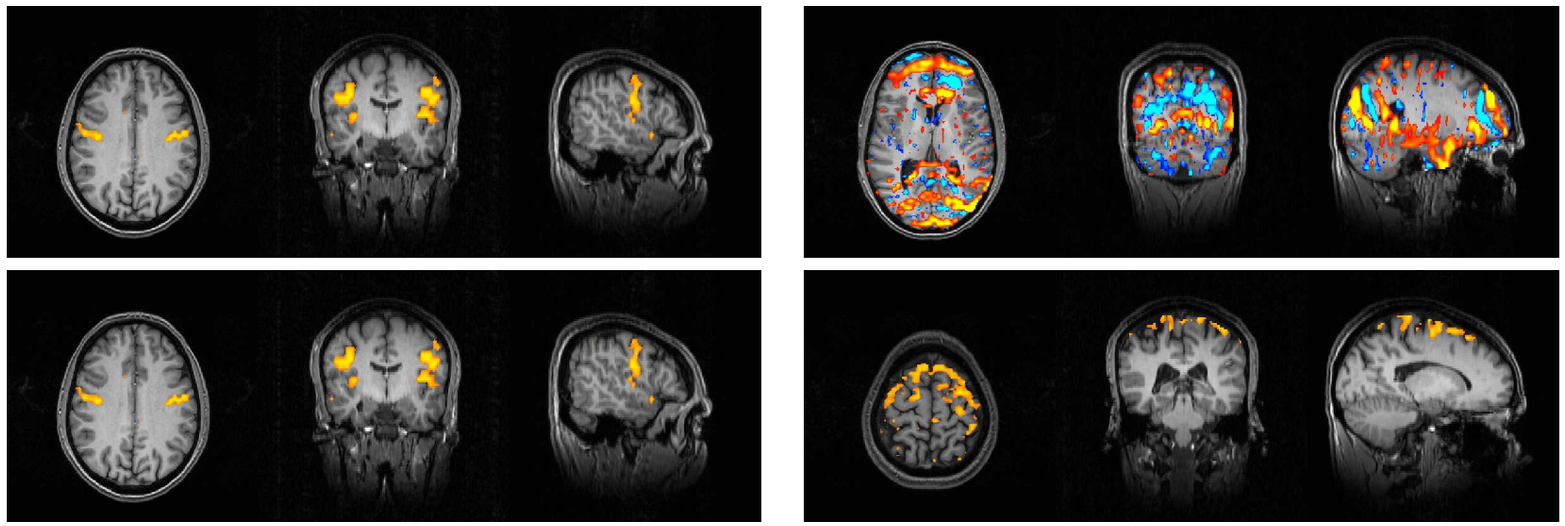

PCA cut-off

$r_B^{12} \simeq 0.3$

- PCA will represent effect 1 differently in the two subjects

Difference in signal representation within the major subspace

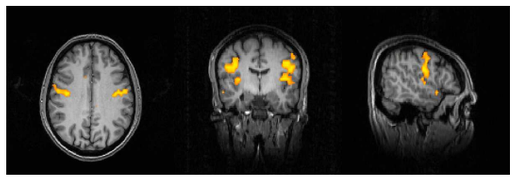

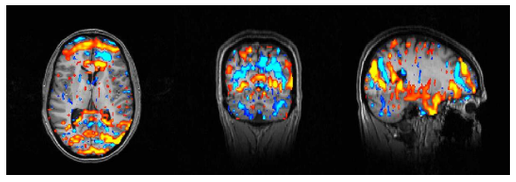

A

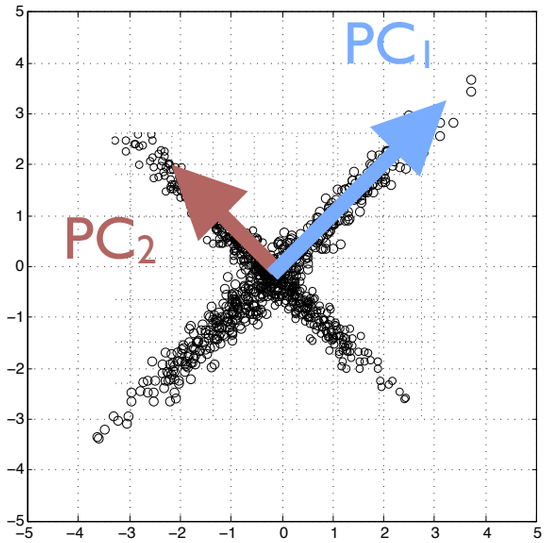

$r_A^{12} \simeq 0$

B

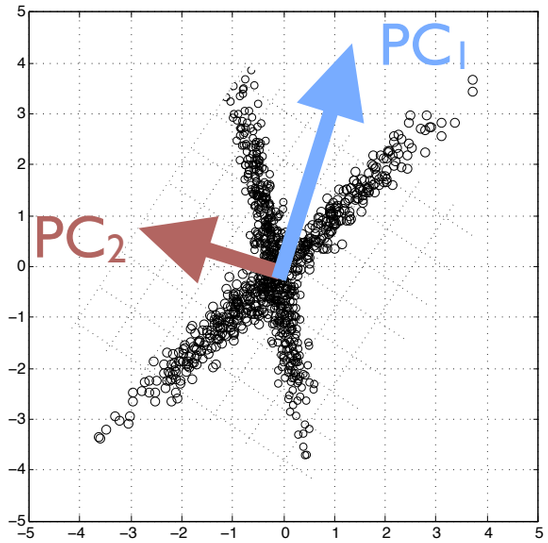

$r_B^{12} \simeq 0.3$

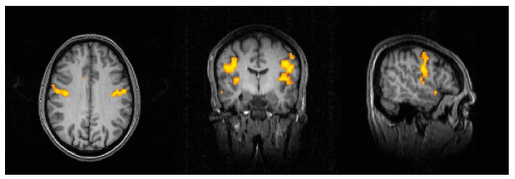

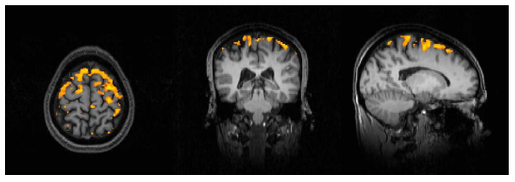

- Inverting PCA will use deflected vectors and over- or under-estimate effects

False-positive or false-negative detection!

Difference in signal representation within the major subspace

A

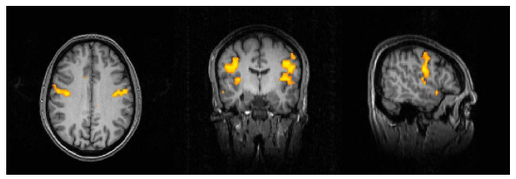

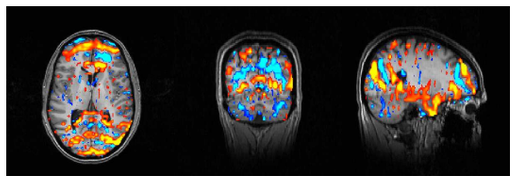

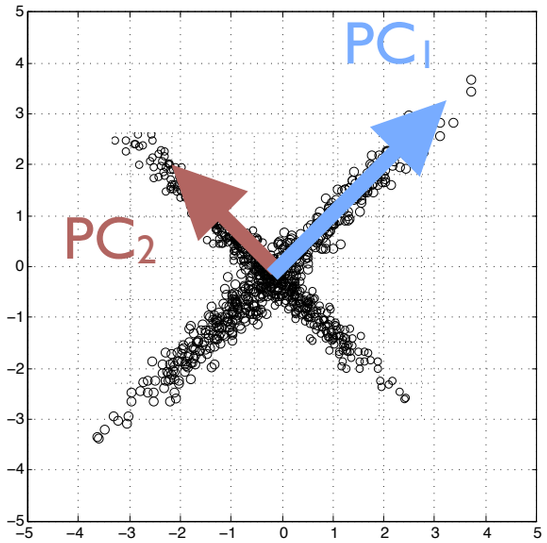

$r_A^{12} \simeq 0$

B

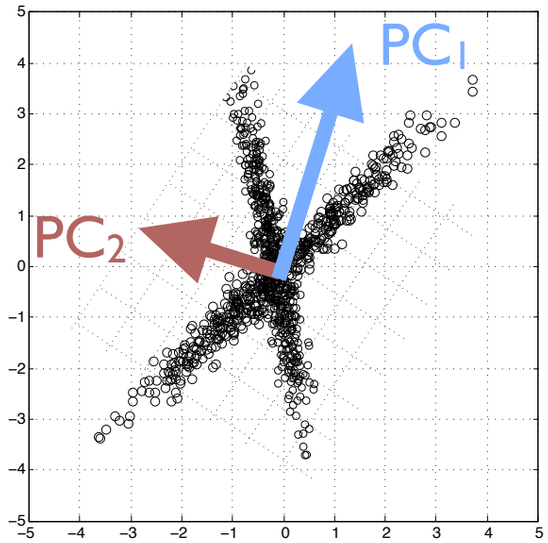

$r_B^{12} \simeq 0.3$

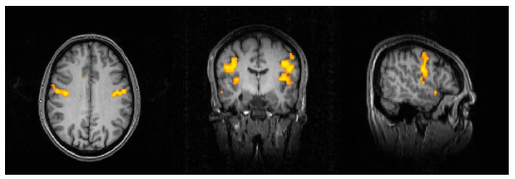

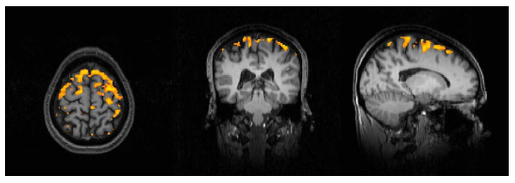

Difference in signal representation within the major subspace

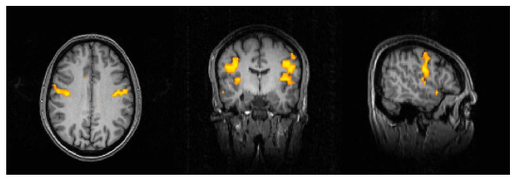

A

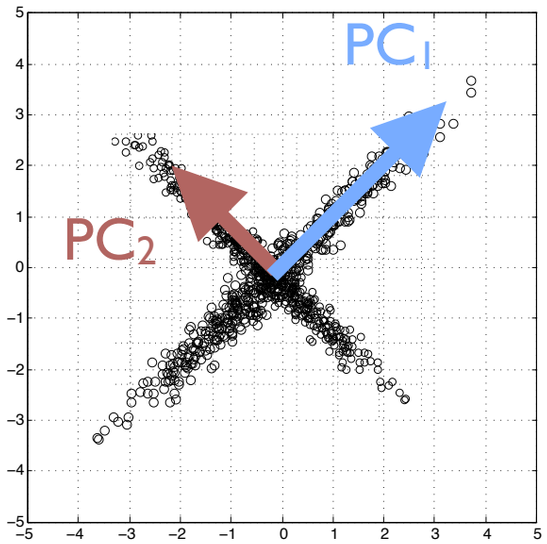

$r_A^{12} \simeq 0$

B

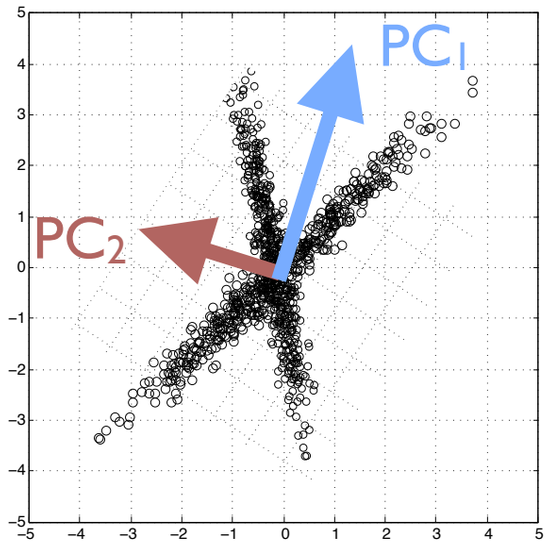

$r_B^{12} \simeq 0.3$

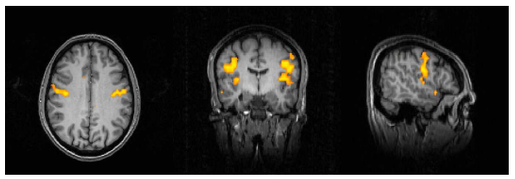

- Note: in higher-dimensional cases the subspaces for A and B will in general not be the same (don;t just differ by rotation)!
- Can only talk about the joint (intersection) space in confidence

How to do multi-subject PCA?

- Ideally want to use the *full* NT x NT covariance matrix

NxT

C_{11}	C_{12}	...	C_{1n}
C_{21}	C_{22}		
⋮		⋱	
C_{n1}			C_{1n}

NxT

How to do multi-subject PCA?

- Ideally want to use the *full* NT x NT covariance matrix
- *subject-specific* PCA uses C_{ii} only

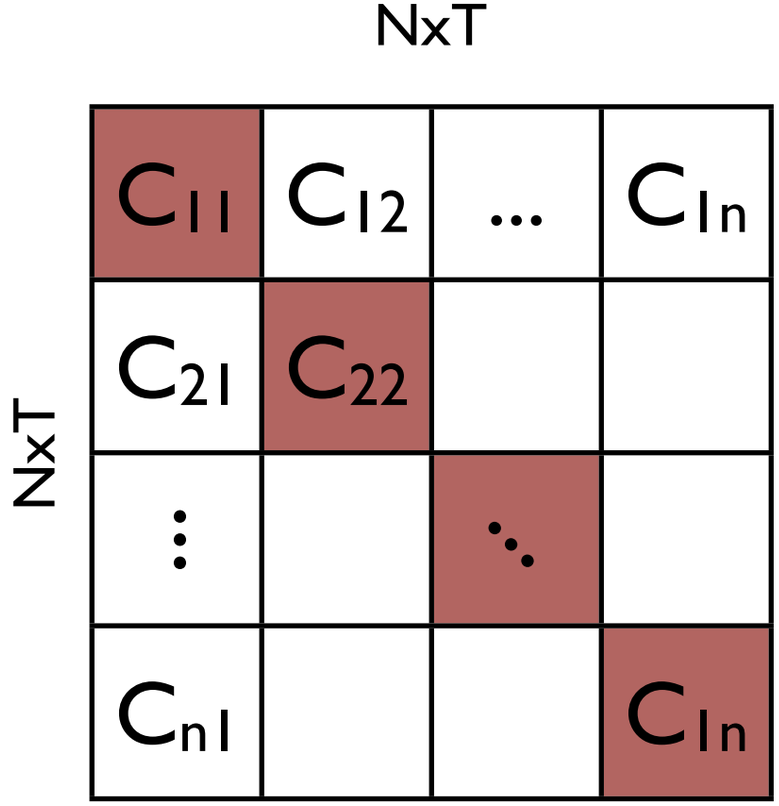

How to do multi-subject PCA?

- Ideally want to use the *full* NT x NT covariance matrix
- *subject-specific* PCA uses C_{ii} only
- $C_{ij\ (i \neq j)}$ contains the relevant cross-subject information
- *subject-specific* PCA ignores these terms!

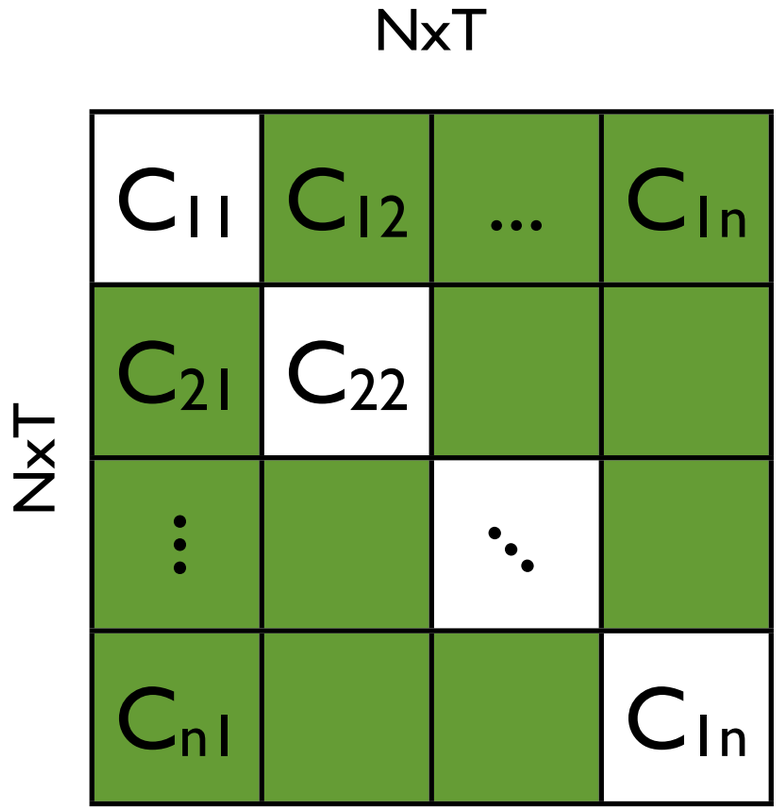

group-PCA

- based on the average data matrix find Eigen-maps

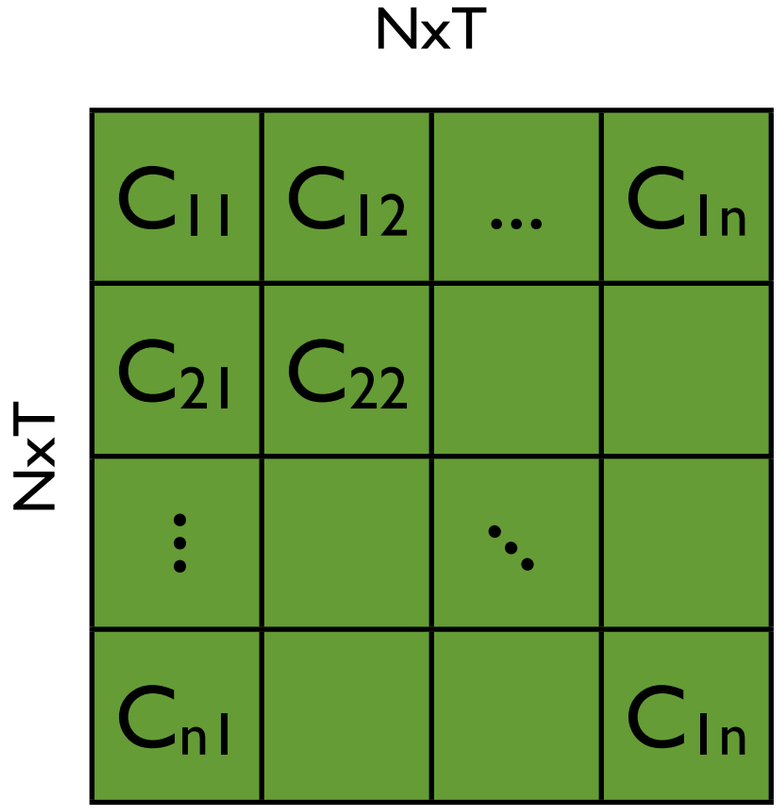

group-PCA

- based on the average data matrix find Eigen-maps

$$\frac{1}{N}\sum_{i} Y^{i} = \widetilde{U}\widetilde{D}V^{t}$$

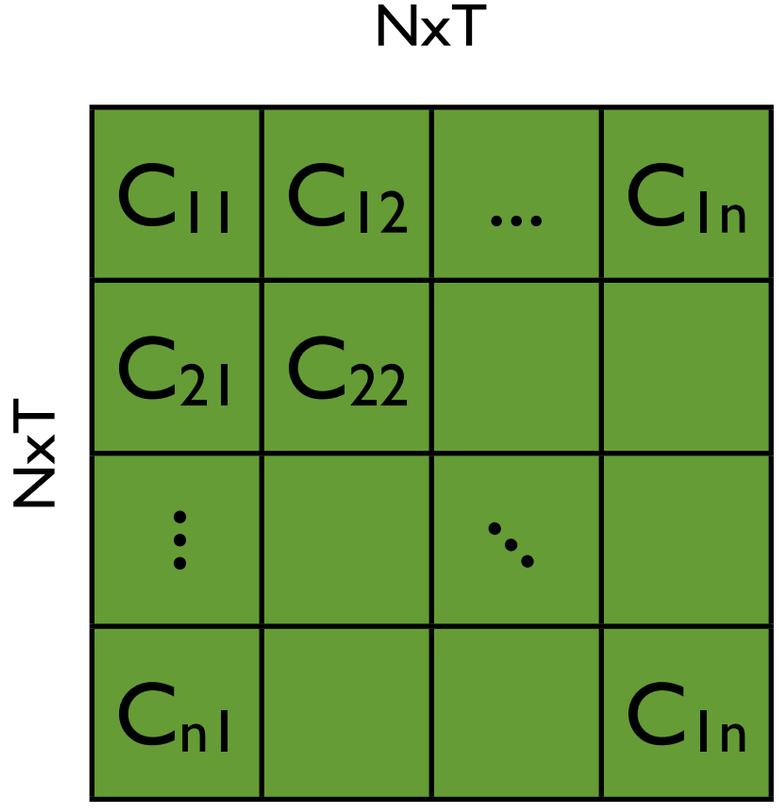

group-PCA

- based on the average data matrix find Eigen-maps

$$\frac{1}{N}\sum_i Y^i = \widetilde{U}\widetilde{D}V^t$$

- solve for $U^i D^i$ s.t.

$$Y^i = U^i D^i V^t$$

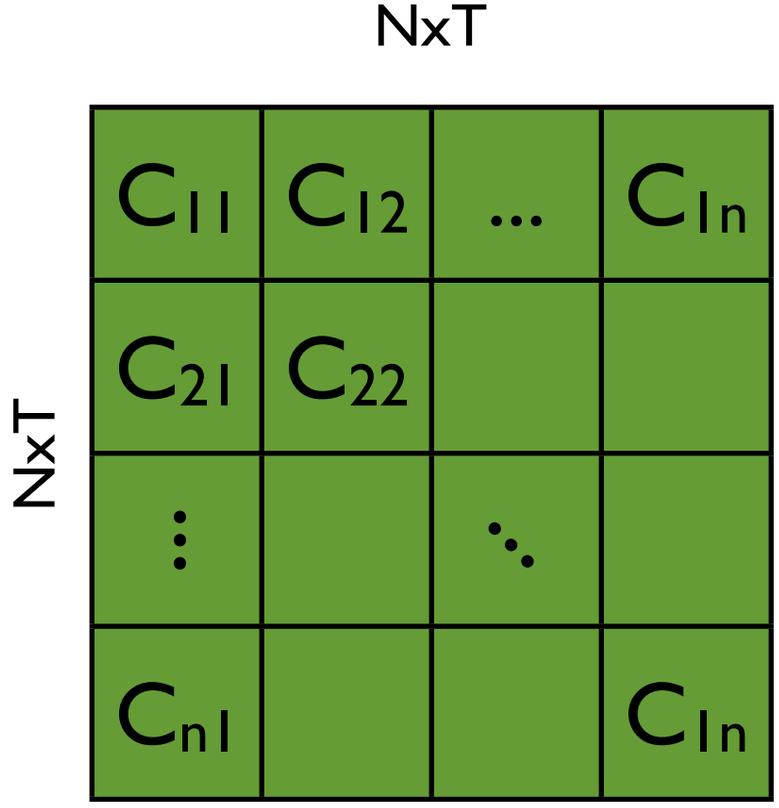

group-PCA

- based on the average data matrix find Eigen-maps

$$\frac{1}{N}\sum_i Y^i = \widetilde{U}\widetilde{D}V^t$$

- solve for U^iD^i s.t.

$$Y^i = U^iD^iV^t$$

- reduce dim. per subject

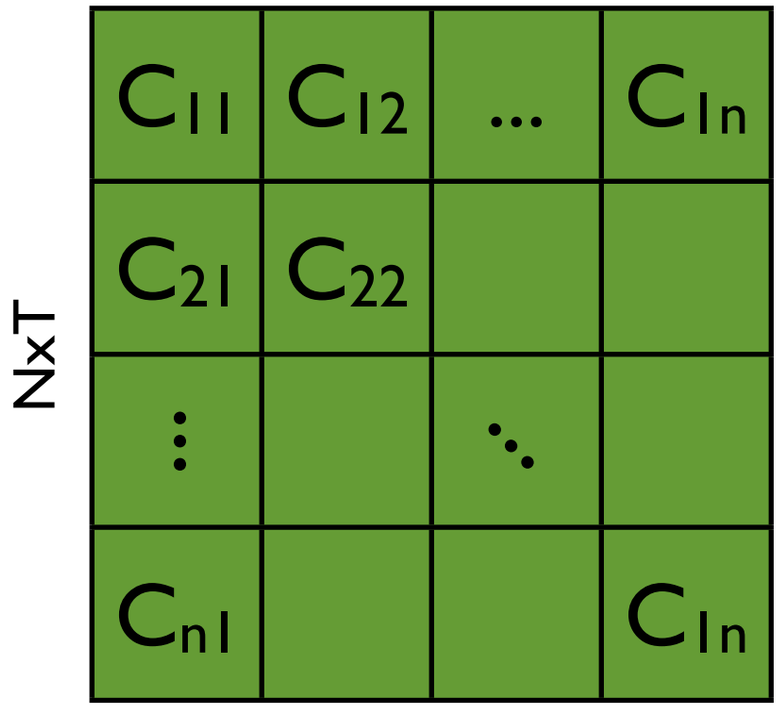

enforces that in *all* subjects the same effects can be *represented and compared*

Concat-ICA

- Concatenate all subjects' data temporally
  (Actually: group-based PCA reduction on each subject, then concat, then PCA reduction)
- then run ICA to obtain group maps

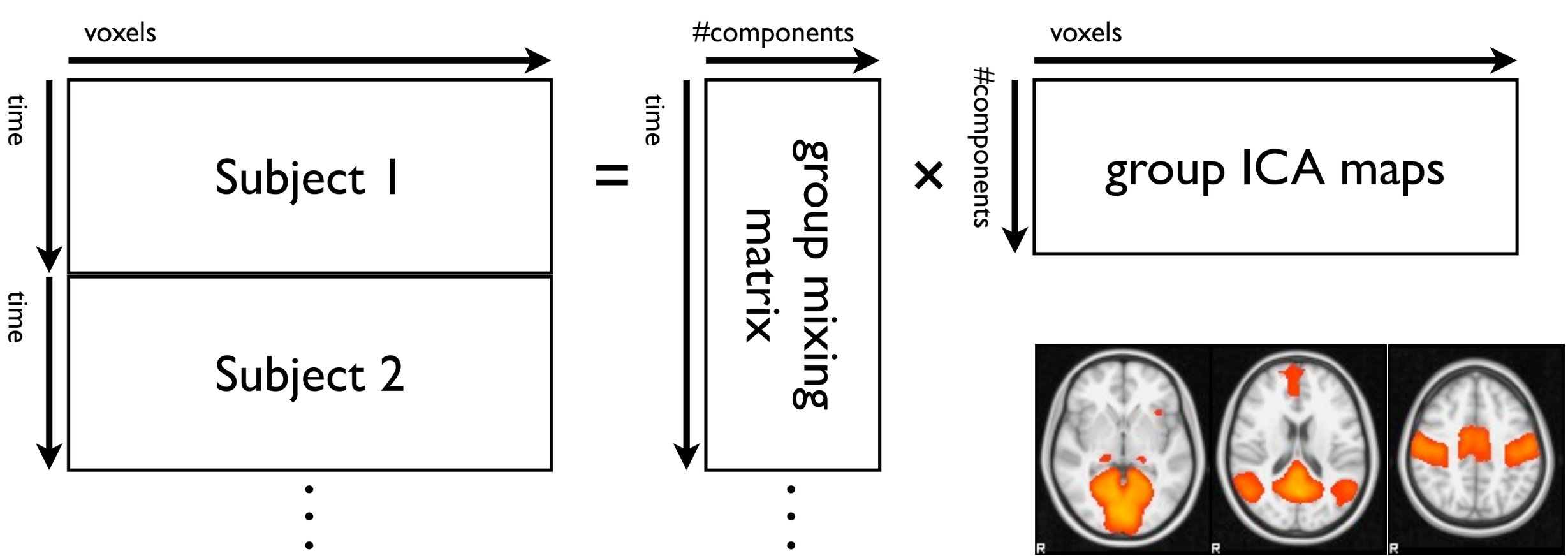

Group maps

How to get subject-specific maps?

- could track all (temporal) transformation F_i used to find spatial group maps, then use inverse, e.g. 'Back-Projection' (Calhoun et al. 2001, HBM)
- but if forward projections are lossy/biased this can't be recovered in the backward projections!
- instead, need to avoid PCA bias
  - remove all dependence on the initial PCA(s)

‘Dual regression’ model

- Model each subject’s data as a linear combination of spatial maps and noise

$$Y^i = S^i A^i + E^i, \quad \text{where} \quad E^i_{\cdot j} \sim \mathcal{N}(0, \sigma^2_Y \boldsymbol{I})$$

- assume all spatial maps are sampled from underlying group maps, e.g. from Concat-ICA

$$S^i = S_g + E_g \quad \text{where} \quad E_g \sim \mathcal{N}(0, \sigma^2_g \boldsymbol{I})$$

‘Dual regression’ model

Hierarchical Normal-Normal model

$$Y^i \sim \mathcal{N}(S^i A^i, \sigma_Y^2 \boldsymbol{I})$$

$$S^i \sim \mathcal{N}(S_g, \sigma_g^2 \boldsymbol{I})$$

S_g known

- can use *Empirical Bayes* for estimation

‘Dual regression’

- wrt temporal modes

$$Y^i = S_g A^i + \widetilde{E} \quad \text{where} \quad \widetilde{E} \sim \mathcal{N}(0, \sigma_g^2 \boldsymbol{I} + \sigma_Y^2 \boldsymbol{I})$$

$$\widehat{A^i} = S_g^{\dagger} Y^i$$

- ...so estimates can be obtained using simple spatial regression of group-ICA maps against data

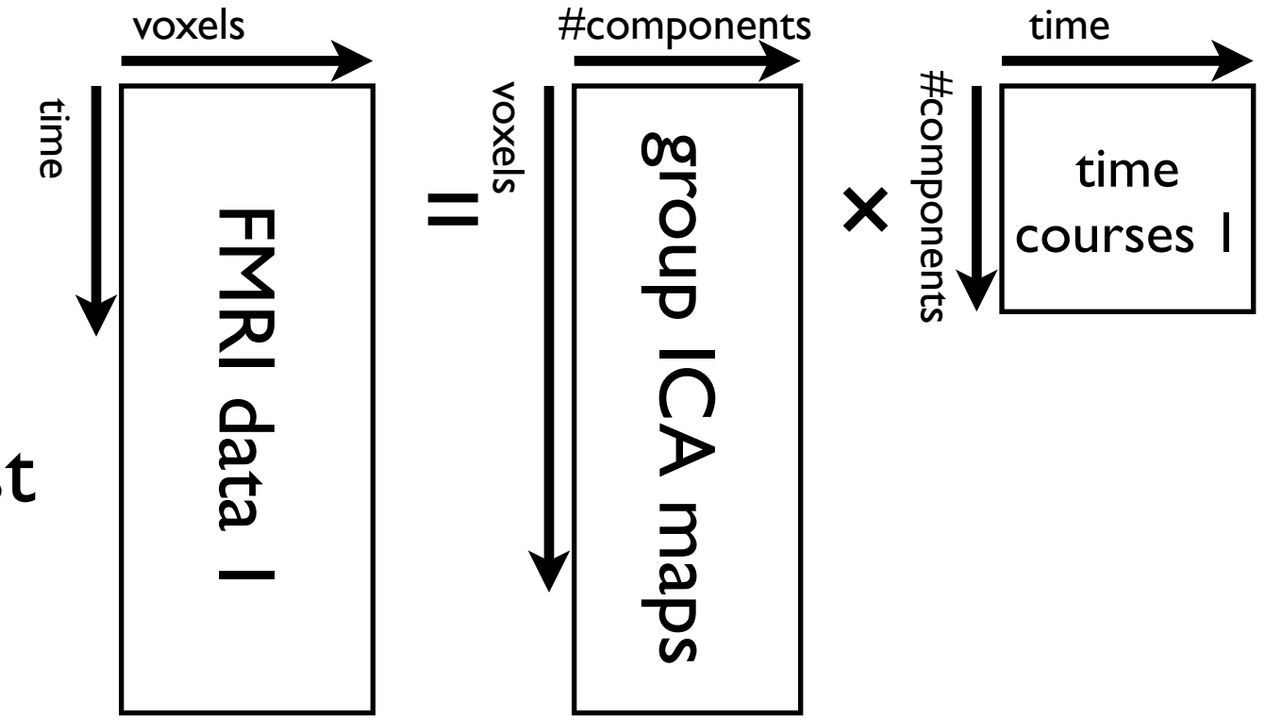

‘Dual regression’

- wrt subject-specific spatial maps

$$S^i \sim \mathcal{N}(\alpha_1 A^{i\dagger} Y^i + \alpha_2 S_g, 1/\beta^2) \quad \text{with}$$

$$\alpha_1 = \frac{1/\sigma_g^2}{1/\sigma_Y^2 + 1/\sigma_g^2}, \qquad \alpha_2 = \frac{1/\sigma_Y^2}{1/\sigma_Y^2 + 1/\sigma_g^2}$$

$$\beta^2 = 1/\sigma_Y^2 + 1/\sigma_g^2$$

‘Dual regression’

- wrt subject-specific spatial maps

$$S^i \sim \mathcal{N}(\alpha_1 A^{i\dagger} Y^i + \alpha_2 S_g, 1/\beta^2) \quad \text{with}$$

$$\alpha_1 = \frac{1/\sigma_g^2}{1/\sigma_Y^2 + 1/\sigma_g^2}, \qquad \alpha_2 = \frac{1/\sigma_Y^2}{1/\sigma_Y^2 + 1/\sigma_g^2}$$

$$\beta^2 = 1/\sigma_Y^2 + 1/\sigma_g^2$$

for $\sigma_g \gg \sigma_Y$: $\boxed{\widehat{S}^i = \widehat{A}^{i\dagger} Y^i}$

‘Dual regression’

- Regress spatial ICs into each subject’s 4D data to find subject-specific timecourses
- regress these back into the 4D data to find subject-specific spatial ICs associated with the group ICs

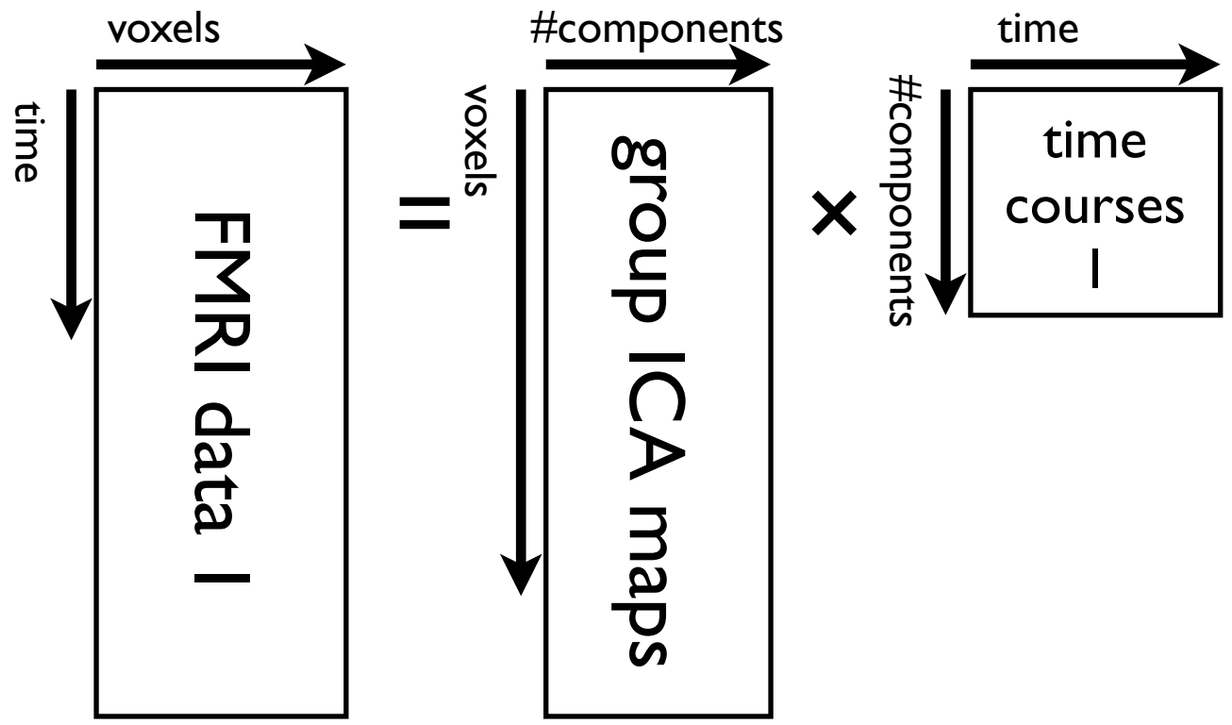

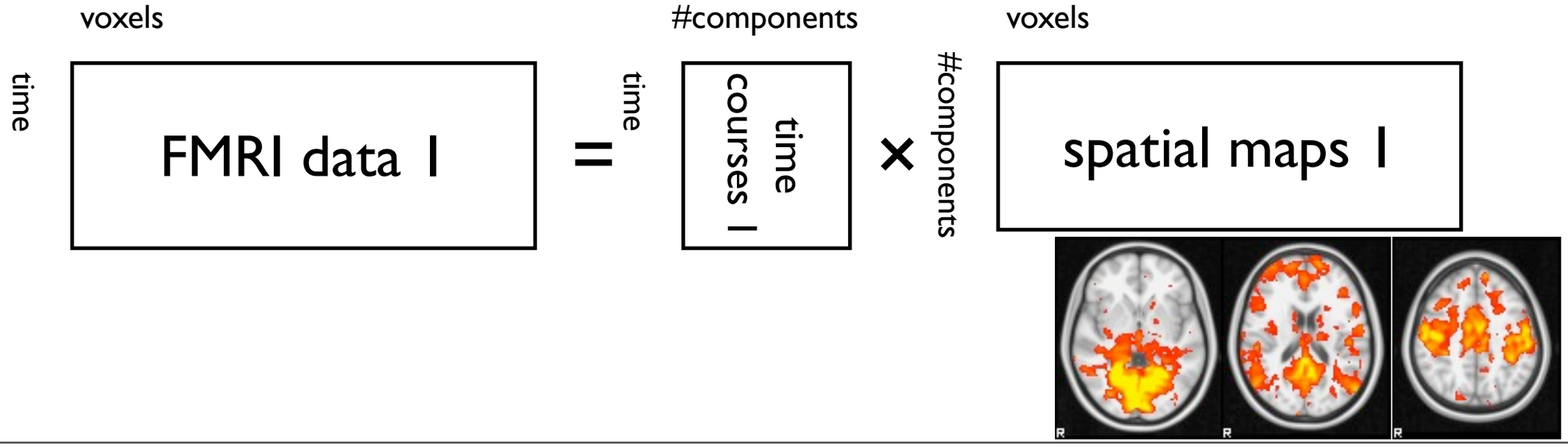

‘Dual regression’

- Collect maps and perform voxel-wise non-parametric randomisation test on GLM

- Can now do voxelwise testing across subjects, separately for each original group ICA map

‘Dual regression’

- Collect maps and perform voxel-wise non-parametric randomisation test on GLM

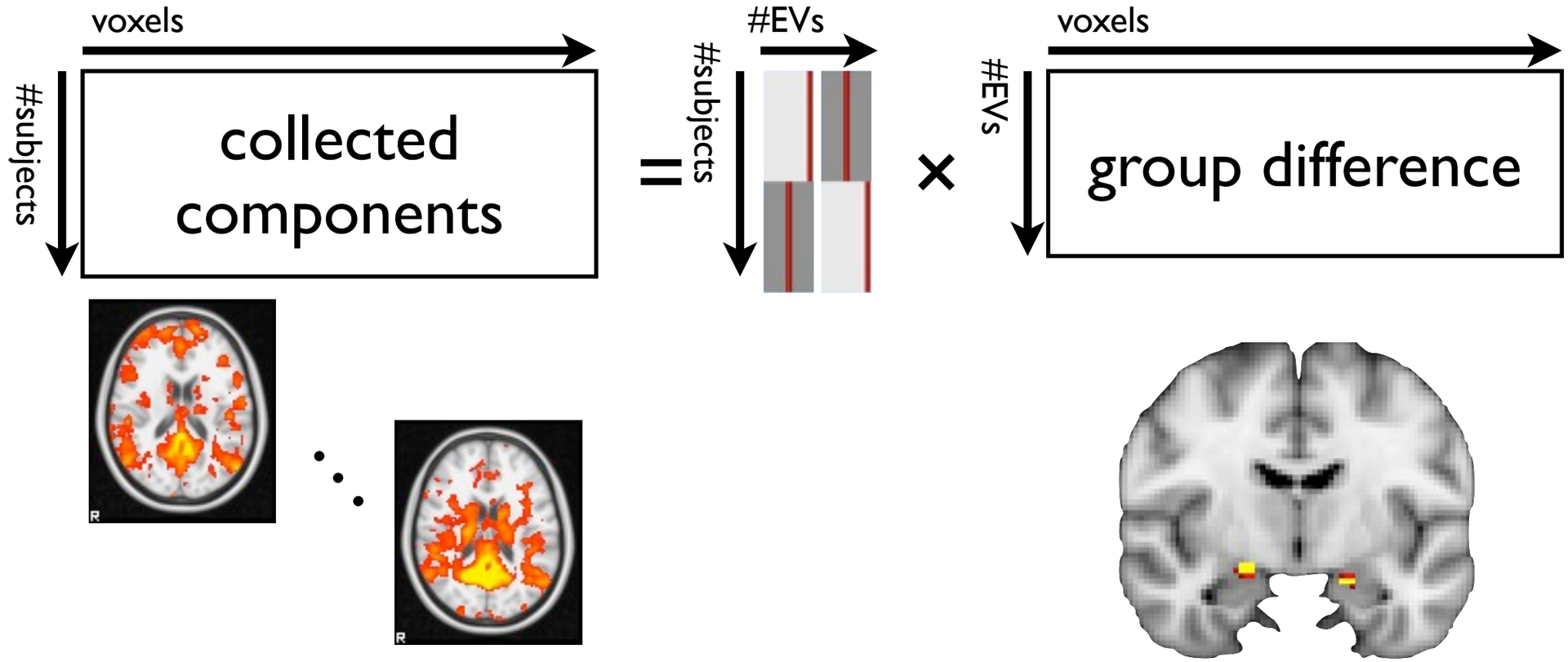

- Can now do voxelwise testing across subjects, separately for each original group ICA map

‘Dual regression’

- Collect maps and perform voxel-wise non-parametric randomisation test on GLM

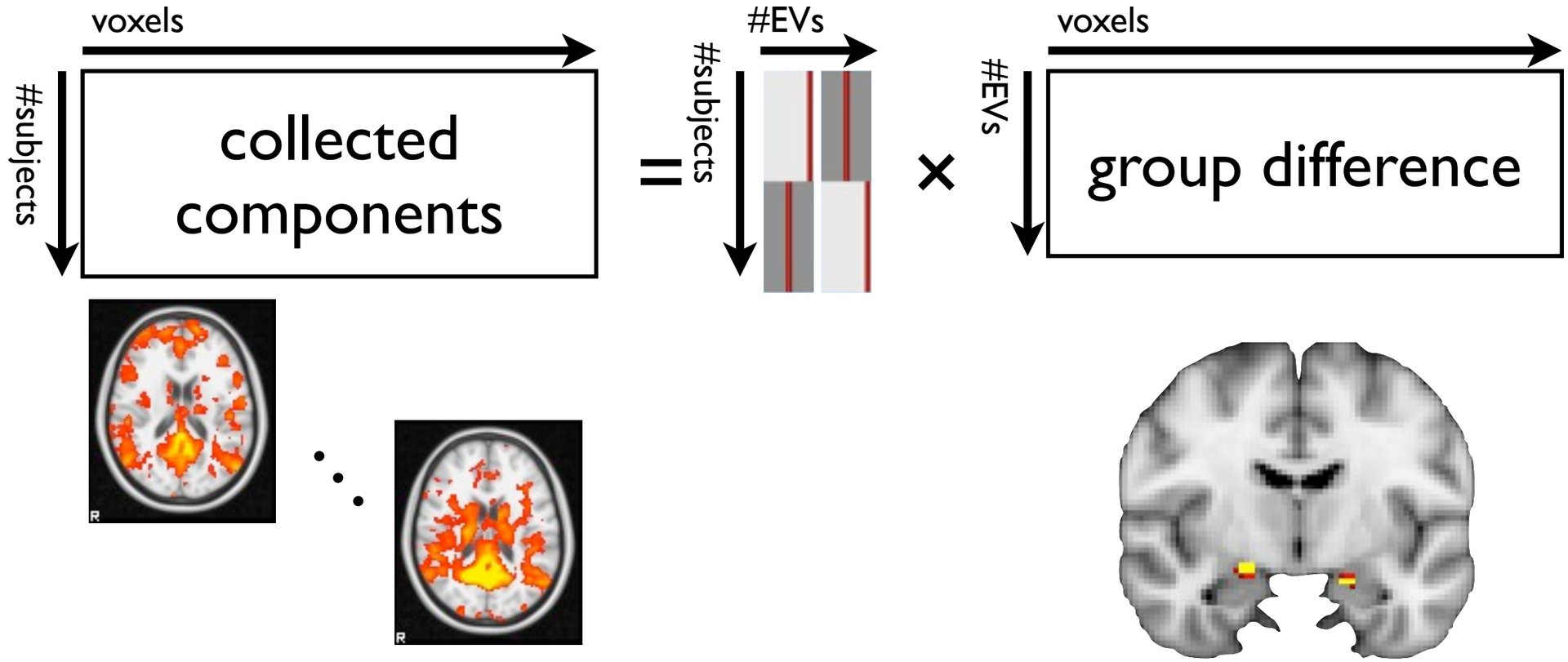

- Can now do voxelwise testing across subjects, separately for each original group ICA map

Dual Regression

Dual Regression

- PCA bias prevents meaningful comparison of differential effects

Dual Regression

- PCA bias prevents meaningful comparison of differential effects
- hard to detect (in sum-of-squares evaluations) so simulations of very limited validity and utility

Dual Regression

- PCA bias prevents meaningful comparison of differential effects
- hard to detect (in sum-of-squares evaluations) so simulations of very limited validity and utility
- need to use unbiased methods when inferring *differences in connectivity* based on maps which show *similarity in connectivity*

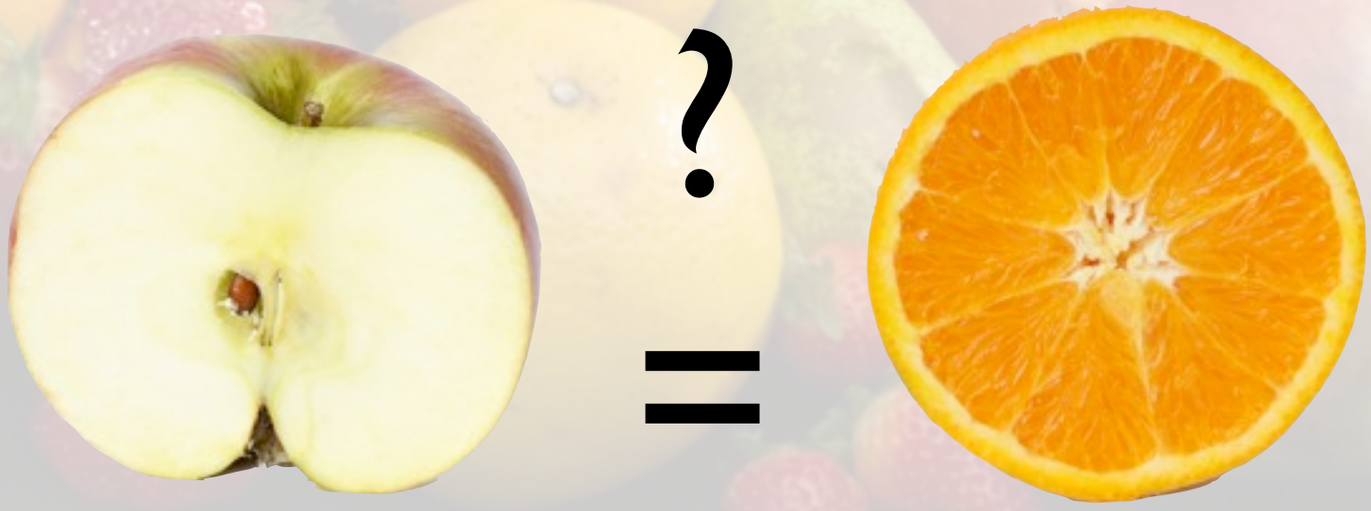

The *functional* architecture of the human brain

PNAS

Correspondence of the brain's functional architecture during activation and rest

Stephen M. Smith[a,1], Peter T. Fox[b], Karla L. Miller[a], David C. Glahn[b,c], P. Mickle Fox[b], Clare E. Mackay[a], Nicola Filippini[a], Kate E. Watkins[a], Roberto Toro[d], Angela R. Laird[b], and Christian F. Beckmann[a,e]

[a]Centre for Functional MRI of the Brain, University of Oxford, Oxford OX3 9DU, United Kingdom; [b]Research Imaging Center, University of Texas Health Science Center, San Antonio, TX 782229; [c]Olin Neuropsychiatry Research Center, Institute of Living, Yale University, New Haven, CT 06106; [d]Human Genetics and Cognitive Function, Institut Pasteur, 75724 Paris, France; and [e]Clinical Neuroscience Department, Imperial College London, London SW7 2AZ, United Kingdom

Edited by Marcus E. Raichle, Washington University School of Medicine, St. Louis, M

Neural connections, providing the substrate for functional networks, exist whether or not they are functionally active at any given moment. However, it is not known to what extent brain regions are continuously interacting when the brain is "at rest." In this work, we identify the major explicit activation networks by carrying out an image-based activation network analysis of thousands of separate activation maps derived from the BrainMap database of functional imaging studies, involving nearly 30,000 human subjects. Independently, we extract the major covarying networks in the resting brain, as imaged with functional magnetic resonance imaging in 36 subjects at rest. The sets of major brain networks, and their decompositions into subnetworks, show close correspondence between the independent analyses of resting and activation brain dynamics. We conclude that the full repertoire of functional networks utilized by the brain in action is continuously and dynamically "active" even when at "rest."

brain connectivity | BrainMap | FMRI | functional connectivity | resting-state networks

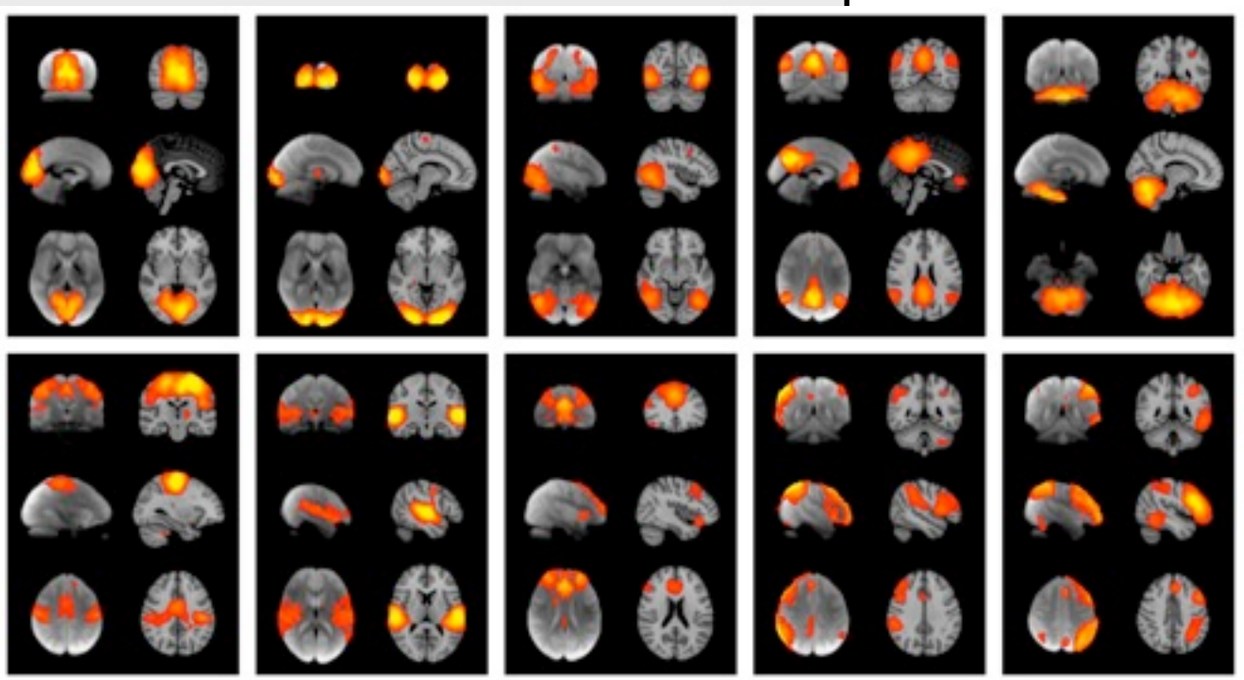

hy cl ac

la pr th st co riz (o la in ex on pr ar tic

vation images" from the list of activation peak locations (18, 19). It is then possible to investigate cooccurrence of different

The *functional* architecture of the human brain:

Correspondence between resting FMRI and task-activation studies

RIC

FMRIB
Oxford Centre for Functional MRI of the Brain

The *functional* architecture of the human brain:

Correspondence between resting FMRI and task-activation studies

RIC

FMRIB
Oxford Centre for Functional MRI of the Brain

FSL

Sleuth v.1.1

BrainMap, RIC, San Antonio

Data

- 1687 FMRI / PET activation studies (19% of all published activation imaging studies)

The *functional* architecture of the human brain:

Correspondence between resting FMRI and task-activation studies

RIC

FMRIB
Oxford Centre for Functional MRI of the Brain

FSL

Sleuth v.1.1

BrainMap, RIC, San Antonio

Data

- 1687 FMRI / PET activation studies (19% of all published activation imaging studies)
- 7342 separate activation conditions/contrasts

The *functional* architecture of the human brain:

Correspondence between resting FMRI and task-activation studies

RIC

FMRIB
Oxford Centre for Functional MRI of the Brain

BrainMap, RIC, San Antonio

Data

- 1687 FMRI / PET activation studies (19% of all published activation imaging studies)
- 7342 separate activation conditions/contrasts
- 29,671 human subjects

The *functional* architecture of the human brain:

Correspondence between resting FMRI and task-activation studies

RIC

FMRIB
Oxford Centre for Functional MRI of the Brain

BrainMap, RIC, San Antonio

Data

- 1687 FMRI / PET activation studies (19% of all published activation imaging studies)
- 7342 separate activation conditions/contrasts
- 29,671 human subjects
- 66 "Behavioural domains" (gross paradigm classifications)

The *functional* architecture of the human brain:

Correspondence between resting FMRI and task-activation studies

RIC

FMRIB
Oxford Centre for Functional MRI of the Brain

FSL

Sleuth v.1.1

BrainMap, RIC, San Antonio

Data

- 1687 FMRI / PET activation studies (19% of all published activation imaging studies)
- 7342 separate activation conditions/contrasts
- 29,671 human subjects
- 66 "Behavioural domains" (gross paradigm classifications)

Resting FMRI data

Data

- 36 healthy subjects, age 20-35
- Subjects at rest, eyes open, fairly dark scanner room
- 6 minutes FMRI, standard BOLD, 3x3x3.5mm

Data & Methods

BrainMap, RIC, San Antonio

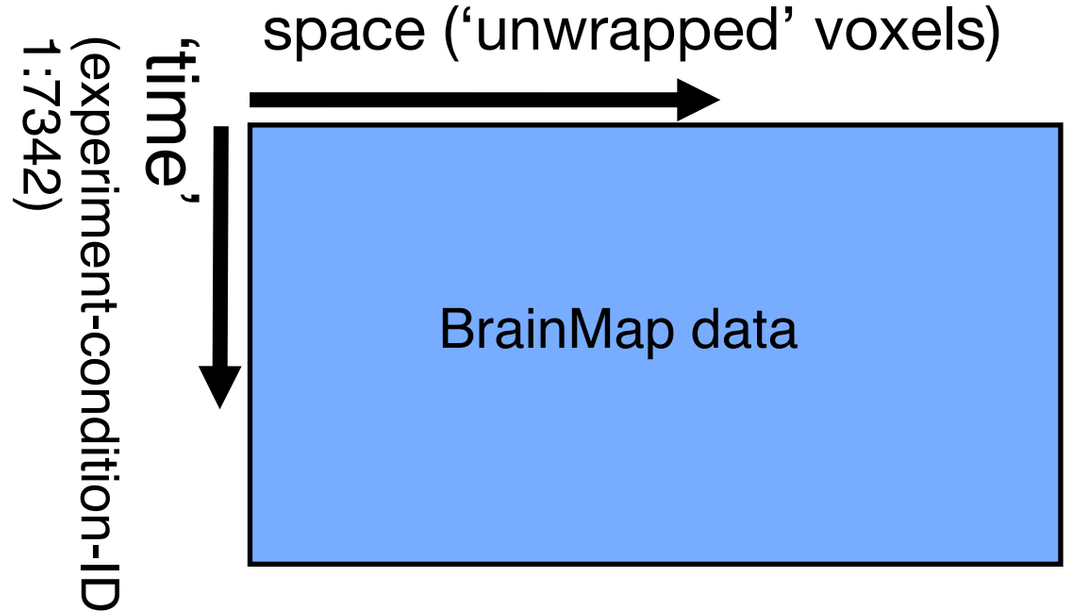

Resting FMRI data

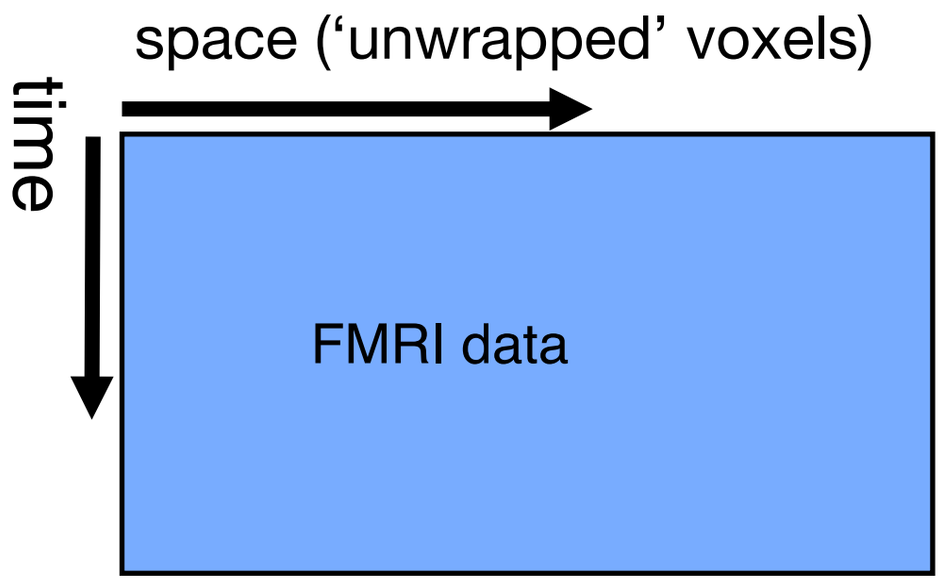

Pairings between RSN maps (left of each pair) and BrainMap maps (right) at ICA dimensionality of 20

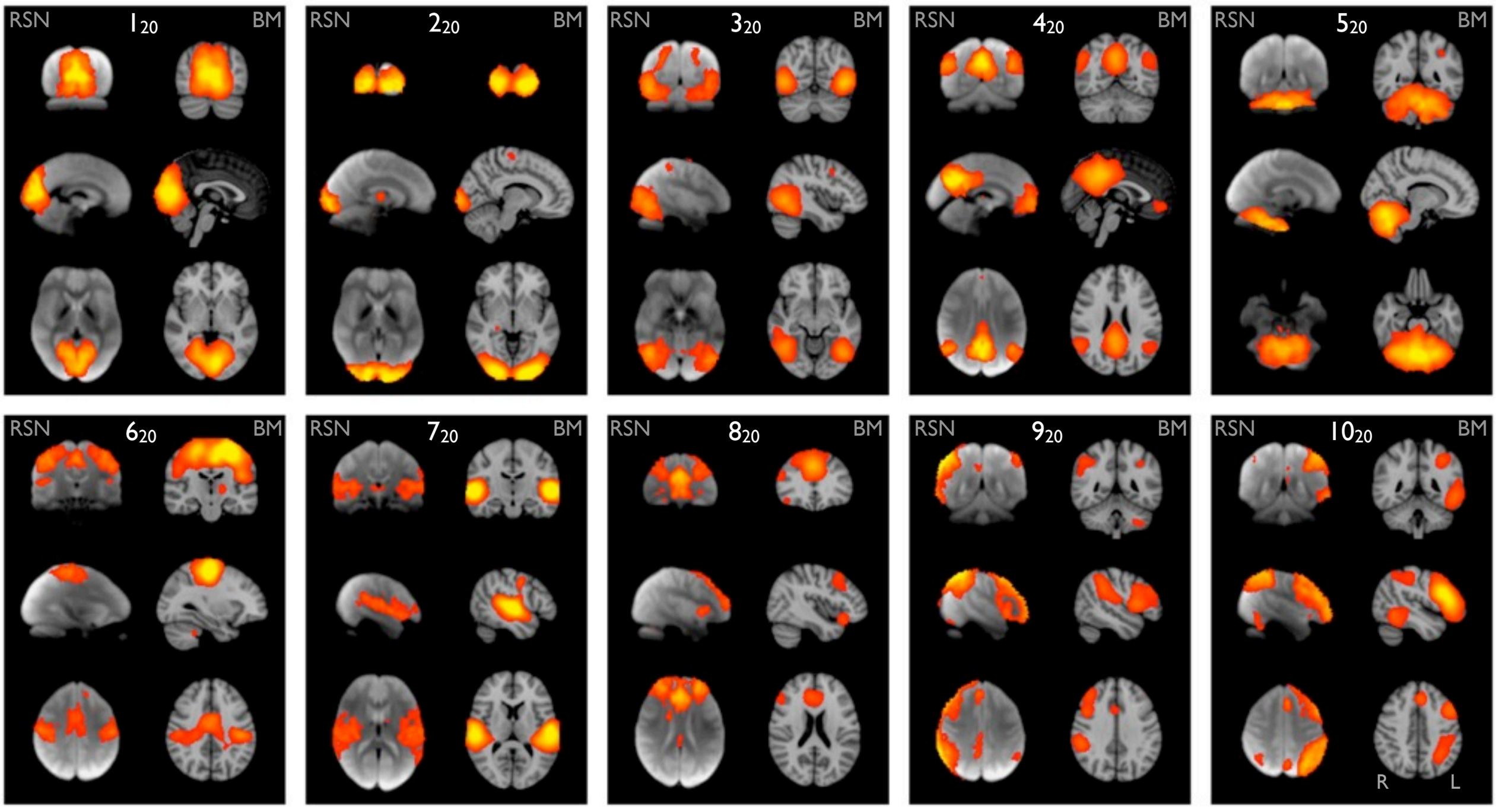

Pairings between RSN maps (left of each pair) and BrainMap maps (right) in the sensori-motor cortex, at ICA dimensionality of 70

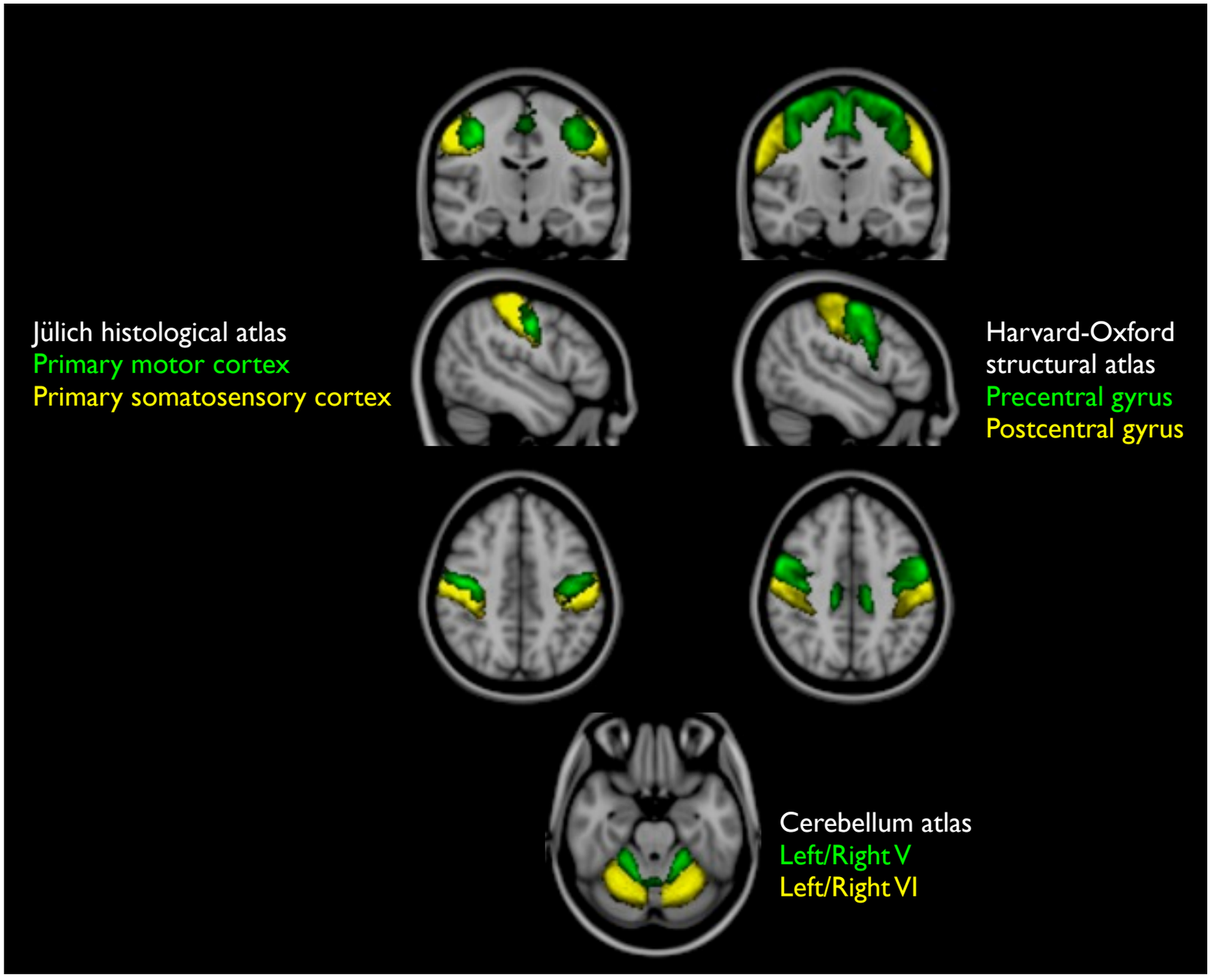

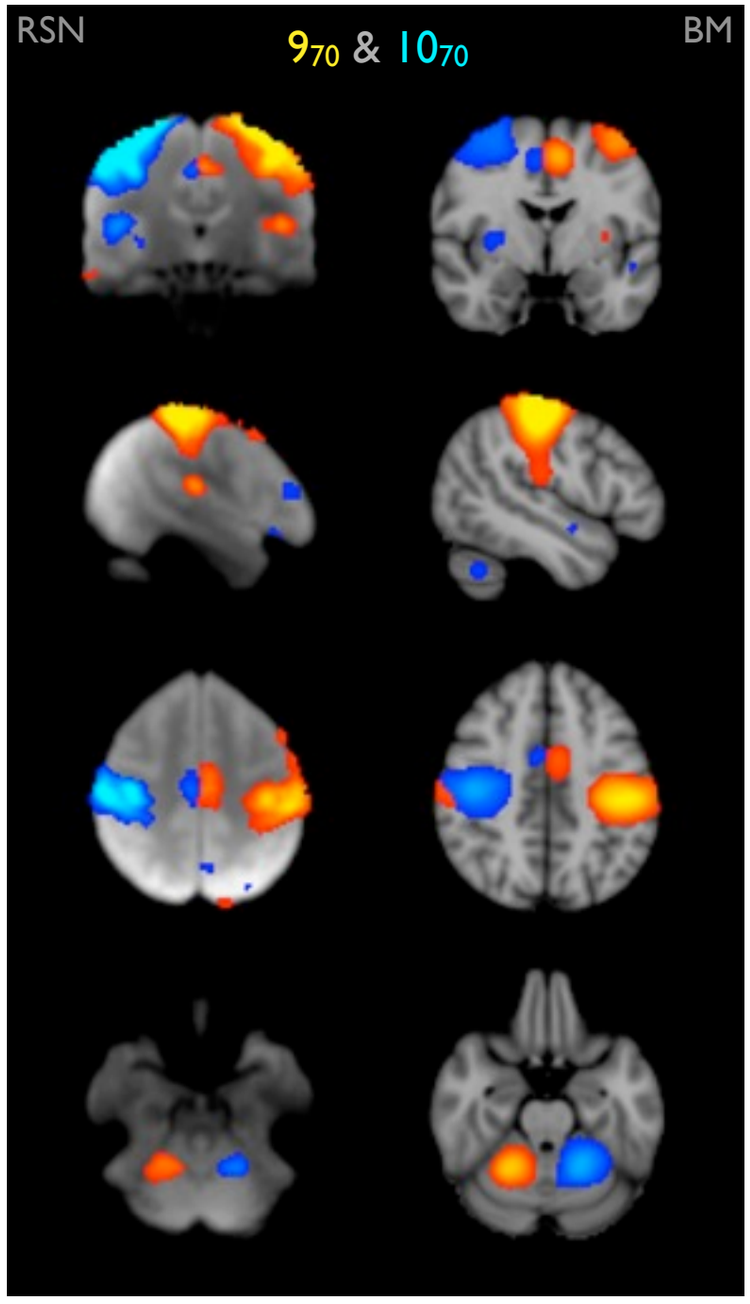

Pairings between RSN maps (left of each pair) and BrainMap maps (right) in visual areas, at ICA dimensionality of 70

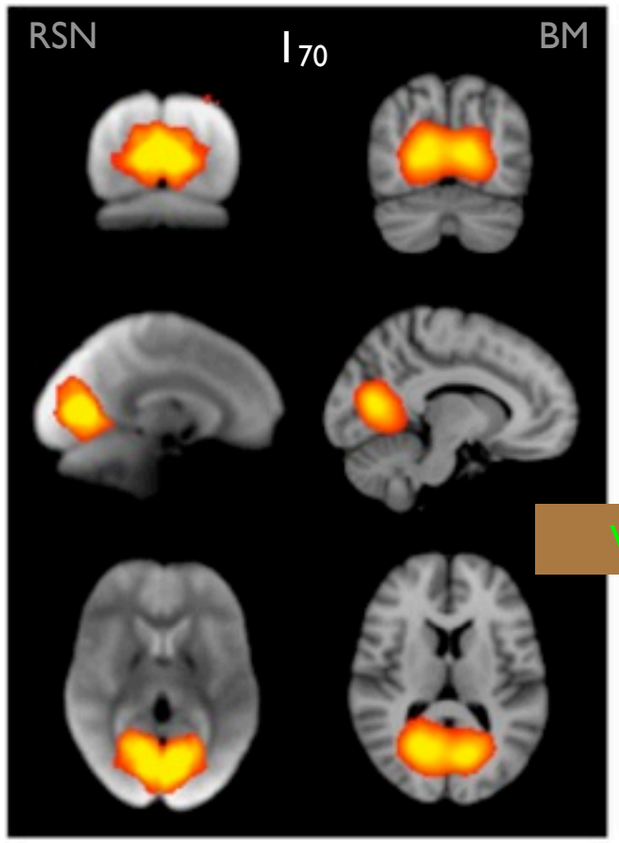

V1

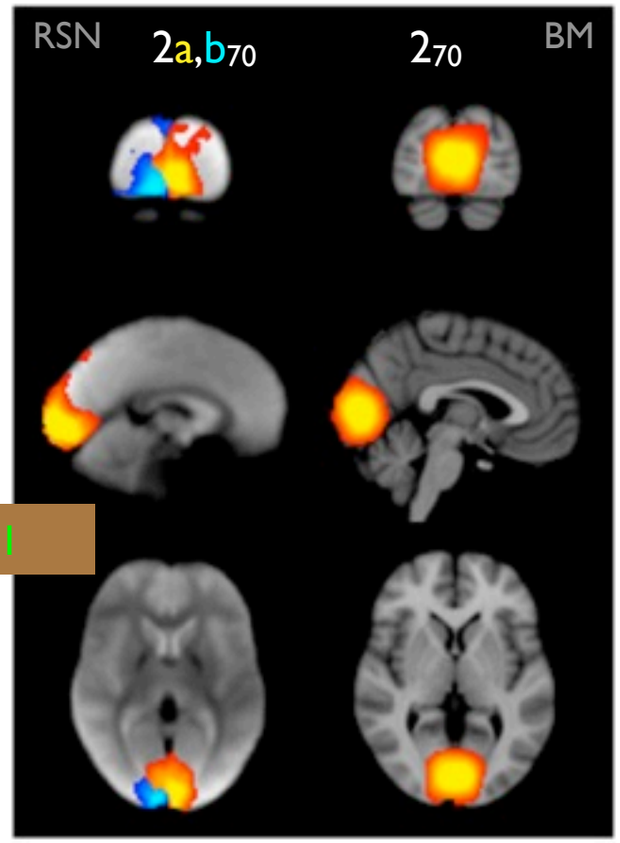

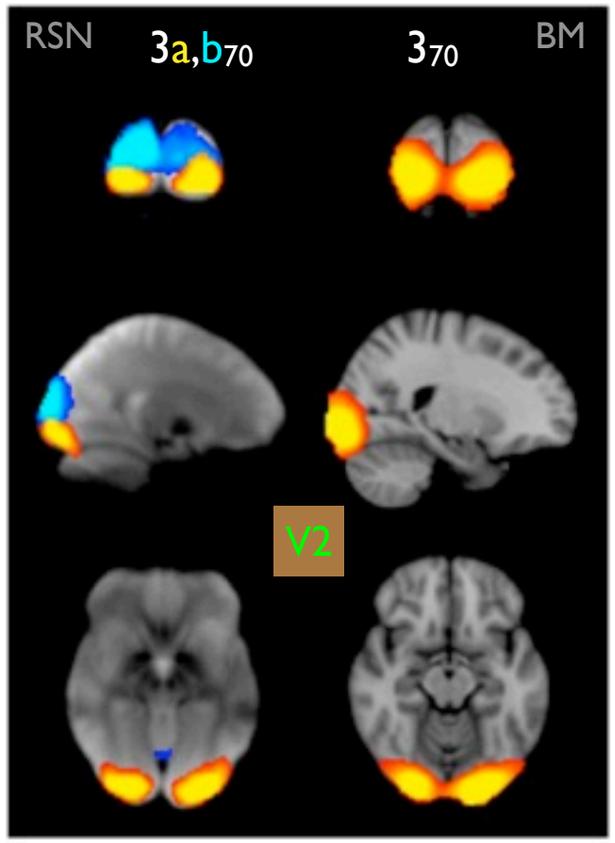

V2

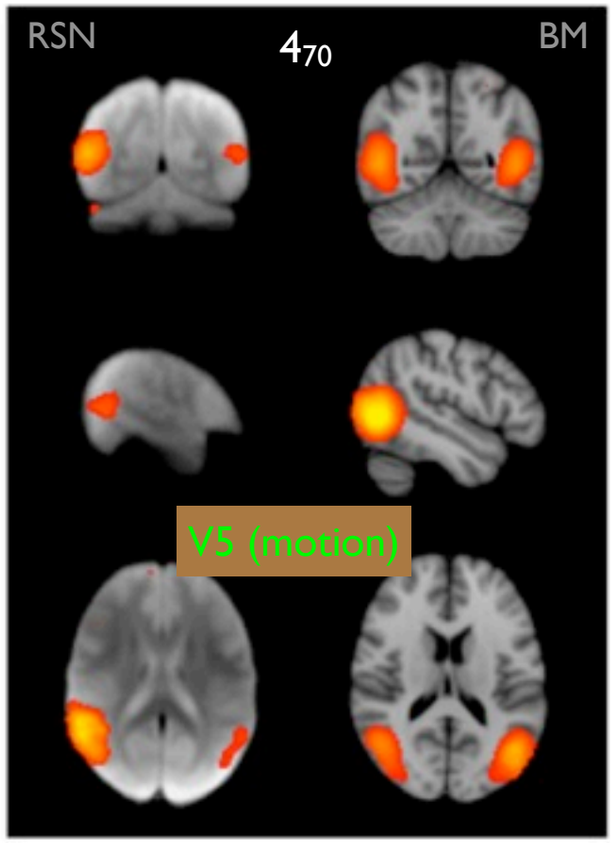

V5 (motion)

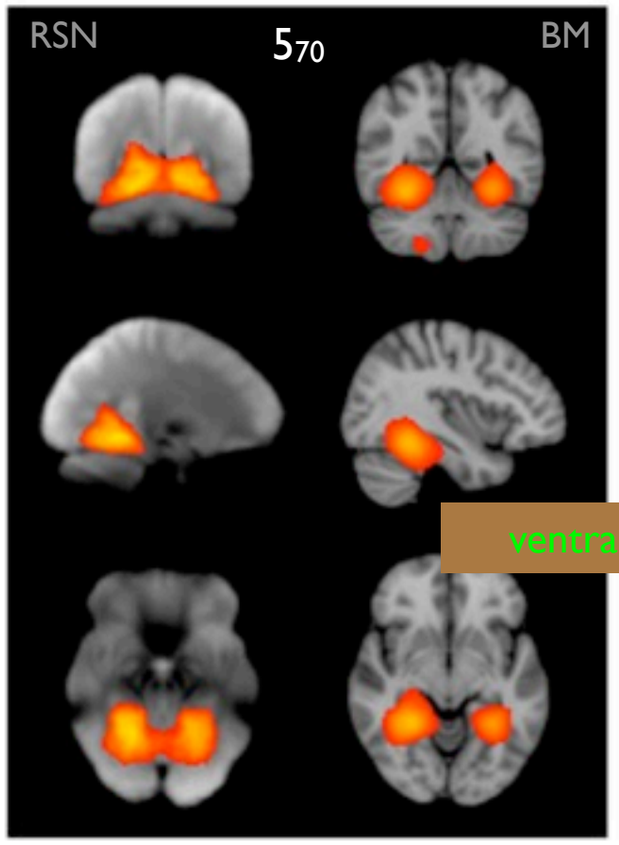

ventral stream

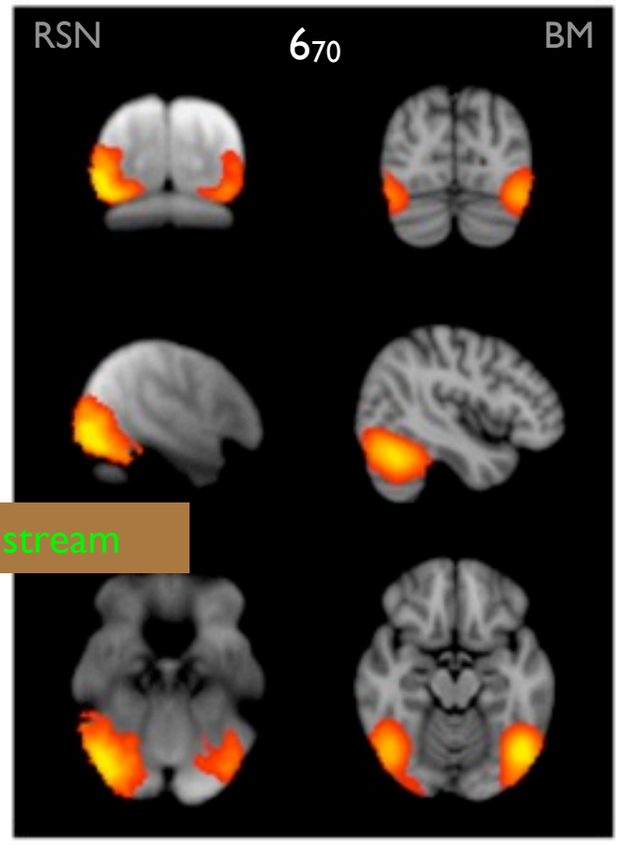

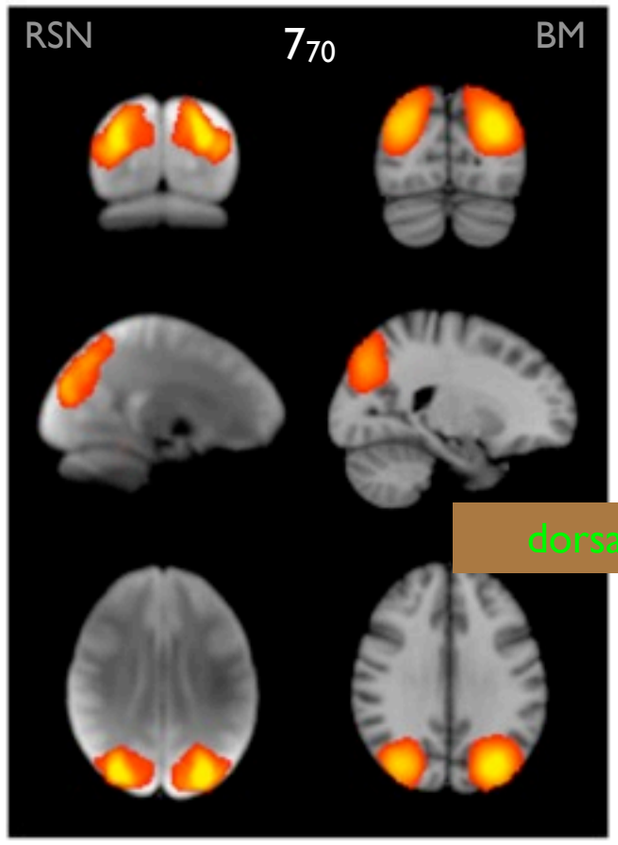

dorsal stream

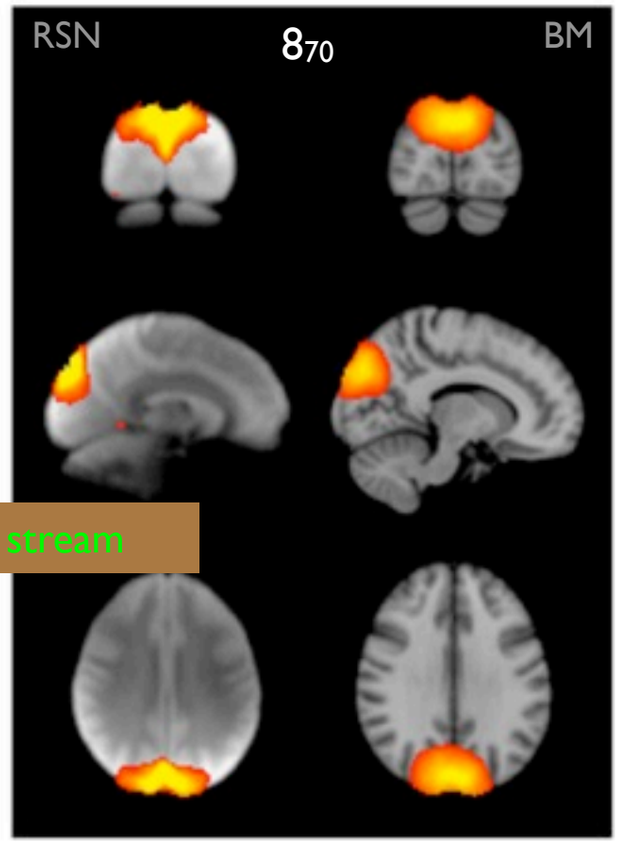

Mapping the 10 paired maps back onto BrainMap "Behavioural Domains"

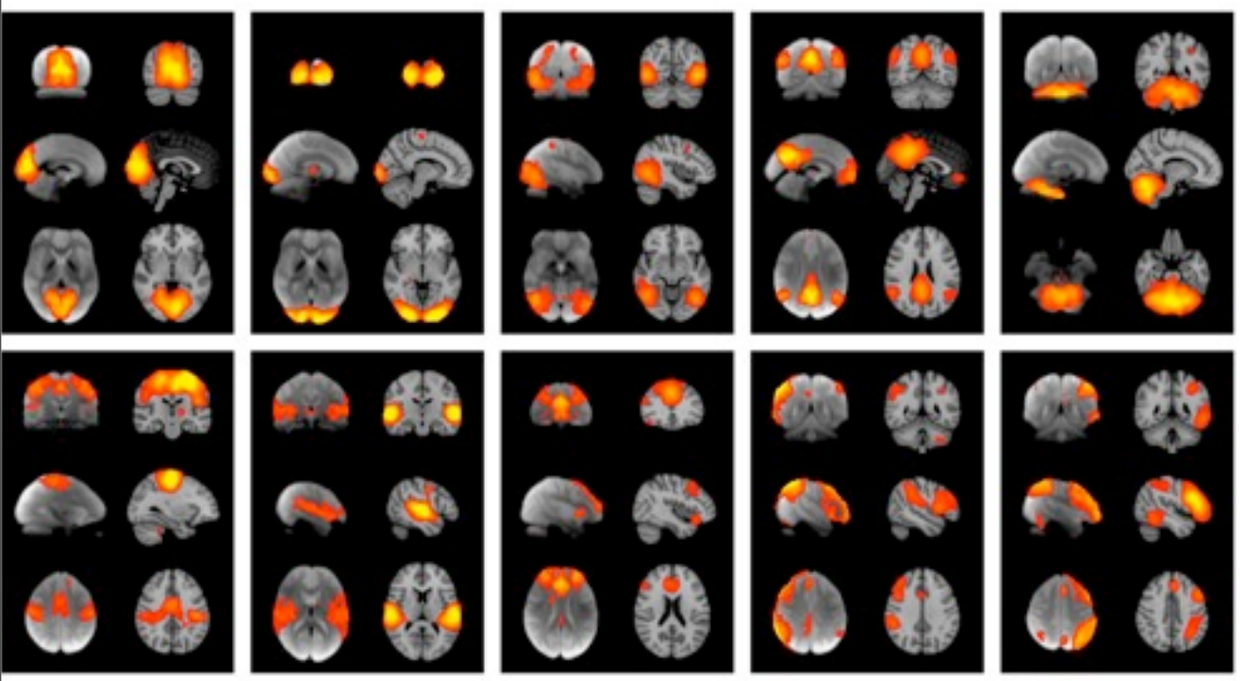

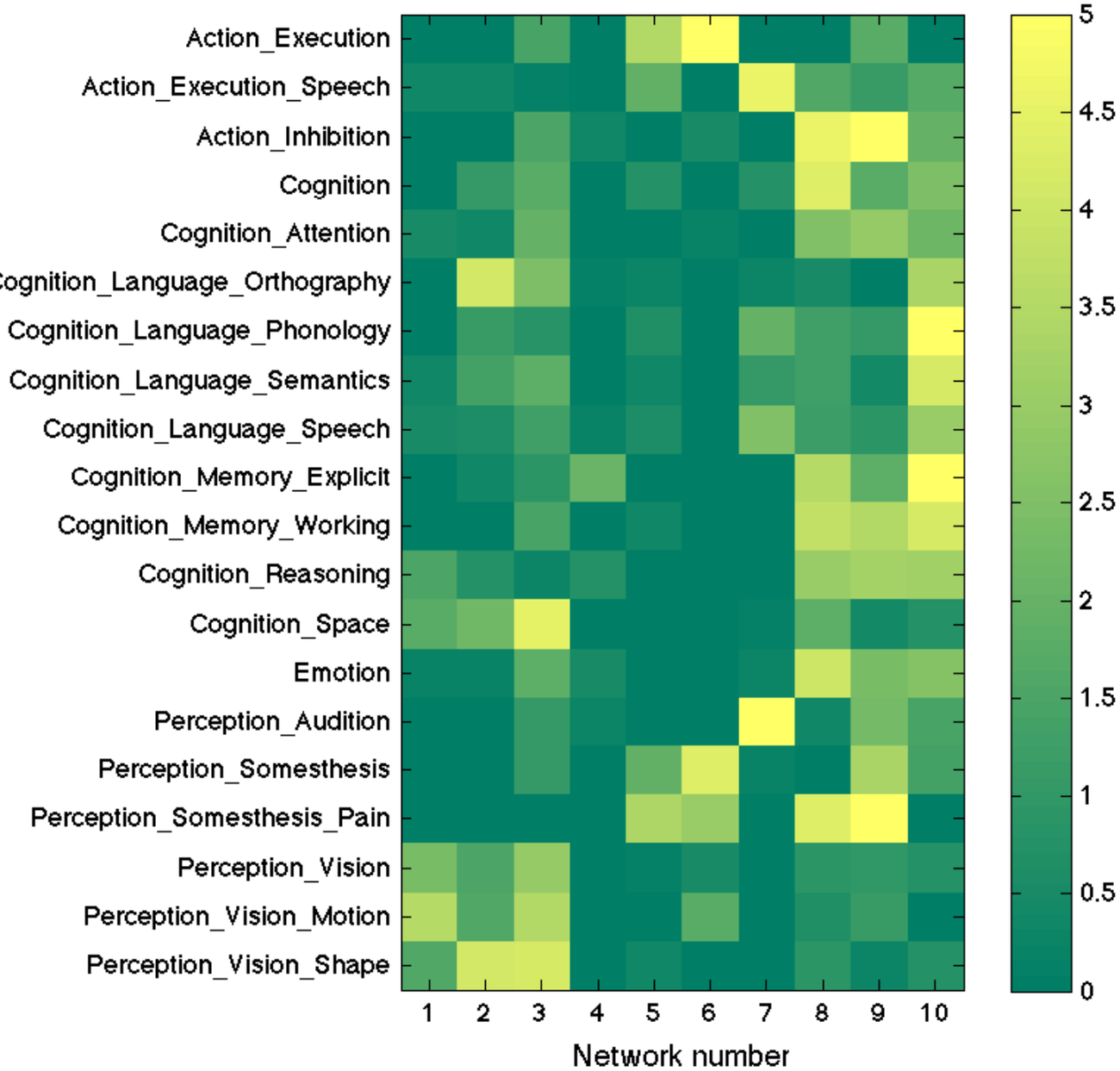

RSNs & neuro-degeneration

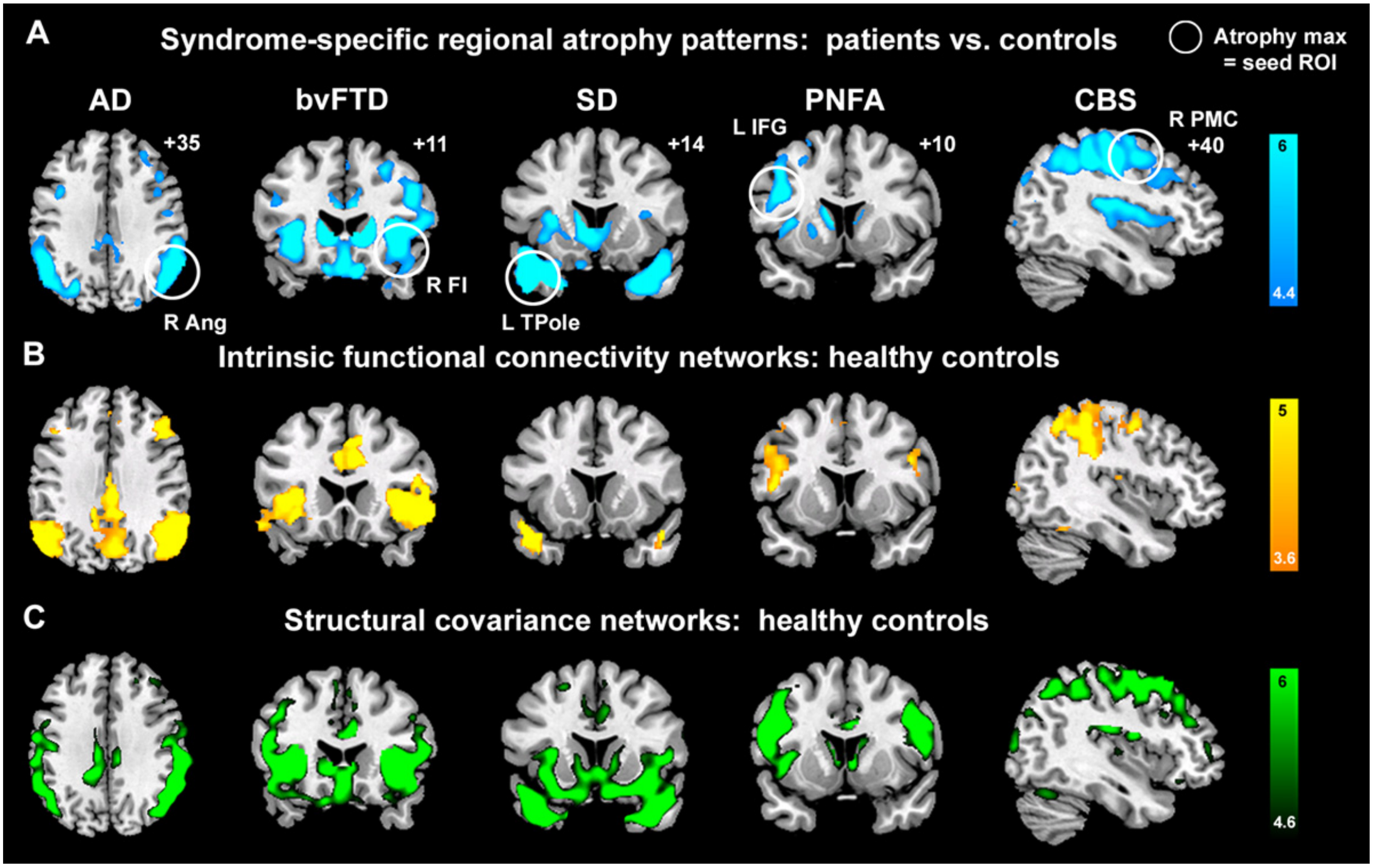

Neurodegenerative diseases target large-scale human brain networks

RSNs & neuro-degeneration

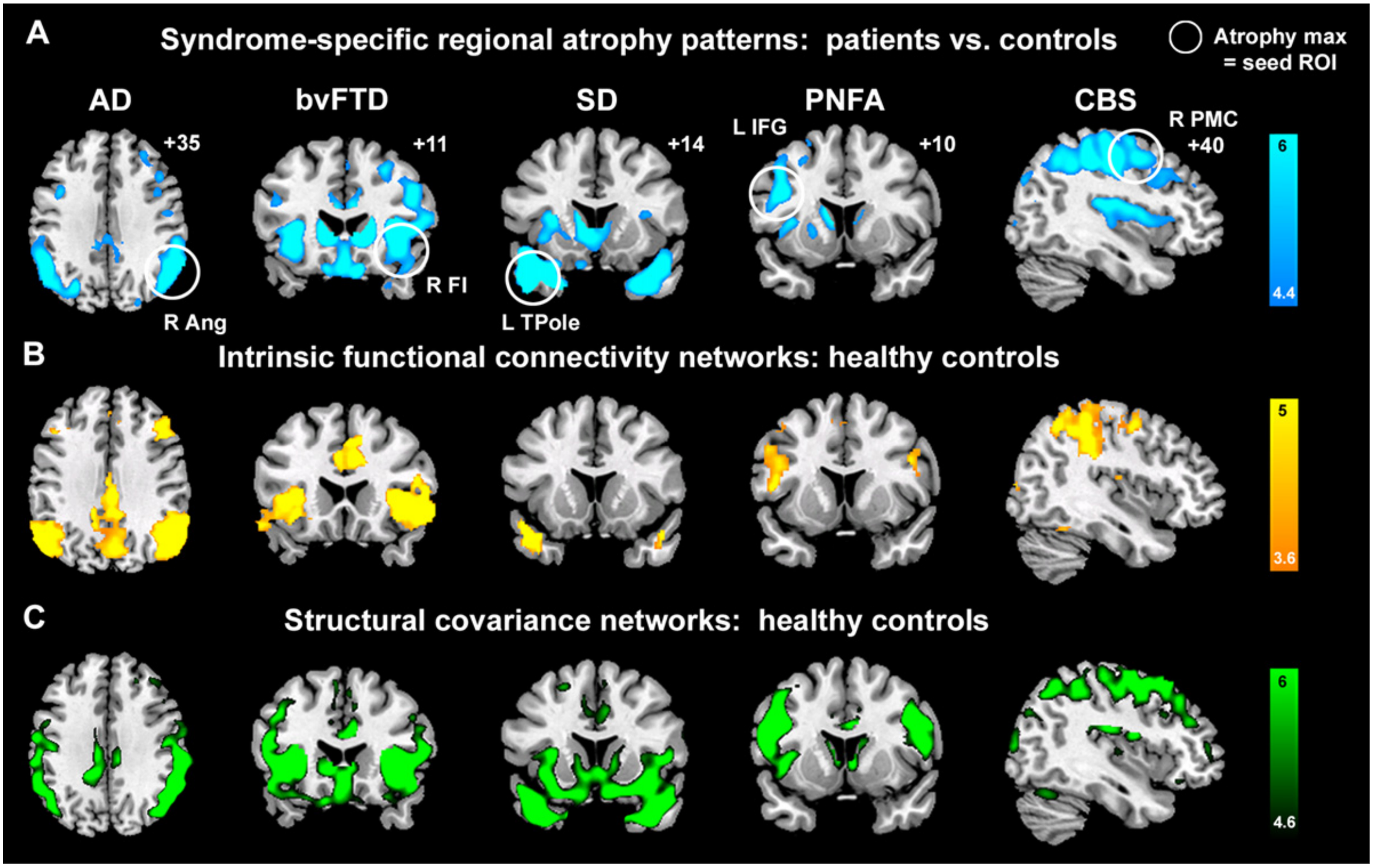

Neurodegenerative diseases target large-scale human brain networks

Seeley et al. (2009) Neuron

DMN in AD

Default Activity

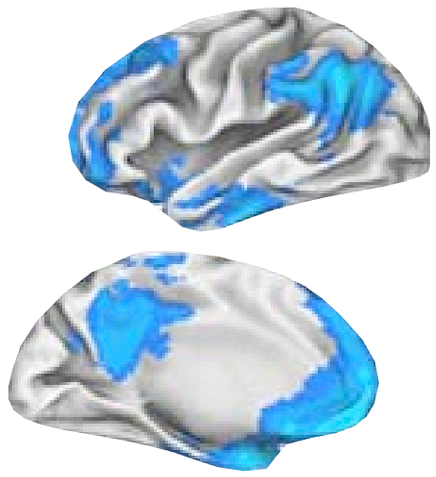

Amyloid Deposition

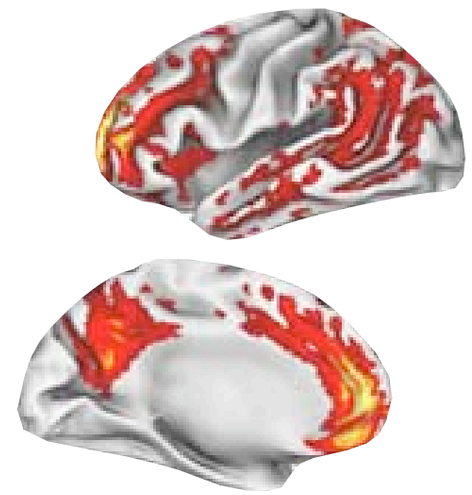

Atrophy

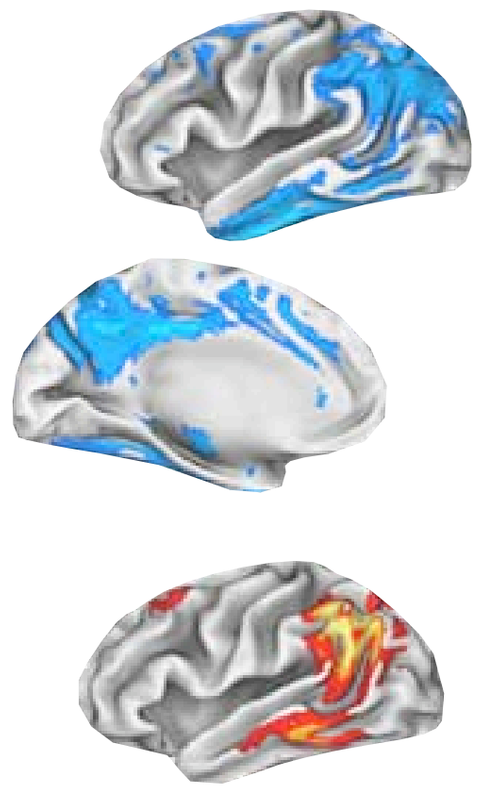

Metabolic Disruption

FDG-PET

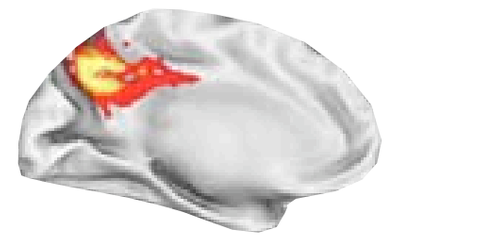

Memory Network

FMRI

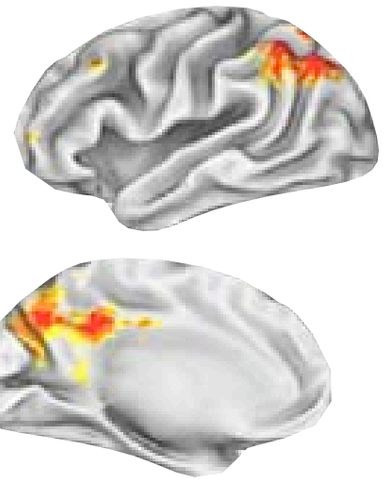

Buckner et al., J Neurosci, 2005

DMN in healthy aging vs AD

Resting FMRI

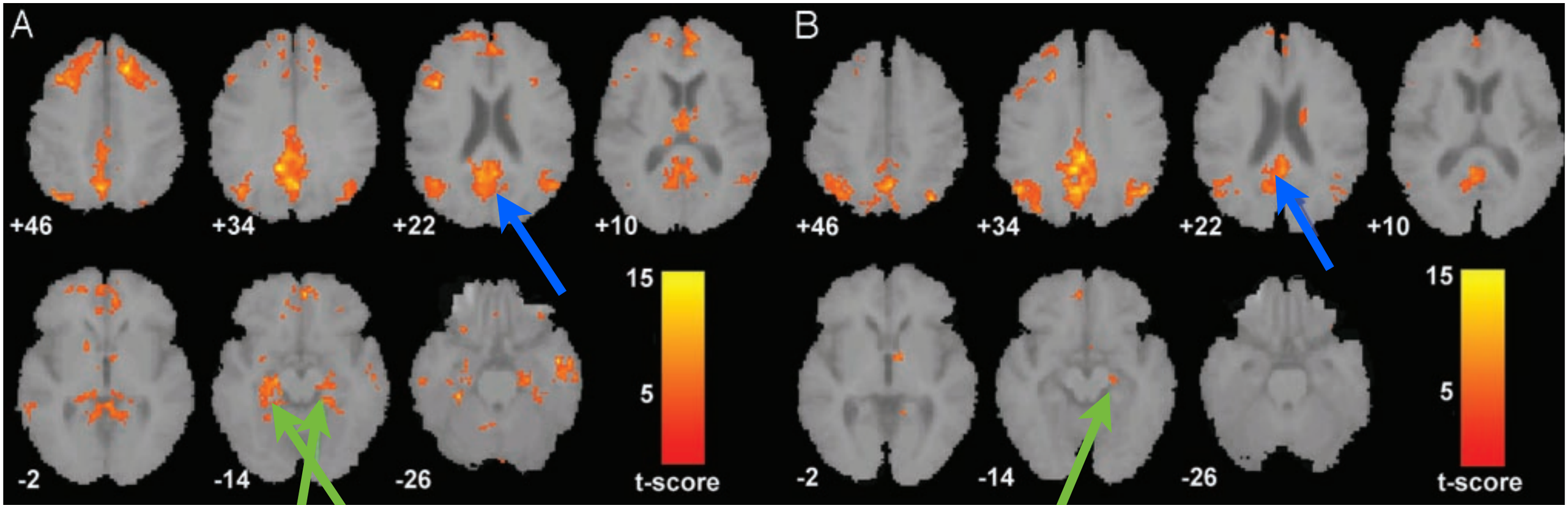

Controls

AD (CDR: 0.5-1)

Greicius et al., PNAS, 2004

Altered functional connectivity in **young, healthy** carriers of APOE-ε4

Collaboration between Oxford & GSK

Distinct patterns of brain activity in young carriers of the *APOE*-ε4 allele

Nicola Filippini[a,b,c], Bradley J. MacIntosh[b], Morgan G. Hough[b], Guy M. Goodwin[a], Giovanni B. Frisoni[c], Stephen M. Smith[b], Paul M. Matthews[d,e], Christian F. Beckmann[b,e], and Clare E. Mackay[a,b,1]

[a]University Department of Psychiatry and [b]Functional Magnetic Resonance Imaging of the Brain Centre, University of Oxford, Oxford OX3 9DU, United Kingdom; [c]Laboratory of Epidemiology, Neuroimaging, and Telemedicine, Istituto di Ricovero e Cura a Carattere Scientifico San Giovanni di Dio-Fatebenefratelli, Brescia 25125, Italy; [d]GlaxoSmithKline Research and Development, Clinical Imaging Centre, London W12 0NN, United Kingdom; and [e]Department of Clinical Neuroscience, Imperial College, Hammersmith Campus London W12 0NN, United Kingdom

Edited by Robert W. Mahley, The J. David Gladstone Institutes, San Francisco, CA, and approved March 6, 2009 (received for review November 25, 2008)

The *APOE* ε4 allele is a risk factor for late-life pathological changes that is also associated with anatomical and functional brain changes in middle-aged and elderly healthy subjects. We investigated structural and functional effects of the *APOE* polymorphism in 18 young healthy *APOE* ε4-carriers and 18 matched noncarriers (age range: 20–35 years). Brain activity was studied both at rest and during an encoding memory paradigm using blood oxygen level-dependent fMRI. Resting fMRI revealed increased ''default mode network'' (involving retrosplenial, medial temporal, and medial-prefrontal cortical areas) coactivation in ε4-carriers relative to noncarriers. The encoding task produced greater hippocampal activation in ε4-carriers relative to noncarriers. Neither result could be explained by differences in memory performance, brain morphology, or resting cerebral blood flow. The *APOE* ε4 allele modulates brain function decades before any clinical or neurophysiological expression of neurodegenerative processes.

hippocampus | memory | neuroimaging | resting connectivity

fMRI studies have tested for early life associations of the *APOE* polymorphism with changes in brain function. Filbey et al. (18) reported greater activation in 8 *APOE* ε4-carriers compared with 8 noncarriers in medial frontal and anterior cingulate areas using a working m
reduced act
ε4-carriers
Both studie
ences brain

Here, we
structural a
APOE ε4-ca
to 35 years
spontaneou
relative to
showing a
frequency fluctuations (less than 0.1 Hz) are defined as ''resting state networks'' (RSNs), and they reflect intrinsic properties of functional brain organization (21). We were specifically inter-

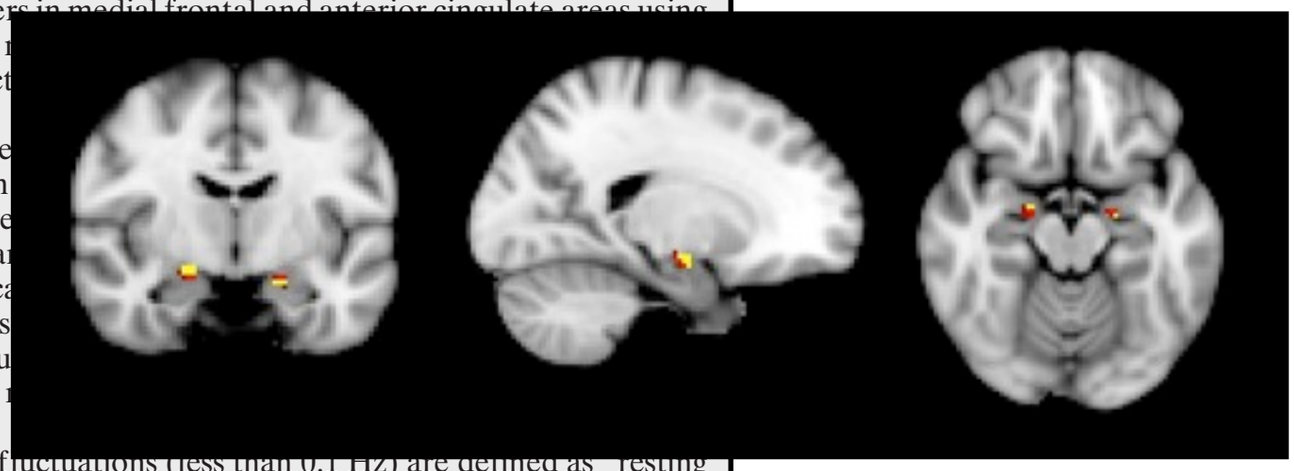

apolipoprotein E - *APOE*

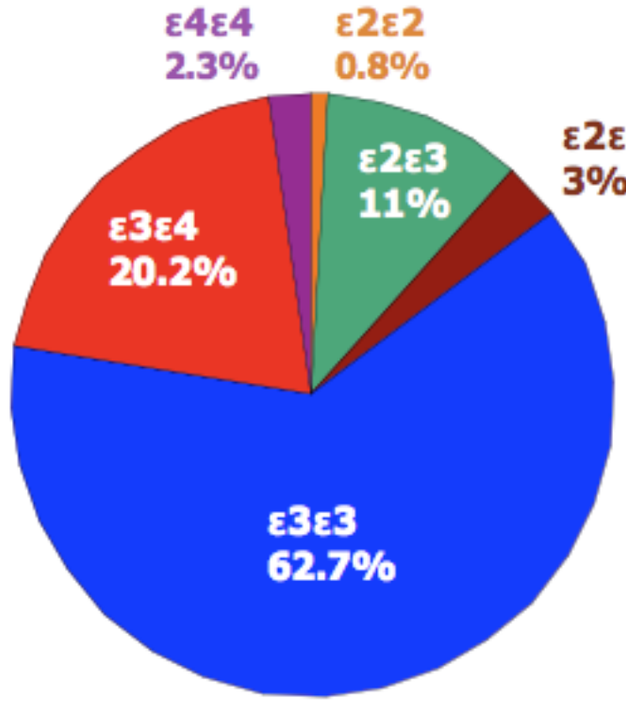

Menzel et al., 1983

apolipoprotein E - *APOE*

- lipid transport protein coded on chromosome 19

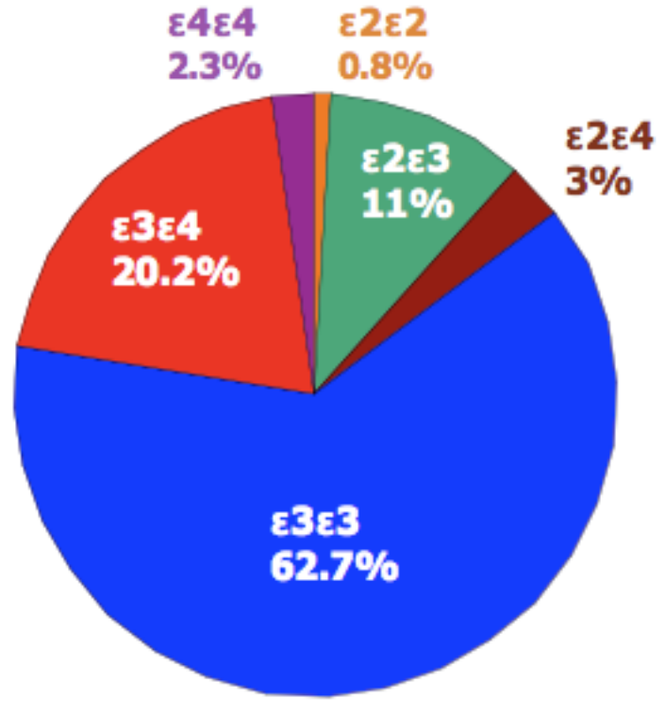

Menzel et al., 1983

apolipoprotein E - *APOE*

- lipid transport protein coded on chromosome 19
- ε4 allele first studied as risk factor for cardiovascular disease

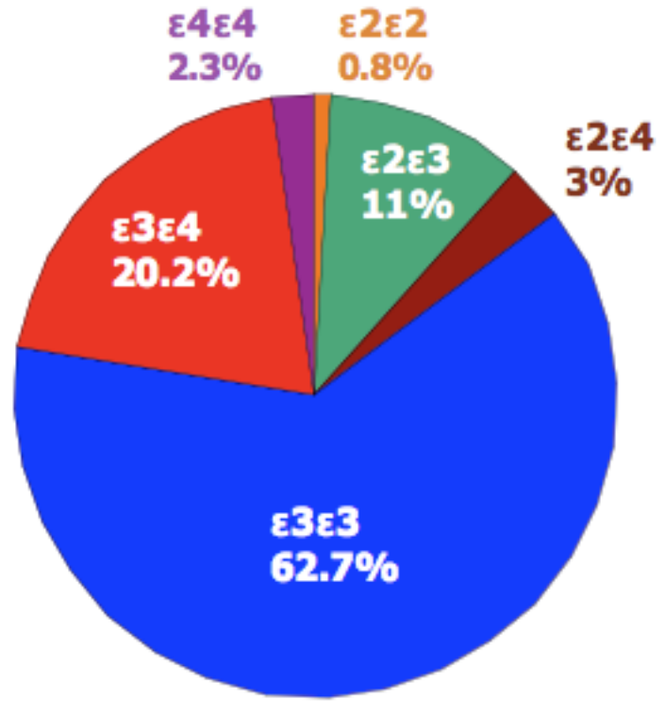

Menzel et al., 1983

apolipoprotein E - *APOE*

- lipid transport protein coded on chromosome 19
- ε4 allele first studied as risk factor for cardiovascular disease
- ε4 Identified as risk for AD in 1993
  - Increased prevalence
  - decreased age of onset
  - gene dose effect

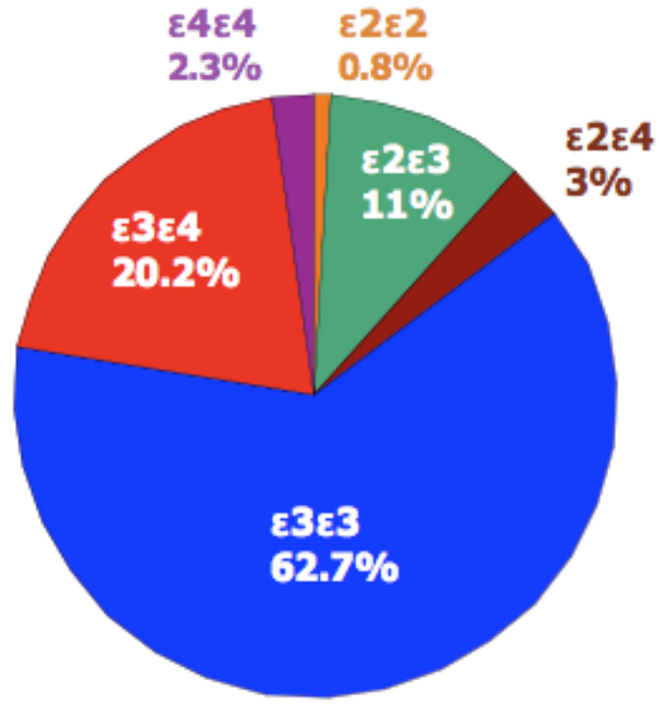

Menzel et al., 1983

What is NOT different

What is NOT different

Structure - Whole brain GM, WM and hippocampal ROIs & VBM not different

What is NOT different

Structure - Whole brain GM, WM and hippocampal ROIs & VBM not different

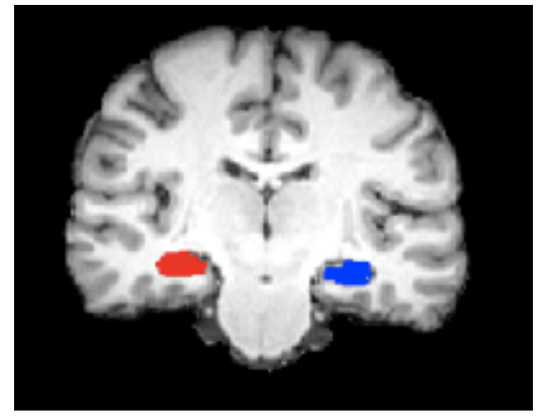

What is NOT different

Structure - Whole brain GM, WM and hippocampal ROIs & VBM not different

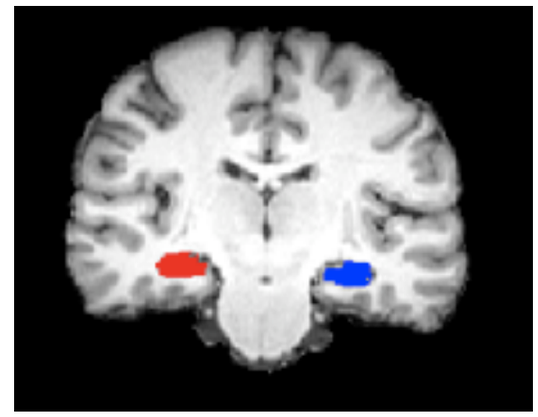

Cerebral blood flow - ASL in hippocampal and lobe ROIs and whole brain not different

What is NOT different

Structure - Whole brain GM, WM and hippocampal ROIs & VBM not different

Cerebral blood flow - ASL in hippocampal and lobe ROIs and whole brain not different

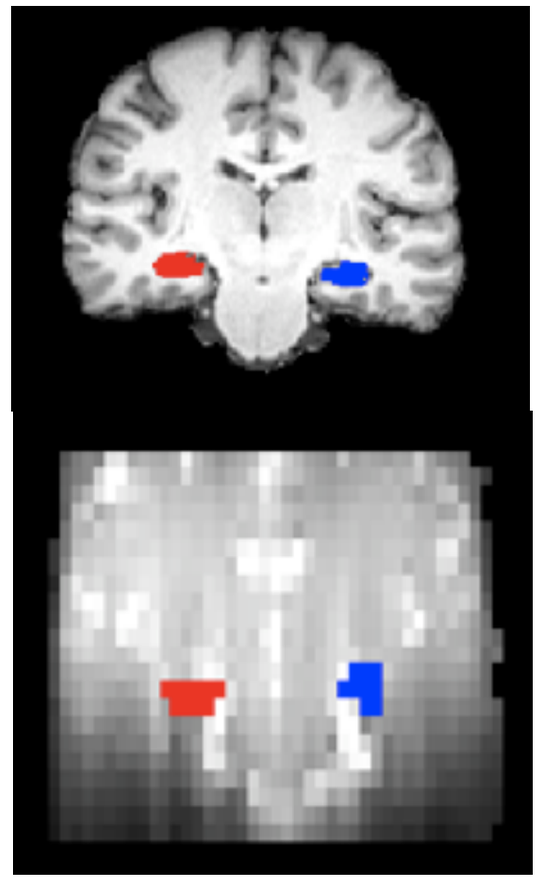

What is NOT different

Structure - Whole brain GM, WM and hippocampal ROIs & VBM not different

Cerebral blood flow - ASL in hippocampal and lobe ROIs and whole brain not different

Memory performance and reaction time not different

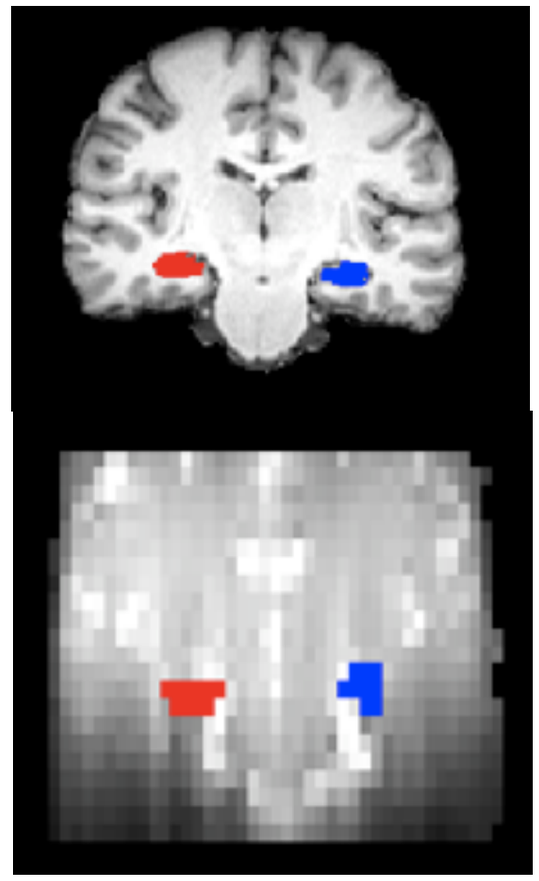

Resting data - DMN

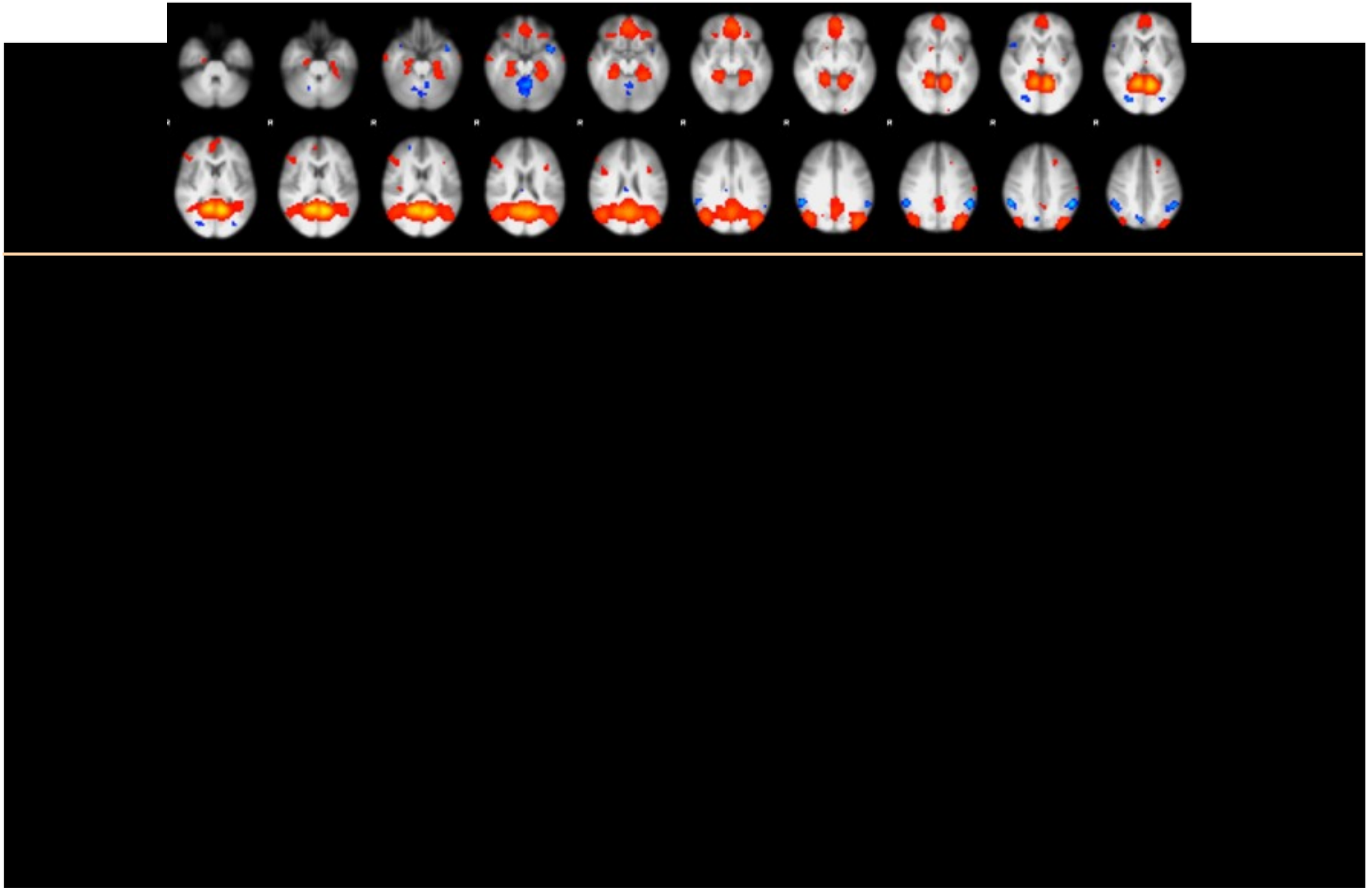

Resting data - DMN

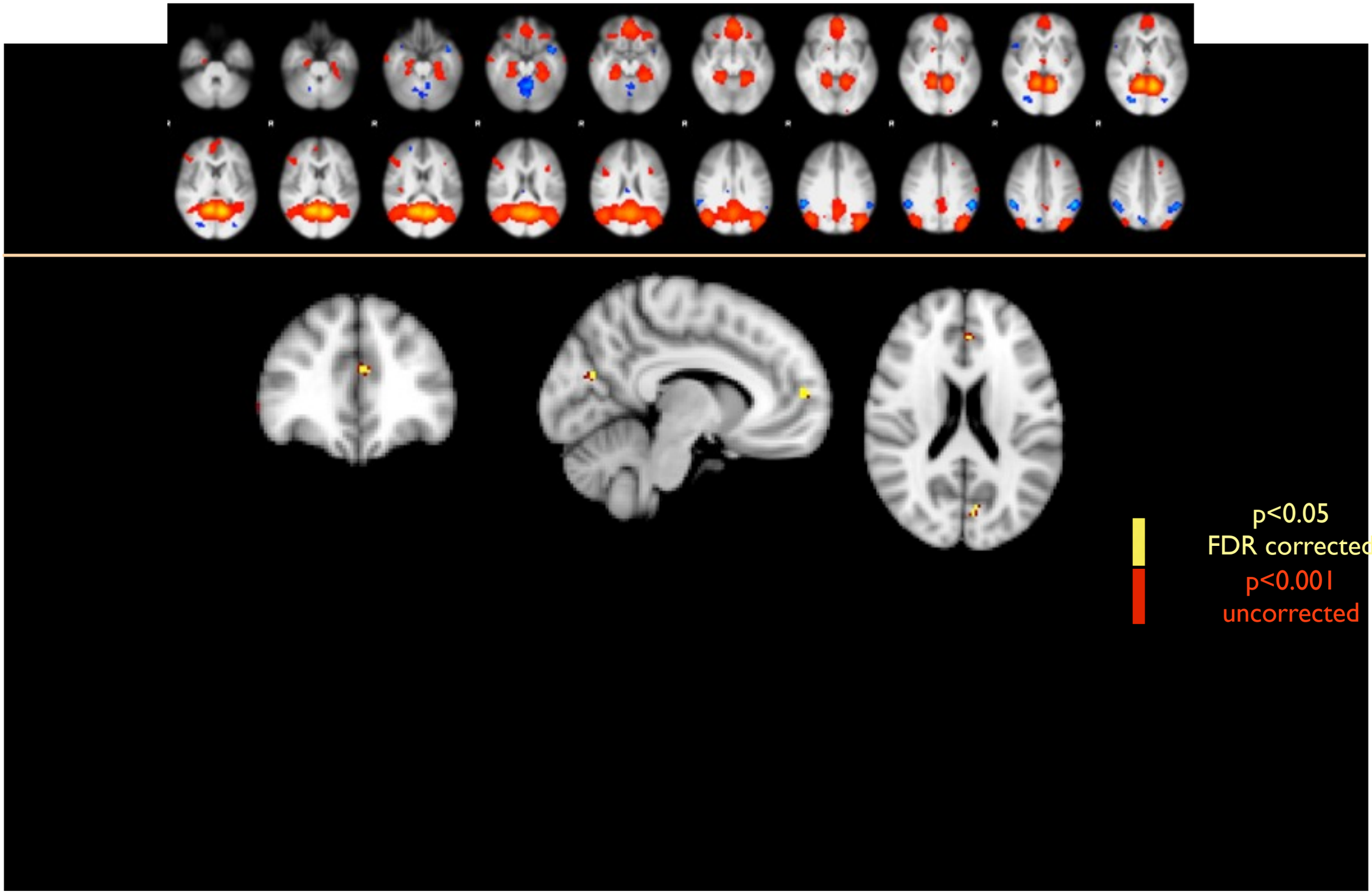

Resting data - DMN

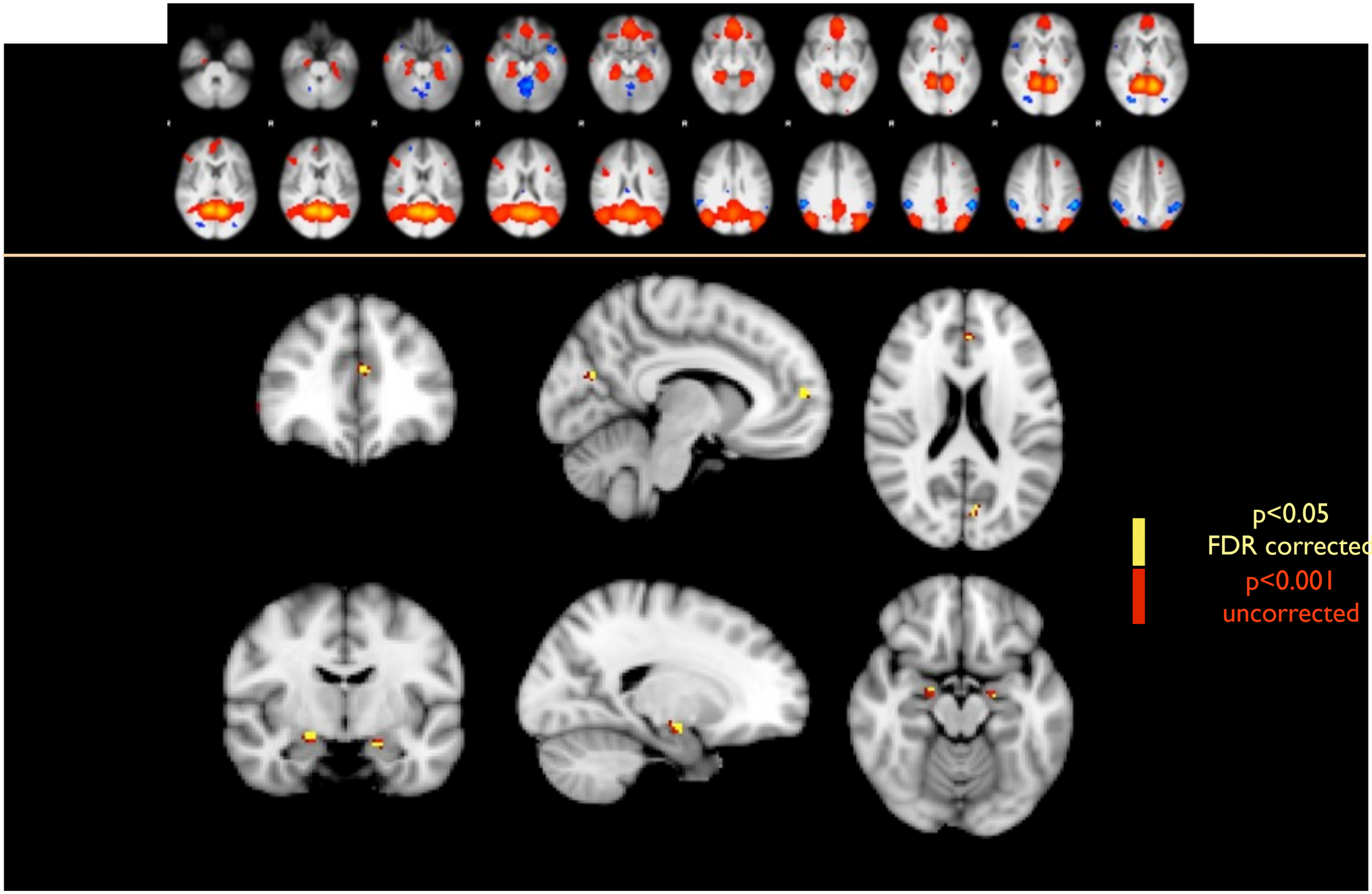

Development of RSNs during gestation

Emergence of resting state networks in the preterm human brain

Valentina Doria[a], Christian F. Beckmann[b,c], Tomoki Arichi[a], Nazakat Merchant[a], Michela Groppo[a], Federico E. Turkheimer[b], Serena J. Counsell[a], Maria Murgasova[d], Paul Aljabar[d], Rita G. Nunes[a], David J. Larkman[a], Geraint Rees[e,f], and A. David Edwards[a,1]

[a]Institute of Clinical Sciences and [b]Centre for Neuroscience, Imperial College London, and Medical Research Council Clinical Sciences United Kingdom; [c]Functional Magnetic Resonance Imaging of the Brain Centre, University of Oxford, Oxford OX3 9DU, United King Processing Group, Department of Computing, Imperial College London, London SW7 2AZ, United Kingdom; [e]University College Lon Neuroscience, London WC1N 3AR, United Kingdom; and [f]Wellcome Trust Centre for Neuroimaging at UCL, London WC1N 3BG, U

Edited by Marcus E. Raichle, The Washington University of St. Louis, St. Louis, MO, and approved September 28, 2010 (received f

The functions of the resting state networks (RSNs) revealed by functional MRI remain unclear, but it has seemed possible that networks emerge in parallel with the development of related cognitive functions. We tested the alternative hypothesis: that the full repertoire of resting state dynamics emerges during the period of rapid neural growth before the normal time of birth at term (around 40 wk of gestation). We used a series of independent analytical techniques to map in detail the development of different networks in 70 infants born between 29 and 43 wk of postmenstrual age (PMA). We characterized and charted the development of RSNs from recognizable but often fragmentary elements at 30 wk of PMA to full facsimiles of adult patterns at term. Visual, auditory, somatosensory, motor, default mode, frontoparietal, and executive control networks developed at different rates; however, by term, complete networks were present, several of which were integrated with thalamic activity. These results place the emergence of RSNs largely during the period of rapid neural growth in the third trimester of gestation, suggesting that they are formed before the acquisition of

between 29 and 43 wk of PMA. We used
including improved registration and a uniqu
of the developing brain with consistent thres
data-driven exploratory analysis and hypoth
to show that synchronous BOLD activity de
tary RSNs in preterm infants into facsimile
term, including involvement of relevant th
quantify the growing network coherence du

Results

Identification of RSNs During the Third Tri
probabilistic independent component analysi
free detection of RSNs (Fig. 1). We analyz
from resting state fMRI in early preterm, pre
(full details are presented in *Methods* and S
ysis revealed correlated low-frequency (0
distributed BOLD signals that characterized recognizable neuroanatomical systems comparable to adult networks, including vi-

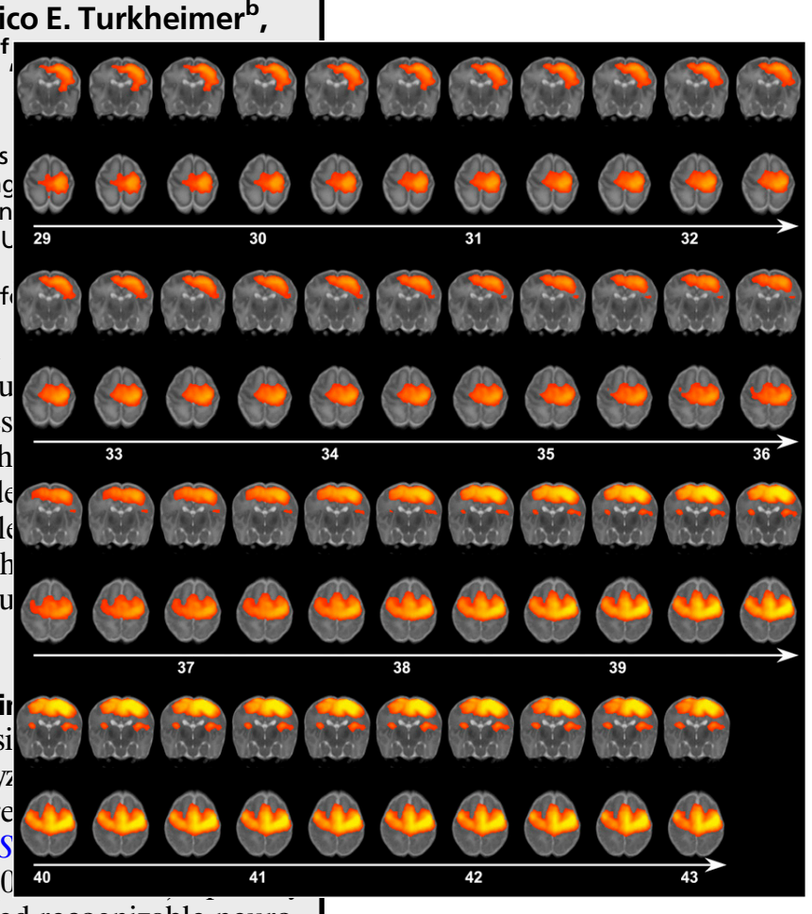

RSNs in infants

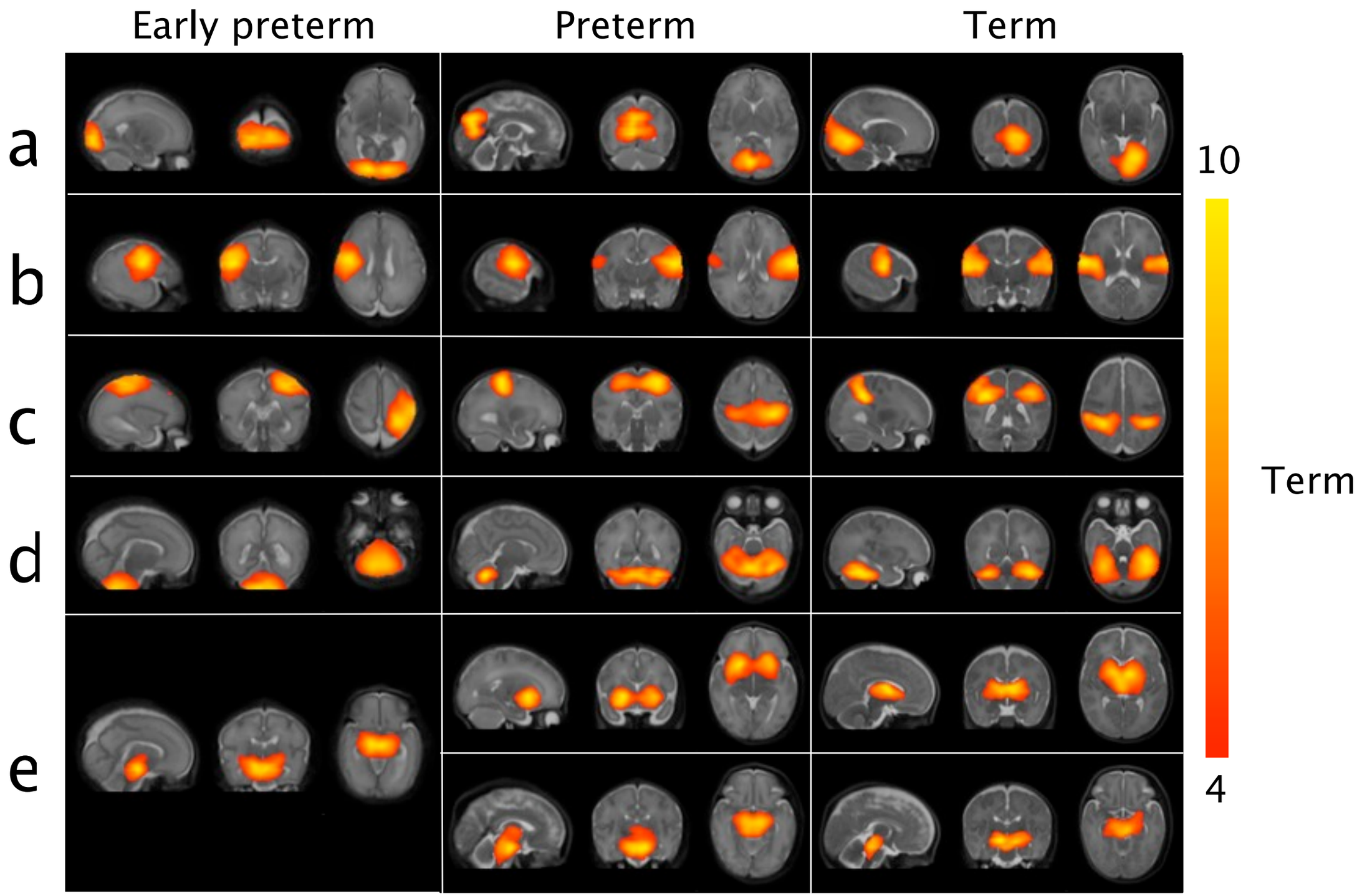

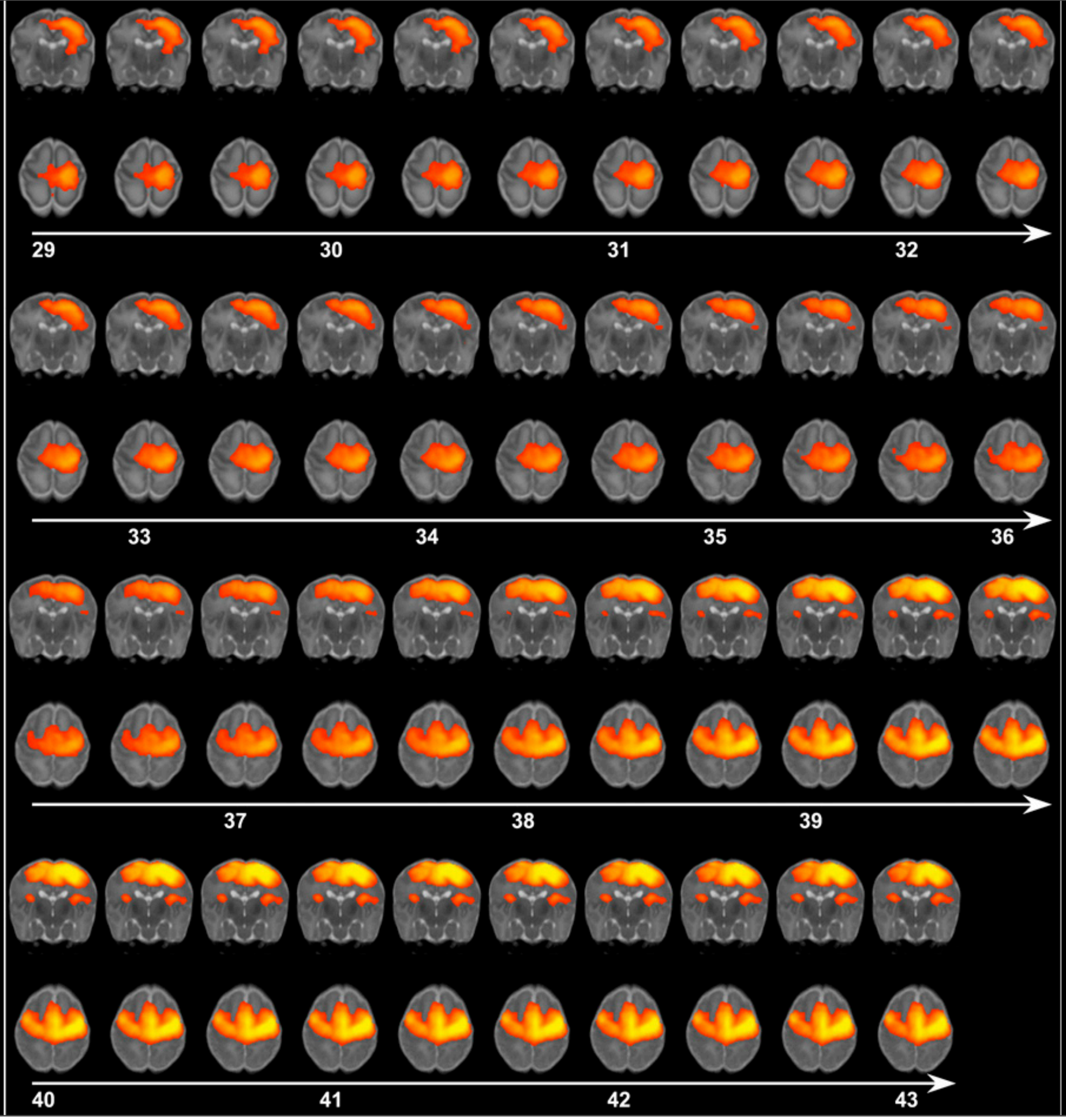
29
30
31
32
33
34
35
36
37
38
39
40
41
42
43

Dynamics of RSNs

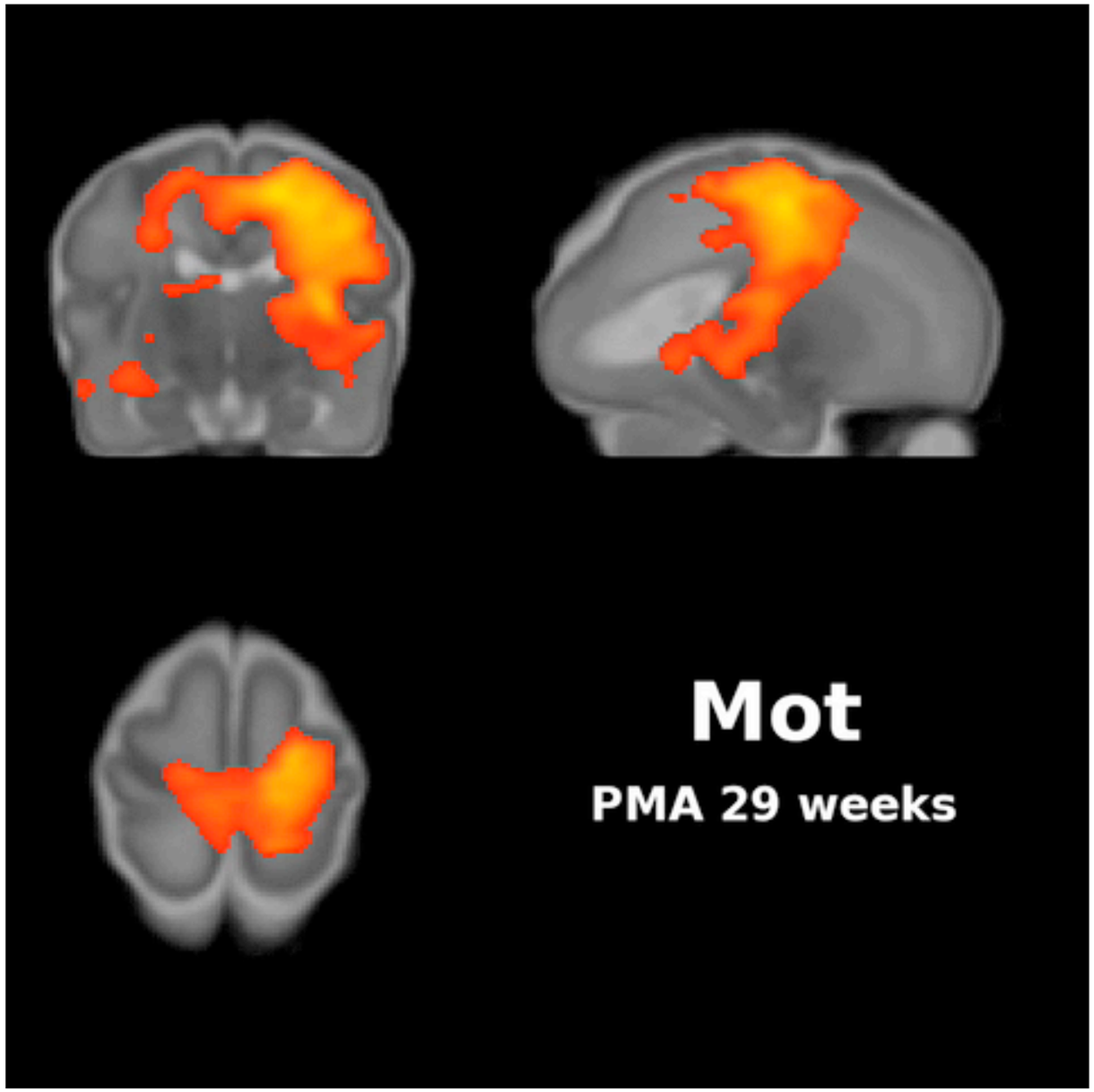

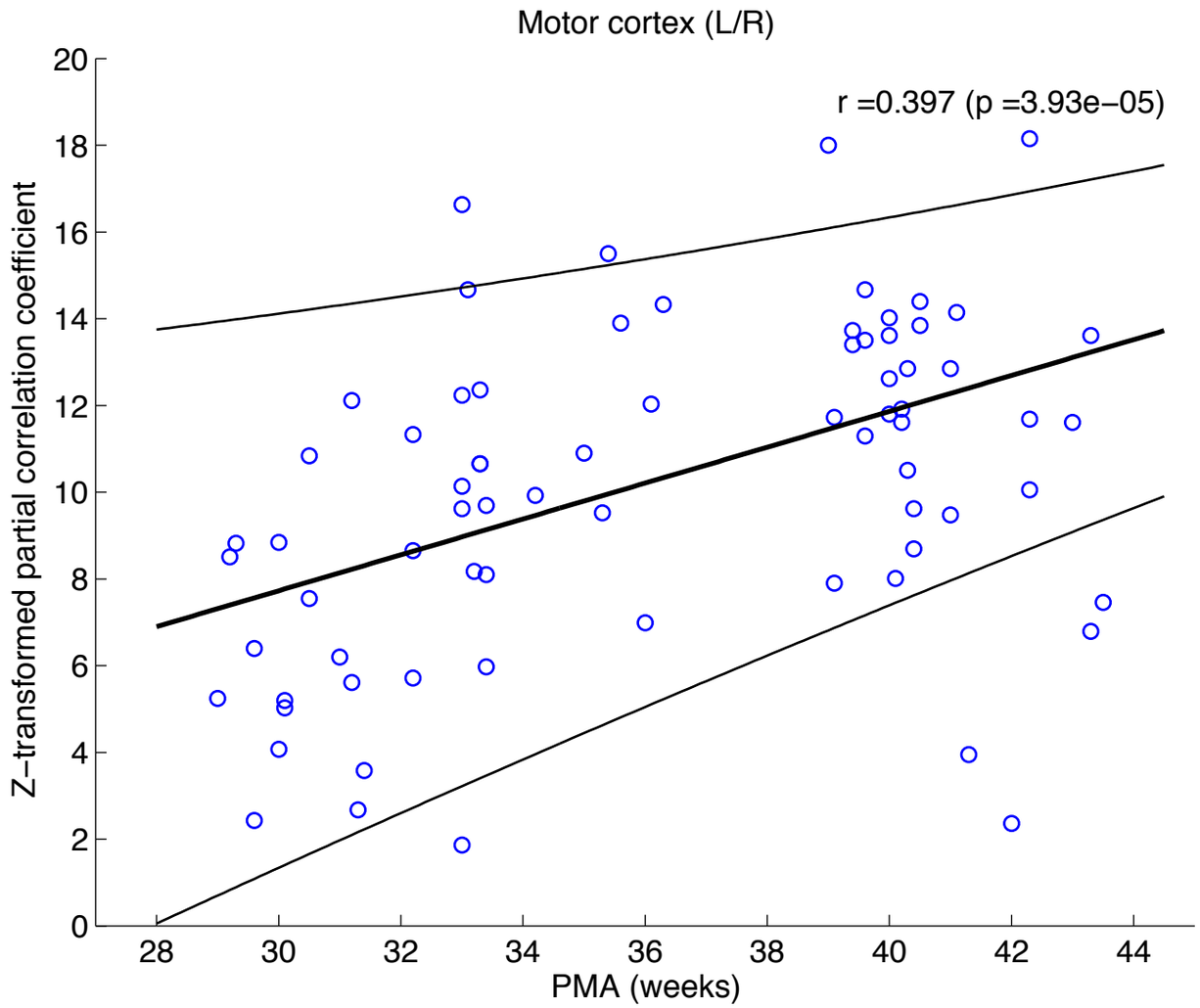

Doria, V. et al, PNAS 2010

Dynamics of RSNs

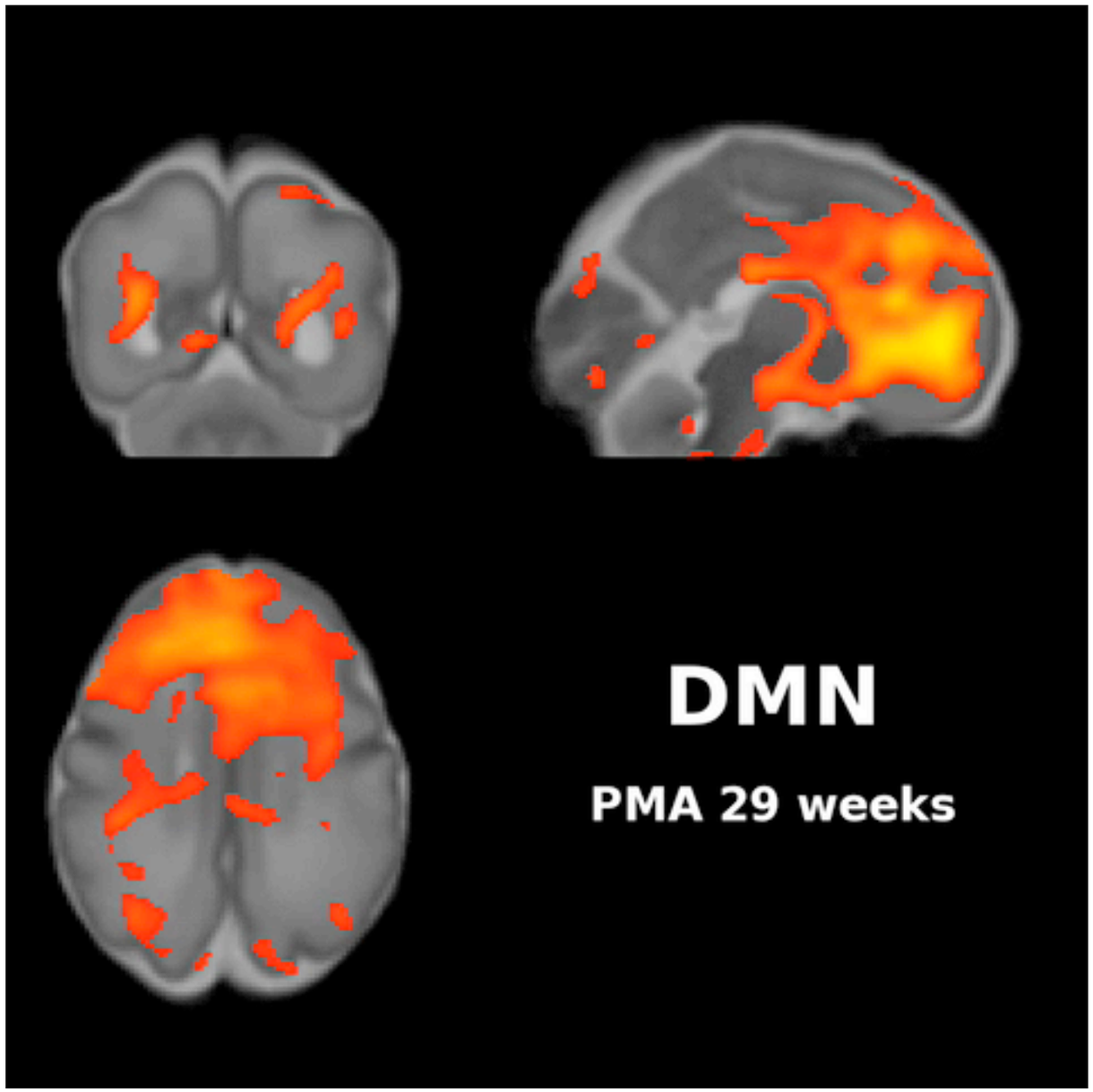

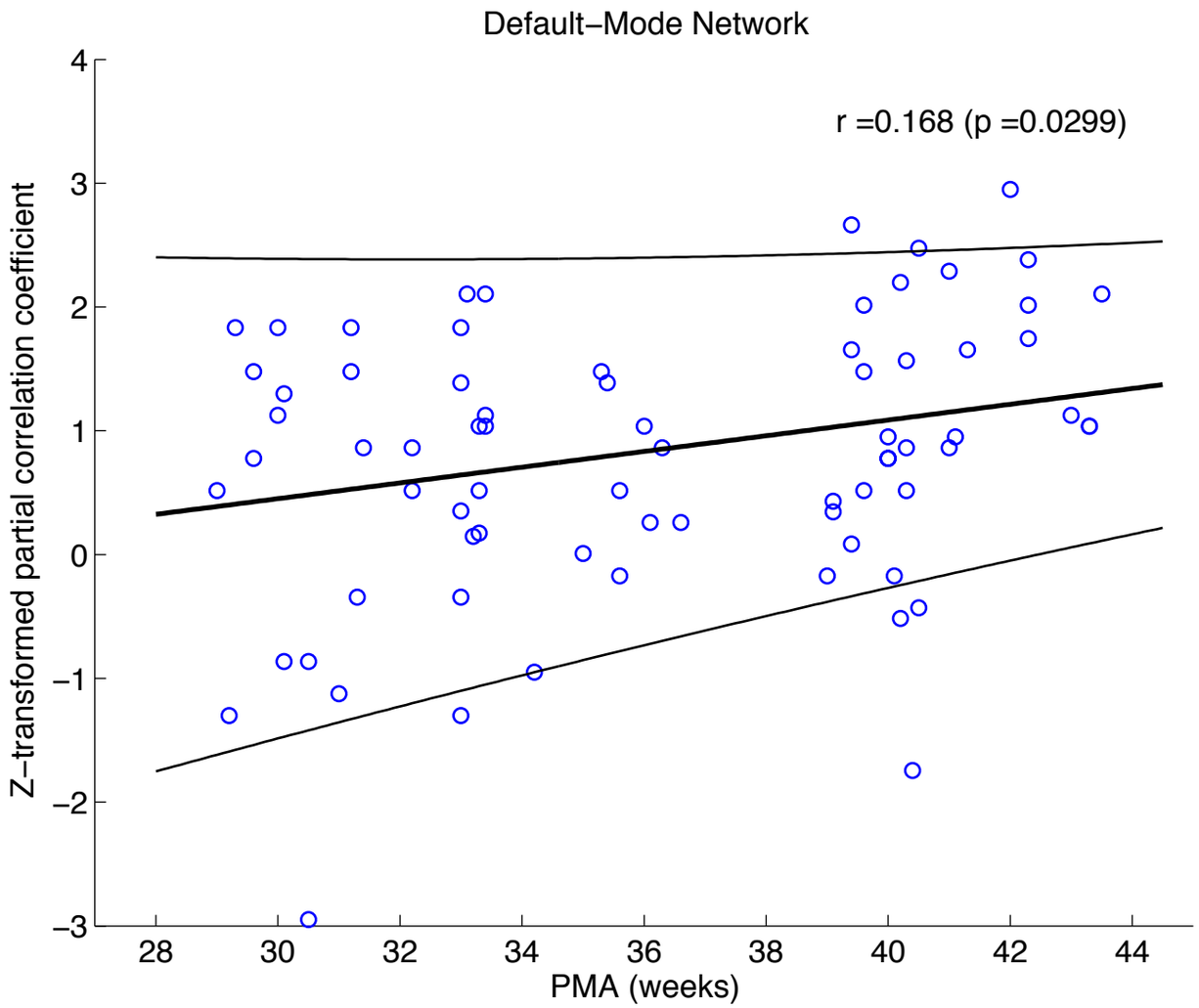

Doria, V. et al, PNAS 2010

Network Modelling

- Seed-correlation maps, or low-dim ICA, give "networks"

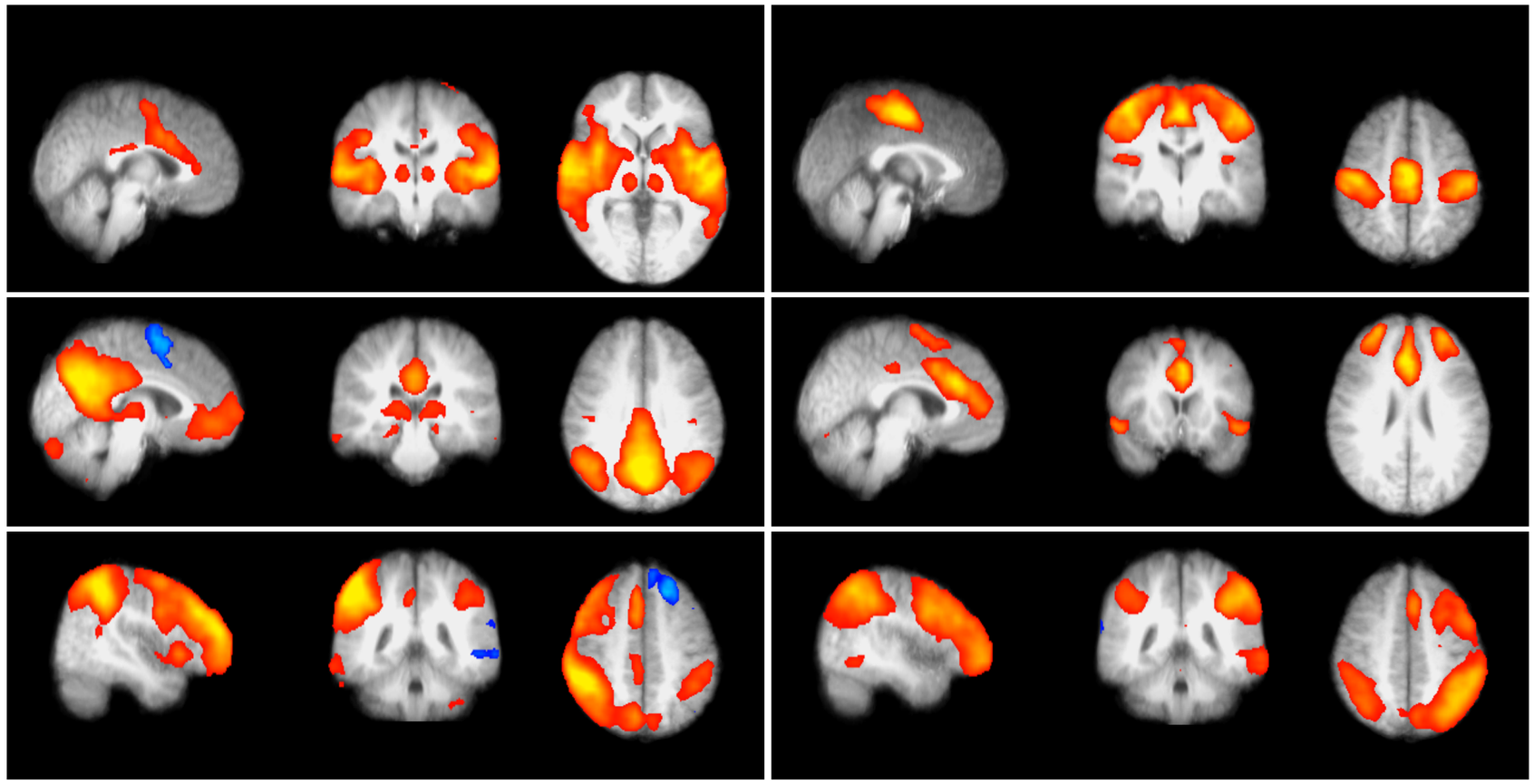

- But these are gross patterns
  - Each map summarised by single timecourse
  - Too simple a model to do more detailed network analysis
- Instead, get detailed parcellation....

Detailed Network Analyses

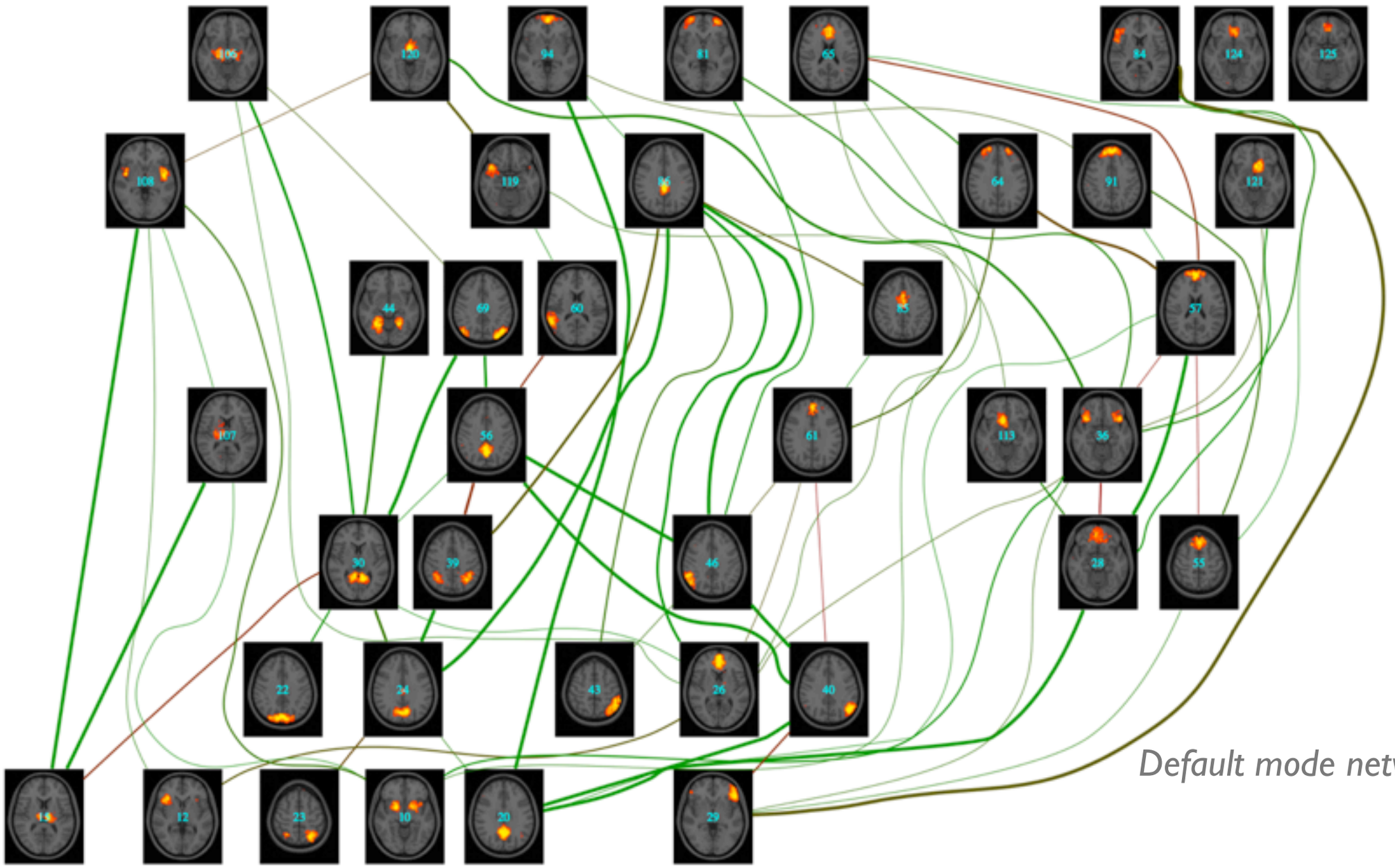

Default mode network

A network model comprises:

- "**Nodes**" distinct functional voxels/regions
- "**Edges**" connections between nodes

Nodes: e.g. from high-dimensional ICA

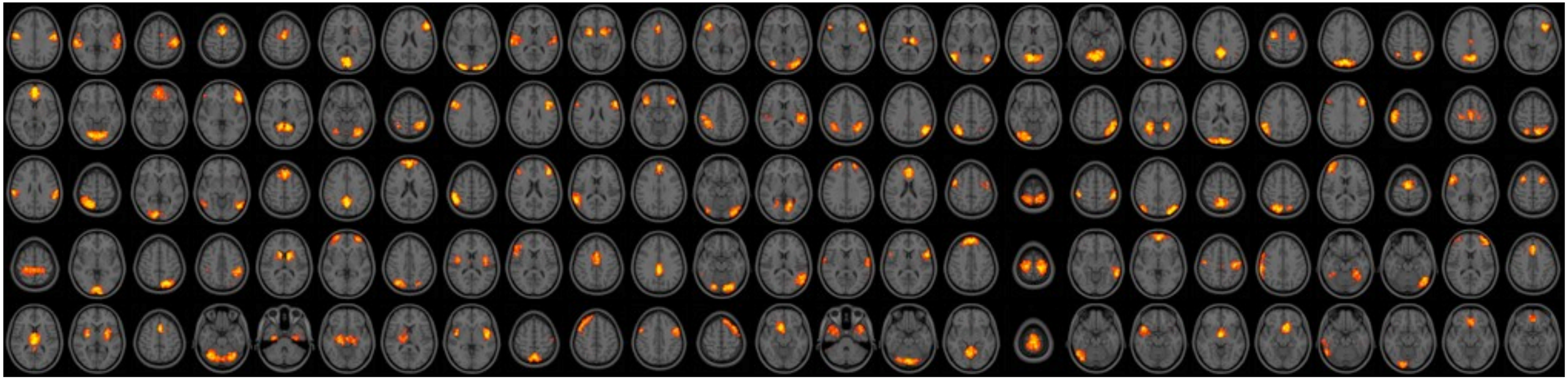

- *Kiviniemi NeuroImage 2009*
- *Smith PNAS 2009*

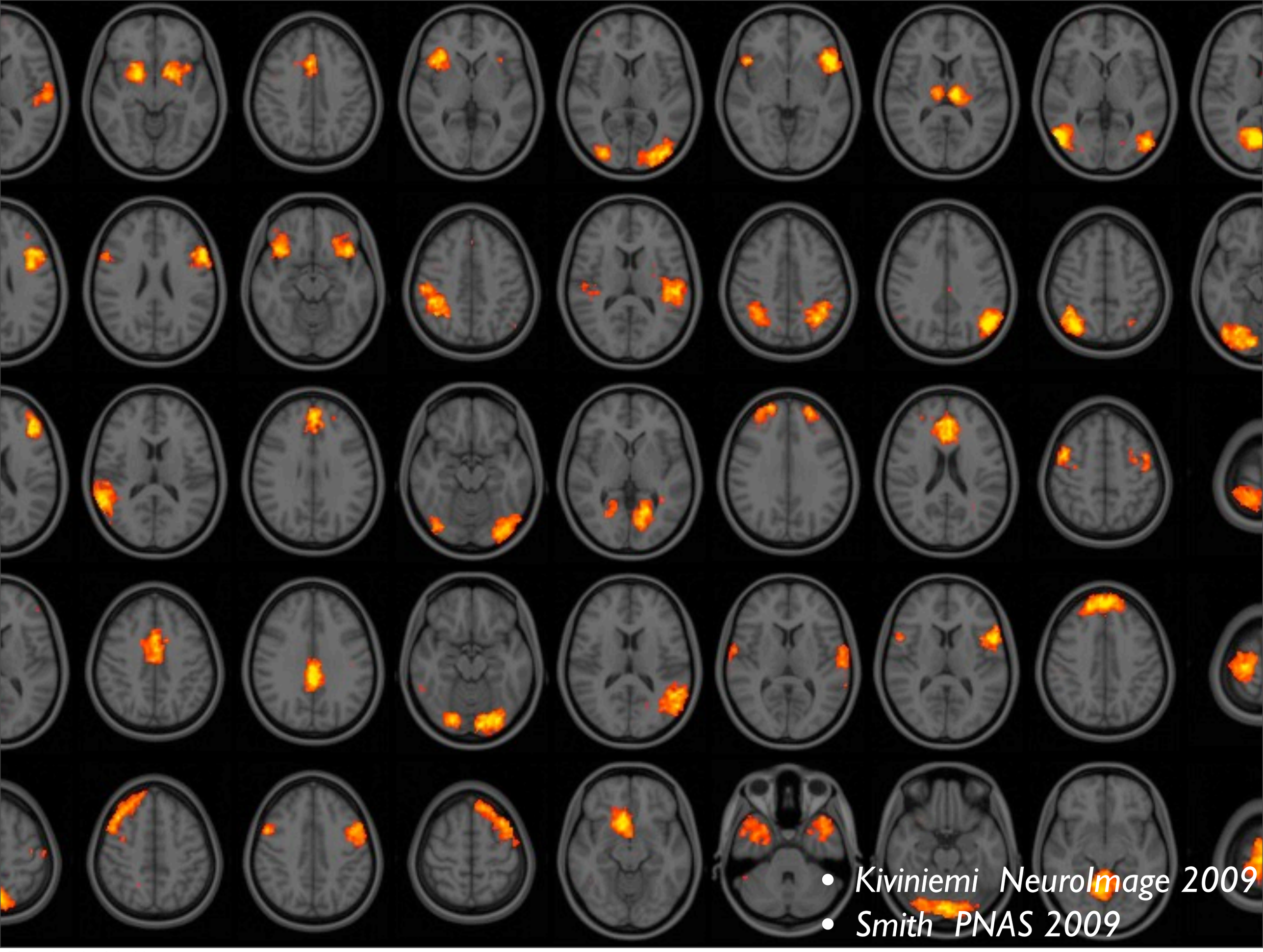
• Kiviniemi NeuroImage 2009
• Smith PNAS 2009

Edges: estimate connectivity between all pairs of nodes

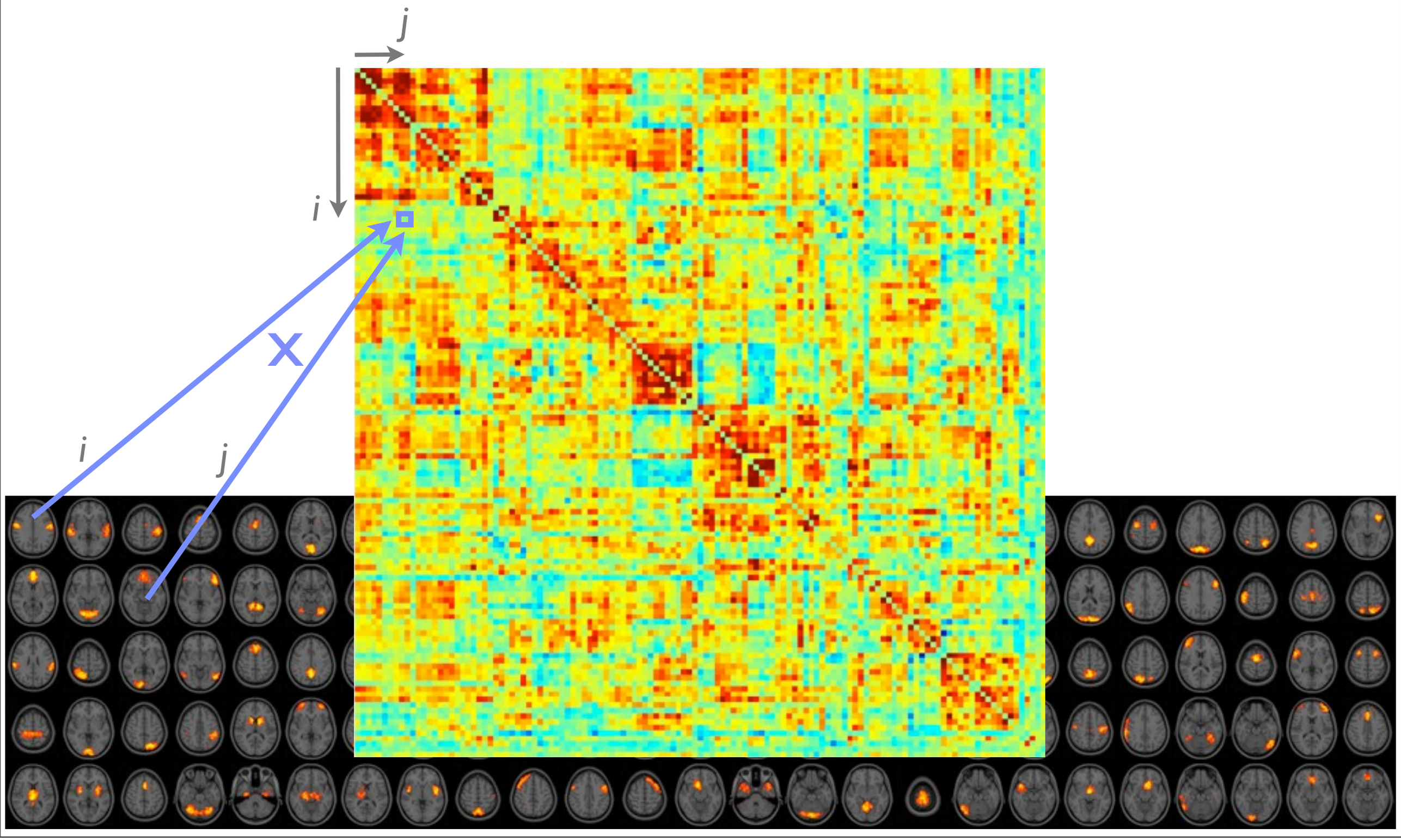

Edges: estimate connectivity between all pairs of nodes

But: what is the right method for estimating connectivity, based on FMRI timeseries?

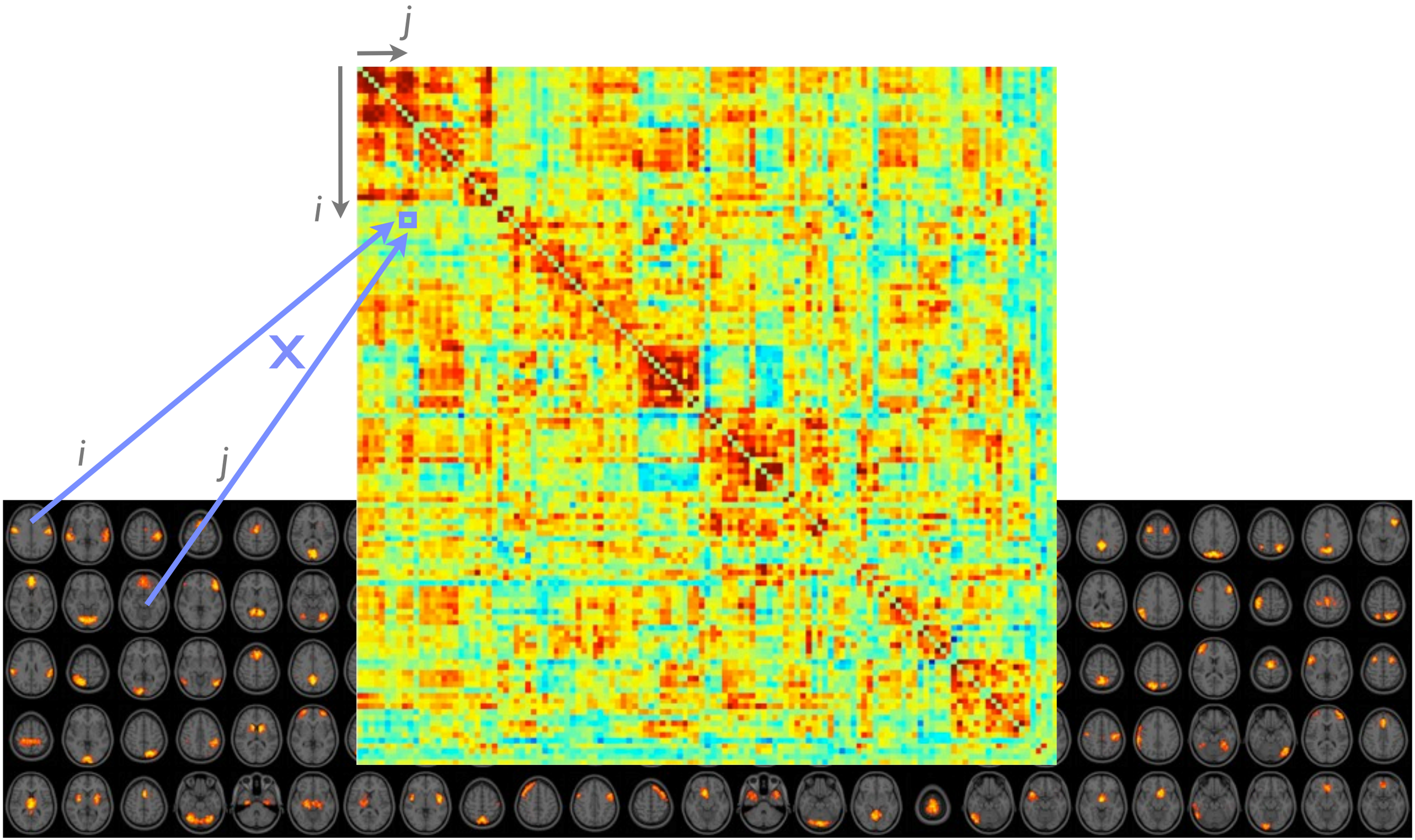

so we get a *Nodes x Nodes* network matrix

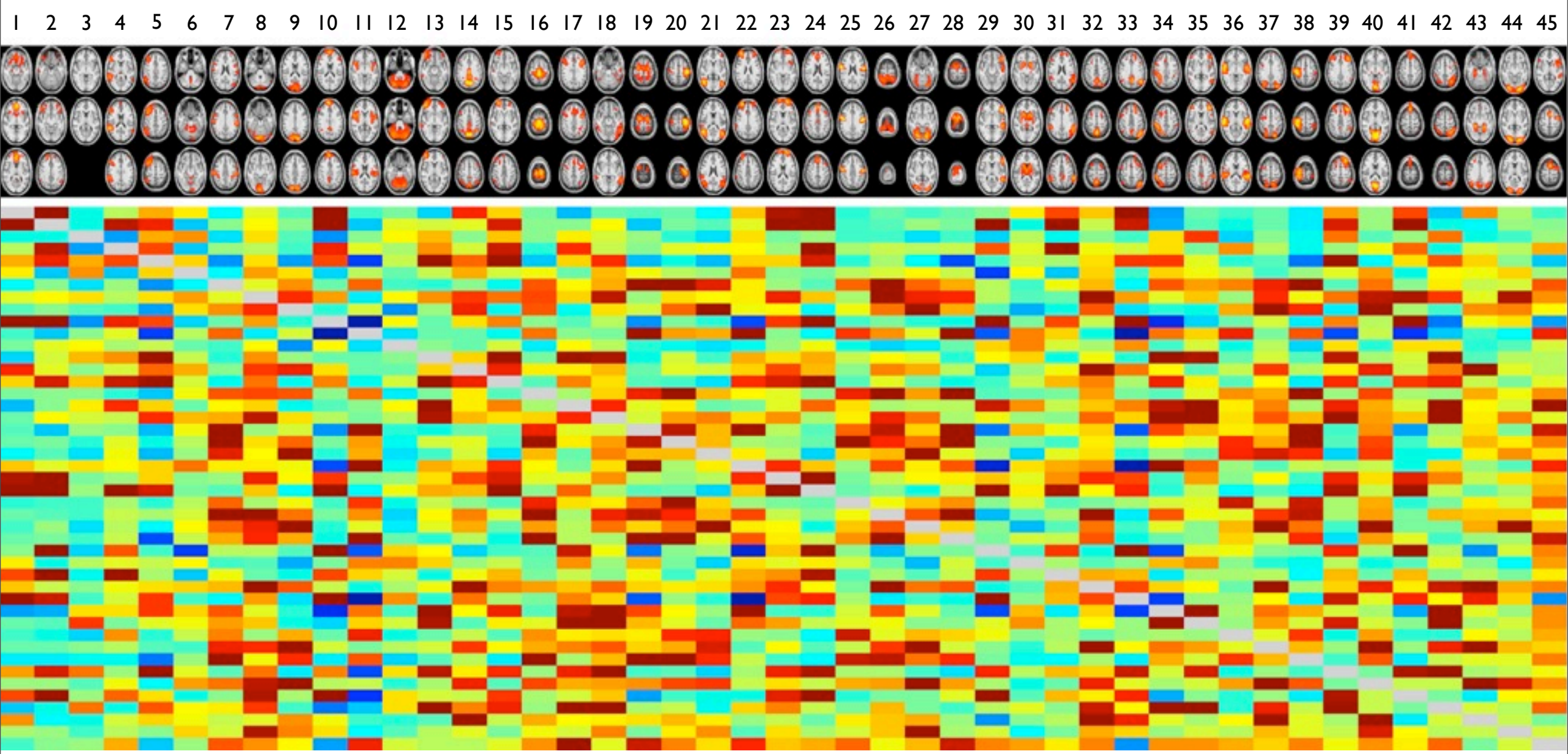

reorder node ordering to find clusters

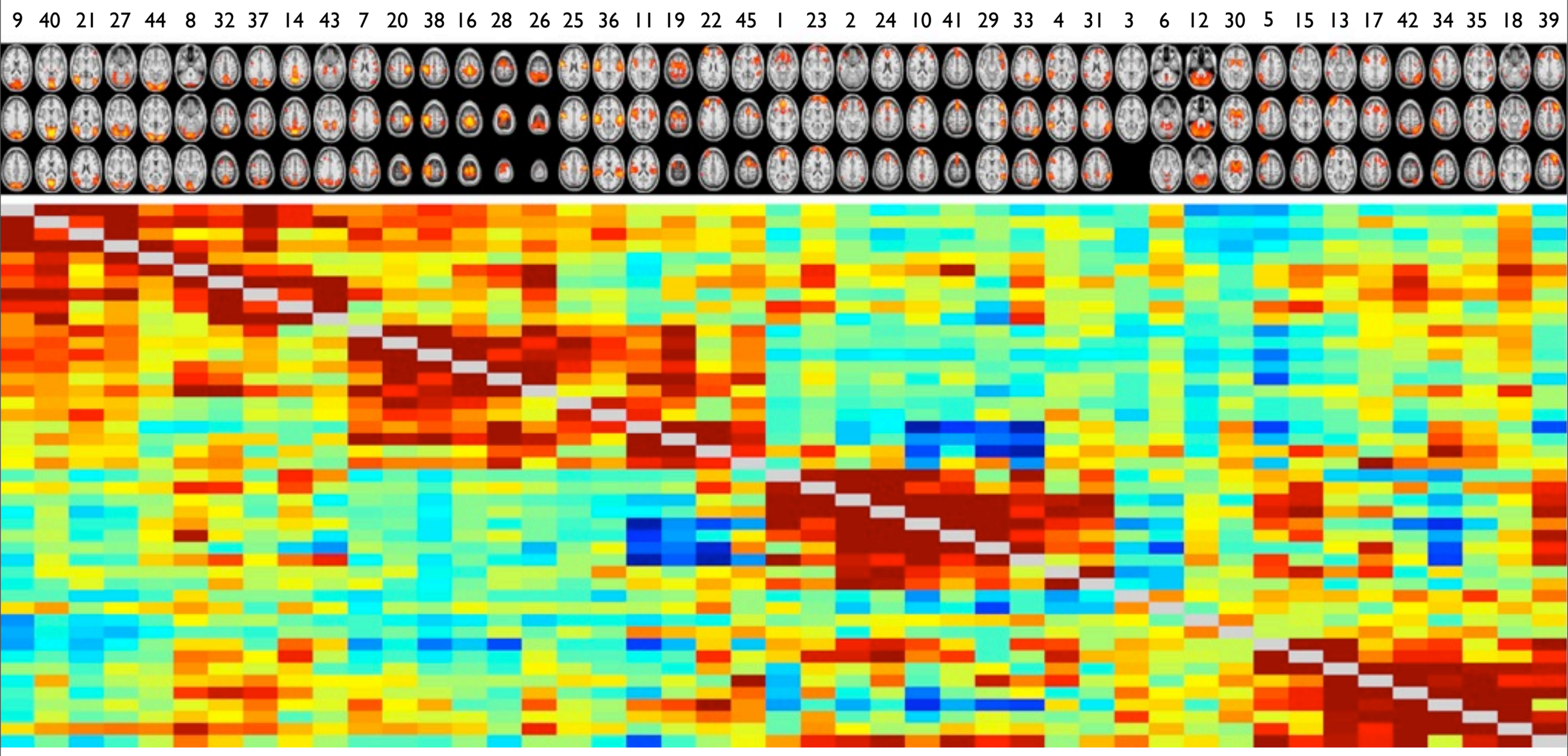

can view hierarchy of clusters

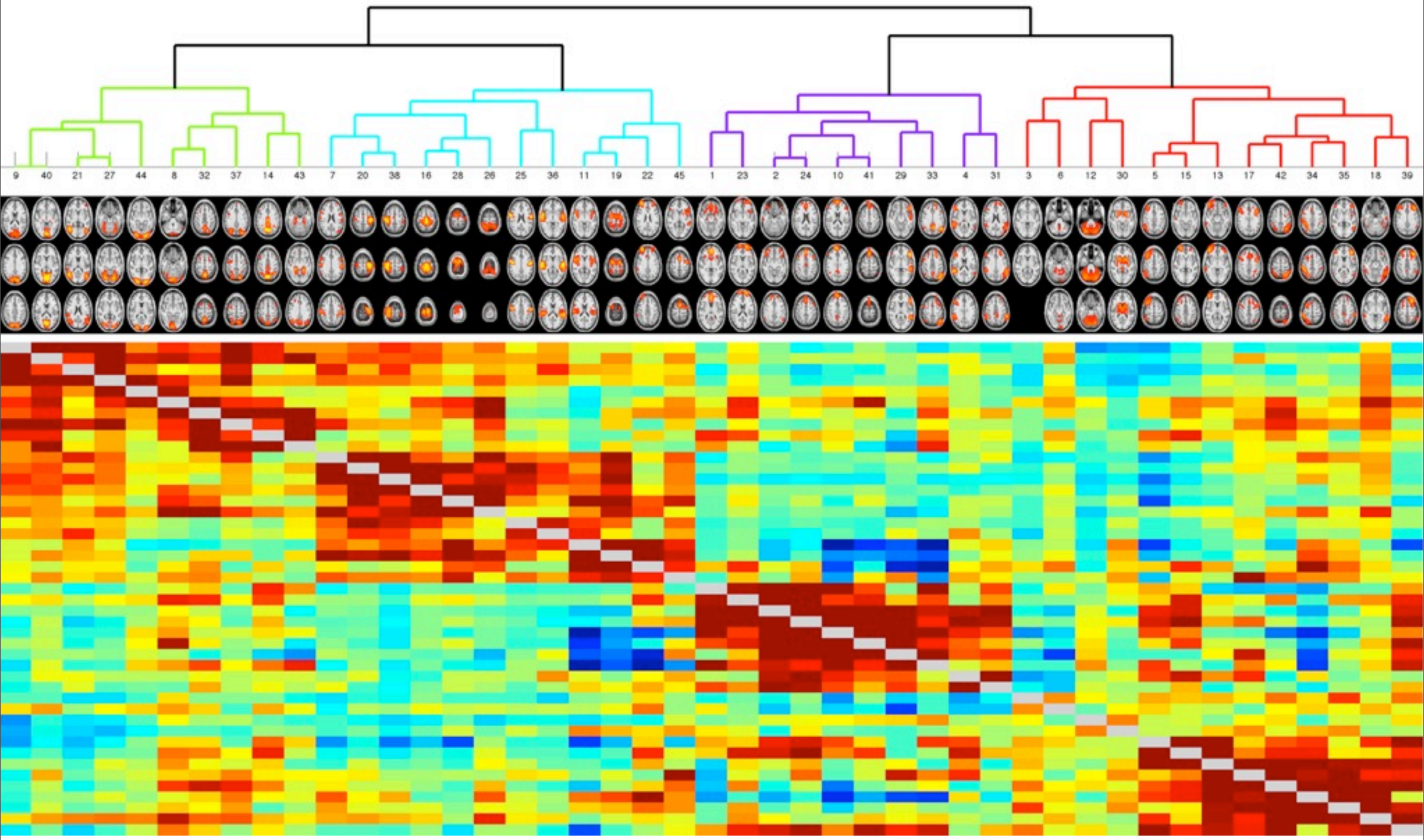

- *Cordes MRI 2002*
- *Salvador Cerebral Cortex 2005*

Brain Networks!

- Take each of the clusters of nodes ("sub-networks") from RSNs
  - Include connected nodes from other clusters ("off-diagonals")
  - Plot all connections - thicker is stronger

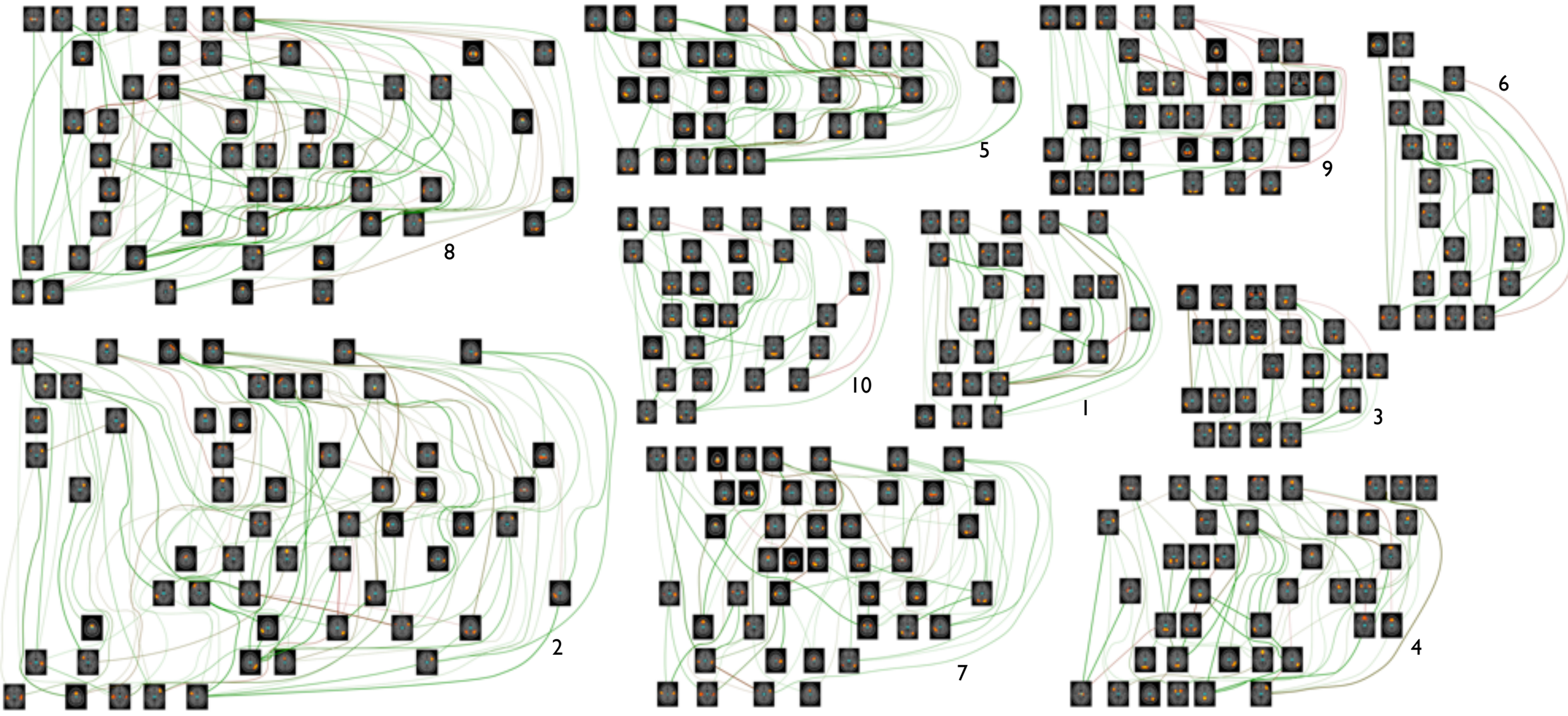

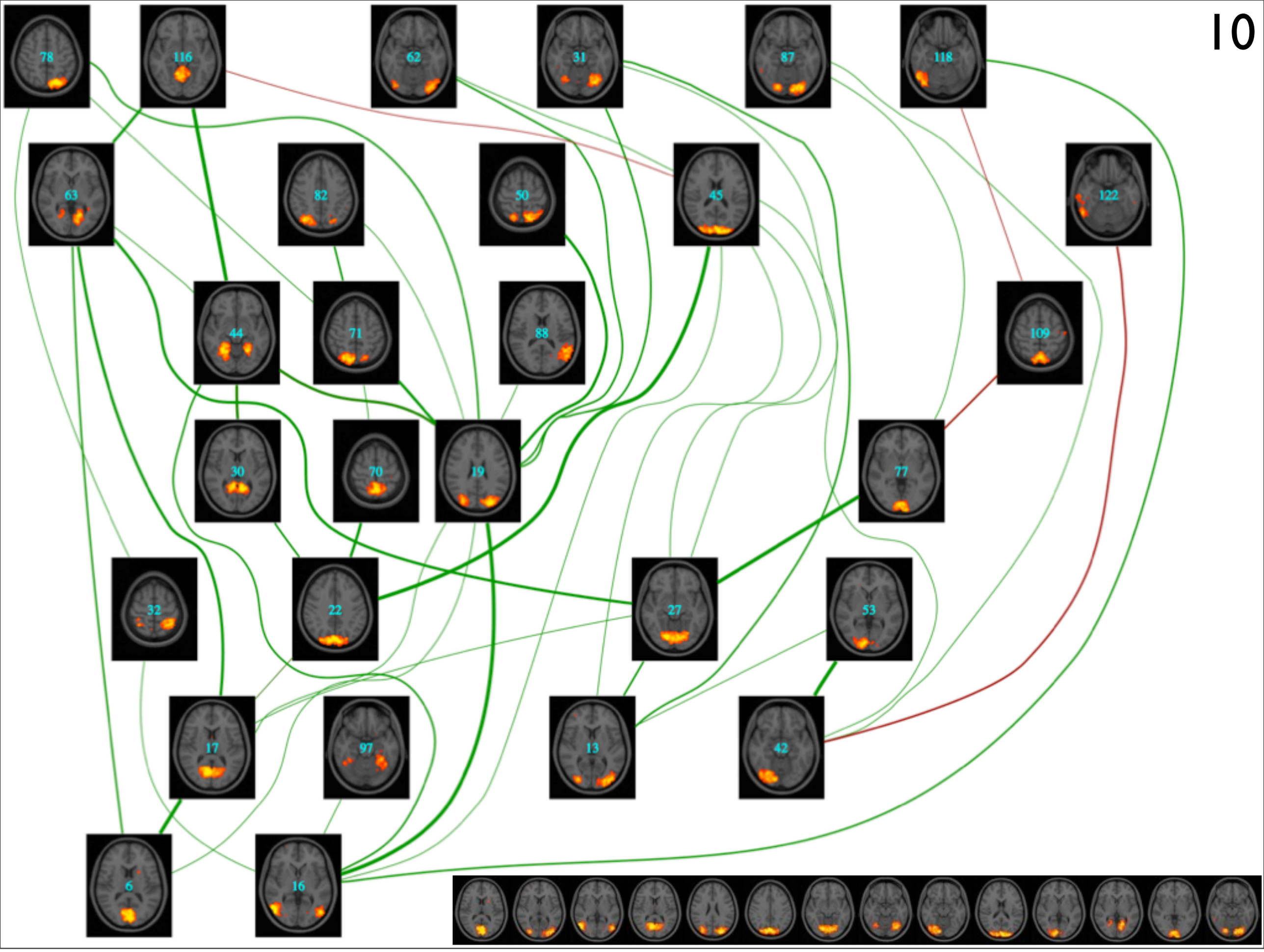
78
116
62
31
87
118
63
82
50
45
122
44
71
88
109
30
70
19
77
32
22
27
53
17
97
13
42
6
16

Acknowledgements

- *Steve Smith*, Clare Mackay, Nicola Filippini, Mark Woolrich, Tim Behrens, Heidi Johansen-Berg (FMRIB Oxford)
- David Cole, Tomoki Arichi, David Edwards, Valentina Doria (Imperial College London)
- Serge Rombouts(LUMC Leiden)
- Lisa Nickerson (Boston)
- *The Human Connectome Project*
- Rami Niazy (Rijad)
- Peter Fox, Angie Laird (RIC San Antonio)

That’s all folks